

# Research & Technology 1996

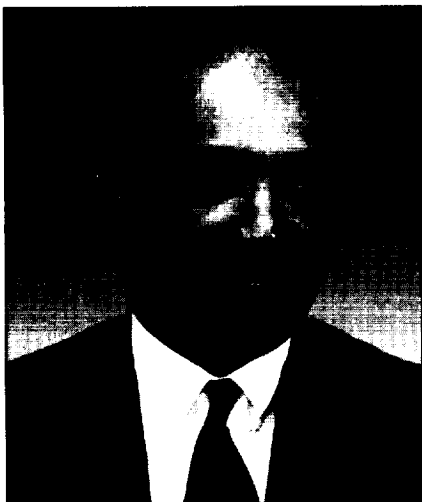


National Aeronautics and  
Space Administration

**Lewis Research Center**  
Cleveland, Ohio 44135

TM-107350

Trade names or manufacturers' names are used in this report for identification only. This usage does not constitute an official endorsement, either expressed or implied, by the National Aeronautics and Space Administration.



# Introduction


The NASA Lewis Research Center, a unique facility located in an important geographical area, has a long and distinguished history of performing research and developing technology in support of NASA's mission and the Nation's needs. Our mission is to work as a team to develop and transfer critical technologies to aerospace and nonaerospace industries, universities, and government institutions. To fulfill this mission, Lewis is committed to maximizing the return on the taxpayer's investment, to improving management and business practices, and to striving for diversity and value in the workforce.

In 1996, Lewis Research Center continued to increase its commitment to the mission of effective technology transfer. On September 19, we held our first "Lewis Business and Industry Summit." Through special sessions, tours, and over 140 exhibits, this event showcased our key technologies, capabilities, and facilities to over 500 participants from more than 300 companies. The event was such a success that we plan to make it a permanent part of our strategy to reach you—our customer.

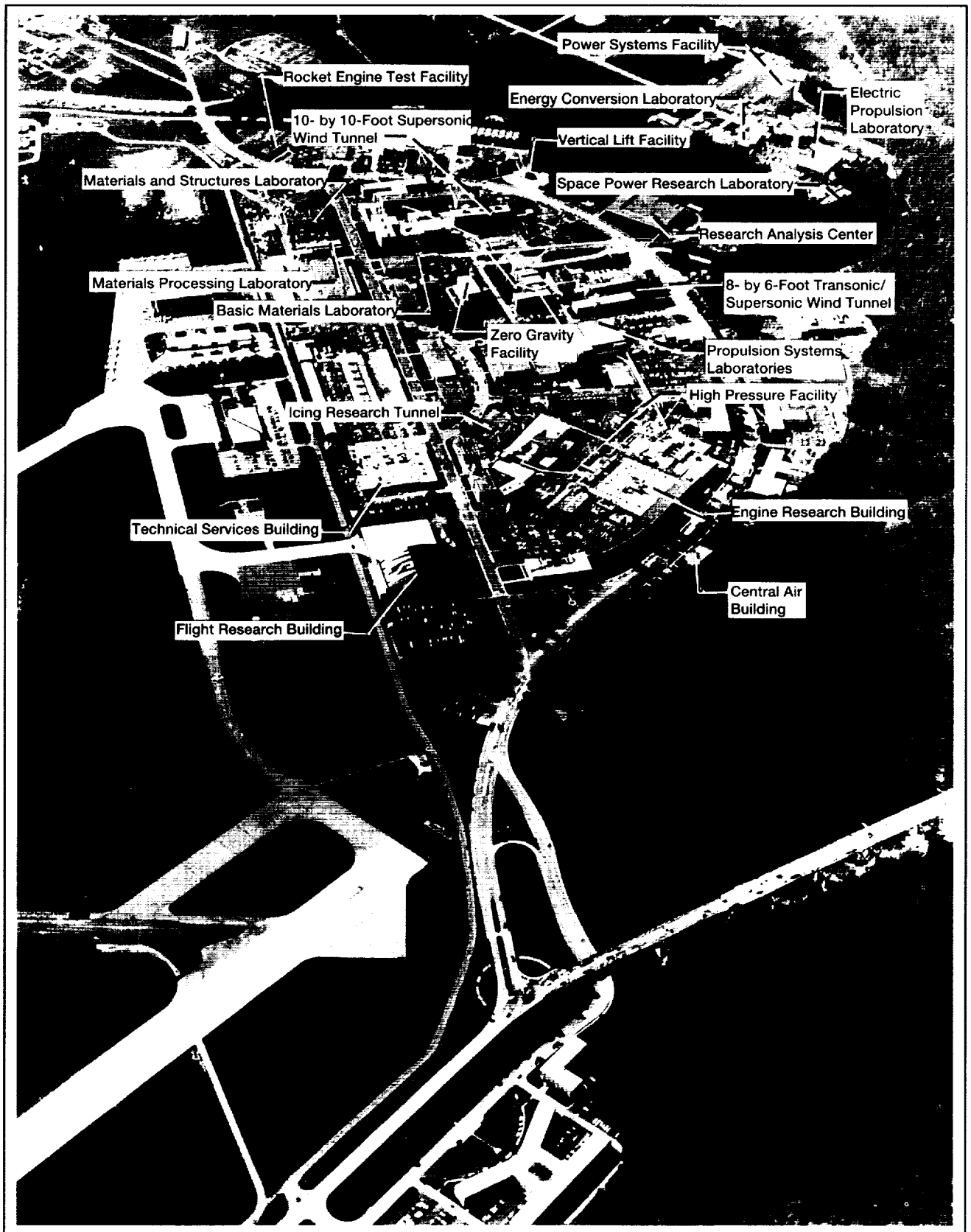
The 1996 Research & Technology report helps us to accomplish our mission by communicating our technical accomplishments to others and providing an avenue to expand their application. This report gives a brief, but comprehensive, review of Lewis' technical accomplishments during the past year. It is a testimony to the dedication and competence of all the employees, civil servants and contractors alike, who make up the staff.

The report is organized so that a broad cross section of the community can readily use it. A short introductory paragraph begins each article and will prove to be an invaluable tool for the layperson. The articles summarize the progress made during the year in various technical areas and portray the technical and administrative support associated with Lewis' technology programs.

We hope this information is useful to all. If additional information is desired, the reader is encouraged to contact the researchers identified in the articles and to visit Lewis on the World Wide Web (<http://www.lerc.nasa.gov>). This document is available on the World Wide Web (<http://www.lerc.nasa.gov/WWW/RT/>).

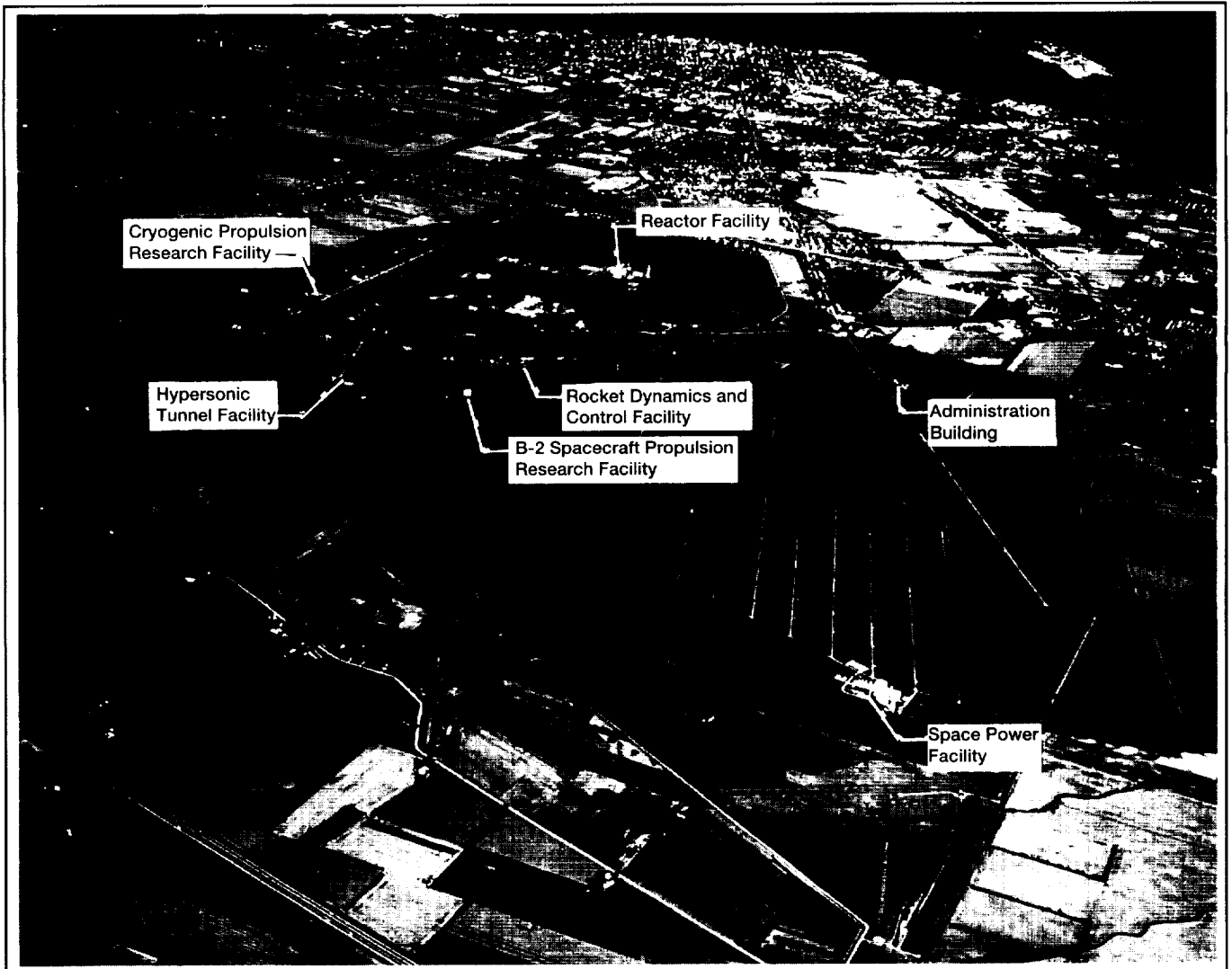


Donald J. Campbell  
Director



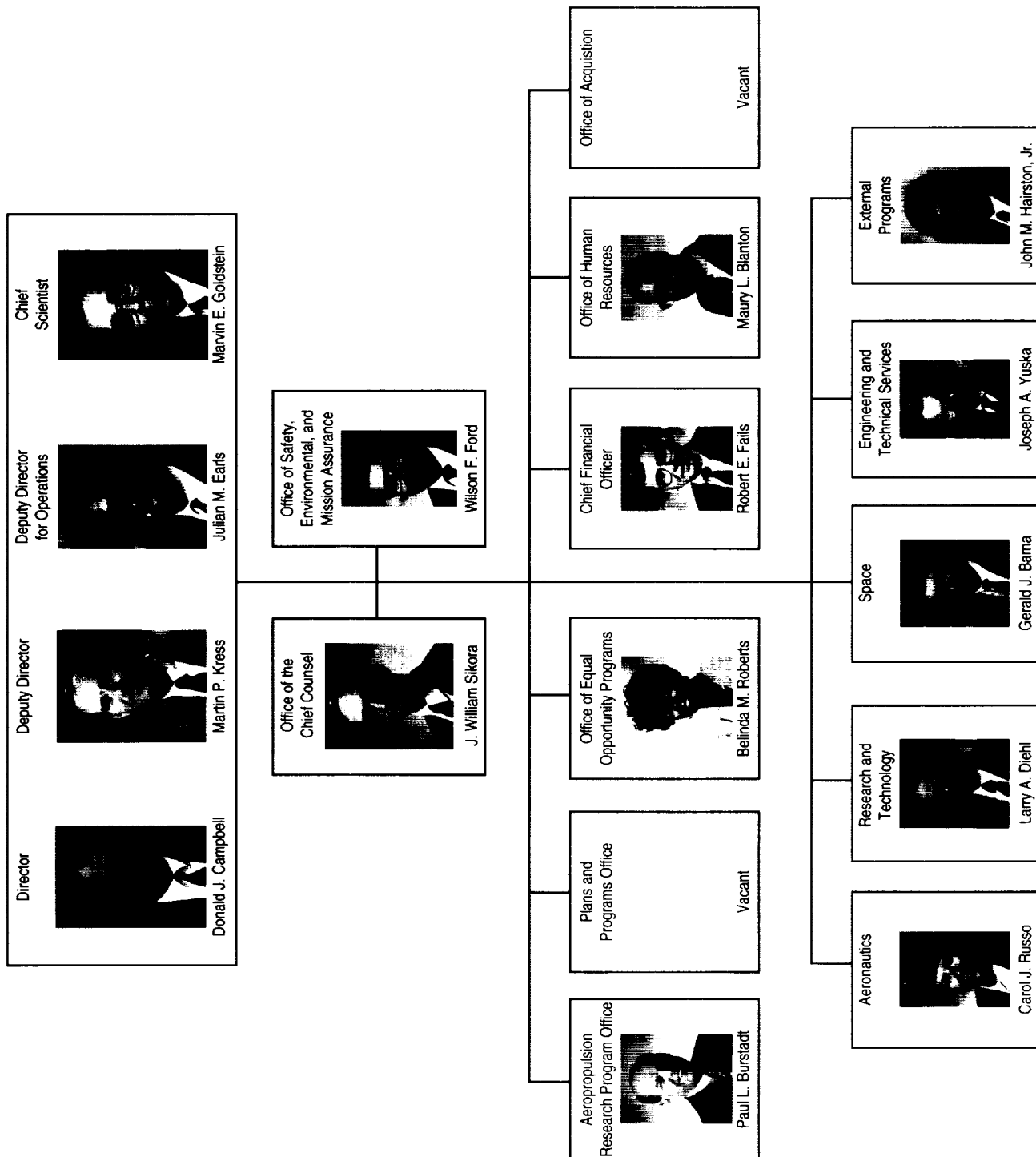
*Lewis Research Center, Cleveland, Ohio*



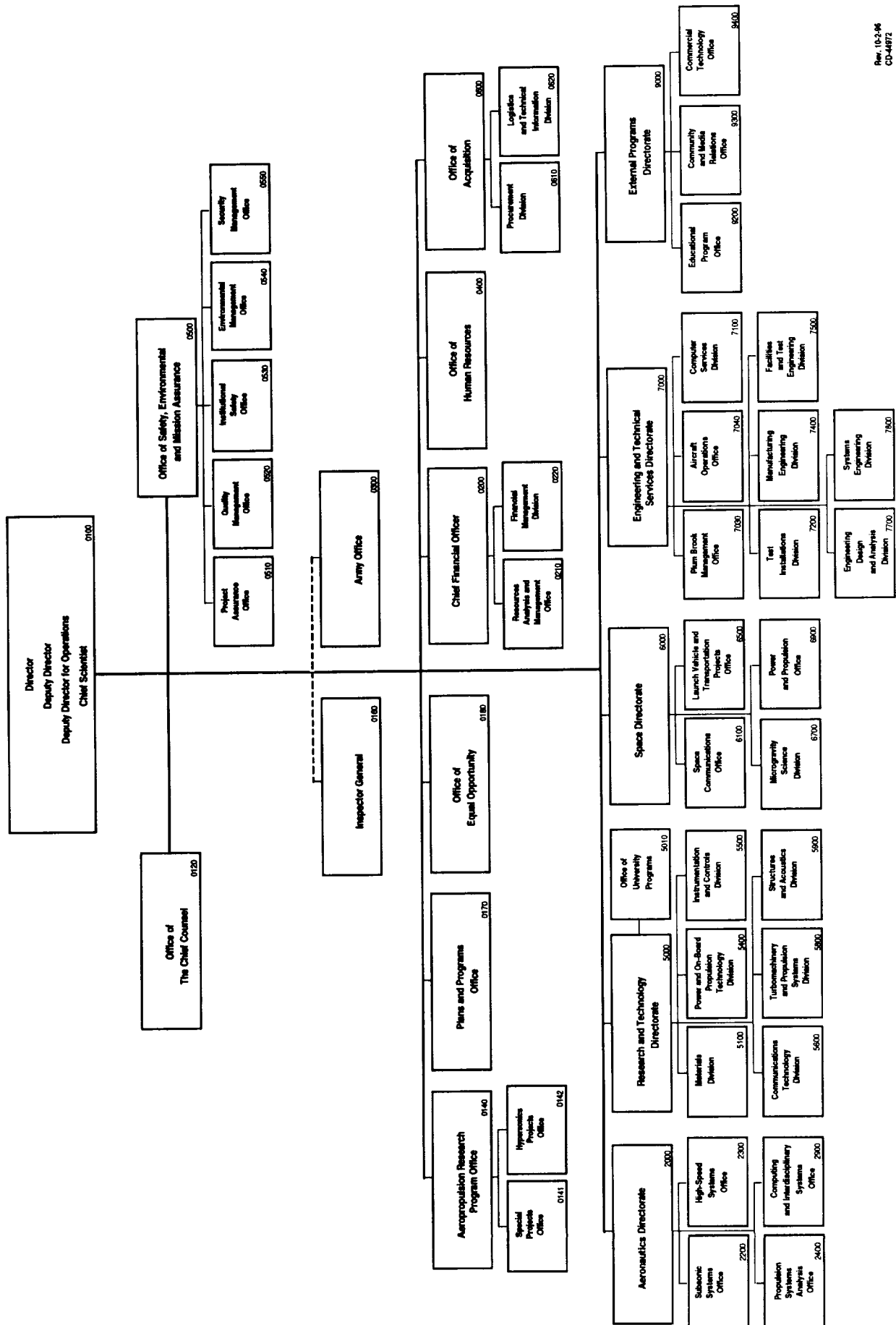


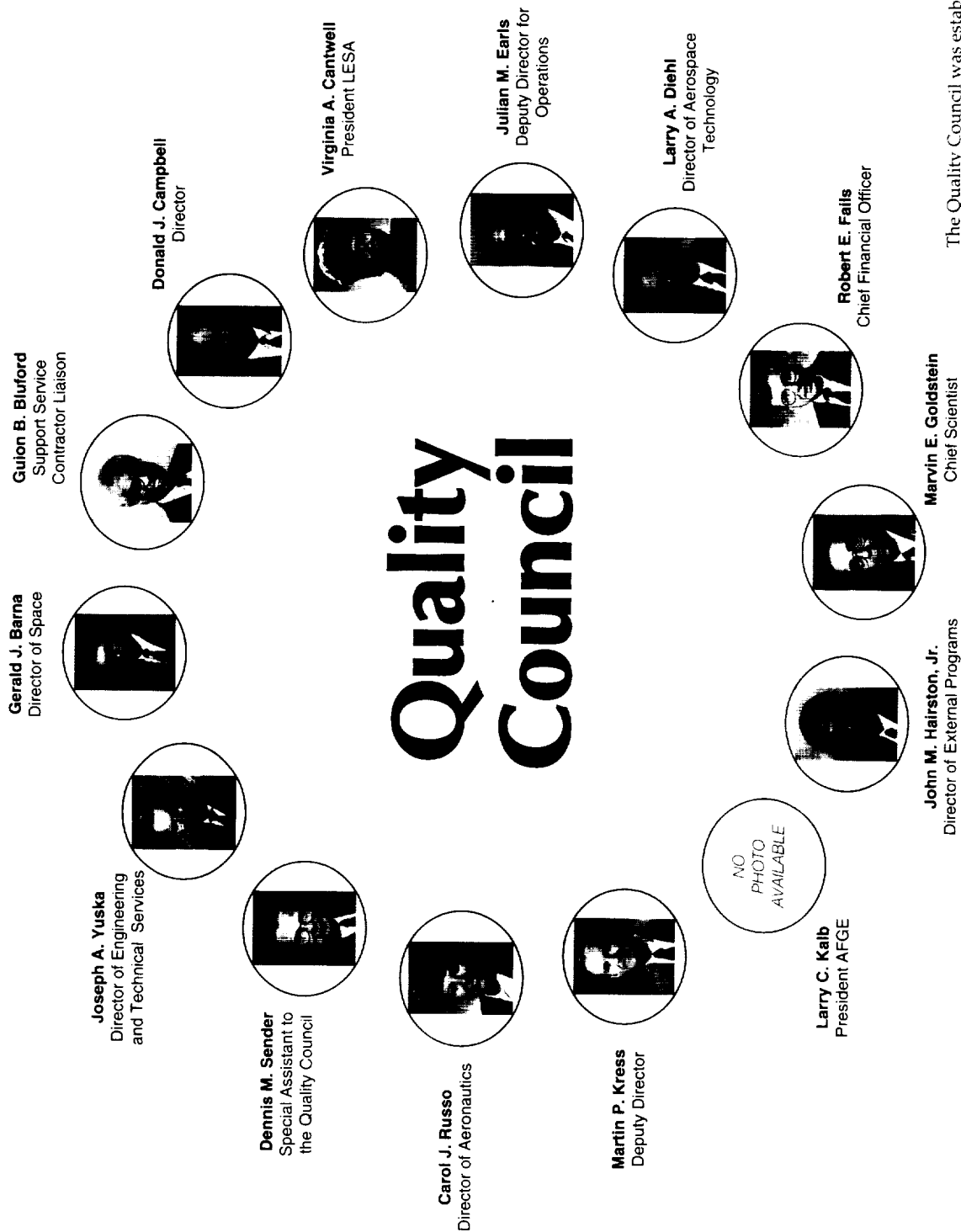
*Plum Brook Station, Sandusky, Ohio*

# NASA Lewis Research Center Senior Management



# NASA Lewis Research Center





The Quality Council was established in October 1992 to adopt and implement a Total Quality (TQ) plan for Lewis. It is composed of Executive Council members as well as the president of the American Federation of Government Employees (AFGE), Local 2812, and the president of the Lewis Engineers and Scientists Association (LESA). IFPTE Local 28. A representative of major onsite support service contractors serves as a liaison.



# Contents

## Aeronautics

### ***Aeropropulsion Analysis***

Combined Numerical/Analytical Perturbation Solutions of the Navier-Stokes Equations for Aerodynamic (Ejector Nozzle) Flows.....	1
---	---

### ***Instrumentation and Control Technology***

High Gas Temperature Probe.....	3
Thermal Analysis Demonstrated for a Plug-Type Heat Flux Gauge.....	4
Reliable Breakdown Obtained in Silicon Carbide Rectifiers.....	6
Ultraviolet Molecular Rayleigh Scattering Used to Measure Velocity in High-Speed Flow.....	8
Chaotic Time Series Analysis Method Developed for Stall Precursor Identification in High-Speed Compressors.....	9
Controls/CFD Interdisciplinary Research Software Generates Low-Order Linear Models for Control Design From Steady-State CFD Results.....	11
Single-Lever Power Control for General Aviation Aircraft Promises Improved Efficiency and Simplified Pilot Controls.....	12

### ***Internal Fluid Mechanics***

National Combustion Code: A Multidisciplinary Combustor Design System.....	14
Interactive Educational Tool for Turbofan and Afterburning Turbojet Engines.....	15
Rotor-Stator Interaction Performance Effects.....	15
Stator Indexing in Multistage Compressors.....	16
Bleed Hole Flow Phenomena Studied.....	17
Internal Mixing Studied for GE/ARL Ejector Nozzle.....	19

### ***Propulsion Systems***

High-Pressure Combustion Testing Reveals Promise of Low-Emission Combustors for Advanced Subsonic Gas Turbines.....	20
Computational Fluid Dynamics Analysis Method Developed for Rocket-Based Combined Cycle Engine Inlet.....	21
Fluidic Injection for Throat-Area Control and Thrust Vectoring.....	23
Oscillating Cascade Aerodynamics at Large Mean Incidence Angles.....	24
SWIFT: Multistage Turbomachinery Analysis Code Developed.....	25
Effects of Rotor Wake on Film Cooling Investigated.....	26
Forward Swept Compressor Testing.....	27
Low Pressure Turbine Flow Physics Program.....	29
Vacuum Cleaner Fan Being Improved.....	30
Acoustic Barrier Facilitates Inlet Noise Measurements for Aft-Dominated Fans.....	31

### ***Aeropropulsion Facilities and Experiments***

Scale Model Icing Research Tunnel.....	33
Supersonic Wind Tunnel Capabilities Expanded Into Subsonic Region.....	34

### ***Interdisciplinary Technology***

pV3-Gold Visualization Environment for Computer Simulations.....	36
Steady-State Cycle Deck Launcher Developed for Numerical Propulsion System Simulation.....	38
Configuration Management File Manager Developed for Numerical Propulsion System Simulation.....	39
Portable Extensible Viewer.....	40
Visual Computing Environment.....	42

A Vision in Aeronautics—The K-12 Wind Tunnel Project.....	43
Flow Analysis of a Gas Turbine Low-Pressure Subsystem.....	44

## Aerospace Technology

### **Materials**

Advanced High-Temperature Engine Materials Technology Progresses.....	47
Natural Strain.....	48
BFS Method for Alloys Optimized and Verified for the Study of Ordered Intermetallic Materials.....	49
Orthorhombic Titanium Matrix Composite Subjected to Simulated Engine Mission Cycles.....	51
Development of Creep-Resistant NiAl(Ti,Hf) Single-Crystal Alloys.....	53
Oxygen Compatibility Screening Tests in Oxygen-Rich Combustion Environment.....	54
Alternative Processing Method Leads to Stronger Sapphire-Reinforced Alumina Composites.....	56
Single-Tow Minicomposite Test Used to Determine the Stressed-Oxidation Durability of SiC/SiC Composites.....	57
First Single-Crystal Mullite Fibers.....	58
Method for Efficient Joining of Silicon Carbide-Based Ceramic Materials Developed.....	59
Unique Tuft Test Facility Dramatically Reduces Brush Seal Development Costs.....	60
Ion Implantation of Perfluoropolyether-Lubricated Surfaces for Improved Tribological Performance.....	61
Test Method Designed to Evaluate Cylinder Liner-Piston Ring Coatings for Advanced Heat Engines.....	62
Compressor Case Manufactured Using High-Temperature Polyimides.....	64
Oxidation-Resistant Coating Alloy for Gamma Titanium Aluminides.....	66
Environmental Studies on Titanium Aluminide Alloys.....	67
Volatile Reaction Products From Silicon-Based Ceramics in Combustion Environments Identified.....	69
Oxidation Resistance and Critical Sulfur Content of Single-Crystal Superalloys.....	70

### **Structures**

Probabilistic Thermomechanical Fatigue of Polymer Matrix Composites.....	72
T/Best: Technology Benefit Estimator for Composites and Applications to Engine Structures.....	74
Effect of Cyclic Thermal Loads on Fatigue Reliability in Polymer Matrix Composites.....	75
ICAN Computer Code Adapted for Building Materials.....	76
Micromechanical Modeling Efforts for Advanced Composites.....	77
COMETBOARDS Can Optimize Performance of Wave-Rotor-Topped Gas Turbine Engine.....	79
Transient Finite Element Analyses Developed to Model Fan Containment Impact Events.....	80
High-Temperature Adhesive Strain Gage Developed.....	81
Novel Multidisciplinary Models Assess the Capabilities of Smart Structures to Manage Vibration, Sound, and Thermal Distortion in Aeropropulsion Components.....	82
Enabling Propulsion Materials (EPM) Structural Component Successfully Tested Under Pseudo-Operating Conditions.....	84
Retirement for Cause as an Alternate Means of Managing Component Lives.....	85
Model Determined for Predicting Fatigue Lives of Metal Matrix Composites Under Mean Stresses.....	86
Oxidation Embrittlement Observed in SiC/SiC Composites.....	87
TURBO-AE: An Aeroelastic Code for Propulsion Applications.....	89
Rotordynamics on the PC: Transient Analysis With ARDS.....	90
Space Mechanisms Lessons Learned and Accelerated Testing Studies.....	92
More-Electric Gas Turbine Engines.....	94
Measurement of Gust Response on a Turbine Cascade.....	95
Fan Blade Deflection Measurement and Analyses Correlation.....	96

Feasibility of Rope Seal Technology Demonstrated for an Industrial Application.....	97
X-Ray Computed Tomography Monitors Damage in Composites.....	98
Stress Intensity Factor Solutions for Multiple Edge Cracks in Ceramic Matrix Composites.....	99
Award-Winning CARES/Life Ceramics Durability Evaluation Software Is Making Advanced Technology Accessible.....	100
Capability of Thermographic Imaging Defined for Detection in High-Temperature Composite Materials.....	102

### ***Space Propulsion Technology***

Rocket Engine Numerical Simulator (RENS).....	104
Ablative Material Testing at Lewis Rocket Lab.....	105
Real-Time Sensor Validation System Developed for Reusable Launch Vehicle Testbed.....	106
Demonstration of Oxygen and Carbon Monoxide Propellants for Mars Missions.....	108
Metallized Gelled Propellant Heat Transfer Tests Analyzed.....	109
Fuels and Space Propellants for Reusable Launch Vehicles: A Small Business Innovation Research Topic and Its Commercial Vision.....	110
Electric Propulsion.....	112
On-Board Chemical Propulsion.....	113
Gas Wave Bearings: A Stable Alternative to Journal Bearings for High-Speed Oil-Free Machines.....	114

### ***Power Technology***

SCARLET Photovoltaic Concentrator Array Selected for Flight Under NASA's New Millennium Program.....	116
Thermophotovoltaic Cell Technology Transferred to the Department of Energy Laboratory and a Commercial Manufacturer.....	117
Balloon Fuel Cell Power System.....	118
Lithium Ion Batteries.....	119
High Capacity Battery Cell Flight Qualified.....	120
NASA Flywheel Program.....	121
Investigation of Teflon FEP Embrittlement on Spacecraft in Low-Earth Orbit.....	122
Cryogenic Electronics in Support of Deep-Space Missions.....	123
New Electromagnetic Interference Shielding Material Demonstrated.....	124
High-Temperature Passive Power Electronics.....	125
Protective Coating Enhances the Durability of Retroreflectors for the International Space Station.....	126

### ***Space Electronics***

High-Power, High-Temperature Superconductor Technology Development.....	127
Digital Audio Radio Field Tests.....	128
Lewis Investigates Frequency Sharing Between Future NASA Space Systems and Local Multipoint Distribution Systems in the 27-GHz Band.....	130
Computer Simulation of Microwave Devices.....	131
High-Temperature Superconducting/Ferroelectric Structures for Tunable Microwave Components.....	132
Miniaturized High-Temperature Superconducting/Dielectric Multilayer Filters for Satellite Communications.....	133
Root-Raised Cosine Filter Implementation That Uses Canonical Signed Digits for High-Speed Digital Filter Applications.....	135

## **Space Flight Systems**

### ***Space Experiments***

Shuttle Fire Tests Are Radiant.....	137
-------------------------------------	-----



Comparative Soot Diagnostics Experiment Looks at the Smoky World of Microgravity Combustion.....	139
Pool Boiling Experiment Has Five Successful Flights.....	140
Colloidal Disorder–Order Transition Experiment Probes Particle Interactions in Microgravity.....	142
Surface Tension Driven Convection Experiment Completed.....	143
Isothermal Dendritic Growth Experiment (IDGE) Is the First United States Microgravity Experiment Controlled From the Principal Investigator’s University.....	145
Smoldering News From STS–77 Endeavour.....	147
Facilitating Science—The International Space Station Fluids and Combustion Facility.....	148
Burning Candles in the Microgravity of Space.....	150
Measured Success—The Microgravity Measurement and Analysis Project.....	151

### ***Power Systems***

Mir Cooperative Solar Array.....	153
Advanced Power System Analysis Capabilities.....	155
Dark Forward Electrical Testing of the Mir Cooperative Solar Array.....	157
Stability of Large Direct-Current Power Systems That Use Switching Converters and the Application of Switching Converters to the International Space Station.....	158
Hybrid Turbine Electric Vehicle.....	159

## **Engineering & Computational Support**

### ***Computational Support***

Integrated Digital Video and Experimental Data Analysis for Microgravity Combustion Experiment.....	161
Automated Status Notification System.....	162

### ***Engineering Support***

Wavelet Methods Developed to Detect and Control Compressor Stall.....	163
Manipulating Liquids With Acoustic Radiation Pressure.....	165
Nonlinear Dynamic Behavior in the Cassini Spacecraft Modal Survey.....	166
Aircraft Anti-Icing and Deicing Protection Using Ultrasound Technology.....	168

## **Lewis Research Academy**

Turbomachinery Flows Modeled.....	169
New Theoretical Technique for Alloy Design.....	170
Thermal Radiation Effects Analyzed in Translucent Composite and Thermal Barrier Coating.....	171

## **Technology Transfer**

Lewis Business and Industry Summit.....	173
Innovative Ultrasonic Imaging Method Wins R&D 100 Award.....	176
Lewis-Developed Ion Exchange Material Licensed to Several Companies.....	177
Lewis Incubator for Technology.....	177

## **Appendixes**

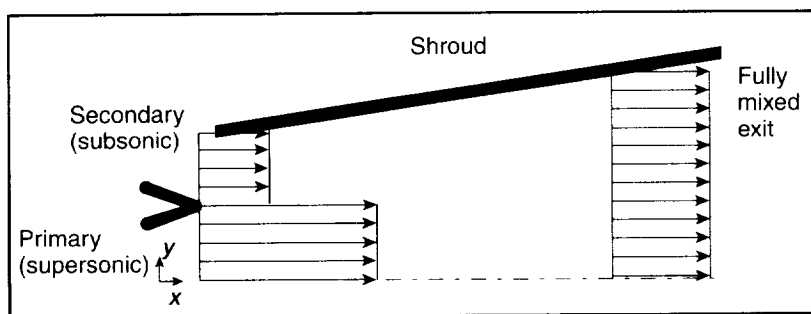
NASA Headquarters Program Offices.....	178
Index of Authors and Contacts.....	179



## Aeropropulsion Analysis

### Combined Numerical/Analytical Perturbation Solutions of the Navier-Stokes Equations for Aerodynamic (Ejector Nozzle) Flows

In spite of the rapid advances in both scalar and parallel computational tools, the large number and breadth of variables involved in aerodynamic systems make the use of parabolized or even boundary layer fluid flow models impractical for both preliminary design and inverse design problems. Given this restriction, we have concluded that reduced or approximate models are an important family of tools for design purposes. This study of a combined perturbation/numerical modeling methodology with an application to ejector-mixer nozzles (shown schematically in the following figure) is nearing completion. The work is being funded by a grant from the NASA Lewis Research Center (Grant NGT 51244) to Texas A&M University.



*Ejector nozzle schematic. The high-speed primary jet (engine core) entrains fluid (viscous and local pressure differential), thus causing the secondary stream.*

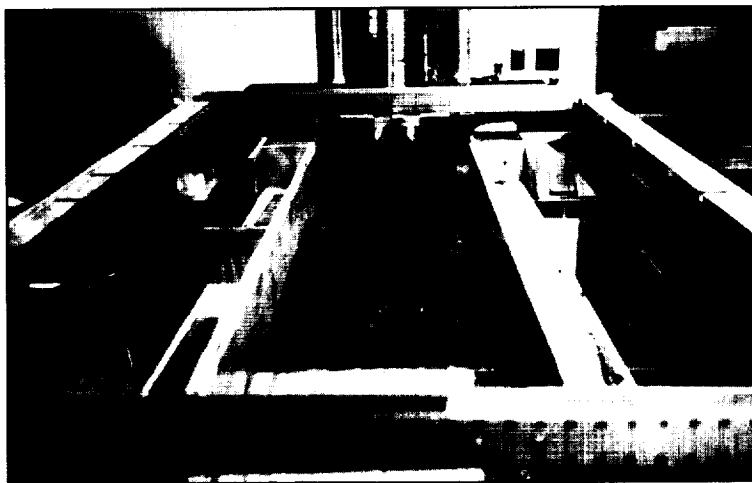
These ejector-mixer nozzle models are designed to be of use to the High Speed Civil Transport Program and may be adopted by both NASA and industry. A computer code incorporating the ejector-mixer models is under development. This code, the Differential Reduced Ejector/Mixer Analysis (DREA), can be run fast enough to be used as a subroutine or to be called by a design optimization routine. Simplified conservation equations— $x$ -momentum, energy, and mass conservation—are used to define the model.

Unlike other preliminary design models, DREA requires minimal empirical input and includes vortical mixing and a fully compressible formulation among other features. DREA is being validated by comparing it with results obtained from

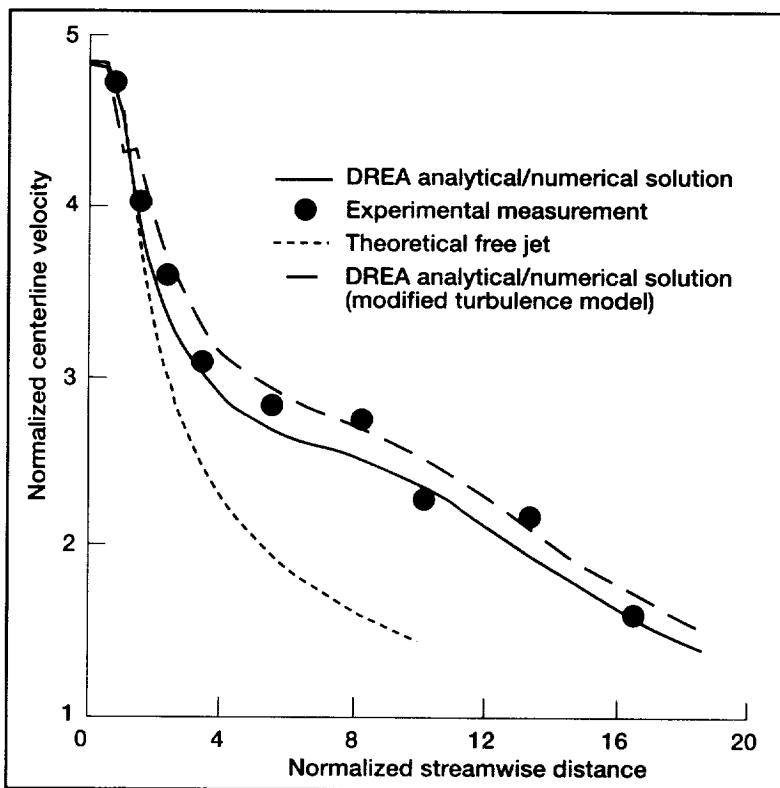
open literature and proprietary industry data. Preliminary results for a subsonic ejector and supersonic ejector are shown in the figures on the facing page.

In addition, dedicated experiments have been performed at Texas A&M. These experiments use a hydraulic/gas flow analog to provide information about the inviscid mixing interface structure (see the photo below).

Final validation and documentation of this work is expected by May of 1997. However, preliminary versions of DREA can be expected in early 1997. In summary, DREA provides a sufficiently detailed and realistic ejector-mixer nozzle model at a computational cost compatible with preliminary design applications.



*Hydraulic analog model of an ejector-mixer nozzle.*



DREA subsonic ejector solution compared with two-dimensional ejector (ref. 1).

## References

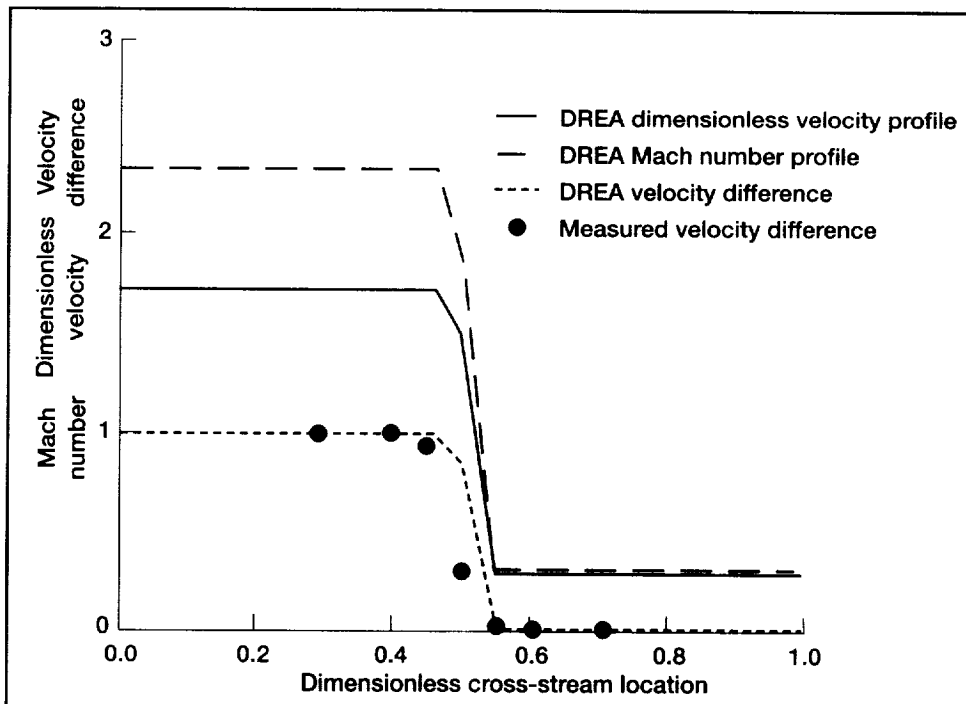
1. Gilbert, G.B.; and Hill, P.G.: Analysis and Testing of Two-Dimensional Slot Nozzle Ejectors With Variable Area Mixing Sections. NASA CR-2251, 1973.
2. Goebel, S.G.; and Dutton, J.C.: Experimental Study of Compressible Turbulent Mixing Layers. AIAA J., vol. 29, April 1991, pp. 538-546.

## Lewis contact:

Shari-Beth Nadell, (216) 977-7035,  
nadell@lerc.nasa.gov

Author: Lawrence J. De Chant

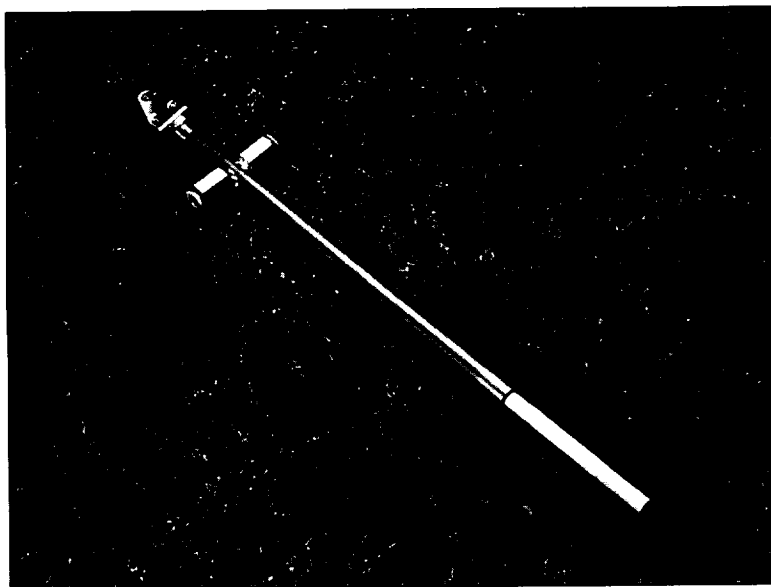
Headquarters program office: OA



DREA supersonic ejector solution for a mixing problem compared with experimental results (ref. 2) at a streamwise location,  $X$ , of 50 mm.

# Instrumentation and Control Technology

## High Gas Temperature Probe



*High gas temperature probe.*

A probe has been designed at the NASA Lewis Research Center and built for use in oxidizing atmospheres to temperatures exceeding 2000 °C. Conventional platinum-based probes are useable to only about 1500 °C. In contrast, this new probe consists of a tungsten-rhenium thermocouple (useable to 2300 °C, but very susceptible to oxidation at high temperatures) surrounded by a beryllium oxide tube. The inside of this tube is filled with argon to protect the thermocouple from oxidation. Beryllium oxide was chosen as the tube material because of its high melting point, good electrical properties at high temperatures, and excellent resistance to thermal shock.

Two probes were tested at NASA Lewis. The first survived several cycles (a total of roughly 4 hours) between room temperature and about 2040 °C, before being destroyed by debris in the test section. The second suffered mechanical damage during installation. After testing, the design was revised to make it more rugged without compromising the thermal properties of the probe.

Development of this probe is part of a strategy to explore the use of conventional probes as well as optical probes to measure gas temperatures within test combustors.

**Lewis contact:** Gustave C. Fralick, (216) 433-3645, [Gustave.C.Fralick@lerc.nasa.gov](mailto:Gustave.C.Fralick@lerc.nasa.gov)

**Author:** Gustave C. Fralick

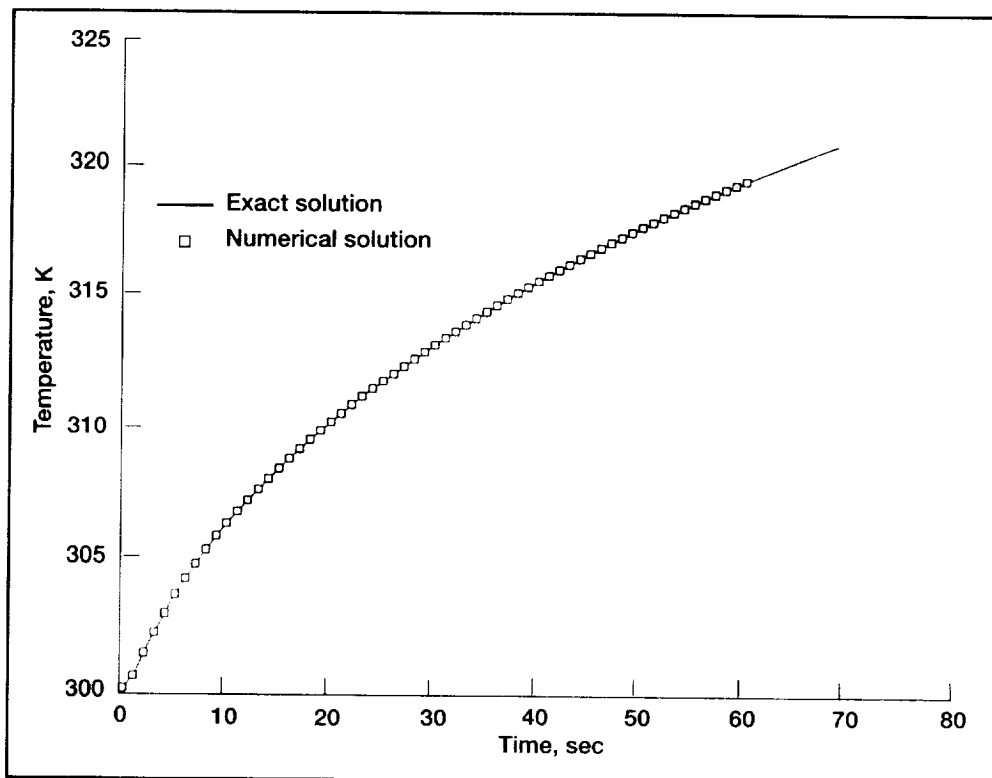
**Headquarters program office:** OA

# Thermal Analysis Demonstrated for a Plug-Type Heat Flux Gauge

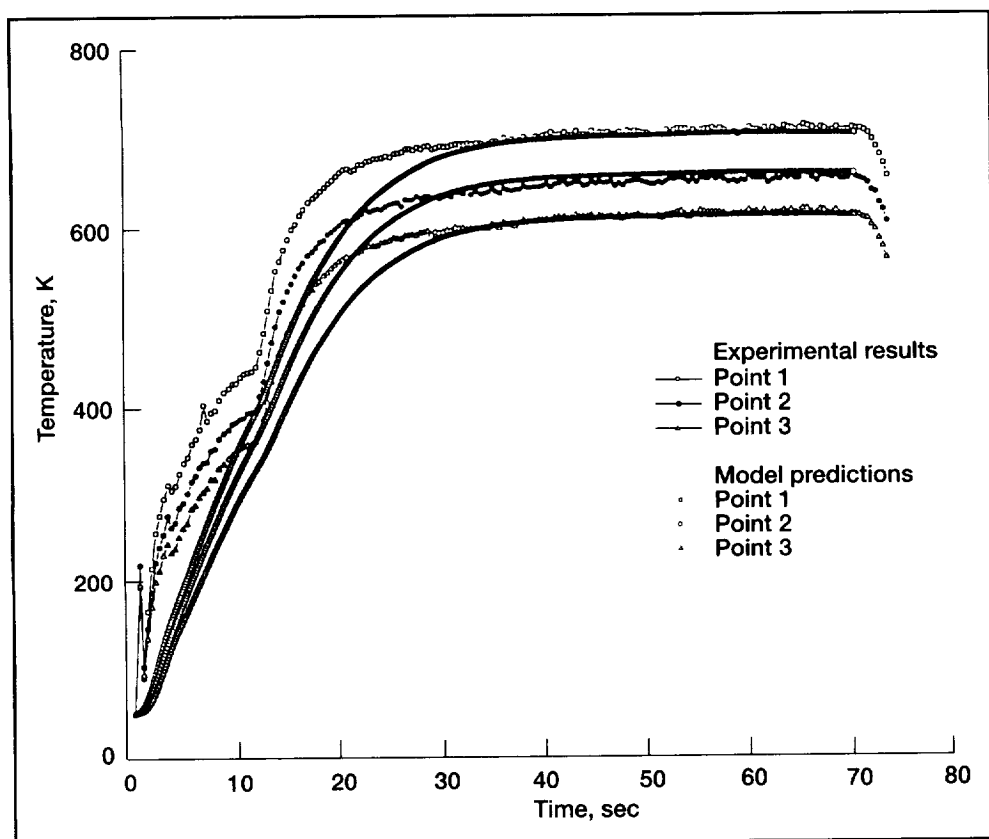
The NASA Lewis Research Center and the University of Akron have developed and demonstrated a two-dimensional, transient, numerical finite difference model of a plug-type heat flux gauge/probe assembly incorporating temperature-dependent material properties and surface radiation. The model's predictions have been compared with experimental results, showing that it can properly predict steady-state temperatures measured along the post of the gauge and in the surrounding material in which the gauge is mounted. The model, which has aided in quantifying expected two-dimensional conduction effects, can be used for future studies involving different applications.

We found that the temperature of the outer periphery of the gauge has a strong effect on temperatures of the gauge post but a much smaller effect on the temperature gradients along the post. Radial temperature gradients were predicted in the post, particularly near the ends, but in general, they were negligible. However, in the application studied here, radial temperature gradients were predicted to be significant above the post near the gauge centerline. As a result, the heat flux predicted at the surface of the gauge was not the same as the heat flux predicted along the post. The magnitude of the difference depends on the particular application since both the level of heat flux and the temperature of the surrounding material influence the two-dimensional heat transfer effects.

Advantages of the plug-type heat flux gauge include not disrupting the aerodynamic flow and its proven ability to withstand extremely harsh conditions. The numerical predictions of the present study suggest that possible design improvements include increasing the post radius, decreasing the air gap outer radius, decreasing the thickness of the hot surface above the post, and back-filling the air gap with a thermally conducting, but electrically nonconducting, material.



Results for the simplified version of the model compared with those for the analytical solution for temperatures at a 0.3-cm depth in a 2.54-cm slab. Step change in ambient fluid temperature to 500 K; material initially 300 K throughout; front surface convective; back face fixed at 300 K; 2.54-cm (axial), 0.5-cm (radial) axisymmetric model; no radiation; exact solution from reference 1. Constant properties: thermal conductivity,  $k$ , 11.685 W/m-K; thermal diffusivity,  $\alpha$ ,  $3.108 \times 10^{-6}$  m/sec<sup>2</sup>.



Post temperatures for model compared with those for experimental results.

This work was performed by Steve Rooke of The University of Akron and Gustave C. Fralick and Curt H. Liebert of the NASA Lewis Research Center.

#### Reference

1. Carslaw, H.S.; and Jaeger, J.C.: Conduction of Heat in Solids. 2nd edition, Oxford University Press, New York. (ISBN 0-19-853368-3)

**Lewis contact:** Gustave C. Fralick, (216) 433-3645, [Gustave.C.Fralick@lerc.nasa.gov](mailto:Gustave.C.Fralick@lerc.nasa.gov)

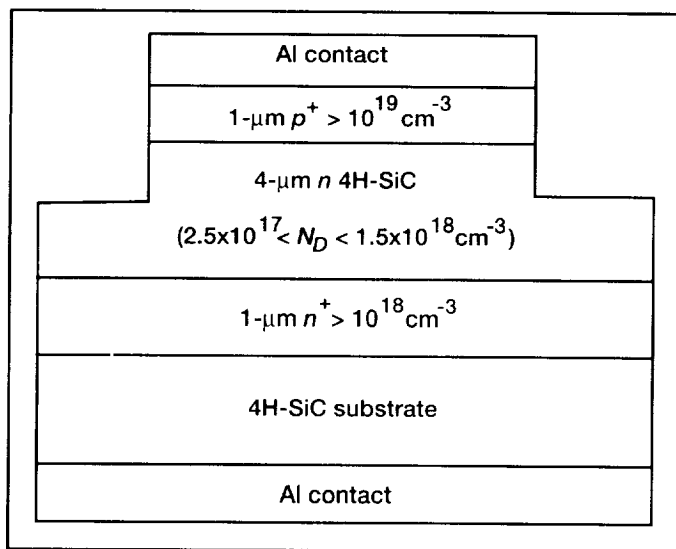
**Author:** Gustave C. Fralick

**Headquarters program office:** OA

# Reliable Breakdown Obtained in Silicon Carbide Rectifiers

The High Temperature Integrated Electronics and Sensor (HTIES) Program at the NASA Lewis Research Center is currently developing silicon carbide (SiC) for use in harsh conditions where silicon, the semiconductor used in nearly all of today's electronics, cannot function. Silicon carbide's demonstrated ability to function under extreme high-temperature, high-power, and/or high-radiation conditions will enable significant improvements to a far-ranging variety of applications and systems. These range from improved high-voltage switching for energy savings in public electric power distribution and electric vehicles, to more powerful microwave electronics for radar and cellular communications, to sensor and controls for cleaner-burning, more fuel-efficient jet aircraft and automobile engines.

For power distribution, SiC semiconductor switches offer the promise of 10-fold to 100-fold performance improvements over present-day silicon-based devices. Before these improvements can be realized, however, present-day prototype SiC devices must be improved and made reliable. One reliability requirement of modern power rectifiers is that they must be able to withstand transient overvoltage glitches that commonly occur in power system circuits. Silicon power rectifiers in use today operate with high reliability in part because they exhibit a stabilizing property known as a positive temperature coefficient of breakdown voltage. This property permits them to withstand and recover from overvoltage glitches without sustaining permanent damage.



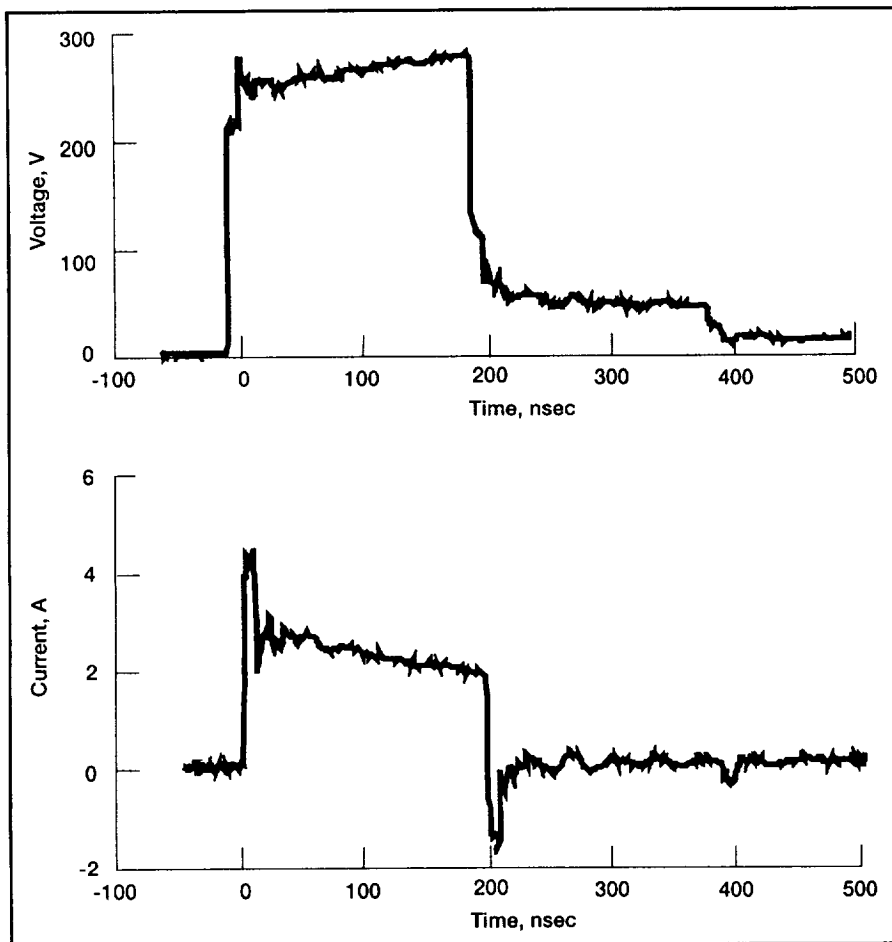
Prototype NASA Lewis SiC rectifier. ( $N_D$  is the donor dopant concentration.)

Prior to this work, prototype SiC rectifiers exhibited a negative temperature coefficient of breakdown voltage; those rectifiers could not reliably withstand overvoltage glitches. Such rectifiers, no matter how well they outperformed silicon rectifiers in voltage, current, and switching speed ratings, could not be incorporated into aerospace power systems where reliable operation is critical.

The figure below shows a schematic cross section of the first SiC rectifiers to exhibit a positive temperature coefficient of breakdown voltage, enabling these Lewis-fabricated rectifiers to repeatedly withstand large overvoltage glitches. The figure on the facing page shows the current and voltage waveforms recorded when one of these devices was subjected to a 200-nsec overvoltage glitch pulse. The device clearly exhibits a positive temperature coefficient of breakdown voltage: as the rectifier self-heats over the pulse duration, the voltage across the device increases (top waveform) while the current through the device decreases (bottom waveform). If one ignores the unimportant displacement current spikes at the rising and falling edges of the pulse, the peak conduction current of ~2.5 A at 20 nsec corresponds to a current density in excess of 50,000 A/cm<sup>2</sup>.

This work demonstrates for the first time that robust SiC power devices with excellent reliability and immunity from glitches will be achievable as SiC technology matures.





*Voltage and current response of the NASA Lewis SiC rectifier subjected to a 200-nsec overvoltage glitch.*

**Find out more about our research on the World Wide Web:**

<http://www.lerc.nasa.gov/WWW/SiC/SiC.html>

**Lewis contact:** Dr. Philip G. Neudeck, (216) 433-8902, [Phil.Neudeck@lerc.nasa.gov](mailto:Phil.Neudeck@lerc.nasa.gov)

**Author:** Dr. Philip G. Neudeck

**Headquarters program office:** OA

# Ultraviolet Molecular Rayleigh Scattering Used to Measure Velocity in High-Speed Flow

Molecular Rayleigh scattering offers a means to measure gas flow parameters including density, temperature, and velocity. No seeding of the flow is necessary. The Rayleigh scattered power is proportional to the gas density, the spectral width is related to the gas temperature, and the shift in the frequency of the spectral peak is proportional to one component of the fluid velocity. Velocity measurements based on Rayleigh scattering are more suitable for high-speed flow, where the bulk fluid velocity is on the order of, or larger than, the molecular thermal velocities. Use of ultraviolet wavelengths for Rayleigh scattering diagnostics is attractive for two reasons. First, the Rayleigh scattering cross section is proportional to the inverse 4th power of the wavelength. And second, the reflectivity of metallic surfaces is generally less than it is at longer wavelengths. This is of particular interest in confined flow situations, such as in small wind tunnels and aircraft engine components, where the stray laser light scattered from the windows and internal surfaces in the test facility limits the application of Rayleigh scattering diagnostics.

In this work at the NASA Lewis Research Center, molecular Rayleigh scattering of the 266-nm fourth harmonic of a pulsed, injection-seeded Nd:YAG (neodymium:yttrium-aluminum-garnet) laser was used to measure velocity in a supersonic free air jet with a 9.3-mm exit diameter. The frequency of the Rayleigh scattered light was analyzed with a planar mirror Fabry-Perot interferometer used in a static imaging mode, with the images recorded on a cooled, high-quantum-efficiency charge-coupled discharge (CCD) camera.

In addition, some unshifted light from the same laser pulse was imaged through the interferometer to generate a reference. Data were obtained with single laser pulses at velocities up to Mach 1.3. The measured velocities were in good agreement with velocities calculated from isentropic flow relations.

Our conclusion from this study was that ultraviolet Rayleigh scattering is preferable in confined flow situations because of the increase in the ratio of Rayleigh scattering signal to stray laser light. On the other hand, in open flows, such as free jets and larger wind tunnels where stray laser light can be controlled, visible Rayleigh scattering is preferable.

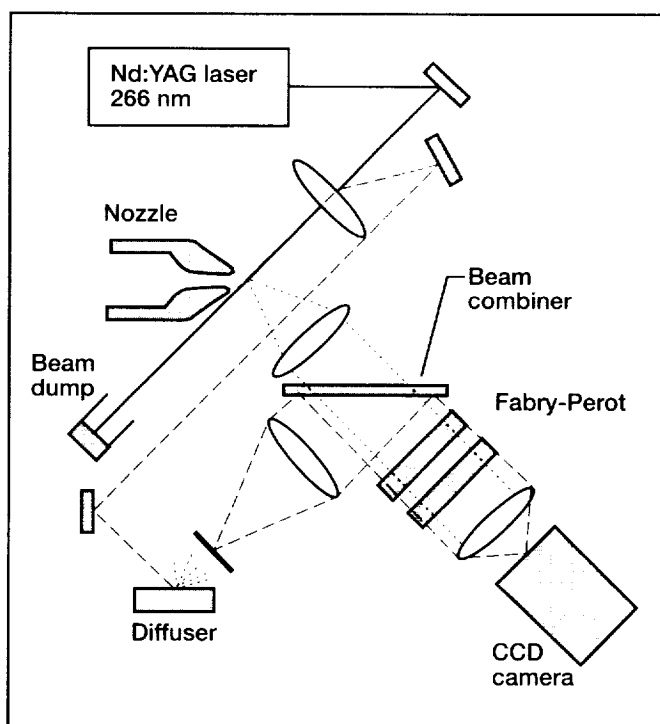
## Bibliography

Seasholtz, R.G.: Single-Shot Spectrally Resolved UV Rayleigh Scattering Measurements in High Speed Flow. NASA TM-107323, 1996.

## Lewis contact:

Dr. Richard G. Seasholtz,  
(216) 433-3754,  
Richard.G.Seasholtz@lerc.nasa.gov

**Author:** Dr. Richard G. Seasholtz  
**Headquarters program office:** OA



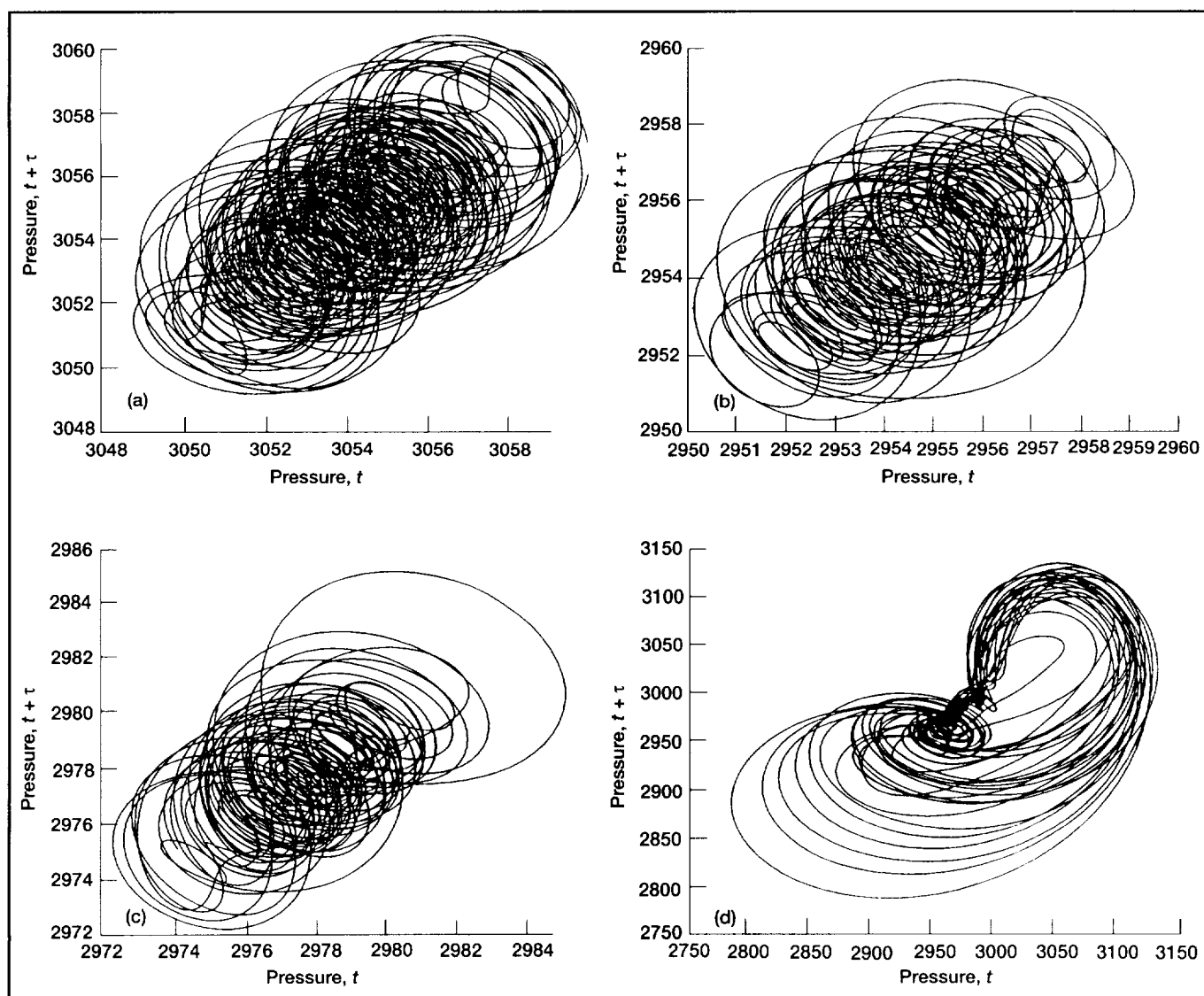
*Setup for Rayleigh scattering measurements in free jet.*

# Chaotic Time Series Analysis Method Developed for Stall Precursor Identification in High-Speed Compressors

A new technique for rotating stall precursor identification in high-speed compressors has been developed at the NASA Lewis Research Center. This pseudocorrelation integral method uses a mathematical algorithm based on chaos theory to identify nonlinear dynamic changes in the compressor. Through a study of four various configurations of a high-speed compressor stage, a multistage compressor rig, and an axi-centrifugal engine test, this algorithm, using only a single pressure sensor, has consistently predicted the onset of rotating stall.

Data for this algorithm have been collected from a single high-frequency-response pressure transducer located one chord length upstream of the rotor and flush mounted in the casing. The pressure signal data are input to

the correlation integral algorithm. The algorithm calculates a phase plane portrait of the pressure data for one window in time. As pressure conditions change in the compressor, specifically through throttle area closing, the algorithm monitors dynamic changes in the phase plane portrait. As the phase portrait shrinks or enlarges, stretches or twists, the correlation integral calculation monitors these changes.



Phase plane portraits of pressure data from a high-speed compressor. (a) Steady phase plane portrait. (b) Phase plane portrait far from stall. (c) Phase plane portrait close to stall. (d) Phase plane portrait in rotating stall.

From calculations performed on four various configurations of a high-speed compressor stage, the data confirm a sharp decrease in the correlation integral prior to the onset of rotating stall.

As an example, the phase plane portraits for a high-speed compressor stage are presented at four operational conditions in the figure. A phase plane portrait displays the pressure data on the  $x$ -axis and a time-delayed version on the  $y$ -axis. Part (a) shows the pressure signal for steady operation of the compressor stage with the throttle fully open. Part (b) shows the phase plane portrait of the compressor with the throttle partially closed, but still far from the stall condition. Part (c) shows the pressure signal very near the stall condition, and part (d) shows the compressor in full rotating stall. The phase plane portraits in parts (a) and (b) are very similar in physical nature, and their correlation integrals are identical. In part (c), the physical nature of the portrait has changed slightly and the correlation integral calculation has decreased. In the rotating stall condition of part (d), the portrait has changed significantly from the previous portraits and the correlation integral has dropped significantly. This decrease in correlation integral prior to rotating stall, which is a precursive signal that rotating stall will occur, is present in all test cases.

To provide a basis for comparison, we applied the traveling wave energy technique (ref. 1), which has been used extensively to study prestall data, to identical data sets (ref. 2). The correlation method was shown to have a potential advantage over the traveling wave energy method because it uses a single sensor for detection and does not require the data to detect changes in the behavior of the compressor. Both methods were used in this study to identify stall precursive events in the pressure fluctuations measured from circumferential pressure transducers located at the front face of the compressor rig. The correlation method successfully identified stall formation or changes in the compressor dynamics from data captured from four different configurations of a NASA Lewis single-stage high-speed compressor while it transitioned from stable operation to stall. The traveling-wave energy technique, which requires eight circumferentially located transducers, was not able to predict the onset of rotating stall for one of the test cases. The experimental results indicate that the correlation method provides warning of the onset of rotating stall at high speed. This method is being expanded into an online diagnostic and prediction tool as part of an integrated active stall control system.

## References

1. Tryfonidis, M., et al.: Prestall Behavior of Several High-Speed Compressors. *J. Turbomachinery*, vol. 117, Jan. 1995, pp. 62–80.
2. Bright, M.M., et al.: Stall Precursor Identification in High Speed Compressor Stages Using Chaotic Time Series Analysis Methods. ASME Paper 96–GT–370, 1996. [Accepted for publication in the *Journal of Turbomachinery*, 1997].

**Lewis contact:** Michelle M. Bright, (216) 433–2304,  
Michelle.M.Bright@lerc.nasa.gov

**Author:** Michelle M. Bright

**Headquarters program office:** OA

# Controls/CFD Interdisciplinary Research Software Generates Low-Order Linear Models for Control Design From Steady-State CFD Results

The NASA Lewis Research Center is developing analytical methods and software tools to create a bridge between the controls and computational fluid dynamics (CFD) disciplines. Traditionally, control design engineers have used coarse nonlinear simulations to generate information for the design of new propulsion system controls. However, such traditional methods are not adequate for modeling the propulsion systems of complex, high-speed vehicles like the High Speed Civil Transport. To properly model the relevant flow physics of high-speed propulsion systems, one must use simulations based on CFD methods. Such CFD simulations have become useful tools for engineers that are designing propulsion system components. The analysis techniques and software being developed as part of this effort (ref. 1) are an attempt to evolve CFD into a useful tool for control design as well.

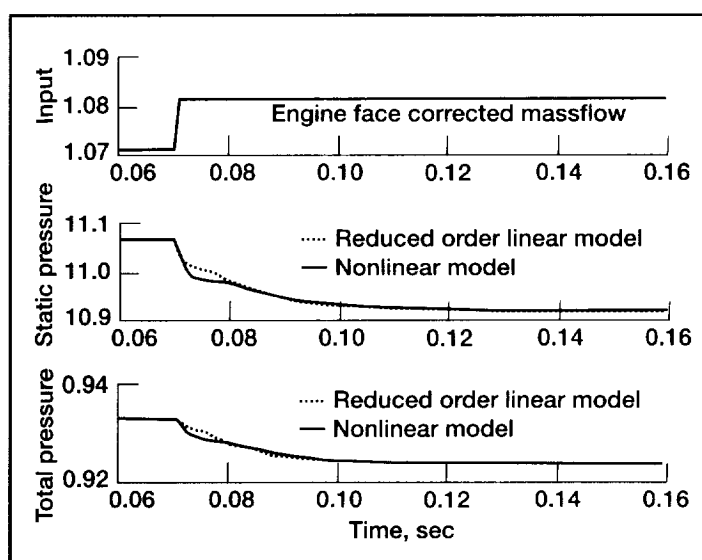
One major aspect of this research is the generation of linear models from steady-state CFD results. CFD simulations, often used during the design of high-speed inlets, yield high-resolution operating point data. Under a NASA grant, the University of Akron has developed analytical techniques and software tools that use these data to generate linear models for control design. The resulting linear models have the same number of states as the original CFD simulation, so they are still very large and computationally cumbersome. Model reduction techniques have been successfully applied to reduce these large linear models by several orders of magnitude without significantly changing the dynamic response. The result is an accurate, easy to use, low-order linear model that takes less time to generate than those generated by traditional means.

The development of methods for generating low-order linear models from steady-state CFD is most complete at the one-dimensional level (ref. 2), where software is available to generate models with different kinds of input and output variables. One-dimensional methods have been extended somewhat so that linear models can also be generated from two- and three-dimensional steady-state results. Standard techniques are adequate for reducing the order of one-dimensional CFD-based linear models. However, reduction of linear models based on two- and three-dimensional CFD results-based models is complicated by very sparse, ill-conditioned matrices. Some novel approaches are being investigated to solve this problem.

Currently available software uses one-dimensional CFD results to generate linear models for a number of different input variables. Upstream input variables can be Mach numbers or static temperatures. Exit plane input variables can be Mach number, static

pressure, or corrected mass flow. Internal input variables can be the massflow rate for bleed or bypass regions. Note that a linear model must be generated for each input variable of interest. Superposition can then be used to combine several linear models into a single multi-input, multi-output linear model. Each linear model can output the Mach number, static pressure, and total pressure for any node in the CFD grid. Furthermore, bounds can be calculated to describe the uncertainty of the model due to linearization and order reduction.

The figure shows how the time response of a reduced-order linear model (with 20 states) compares with the response of the original nonlinear model (with 123 states). The results shown here were generated from a quasi-one-dimensional model of a mixed-compression inlet



*Diffuser pressure response to a 1-percent step in engine face corrected mass flow. Reduced-order linear model response compared with nonlinear model response. Vertical axes show nondimensional values for parameters.*

being developed for the High Speed Civil Transport program. They represent the pressure response at a point in the subsonic diffuser to a 1-percent increase in exit plane corrected mass flow. The strong agreement between the responses of the reduced-order model and those of the nonlinear model increases confidence in the use of the reduced-order model for control design. The linearization process has been identified as the cause of the difference between the transient response of the two models. Current research is focused on improving this process.

**Find out more about this research on the World Wide Web:**

<http://controls.lerc.nasa.gov:8080/projects/cntrlcfd/>

<http://www.lerc.nasa.gov/WWW/IFMD/2620/homepage.html>

**References**

1. Chicatelli, A.K., et al.: Interdisciplinary Modeling Using Computational Fluid Dynamics and Control Theory. Proceedings of the American Control Conference, June 1994, pp. 3438-3443.
2. Chicatelli, A.K.; and Hartley, T.T.: A Method for Generating Reduced Order Linear Models of Supersonic Inlets. NASA CR-198538, 1996.

**Lewis contact:** Kevin J. Melcher, (216) 433-3743, [kmelcher@lerc.nasa.gov](mailto:kmelcher@lerc.nasa.gov)

**Author:** Kevin J. Melcher

**Headquarters program office:** OA (HPCCO)

## Single-Lever Power Control for General Aviation Aircraft Promises Improved Efficiency and Simplified Pilot Controls

General aviation research is leading to major advances in internal combustion engine control systems for single-engine, single-pilot aircraft. These advances promise to increase engine performance and fuel efficiency while substantially reducing pilot workload and increasing flight safety. One such advance is a single-lever power control (SLPC) system, a welcome departure from older, less user-friendly, multilever engine control systems. The benefits of using single-lever power controls for general aviation aircraft are improved flight safety through advanced engine diagnostics, simplified powerplant operations, increased time between overhauls, and cost-effective technology (extends fuel burn and reduces overhaul costs). The single-lever concept has proven to be so effective in preliminary studies that general aviation manufacturers are making plans to retrofit current aircraft with the technology and are incorporating it in designs for future aircraft.

To aid in this effort, nine industry members of the Advanced General Aviation Transport Experiment (AGATE) consortium have teamed together to further develop SLPC technology. This consortium consists of Government, industry, and academia members who are joining forces to revitalize the nation's general aviation sector by designing integrated advanced flight systems that will improve safety and reduce the cost and time for learning to fly. SLPC technology is a vital element of this effort. SLPC team members range from aircraft manufacturers to suppliers, with the propulsion control system specialists at the NASA Lewis Research Center managing the effort.

### How Does a Single Lever Work to Control an Internal Combustion Engine?

A single lever is used in tandem with a digital engine control system known as full-authority digital engine control. The combined system controls engine power on an airplane much like an automobile accelerator provides speed. Movement of the power lever automatically sets the amount of fuel flow, air flow, ignition timing, and propeller pitch to achieve requested thrust levels from the engine and propeller during the takeoff, cruise, and landing phases of flight. The single-lever power control increases fuel efficiency, decreases the time between overhauls, and ensures the best engine/propeller performance for all flight phases. SLPC greatly simplifies engine control in comparison to older

systems—which use a 50-year-old technology and require the use of as many as five levers for power control.

Mechanical versions of single-lever power control were developed 15 years ago for light aircraft engines. However, their implementation was limited because of their complexity and inability to compensate for variations in air density. Later, researchers found that digital computer technology greatly enhances the accuracy and usefulness of the system as standalone equipment or integrated with an advanced cockpit display system. Single-lever power systems are commonly found today on turbine engines that use NASA-developed fly-by-wire digital control technology. This technology is used in present-day, high-performance military jet fighters and commercial transports.

### A New Outlook and the Future

Thanks to the establishment of the AGATE consortium in the spring of 1995, companies are now heavily engaged in single-lever development for light aircraft, working together to eliminate any remaining glitches and to further refine the technology. Work is underway to include engine monitoring and diagnostic capability in the full-authority digital engine control to enhance pilot awareness of engine status during flight and to provide a postflight diagnostic capability.

The team effort has led to reduced development risks and costs, which are shared equally between NASA and industry partners. Pooling of team members' resources and sharing of development costs have also dramatically speeded the development of this technology and are helping to bring new engine controls to market rapidly. SLPC developers plan on developing guidelines, standards, and certification methods for future technology applications. They foresee the day when all general aviation engines will be completely operated by electronic systems, helping to fulfill the broader AGATE vision of creating "highways in the sky."

For additional information, visit the AGATE homepage on the World Wide Web: <http://agate.larc.nasa.gov>

And write for *The AGATE Flier*, vol. II, issue 1, May 1996:  
c/o Office of Communications, RTI  
P.O. Box 12194  
Research Triangle Park, NC  
27709-2194

**Lewis contact:**  
Jeffrey L. Musgrave, (216) 433-6472,  
[Jeffrey.Musgrave@lerc.nasa.gov](mailto:Jeffrey.Musgrave@lerc.nasa.gov)  
**Author:** Jeffrey L. Musgrave  
**Headquarters program office:** OA

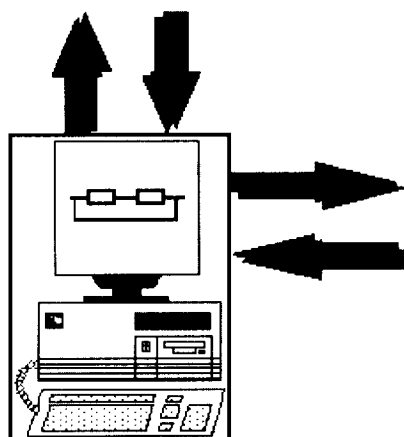


(Courtesy of JetStream Catalog.)

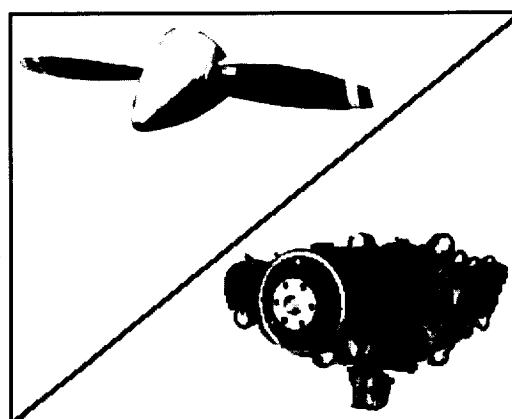
### Advantages of a Single Lever

The benefits of using single lever power controls for general aviation aircraft are

- Improved flight safety through advanced engine diagnostics
- Simplified powerplant operations
- Increased time between overhauls
- Cost-effective technology (increases fuel efficiency and reduces overhaul costs)



Pilot inputs are processed by the engine control system, which regulates engine rpm, mixture ratio, ignition timing, and fuel flow.



General aviation engine and propeller.

*Movement of the single lever automatically controls engine thrust levels.*

# Internal Fluid Mechanics

## National Combustion Code: A Multidisciplinary Combustor Design System

The Internal Fluid Mechanics Division conducts both basic research and technology, and system technology research for aerospace propulsion systems components. The research within the division, which is both computational and experimental, is aimed at improving fundamental understanding of flow physics in inlets, ducts, nozzles, turbomachinery, and combustors. This article and the following three articles highlight some of the work accomplished in 1996.

A multidisciplinary combustor design system is critical for optimizing the combustor design process. Such a system should include sophisticated computer-aided design (CAD) tools for geometry creation, advanced mesh generators for creating solid model representations, a common framework for fluid flow and structural analyses, modern postprocessing tools, and parallel processing. The goal of the present effort is to develop some of the enabling technologies and to demonstrate their overall performance in an integrated system called the National Combustion Code.

The development of the National Combustion Code is currently being pursued under a NASA/Department of Defense/Department of Energy/U.S. industry partnership. Recent efforts have been focused on developing a computational combustion dynamics capability that meets combustor designer requirements for model accuracy and analysis turnaround time, incorporating both short-term and long-term technology goals. As a first step, a baseline solver for turbulent combustion flows, CORSAIR-CCD, was developed under a joint modeling and code development effort between Pratt & Whitney and the NASA Lewis Research Center. CORSAIR-CCD is a Navier-Stokes flow solver based on an explicit four-stage Runge-Kutta scheme that uses unstructured meshes and runs on networked workstations. The solver can be linked to any computer-aided design system via the Patran file system. Turbulence closure is obtained via the standard  $k-\epsilon$  model with a high Reynolds number wall function. The following combustion models have been implemented into the code: finite-rate chemical kinetics emulations for Jet-A and methane fuels, turbulence-chemistry interactions via an assumed probability density function for temperature fluctuations, and thermal emissions of nitrogen oxides. CORSAIR-CCD can switch between a parallel virtual machine (PVM) interface and a message-passing interface (MPI) by using compiler flags. Its parallel performance on several platforms has been analyzed, and on the basis of the results, several improvements have been made.

**Lewis contact:** Dr. Robert M. Stubbs, (216) 433-6303,  
Robert.M.Stubbs@lerc.nasa.gov

**Authors:** Dr. Nan-Suey Liu and Dr. Robert M. Stubbs

**Headquarters program office:** OA



## Interactive Educational Tool for Turbofan and Afterburning Turbojet Engines

A workstation-based, interactive educational computer program has been developed at the NASA Lewis Research Center to aid in the teaching and understanding of turbine engine design and analysis. This tool has recently been extended to model the performance of two-spool turbofans and afterburning turbojets. The program solves for the flow conditions through the engine by using classical one-dimensional thermodynamic analysis found in various propulsion textbooks. Either an approximately thermally perfect or calorically perfect gas can be used in the thermodynamic analysis. Students can vary the design conditions through a graphical user interface; engine performance is calculated immediately. A variety of graphical formats are used to present results, including numerical results, moving bar charts, and student-generated temperature versus entropy ( $T$ - $s$ ), pressure versus specific volume ( $p$ - $v$ ), and engine performance plots. The package includes user-controlled printed output, restart capability, online help screens, and a browser that displays teacher-prepared lessons in turbomachinery. The program runs on a variety of workstations or a personal computer using the UNIX operating system and X-based graphics. It is being tested at several universities in the midwestern United States; the source and executables are available free from the author.

**Lewis contact:** Thomas J. Benson, (216) 433-5920, Thomas.J.Benson@lerc.nasa.gov

**Author:** Thomas J. Benson

**Headquarters program office:** OA

## Rotor-Stator Interaction Performance Effects

Decreased axial spacing between blade rows in an axial compressor stage is thought to increase stage performance because of an unsteady process that occurs in the downstream blade row and acts on the upstream blade row wakes. This process results in the "recovery" of part of the wake energy before all of this energy is irreversibly lost due to viscous diffusion. To study the wake-blade interaction mechanism, researchers at the NASA Lewis Research Center acquired two-component Laser Fringe Anemometer measurements of the rotor wake in the single-stage transonic compressor at two stage loading levels. The detailed measurements were acquired for one stator pitch in circumference at axial positions from the rotor trailing edge to 20 percent of the stator axial chord, at the exit of the stator passage, and downstream of the stator row including the stator wake. These data show that the changes in wake energy that occur inside the stator passage are not due to viscous dissipation alone, and thus the data provide evidence that "wake recovery" is occurring.

A time-accurate, three-dimensional Navier Stokes simulation of the compressor stator was done at the corresponding stage loading levels. The measurements and simulations are being used in combination to show the effects of stator blade loading, quantify the effects of viscosity, and quantify the stage efficiency gain due to the wake recovery process. The accuracy of

simple models of the wake recovery process is being evaluated in an effort to include the effects of wake recovery in the NASA-developed Average Passage code for multi-stage turbomachinery simulations.

**Lewis contact:**

Dale E. Van Zante, (216) 433-3640,

Dale.E.VanZante@lerc.nasa.gov

**Author:** Dale E. Van Zante

**Headquarters program office:** OA

# Stator Indexing in Multistage Compressors

The relative circumferential location of stator rows (stator indexing) is an aspect of multistage compressor design that has not yet been explored for its potential impact on compressor aerodynamic performance. Although the inlet stages of multistage compressors usually have differing stator blade counts, the aft stages of core compressors can often have stage blocks with equal stator blade counts in successive stages. The potential impact of stator indexing is likely greatest in these stages. To assess the performance impact of stator indexing, researchers at the NASA Lewis Research Center used the 4-ft-diameter, four-stage NASA Low Speed Axial Compressor for detailed experiments. This compressor has geometrically identical stages that can circumferentially index stator rows relative to each other in a controlled manner; thus it is an ideal test rig for such investigations.

Measurements were made to first determine the indexing pattern that would result in the wakes of each stator impacting the leading edge of the adjacent downstream stators. This pattern served as the initial indexing configuration from which detailed performance measurements were then acquired as a function of stator indexing at peak efficiency and peak pressure operating conditions. These performance measurements showed that stator indexing had a small but measurable effect on performance. For the stator indexing configurations corresponding to the maximum and minimum performance at each operating condition, areas upstream and downstream of the third-stage blade rows were traversed in detail to assess the effects of stator indexing on blade element performance parameters. Finally, for a given stator indexing configuration, blade element performance was measured across two different stator blade passages to assess the level of passage-to-passage performance differences. Results indicate that the measured performance differences due to manufacturing and assembly tolerances are of the same order as those due to stator indexing, which further indicates that stator indexing has a small impact on performance.

**Lewis contact:** Wendy S. Barankiewicz, (216) 433-8706,  
Wendy.S.Barankiewicz@lerc.nasa.gov  
**Author:** Wendy S. Barankiewicz  
**Headquarters program office:** OA

## Bleed Hole Flow Phenomena Studied

Boundary-layer bleed is an invaluable tool for controlling the airflow in supersonic aircraft engine inlets. Incoming air is decelerated to subsonic speeds prior to entering the compressor via a series of oblique shocks. The low momentum flow in the boundary layer interacts with these shocks, growing in thickness and, under some conditions, leading to flow separation. To remedy this, bleed holes are strategically located to remove mass from the boundary layer, reducing its thickness and helping to maintain uniform flow to the compressor. The bleed requirements for any inlet design are unique and must be validated by extensive wind tunnel testing to optimize performance and efficiency.

To accelerate this process and reduce cost, researchers at the NASA Lewis Research Center initiated an experimental program to study the flow phenomena associated with bleed holes. Knowledge of these flow properties will be incorporated into computational fluid dynamics (CFD) models that will aid engine inlet designers in optimizing bleed configurations before any hardware is fabricated. This ongoing investigation is currently examining two hole geometries,  $90^\circ$  and  $20^\circ$  (both with 5-mm diameters), and various flow features (see the figure below):

- The shock structure in and around the hole
- Multihole interaction
- Slant hole flow misalignment
- Orifice scaling relative to the boundary layer thickness
- Flow separation inside the bleed orifice
- The vortex structure around the hole

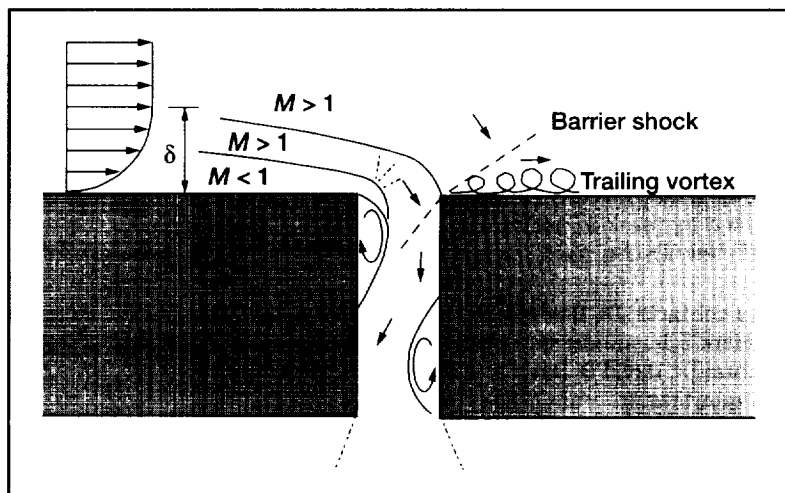
The tests are being conducted in NASA Lewis' 15- by 15-Centimeter Supersonic Wind Tunnel, which is an open-loop, continuous-flow facility. Mach number variation is provided by interchangeable, fixed-geometry nozzle blocks. The tunnel can be run subsonically from Mach 0.2 to 0.8, and supersonically at discrete Mach numbers of 1.67, 2.0, 2.5, and 3.0.

To date, several of these areas have been investigated. For both  $90^\circ$  and  $20^\circ$  holes, pitot and five-hole probe surveys downstream of single bleed holes revealed an oblique barrier shock originating from the back lip of the hole. Pressure sensitive paint applied to the wall indicated flow expansion and compression regions in the vicinity of these orifices (see the figure on the facing page).

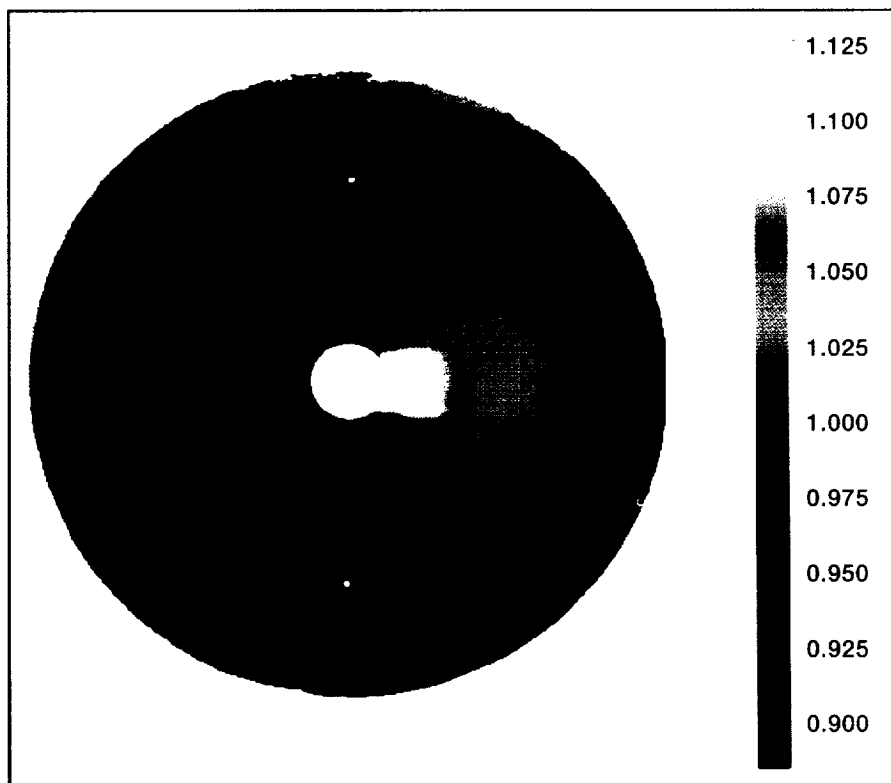
For the  $20^\circ$  hole, alignment with the local flow direction was found to be critical for supersonic Mach numbers. The misalignment of a slanted hole fabricated in a rotatable plug was varied between  $0^\circ$  and  $30^\circ$  at Mach numbers of 0.60, 1.67, and 2.50. For each angle, a mass flow survey was taken for plenum pressures varying between full bleed and no bleed. It was found that at Mach 2.50 as little

as one degree of flow misalignment resulted in a drop in mass flow through the orifice. The lower Mach number test showed similar behavior; however, mass flow hindrance proved less severe.

In inlet applications, holes are arranged in fields, each on the order of two to three diameters away from neighboring holes, so a two-hole interaction for this type of arrangement was studied. Two  $90^\circ$  holes with the rotatable plug geometry were located two diameters from each other: one hole was at the center of the plug and the other was offset from the center. The plug was then rotated between  $0^\circ$  (holes lie in a plane normal to the flow direction) and  $90^\circ$  (holes lie in a plane parallel to the flow direction). Mass flow surveys were again taken for each angle. As with the  $20^\circ$  misalignment experiment, sensitivity to location increased with Mach number. However, although shallow orientations resulted in a drop in the flow coefficient, at angles above  $50^\circ$ , the flow coefficient improved. This shows the potential for multihole



Flow in the vicinity of a  $90^\circ$  bleed hole. Boundary layer thickness,  $\delta$ .



*Normalized surface pressure ( $P_w/P_{w,0}$ ) at Mach 2.5 in the vicinity of a 90° bleed hole.*

configurations to exhibit more efficient bleed properties than their single-hole counterparts.

Continuing research is being conducted to study various other phenomena. As air enters a 90° hole, it separates from the hole wall, creating a blockage throat that hinders the hole's performance. Flow-visualization experiments using oil trace techniques verified this feature; however, flow-field measurements in the hole are yet to be recorded. Surveys of the trailing vortices created by bleed holes are also planned, as well as studies of the problems and benefits of bleed hole scaling.

### **Bibliography**

Bodner, J.P.; and Greber, I.: Experimental Investigation of the Effect of a Single Bleed Hole on a Turbulent Supersonic Boundary-Layer. AIAA Paper 96-2797, 1996.

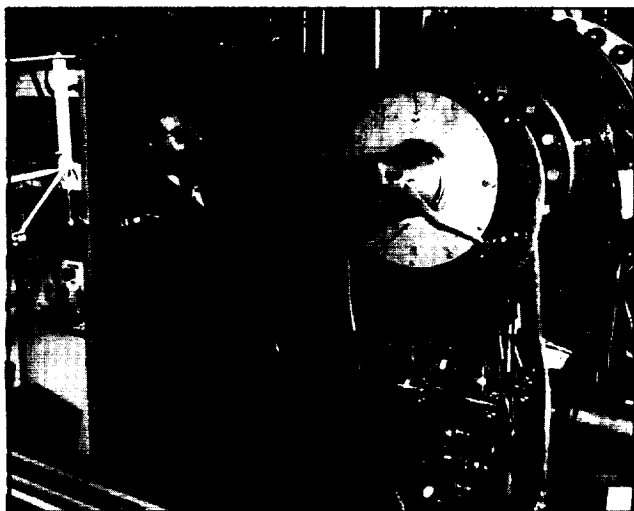
Davis, D.O.; Grimes, M.; and Schoenenberger, M.: Effect of Flow Misalignment and Multi-Hole Interaction on Boundary-Layer Bleed Hole Flow Coefficient Behavior. Prepared for the 1996 International Mechanical Engineering Congress and Exhibit, ASME, Nov. 17-24, 1996.

**Lewis contacts:** Dr. David O. Davis, (216) 433-8116, David.O.Davis@lerc.nasa.gov; and Mark Schoenenberger, (216) 433-5905, Mark.Schoenenberger@lerc.nasa.gov

**Authors:** Dr. David O. Davis and Mark Schoenenberger

**Headquarters program office:** OA

# Internal Mixing Studied for GE/ARL Ejector Nozzle



Mixer-ejector nozzle mounted on the jet facility.

reduce the jet velocity and, hence, the jet noise. It is desirable to mix the two streams as fast as possible in order to minimize the length and weight of the ejector.

An earlier model of the mixer-ejector nozzle was tested extensively in the Aerodynamic Research Laboratory (ARL) of GE Aircraft Engines at Cincinnati, Ohio. While testing was continuing with later generations of the nozzle, the earlier model was brought to the NASA Lewis Research Center for relatively fundamental measurements. Goals of the Lewis study were to obtain details of the flow field to aid computational fluid dynamics (CFD) efforts and obtain a better understanding of the flow mechanisms, as well as to experiment with mixing enhancement devices, such as tabs. The measurements were made in an open jet facility for cold (unheated) flow without a surrounding coflowing stream. The photo shows the experimental setup. Distributions of streamwise vorticity as well as turbulent stresses were obtained using hot-wire anemometry for a low nozzle pressure ratio. Pitot probe surveys were conducted for higher nozzle pressure ratios.

The figure shows the mean velocity distribution inside the ejector. The outline of the interior of the ejector is shown for reference. The distribution exhibits a cellular pattern because of varying velocities through the primary and secondary chutes. Corresponding streamwise vorticity data show that pairs of counter-rotating vortices

To achieve jet noise reduction goals for the High Speed Civil Transport aircraft, researchers have been investigating the mixer-ejector nozzle concept. For this concept, a primary nozzle with multiple chutes is surrounded by an ejector. The ejector mixes low-momentum ambient air with the hot engine exhaust to

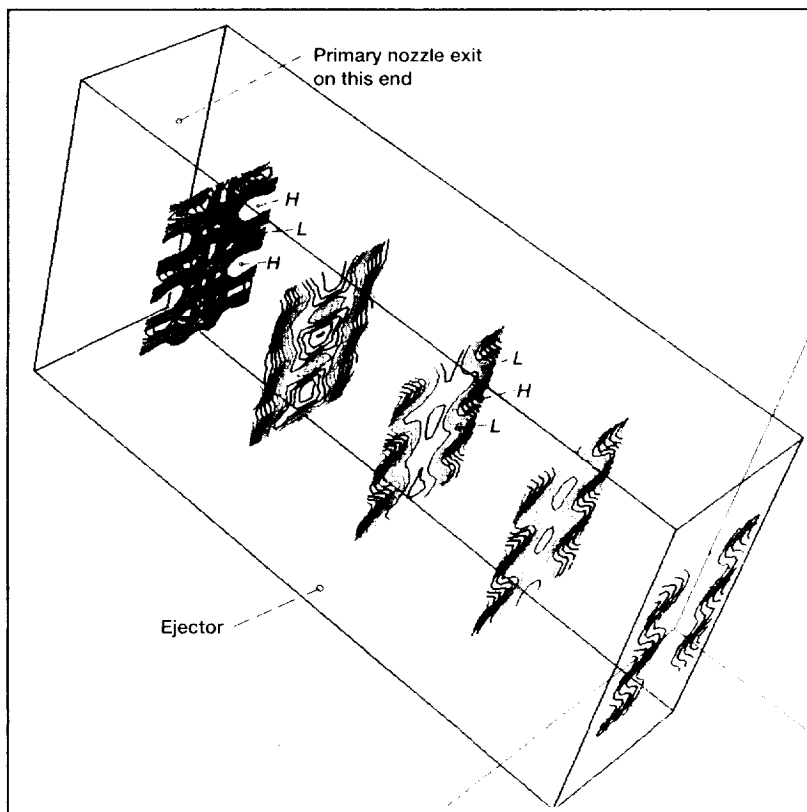
originate from the chutes and persist over the entire length of the ejector. The velocity distributions also reveal, with increasing downstream distance, an interchanging of low-velocity regions (marked with an *L*) with adjacent high-velocity regions (marked with an *H*). This occurs because of the action of the streamwise vortices as fluid is continually transported laterally by the vortex pairs. Although the data shown are for a low-pressure ratio, corresponding distributions at higher pressure ratios exhibit a similar behavior, in some cases, with the interchanging occurring more than once within the ejector.

#### Lewis contact:

Dr. Khairul B. Zaman, (216) 433-5888,  
Khairul.B.Zaman@lerc.nasa.gov

**Author:** Dr. Khairul Zaman

**Headquarters program office:** OA



Mean velocity distribution within the ejector.

# Propulsion Systems

## High-Pressure Combustion Testing Reveals Promise of Low-Emission Combustors for Advanced Subsonic Gas Turbines

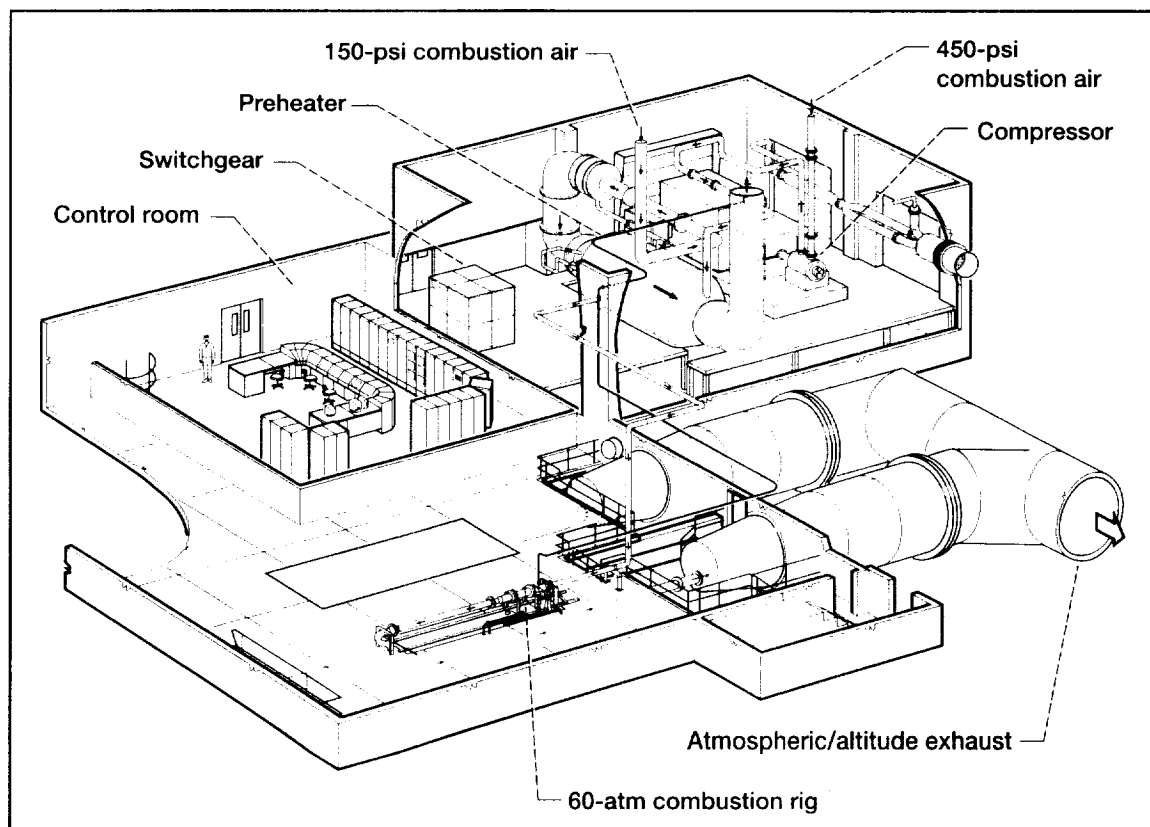
NASA Lewis Research Center's new, world-class, 60-atm combustor research facility, the Advanced Subsonic Combustion Rig (ASCR), is in operation and producing highly unique research data. At operating pressures to 800 psia, emissions of nitrogen oxides were reduced by greater than 70 percent with an advanced fuel injector designed at NASA Lewis. Data, including exhaust emissions and pressure and temperature distributions, were acquired at high pressures and temperatures representative of future subsonic engines. Results to date represent an improved understanding of the formation of nitrogen oxides at these high pressures (twice the pressure of previous combustor tests) and temperatures.

For greater fuel efficiency and performance, future aircraft jet engines will run at higher pressures. This will require new combustor designs to keep the nitrogen oxide and carbon monoxide emissions at environmentally acceptable levels.

To verify the emissions characteristics of gas turbine engines, researchers must duplicate the actual pressures and temperatures found in gas turbine

combustors in a laboratory environment. Recognizing this, the U.S. aircraft gas turbine industry identified a need for a national facility that could duplicate the severe inlet conditions of future combustors.

Because of NASA Lewis' expertise in combustion emissions reduction research and in the design and operation of high-pressure test facilities, the Center was seen as the natural location for such a facility. In addition, as a national laboratory, Lewis could provide these facilities to all U.S. gas turbine engine manufacturers while protecting their proprietary interests.



*Advanced Subsonic Combustion Rig at the NASA Lewis Research Center.*

The Advanced Subsonic Combustion Rig (see the figure) provides pressures to 60 atm at inlet temperatures to 1300 °F and air flow rates up to 38 lb/sec. This represents a doubling of the pressure capability for combustion testing at Lewis and provides a unique continuous flow facility for the nation. Furthermore, the facility offers state-of-the-art diagnostic methods for characterizing advanced combustor concepts.

Lewis continues to work closely with the gas turbine industry so that this low-emissions combustor technology is successfully transferred into engine prototype hardware. Complementary tests in Lewis' currently available 30-atm test facilities are also underway, taking advantage of Lewis' unique laser diagnostic capabilities. After potential combustor concepts are screened in the 30-atm facilities (which simulate aircraft cruise conditions), the most promising will undergo further testing at actual takeoff and advanced cycle cruise conditions in the new 60-atm rig. Utilization of these test facilities and the expertise of both NASA and its industry partners will enable multiple combustor concepts to be conceived and developed in a shorter period of time, bringing new and better low-emission combustors to market sooner. Research performed in the Advanced Subsonic Combustion Rig will make it possible for U.S. engine manufacturers to produce environmentally superior commercial engines, enabling them to compete on a worldwide basis.

**Find out more about the Advanced Subsonic Combustion Rig on the World Wide Web:**

<http://www.lerc.nasa.gov/WWW/AST/propulsion.htm#ascr>

**Lewis contact:**

Dr. Valerie J. Lyons, (216) 433-5970,  
Valerie.J.Lyons@lerc.nasa.gov

**Author:** Dr. Valerie J. Lyons

**Headquarters program office:** OA

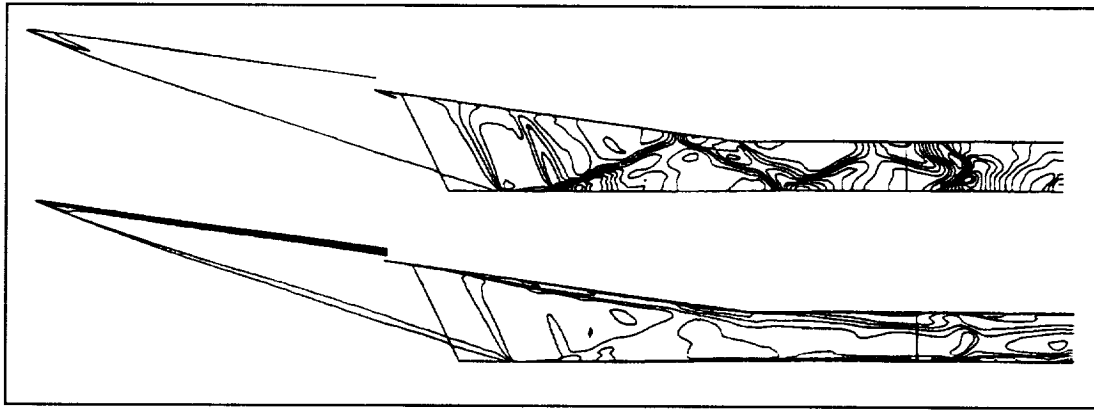
## Computational Fluid Dynamics Analysis Method Developed for Rocket-Based Combined Cycle Engine Inlet

Renewed interest in hypersonic propulsion systems has led to research programs investigating combined cycle engines that are designed to operate efficiently across the flight regime. The Rocket-Based Combined Cycle Engine is a propulsion system under development at the NASA Lewis Research Center. This engine integrates a high specific impulse, low thrust-to-weight, airbreathing engine with a low-impulse, high thrust-to-weight rocket. From takeoff to Mach 2.5, the engine operates as an air-augmented rocket. At Mach 2.5, the engine becomes a dual-mode ramjet; and beyond Mach 8, the rocket is turned back on. One Rocket-Based Combined Cycle Engine variation known as the "Strut-Jet" concept is being investigated jointly by NASA Lewis, the U.S. Air Force, Gencorp Aerojet, General Applied Science Labs (GASL), and Lockheed Martin Corporation. Work thus far has included wind tunnel experiments and computational fluid dynamics (CFD) investigations with the NPARC code.

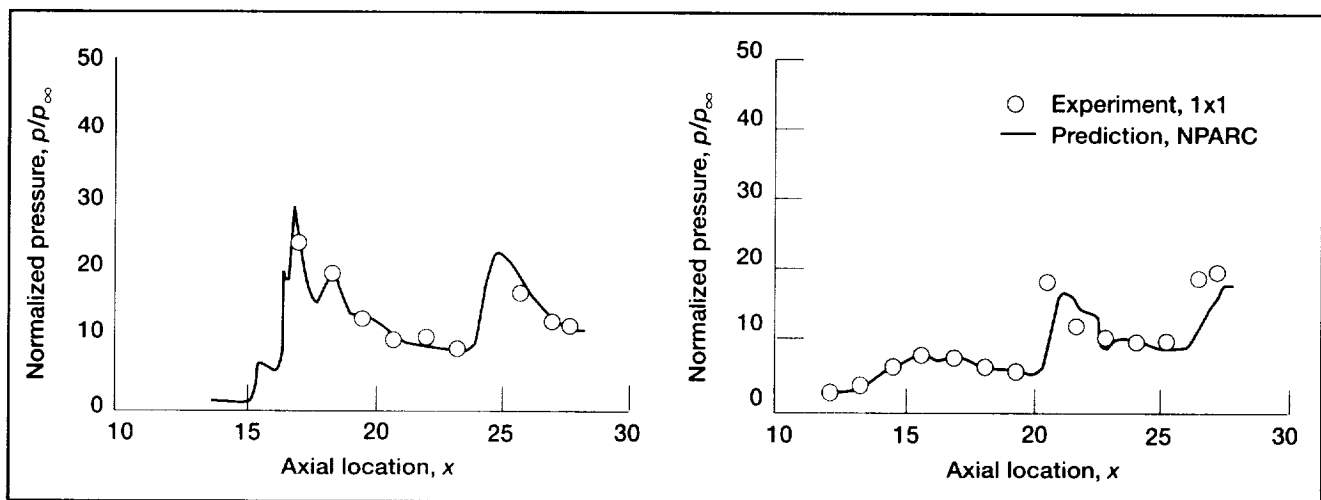
The CFD method was initiated by modeling the geometry of the Strut-Jet with the GRIDGEN structured grid generator. Grids representing a subscale inlet model and the full-scale demonstrator geometry were constructed. These grids modeled one-half of the symmetric inlet flow path, including the precompression plate, diverter, center duct, side duct, and combustor. After the grid generation, full Navier-Stokes flow simulations were conducted with the NPARC Navier-Stokes code. The Chien low-Reynolds-number  $k-\epsilon$  turbulence model was employed to simulate the high-speed

turbulent flow. Finally, the CFD solutions were postprocessed with a Fortran code. This code provided wall static pressure distributions, pitot pressure distributions, mass flow rates, and internal drag. These results were compared with experimental data from a subscale inlet test for code validation; then they were used to help evaluate the demonstrator engine net thrust.

The top contour plot shows contours of static pressure on the inlet centerplane of the subscale inlet. These contours indicate a series of strong oblique shocks initiated by the precompression plate. Mach number contours in the bottom contour plot indicate a large region of low-speed flow along the body side of the inlet resulting from a shock-induced boundary layer



Subscale inlet pressure ( $p/p_\infty$ ) and Mach number contours for a supercritical flow of  $M_\infty = 5$ . Top: pressure contour ranges of 1.4 to 32.2. Bottom: Mach number contour ranges of 0.2 to 5.0.



Subscale inlet pressure ( $p/p_\infty$ ) distribution for a supercritical flow of  $M_\infty = 5$  in the NASA Lewis 1- by 1-Foot Supersonic Wind Tunnel (1x1). Left: Cowl centerline. Right: Body centerline.

separation. The graphs compare the static pressures obtained from the NPARC code to experimental measurements made in NASA Lewis' 1- by 1-Foot Supersonic Wind Tunnel. Very good agreement is observed for the pressures along the cowl and body centerline.

After good agreement was observed between the CFD solutions and subscale wind tunnel experimental data, the NPARC code was applied to the demonstrator engine to provide pretest predictions. Pressure distributions and internal drag force calculations were obtained to guide the demonstrator engine tests. The CFD method developed here (including grid generation, flow computation, and postprocessing) will allow for analyses of future combined-cycle engine concepts.

**For more information about the NPARC Alliance, visit their site on the World**

**Wide Web:** <http://info.arnold.af.mil/nparc/>

### Bibliography

DeBonis, J.R.; and Yungster, S.: Rocket-Based Combined Cycle Engine Technology Development: Inlet CFD Validation and Application. AIAA Paper 96-3145 (Also NASA TM-107274), 1996.

**Lewis contacts:** James R. DeBonis, (216) 433-6581, [James.R.DeBonis@lerc.nasa.gov](mailto:James.R.DeBonis@lerc.nasa.gov); and Nicholas J. Georgiadis, (216) 433-3958, [Nicholas.J.Georgiadis@lerc.nasa.gov](mailto:Nicholas.J.Georgiadis@lerc.nasa.gov)  
**Author:** James R. DeBonis  
**Headquarters program office:** OA



## Fluidic Injection for Throat-Area Control and Thrust Vectoring

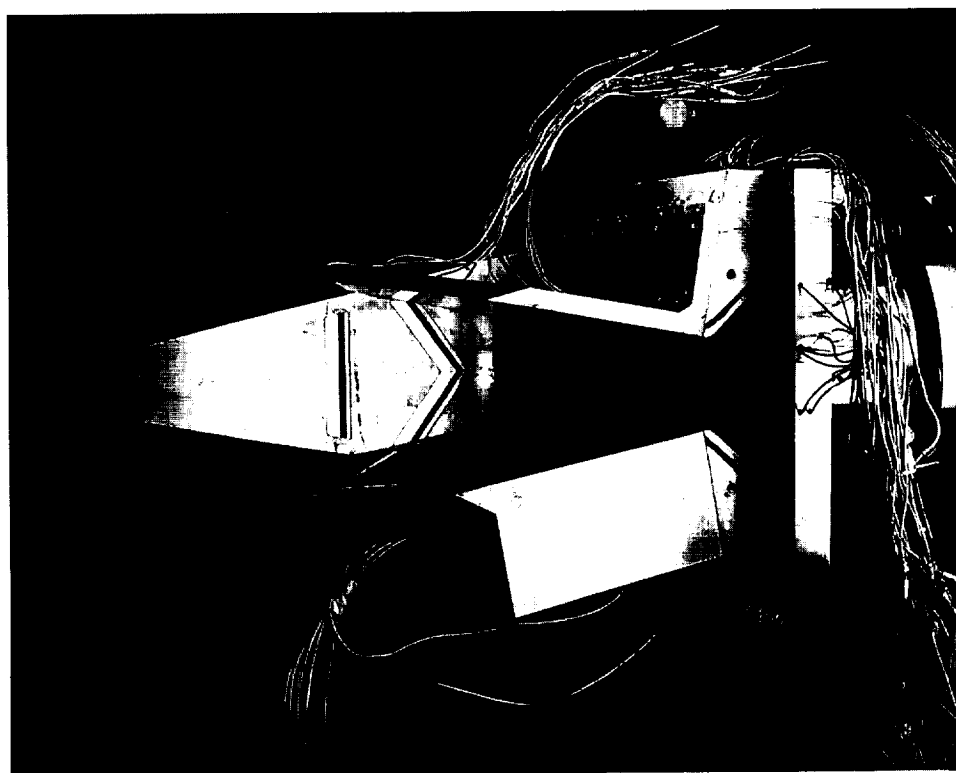
The Fluidic Injection Nozzle Technology program is a national cooperative effort to develop fluidic area control and thrust vectoring concepts for advanced exhaust systems. Exhaust nozzles with vector flow capability will increase the maneuverability and survivability of future fighter aircraft. Currently used mechanical vectoring and area-control systems add weight and complexity to aircraft exhaust systems. With the use of fluidic injection, area-control and vectoring can be achieved without the added weight penalty. Under this program, the NASA Lewis Research Center entered into a cooperative test program with Pratt & Whitney to study the performance of the F119 nozzle with fluidic injection. Our area of interest was to measure flow and thrust coefficients, throat-area reduction, and vector angles.

This experimental program was successfully completed in January 1996 in Lewis' CE-22 facility. Various nozzle throat areas and expansion ratios were tested over a wide range of nozzle pressure ratios. Other model configurations included different injection locations at different injection angles. Results confirmed that fluidic injection is feasible in throat-area reduction and in vectoring. The data obtained from this test program were added to the current database, which can then be used to validate any future performance prediction methodology and computational fluid dynamics (CFD) analysis.

**Lewis contact:** David W. Lam, (216) 433-8875, David.W.Lam@lerc.nasa.gov

**Author:** David W. Lam

**Headquarters program office:** OA



*F119 model with injection slots mounted in CE-22 facility.*

# Oscillating Cascade Aerodynamics at Large Mean Incidence Angles

In a cooperative program with Pratt & Whitney, researchers obtained fundamental separated flow unsteady aerodynamic data in the NASA Lewis Research Center's Oscillating Cascade. These data fill a void that has hindered the understanding and prediction of subsonic and transonic stall flutter. For small-amplitude torsional oscillations, unsteady pressure distributions were measured on airfoils with cross sections representative of an advanced, low-aspect-ratio fan blade. Data were obtained for two mean incidence angles with a subsonic inflow. At high mean incidence angles ( $\alpha = 10^\circ$ ), the mean flow separated at the leading edge and reattached at about 40 percent of the chord. For comparison purposes, data were also obtained for a low incidence angle ( $\alpha = 0^\circ$ ) attached flow.

The figure shows the effects of incidence angle and reduced frequency on the chordwise distribution of the unsteady aerodynamic work per cycle for both the separated and attached flows. Where the high incidence angle flow was separated (from the leading edge to about 40 percent of the chord), the unsteady data are dramatically different. Very near the leading edge, the detached flows have a strongly destabilizing influence but the attached flows are strongly stabilizing. At about 15 percent of the chord, the two sets of curves cross over, with the detached flow becoming stabilizing and the attached flow becoming destabilizing. Beyond the reattachment point, differences in the data are much less dramatic.

## Bibliography

Buffum, D.H., et al.: Oscillating Cascade Aerodynamics at Large Mean Incidence. NASA TM-107247, 1996.

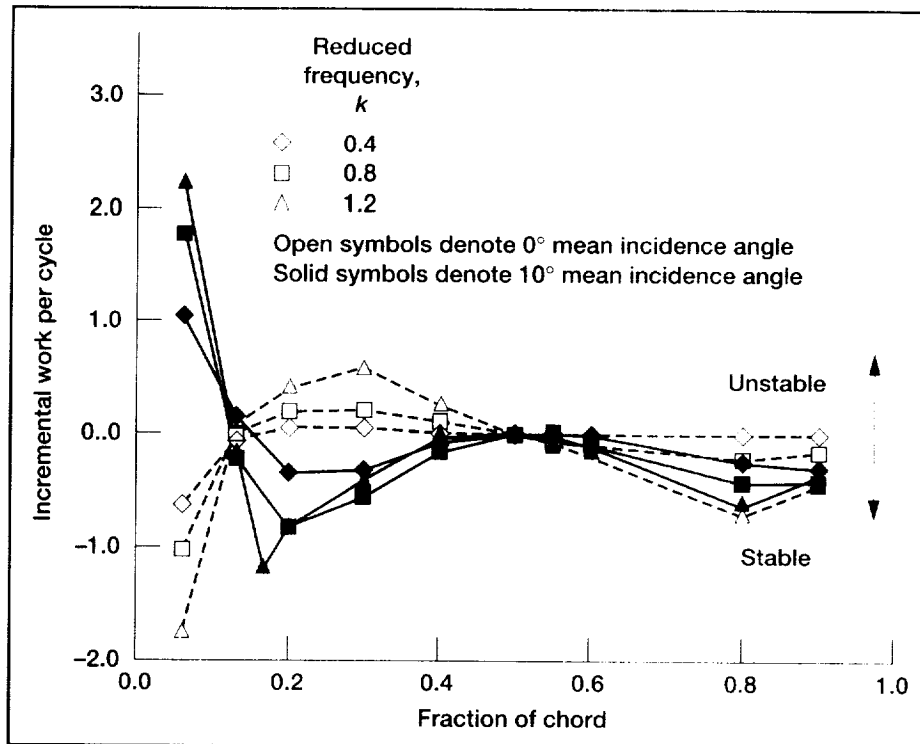
Buffum, D.H., et al.: Experimental Investigation of Unsteady Flows at Large Incidence Angles in a Linear Oscillating Cascade. AIAA Paper 96-2823 (Also NASA TM-107283), 1996.

## Lewis contact:

Dr. Daniel H. Buffum, (216) 433-3759,  
Daniel.H.Buffum@lerc.nasa.gov

**Author:** Dr. Daniel H. Buffum

**Headquarters program office:** OA



Chordwise distribution of unsteady aerodynamic work per cycle at Mach 0.5 and an interblade phase angle,  $\beta$ , of  $180^\circ$ .

# SWIFT: Multistage Turbomachinery Analysis Code Developed



*Space Shuttle Main Engine two-stage fuel turbine pressure contours.*

A new turbomachinery analysis code called SWIFT has been developed at the NASA Lewis Research Center. SWIFT solves thin-layer Navier-Stokes equations with the Baldwin-Lomax turbulence model and an explicit finite-difference scheme. Preconditioning allows the code to be used for all speed ranges, from incompressible to supersonic flows. Multiblock capability allows three types of grids to be patched together to simulate many types of turbomachinery geometries, including hub and tip clearances. In addition, code users can analyze multistage turbomachinery by using a steady averaging-plane approach. This approach uses linearized characteristic boundary conditions to pass information accurately between the stages.

SWIFT has been validated for an isolated transonic compressor rotor and used to look at tip clearance flows in detail (ref. 1). The code has recently been validated for the two-stage Space Shuttle Main Engine fuel turbine. For these calculations, a seven-block grid with just over one million grid points was used. The calculations required about 4 hours of CPU time on the Cray C-90 computer at the NASA Ames Research Center, but they can be run overnight on a fast workstation. The figure shows contours of surface pressure on the four turbine blade rows. Tip clearances were modeled for the rotors, and the tip pressure distributions can be seen. Computed pressure distributions compare well with experimental data on the stators at midspan and on the endwalls. Computed values of surface heat transfer also compare reasonably well with experimental data on the stators and first rotor.

## Reference

1. Chima, R.V.: Calculation of Tip Clearance Effects in a Transonic Compressor Rotor. ASME Paper GT-114 (Also NASA TM-107216), 1996.

## Lewis contact:

Dr. Rodrick V. Chima, (216) 433-5919,  
Rodrick.V.Chima@lerc.nasa.gov

**Author:** Dr. Rodrick V. Chima

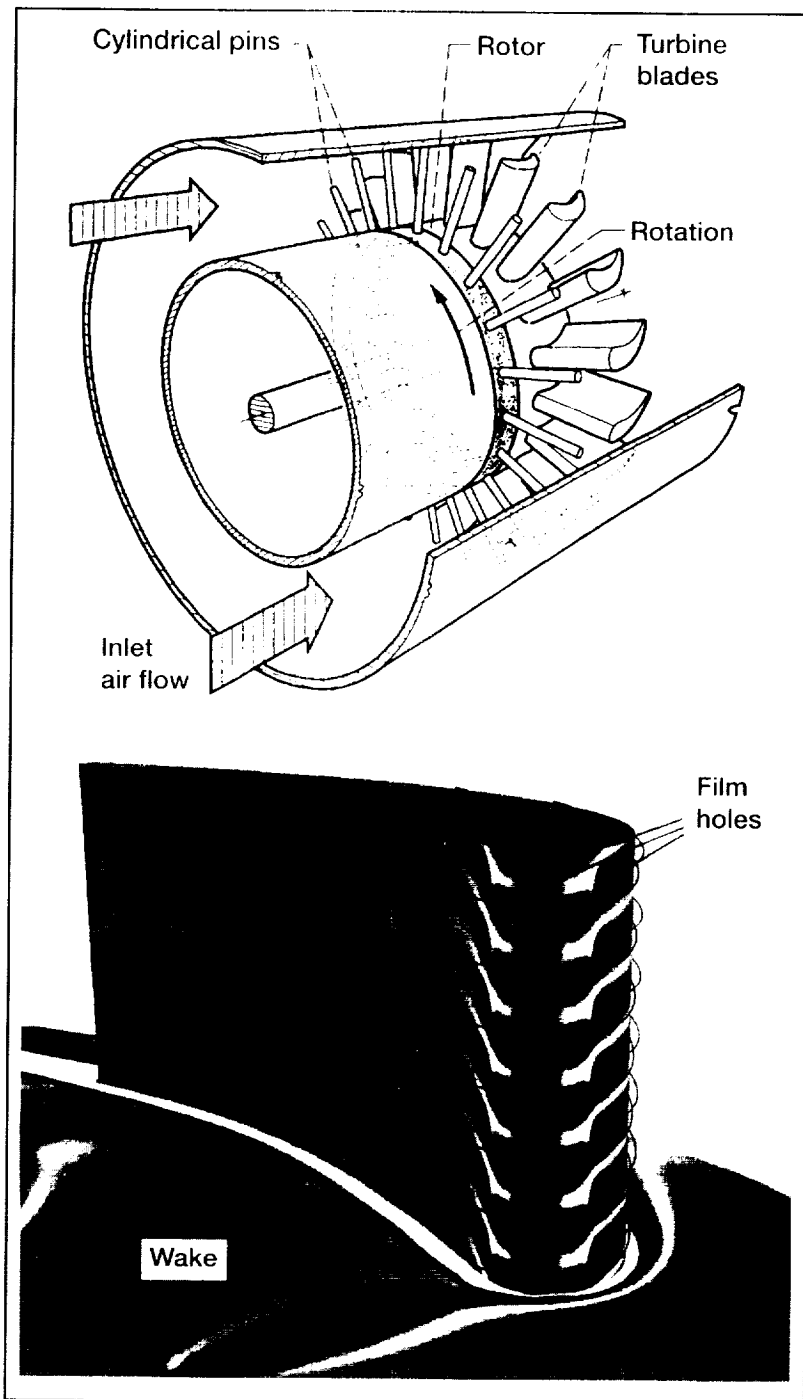
**Headquarters program office:** OA

# Effects of Rotor Wake on Film Cooling Investigated

Through a combination of experimental and computational studies, researchers at the NASA Lewis Research Center investigated the effect of upstream blade-row wake passing on the showerhead (leading edge) film cooling of a downstream turbine. The experiments were performed in a steady-flow annular turbine cascade facility equipped with an upstream rotating row of cylindrical rods to produce a periodic wake field similar to that found in an actual turbine. Spanwise, chordwise, and temporal resolution of the blade surface temperature were achieved through the use of an array of nickel thin-film surface gauges covering one unit cell of a showerhead film hole pattern. Film effectiveness and Nusselt numbers were determined for a test matrix of various injectants, injectant blowing ratios, and wake Strouhal numbers ( $St$ ).

Results indicate a demonstrable reduction in film effectiveness with increasing Strouhal number, as well as the expected increase in film effectiveness with blowing ratio. An equation was developed to correlate the span-average film effectiveness data. The primary effect of wake unsteadiness was found to be correlated well by a chordwise-constant decrement of  $0.094 St$ . Measurable spanwise film effectiveness variations were found near the showerhead region, but meaningful unsteady variations and downstream spanwise variations were not found. Nusselt numbers were less sensitive to wake and injection changes.

Computations were performed with a three-dimensional turbulent Navier-Stokes code that had been modified to model wake passing and film cooling. Unsteady computations were found to agree well with steady computations when the proper time-average blowing ratio and pressure/suction surface flow split were matched. The remaining differences were found to be due to enhanced mixing in the unsteady solution caused by the wake sweeping normally on the pressure surface. Steady computations were found to be in excellent agreement with experimental Nusselt numbers but to overpredict experimental film effectiveness values. This is likely due to the inability of the code to match actual hole exit-velocity profiles and the absence of a credible turbulence model for film cooling.



Top: Rotor-wake facility. Bottom: Computed blade surface temperature and stream-surface entropy.

## Bibliography

Heidmann, J.D.: A Numerical Study of the Effect of Wake Passing on Turbine Blade Film Cooling. AIAA Paper 95-3044 (Also NASA TM-107077), 1995.

Heidmann, J.D.; Lucci, B.L.; and Reshotko, E.: An Experimental Study of the Effect of Wake Passing on Turbine Blade Film Cooling. Accepted for ASME Paper, ASME TURBO EXPO, Orlando, FL, June 1997.

Heidmann, J.D.: The Effect of Wake Passing on Turbine Blade Film Cooling. Ph.D. Dissertation, Case Western Reserve University (Also NASA TM-107380), 1996.

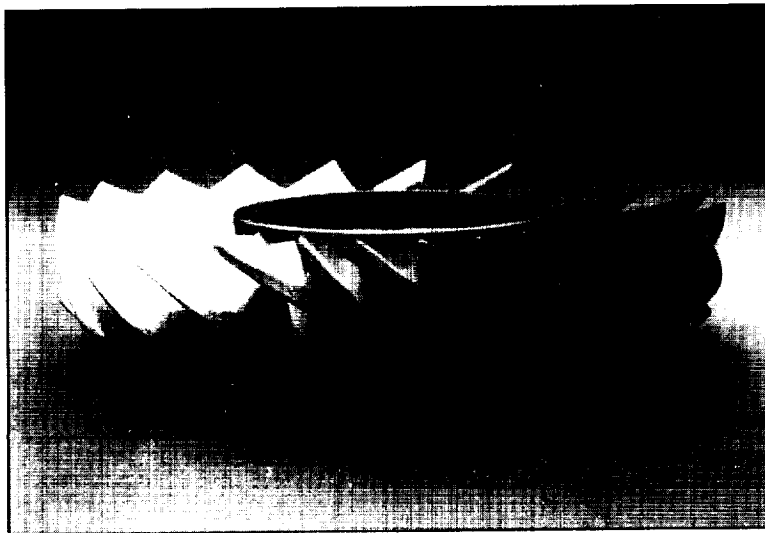
**Lewis contact:** James D. Heidmann, (216) 433-3604 (voice), (216) 433-3918 (fax), toheid@hoops.lerc.nasa.gov

**Author:** James D. Heidmann

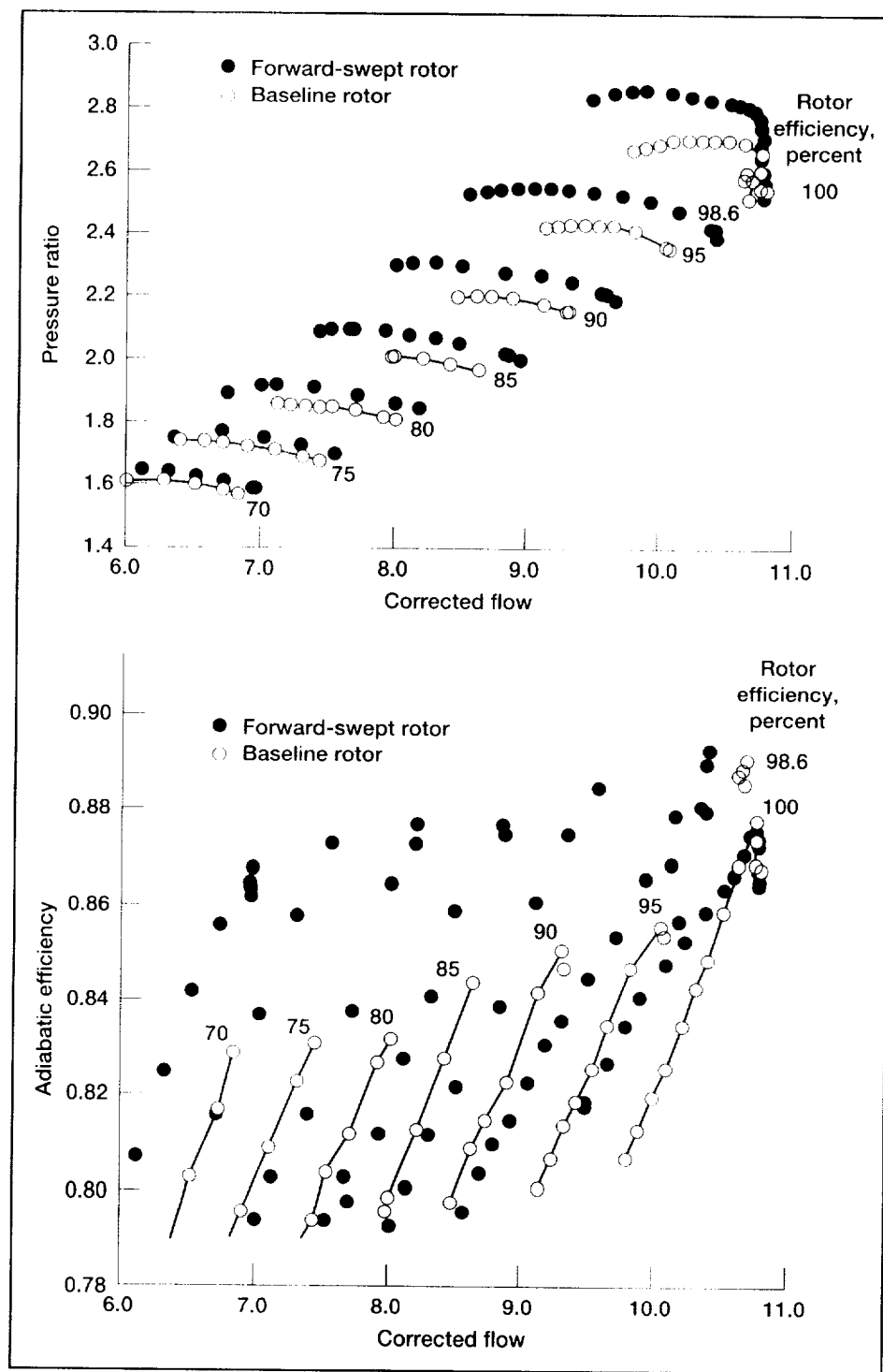
**Headquarters program office:** OA

## Forward Swept Compressor Testing

A new forward-swept rotor designed by Allison Engine Company was tested in NASA Lewis Research Center's CE-18 facility. This testing was a follow-on project sponsored by NASA Lewis to study range enhancements in small turbomachinery. The test was conducted against a baseline rotor design that was also tested in CE-18. The design point for the rotor was a rotor pressure ratio of 2.69, a mass flow of 10.52 lbm/sec, and an adiabatic efficiency of 89.1 percent. Test data indicate that the rotor met the pressure ratio of 2.69 with a 10.77 lbm/sec flow rate, a 87.5-percent adiabatic efficiency, and a 19.5-percent stall margin. The baseline rotor achieved a pressure ratio of 2.69 at a 10.77 lbm/sec flow rate with a stall margin of only 9.2 percent and an adiabatic efficiency of 87.0 percent. The major differences are the significant stall margin increase and the substantially higher off-design peak efficiencies of the forward-swept rotor. The substantially higher performance over the baseline rotor design makes the new design a viable technology candidate for future products.



*Forward-swept rotor design.*



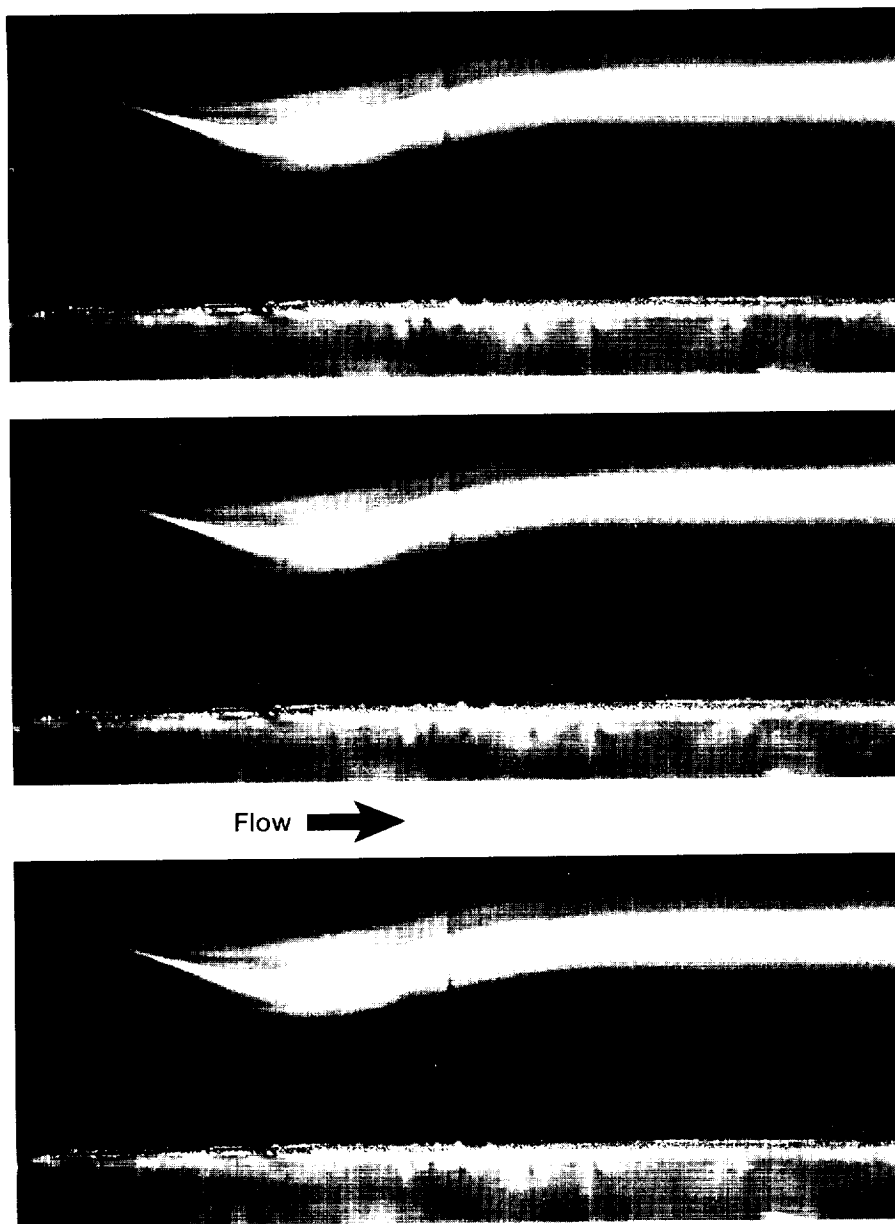
Measured rotor pressure and efficiency maps for baseline and forward-swept rotors. Top: Rotor pressure map. Bottom: Rotor efficiency map.

**Lewis contact:** Dr. David P. Miller, (216) 433-8352, d.p.miller@lerc.nasa.gov

**Author:** Dr. David P. Miller

**Headquarters program office:** OA

## Low Pressure Turbine Flow Physics Program



*Smoke-wire flow visualization of a separation bubble for a free-stream turbulence level of approximately 0.8 percent.*

As part of the collaborative NASA/industry/academia Low Pressure Turbine (LPT) Flow Physics program, smoke flow was visualized from a simulated low-pressure turbine experiment in NASA Lewis Research Center's CW-7 test facility. As shown in the photographs, a laminar separation bubble formed on the bottom flat surface. This is characteristic of the flows in a large-scale, low-pressure turbine operating under off-design conditions. A contoured upper wall was designed to generate a pressure distribution on a flat plate to match the suction surface pressure distribution from a generic low-pressure turbine blade.

This photograph was taken from a 2-sec burn of smoke from a smoke-wire generator located upstream of the test section. At the time, the Reynolds number was 90,000 (based on exit velocity) and the free-stream turbulence intensity was 0.7 percent. The photograph helped to validate the existence and axial location of the separation bubble and provided qualitative features of the bubble such as the large eddy structures in its trailing edge region.

**Lewis contacts:**

Rickey J. Shyne, (216) 433-3595, Rickey.J.Shyne@lerc.nasa.gov; and Dr. Ki-Hyeon Sohn, (216) 433-5949, Ki-Hyeon.Sohn@lerc.nasa.gov

**Authors:** Rickey J. Shyne and Dr. Ki-Hyeon Sohn

**Headquarters program office:** OA

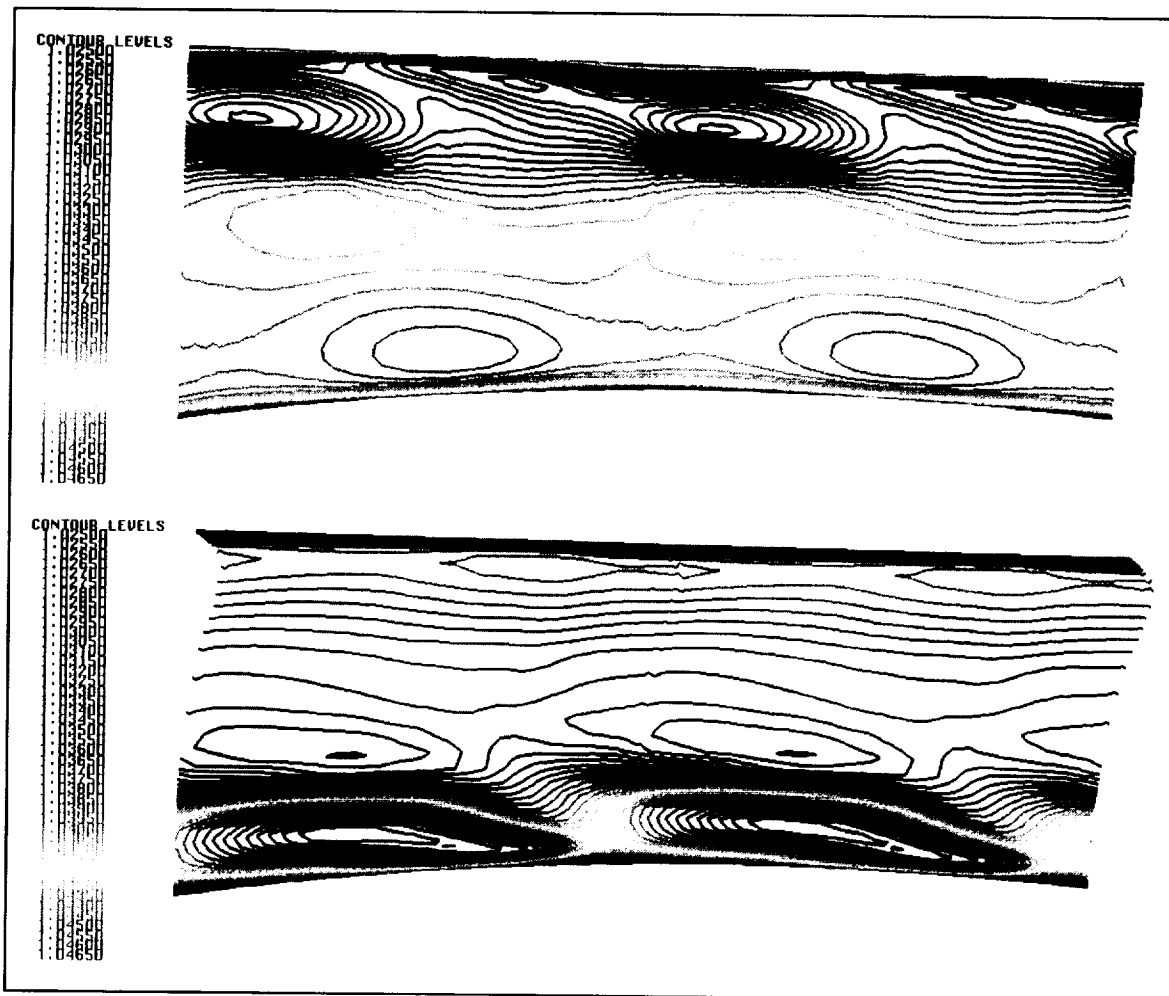
# Vacuum Cleaner Fan Being Improved

As part of the technology utilization program at the NASA Lewis Research Center, efforts are underway to transfer aerospace technologies to new areas of practical application. One such effort involves using advanced computational fluid dynamics (CFD) codes for turbomachinery to analyze the internal fluid dynamics of low-speed fans and blowers. This year, the Kirby Company in Cleveland, Ohio, approached NASA with a request for technologies that could help them improve their vacuum cleaners. Of particular interest to Kirby is the high-frequency blade-passing noise generation of their vacuum cleaner fan at low airflow rates.

To assess the current capability, Lewis researchers studied two Kirby centrifugal fan impellers, a standard (baseline) impeller and a modified (tapered) impeller, analyzing them aerodynamically with a three-dimensional viscous turbomachinery CFD code (RVC3D), that was developed by R.V. Chima at Lewis. Both impellers were simulated at the same airflow ( $102 \text{ ft}^3/\text{min}$ ) and at slightly different rotational speeds corresponding to the measured differences in Kirby tests performed on the two impellers.

The Kirby test data indicated that the tapered impeller generated significantly less noise at all flow rates, but especially at very low flow rates. The main goals of the CFD simulations were to investigate whether substantial differences could be seen in the computed results for a relatively high airflow rate and to determine if those differences suggested the observed trend in noise reduction.

Contour plots of the computed (absolute) total-pressure fields just downstream of the impeller exit for the baseline and tapered impellers



*Fan exit absolute total-pressure fields for Kirby impellers at an airflow of  $102 \text{ ft}^3/\text{min}$ . Top: Kirby baseline propeller at a rotational velocity of 13,500 rpm. Bottom: Kirby tapered impeller at a rotational velocity of 14,000 rpm.*



are shown in the figures. A complete inversion of a high total-pressure region is apparent from the results. In particular, the baseline impeller produces higher total-pressures near the shroud (the top of the passage in the top figure), whereas the tapered impeller produces higher total-pressures near the hub (bottom of the passage in the bottom figure). These differences are much larger than expected since there is only a modest change in the impeller geometry between the baseline and tapered configurations. In view of the spanwise extent and general character of the circumferential (left-to-right) variations in total-pressure, we concluded that the CFD results do allow a reasonable inference about relative noise generation. That is, compared with the baseline impeller, the tapered impeller should generate less noise.

**Lewis contact:** Dr. Daniel L. Tweedt, (216) 433-3592, totweed@cyrus.lerc.nasa.gov

**Author:** Dr. Daniel L. Tweedt

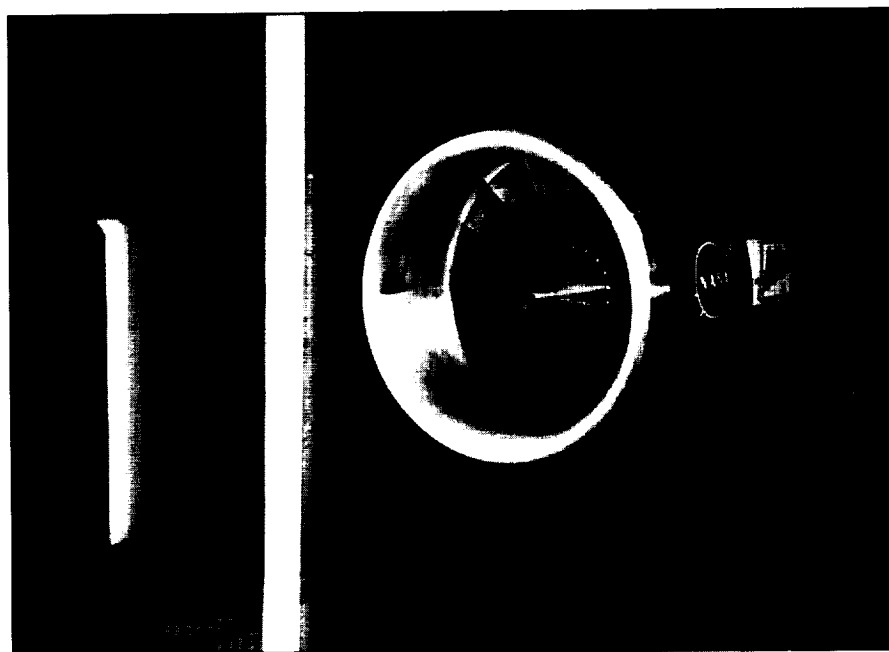
**Headquarters program office:** OA

## Acoustic Barrier Facilitates Inlet Noise Measurements for Aft-Dominated Fans

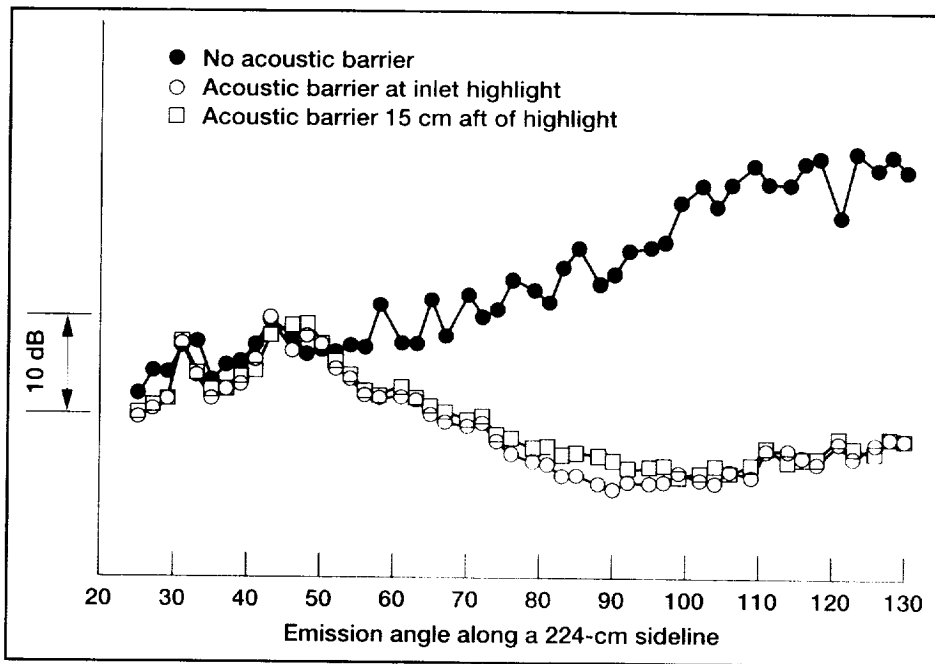
Noise levels for modern high-bypass-ratio subsonic turbofans tend to be aft dominated. That is, the highest flyover noise levels radiate from the fan exit. Measuring fan inlet sound radiation without aft radiation contamination requires selective suppression of the aft noise. In NASA Lewis Research Center's 9- by 15-Foot Low-Speed Wind Tunnel, an acoustic barrier was used to effectively isolate the inlet noise field for a model of an advanced turbofan. This proof-of-concept test was performed on a model turbofan manufactured for NASA Lewis by the Allison Engine Company as part of the Advanced Subsonic Technology program.

The 8-cm-thick acoustic barrier was constructed in sections that were joined upon installation. These sections, which were composed of a wood frame with typically 0.64-cm tempered fiberboard skins, extended from the tunnel's floor to its ceiling and had an axial length of 61 cm. On the fan side of the barrier just downstream of the leading edge, the upstream section had an acoustic treatment—a bulk absorber with a perforated metal skin. It had a nominal full height and an axial length of 46 cm. In addition, an elliptical

leading edge was faired into the upstream barrier section. The barrier was mounted on tracks on the tunnel floor and ceiling at a side-line distance of 15 cm from the fan nacelle. Tests were made with the



*Allison model turbofan in Lewis' 9- by 15-Foot Low-Speed Wind Tunnel. Acoustic barrier shown installed.*



*Aft fan noise suppression due to the wall along the 224-cm sideline.*

barrier leading edge at the fan inlet highlight plane and 15 cm further aft. The barrier extended downstream essentially to the end of the treated tunnel test section.

In the photograph, the acoustic barrier is shown in the upstream position. Acoustic data were taken with a translating microphone on a 224-cm sideline. The directivity plot shows the aft fan noise suppression due to the barrier along the 224-cm sideline. Data are for one-third octave band levels at 6300 Hz, which correspond to the second harmonic of the fan rotor-stator interaction tone. Results are shown for the fan without the barrier present and with the barrier leading edge at the two axial test locations. Aerodynamic data indicate that the barrier does not influence the performance of the fan.

**Lewis contacts:** Richard P. Woodward, (216) 433-3923, Richard.P.Woodward@lerc.nasa.gov; and Christopher E. Hughes, (216) 433-3924, Christopher.E.Hughes@lerc.nasa.gov

**Author:** Richard P. Woodward

**Headquarters program office:** OA (STD)

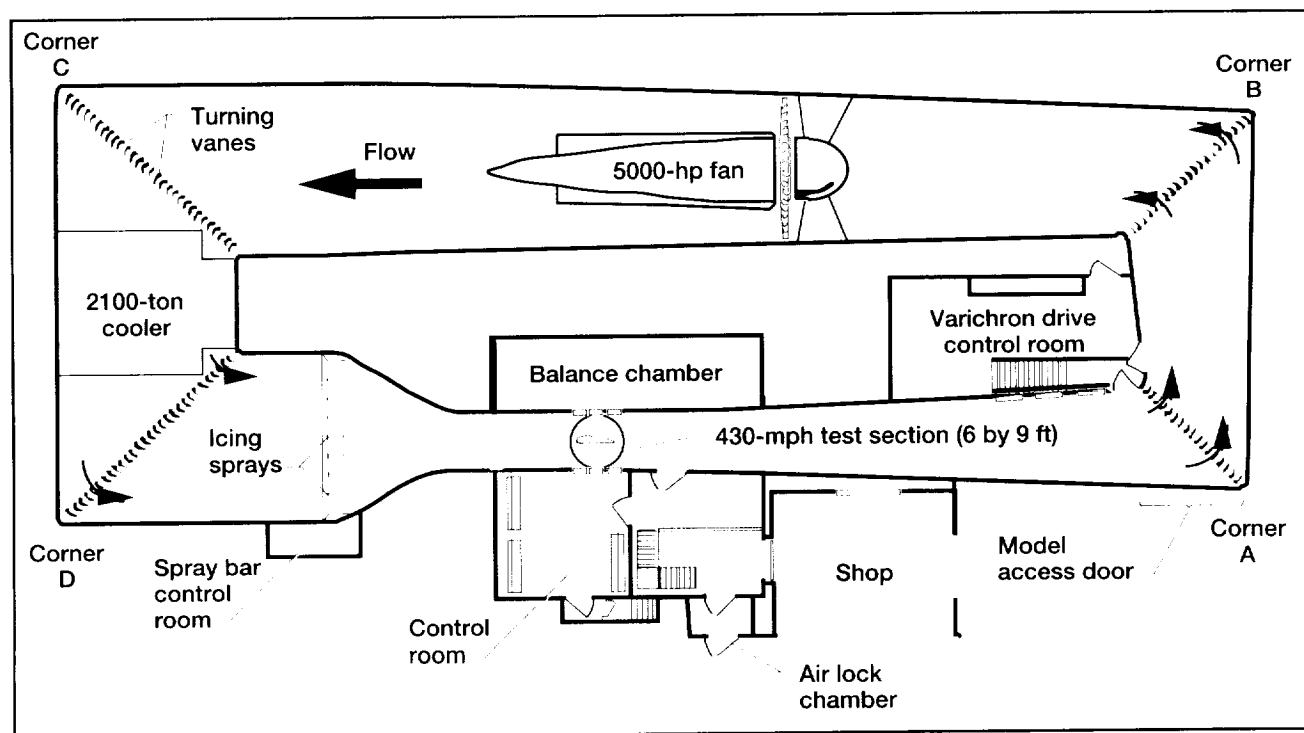
# Aeropropulsion Facilities and Experiments

## Scale Model Icing Research Tunnel

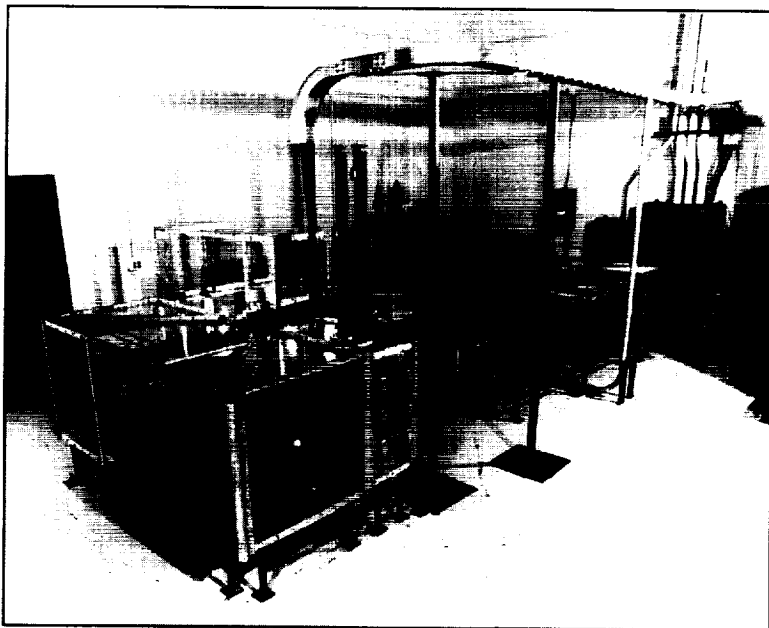
NASA Lewis Research Center's Icing Research Tunnel (IRT) is the world's largest refrigerated wind tunnel and one of only three icing wind tunnel facilities in the United States. The IRT was constructed in the 1940's and has been operated continually since it was built. In this facility, natural icing conditions are duplicated to test the effects of in-flight icing on actual aircraft components as well as on models of airplanes and helicopters. IRT tests have been used successfully to reduce flight test hours for the certification of ice-detection instrumentation and ice protection systems. To ensure that the IRT will remain the world's premier icing facility well into the next century, Lewis is making some renovations and is planning others. These improvements include modernizing the control room, replacing the fan blades with new ones to increase the test section maximum velocity to 430 mph, installing new spray bars to increase the size and uniformity of the artificial icing cloud, and replacing the facility heat exchanger.

Most of the improvements will have a first-order effect on the IRT's airflow quality. To help us understand these effects and evaluate potential improvements to the flow characteristics of the IRT, we built a modular 1/10th-scale aerodynamic model of the facility. This closed-loop scale-model pilot tunnel was fabricated onsite in the various shops of Lewis' Fabrication Support Division. The tunnel's rectangular sections are composed of acrylic walls supported by an aluminum angle framework. Its turning vanes are made of tubing machined to the contour of the IRT turning vanes. The fan leg of the tunnel, which transitions from rectangular to circular and back to rectangular cross sections, is fabricated of fiberglass sections. The contraction section of the tunnel is constructed from sheet aluminum. A 12-bladed aluminum fan is coupled to a turbine powered by high-pressure air capable of driving the maximum test section velocity to 550 ft/sec (Mach 0.45). The air turbine and instrumentation are housed inside a fiberglass nacelle. Total and static pressure measurements can be taken around the loop, and velocity and flow angularity measurements can be taken with hot-wire and five-hole probes at specific locations.

The Scale Model Icing Research Tunnel (SMIRT) is undergoing checkout tests to determine how its airflow characteristics compare with the IRT. Near-term uses for this scale-model tunnel include



Plan view of the Icing Research Tunnel (IRT).



*Scale Model Icing Research Tunnel (SMIRT).*

determining the aerodynamic effects of replacing the 52-year-old W-shaped heat exchanger with a flat-faced heat exchanger. SMIRT is an integral part of the improvements planned for the IRT because testing the proposed IRT improvements in a scale-model tunnel will lower costs and improve productivity.

**Find out more about Lewis' IRT on the World Wide Web:**

<http://www.lerc.nasa.gov/WWW/AFED/facilities/irt.html>

**Lewis contacts:**

Victor A. Canacci, (216) 433-2697, [Victor.A.Canacci@lerc.nasa.gov](mailto:Victor.A.Canacci@lerc.nasa.gov); and Thomas B. Irvine, (216) 433-5369, [Thomas.B.Irvine@lerc.nasa.gov](mailto:Thomas.B.Irvine@lerc.nasa.gov)

**Author:** Victor A. Canacci

**Headquarters program office:** OA

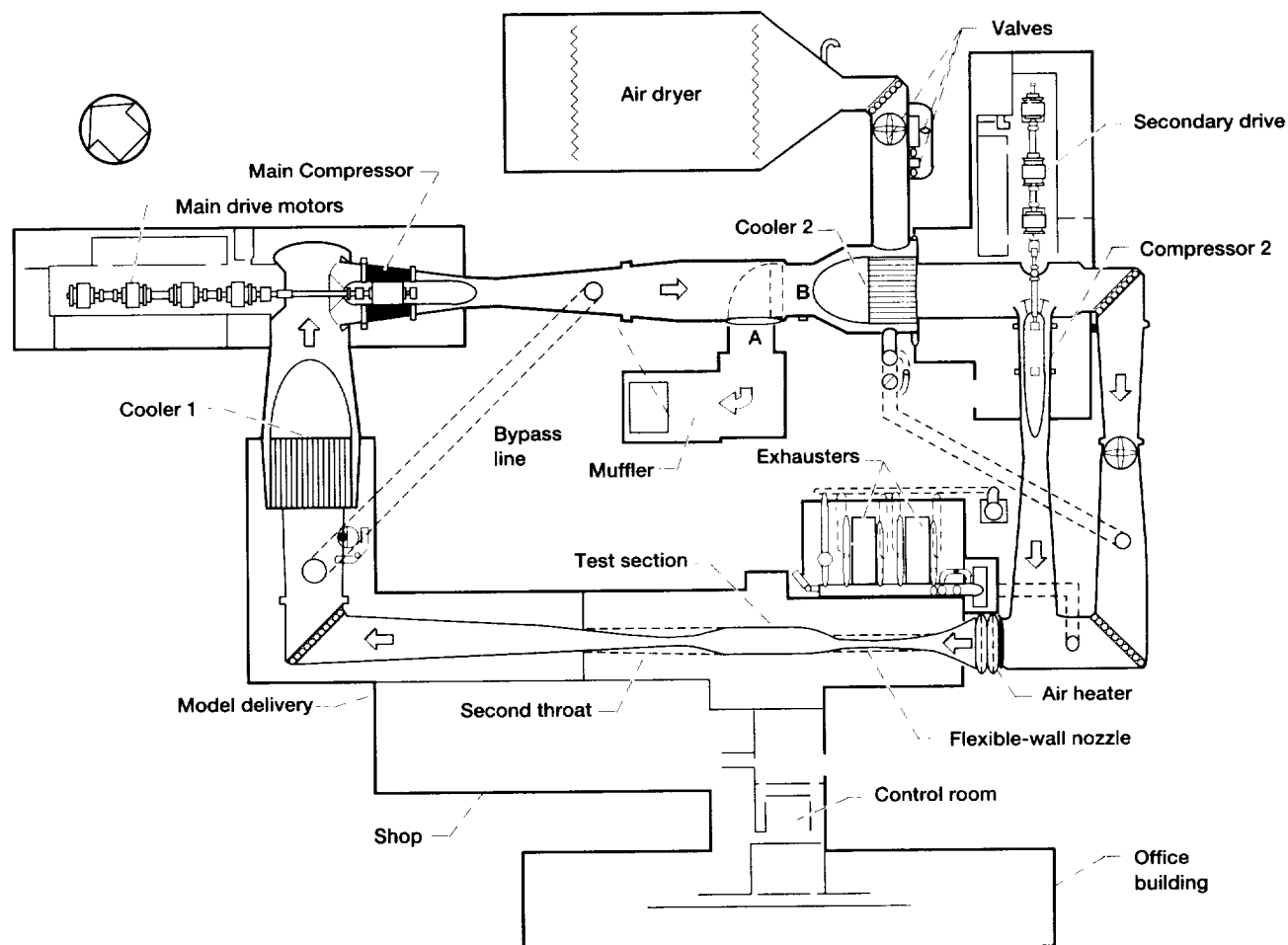
## Supersonic Wind Tunnel Capabilities Expanded Into Subsonic Region

The operating envelope of the Abe Silverstein 10- by 10-Foot Supersonic Wind Tunnel (10×10 SWT) at the NASA Lewis Research Center was recently expanded to include operation at subsonic test section speeds. This new capability generates test section air speeds ranging from Mach 0.05 to 0.35 (32 to 240 kn). Most of the expansion in air speed range was obtained by running the tunnel's main compressor at much lower speeds than ever before. The compressor drive system, consisting of four large electric motors, was run with only one or two motors energized to obtain the lower compressor speed range. This new capability makes the 10×10 SWT more versatile and gives U.S. researchers an enhanced ability to perform subsonic propulsion and aerodynamic testing.

The 10×10 SWT was designed and built in the early 1950's as a supersonic wind tunnel capable of test section speeds of about 2 to 3.5 Mach. However, in the late 1970's, tunnel operation was modified so that subsonic test section speeds could be obtained, roughly 0.1 to 0.35 Mach. The tunnel main compressor was run near its minimum speed, around 565 rpm, with all four of the drive motors energized. This operation caused very high air flow rates and vibrations in the main compressor bypass pipeline and was later stopped because of suspected structural damage. Because of the current high demand for subsonic testing, subsonic operation of the 10×10 SWT was revisited in early 1996.

The new subsonic capability resulted from two efforts. Initially, the old method of subsonic operation was investigated to determine which part of the speed range caused structural problems for the compressor bypass pipeline. Vibration, strain, and displacement instrumentation placed on the bypass line showed that structural vibrations were prohibitive at test section air speeds below Mach 0.25 but were tolerable at test section air speeds of about Mach 0.25 to 0.35.

Next, and more importantly, the main compressor drive motor operation was modified to further reduce the compressor operating speed and, therefore, the amount of compressor bypass line flow. The number of motors energized was



*Lewis' Abe Silverstein 10- by 10-Foot Supersonic Wind Tunnel.*

reduced from four to one or two to achieve new compressor operating speeds, as low as 220 rpm. The resulting test section air speeds range from about 0.05 to 0.25 Mach. Also, by reducing the compressor speed and the number of drive motors, the electric power consumption was significantly reduced, providing energy and dollar savings. The first test program utilizing the new capability was run in the fall of 1996.

**Find out more about the Abe Silverstein 10- by 10-Foot Supersonic Wind Tunnel on the World Wide Web:**

<http://www.lerc.nasa.gov/WWW/AFED/facilities/10x10.html>

**Lewis contacts:** Gary A. Klann, (216) 433-5715, [Gary.A.Klann@lerc.nasa.gov](mailto:Gary.A.Klann@lerc.nasa.gov); and James W. Roeder, Jr., (216) 433-5677, [James.W.Roeder@lerc.nasa.gov](mailto:James.W.Roeder@lerc.nasa.gov)

**Author:** James W. Roeder, Jr.

**Headquarters program office:** OA

# Interdisciplinary Technology

## pV3-Gold Visualization Environment for Computer Simulations

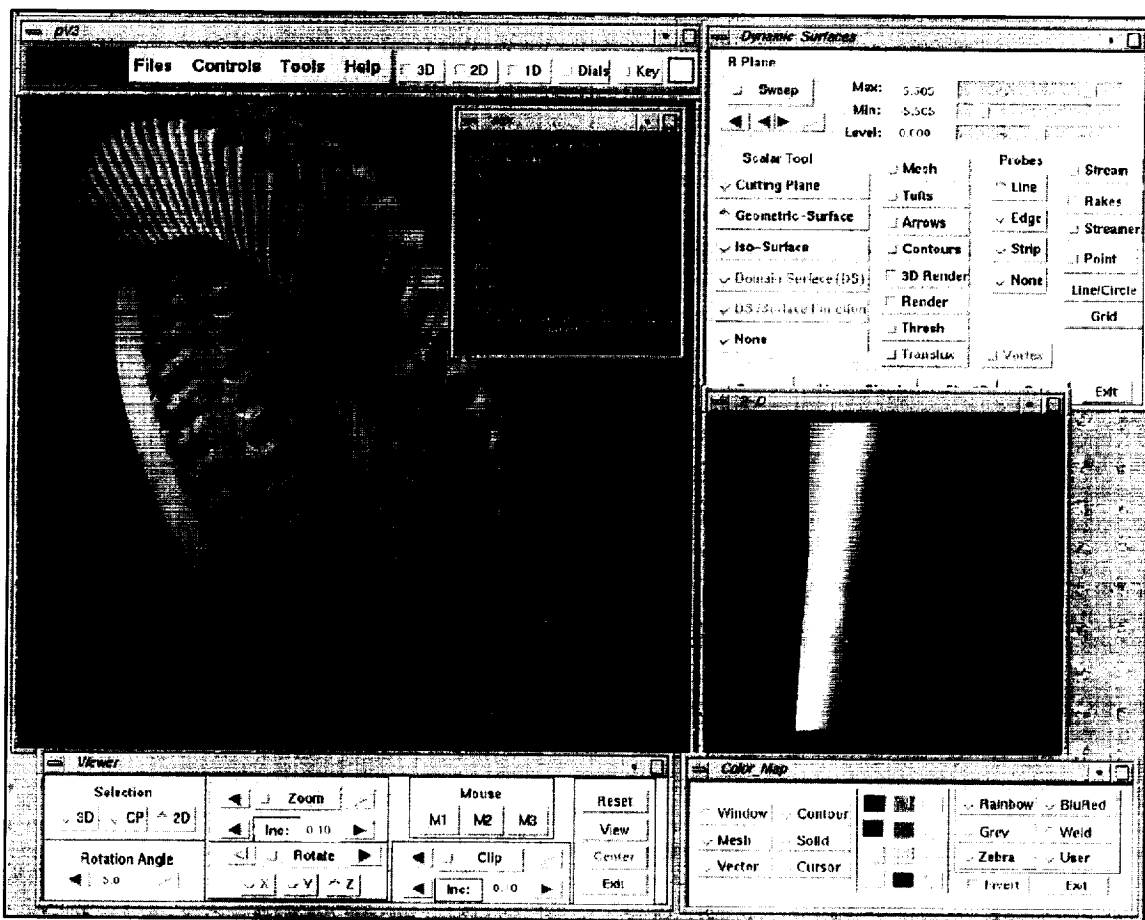
A new visualization environment, pV3-Gold, can be used during and after a computer simulation to extract and visualize the physical features in the results. This environment, which is an extension of the pV3 visualization environment developed at the Massachusetts Institute of Technology with guidance and support by researchers at the NASA Lewis Research Center, features many tools that allow users to display data in various ways.

The pV3-Gold visualization environment is designed for coprocessing multidimensional visualizations of scalar, vector, and tensor data generated in a distributed computing network. It is designed to allow the numerical solver to run as independently as possible. If the numerical procedure takes days to reach a solution, pV3 can periodically connect to the simulation, allowing users to view changing data and then disconnect.

A small amount of programming is required to merge the visualization with the numerical solver, which involves inserting function calls in the numerical solver that pass the solver data to pV3-Gold. If the data are distributed

in a cluster of machines, pV3 handles this, minimizing complications for the user.

pV3-Gold is one of the tools being developed by the United Technologies Research Center as part of the Affordable High Performance Computing Project. Work on the project is being done under a cooperative agreement between NASA Lewis and a team of industry and university partners led by Pratt & Whitney (division of United Technologies). Although the pV3-Gold visualization environment maintains all the original functions of pV3, the



Typical screen of the pV3-Gold visualization tool.

original pV3 interface has been replaced with an intuitive Motif graphical user interface that allows users to visualize data in one-, two- and three-dimensional view windows. Other new functions include annotation, animation recording, and feature extraction. Interactive viewing and steering of a distributed application has been demonstrated with animations recorded to MPEG (Moving Pictures Experts Group) files and video. A visualization and a movie (available on the World Wide Web: <http://danville.res.utc.com/AHPCP/movie.htm>) have been done for more than one cycle of an unsteady three-dimensional turbomachinery simulation. With the pV3-Gold environment, it is now affordable to create many cycled visual representations by extracting the results as the simulation is occurring—a benefit to the aeronautics industry. Thus, the visualization of three-dimensional unsteady simulations can be a daily tool of the aeronautics design engineer.

A number of additional features are currently available in pV3-Gold. The environment handles steady-state data as well as time-varying three-dimensional data in both postprocessing and coprocessing modes, and it provides full support for structured and unstructured meshes. pV3-Gold can render three types of transient data: unsteady, deformation, and structure unsteady. Because pV3-Gold passes only the data that need to be rendered, a high bandwidth is possible. Scalar tools are available to interrogate nodal-based scalar field data such as domain surface maps, planar and arbitrary geometric cuts, and isosurfaces. Vector tools allow users to investigate steady nodal-based vector fields with various types of particles. Probes allow extraction of one-dimensional scalar data from a surface into a one-dimensional plot. Volumes can be broken into any combination of shapes: tetrahedrons, pyramids, prisms, and hexahedrons, polytetrahedral strips, and structured blocks.

The pV3-Gold environment is currently available for beta testing. Future plans for pV3-Gold include developing physical phenomena feature-extraction techniques, designing changes to the graphical user interface to support subsectioning and multidisciplinary visualization, and commercializing the software. We plan to complete these additional features by September 1997.

**Find out more about this research on the World Wide Web:**

<http://danville.res.utc.com/AHPCP/>

**Lewis contact:** Theresa L. Babrauckas, (216) 433-8723, [theresa@lerc.nasa.gov](mailto:theresa@lerc.nasa.gov)

**Author:** Theresa L. Babrauckas

**Headquarters program office:** OA (HPCCO)

# Steady-State Cycle Deck Launcher Developed for Numerical Propulsion System Simulation

One of the objectives of NASA's High Performance Computing and Communications Program's (HPCCP) Numerical Propulsion System Simulation (NPSS) is to reduce the time and cost of generating aerothermal numerical representations of engines, called customer decks. These customer decks, which are delivered to airframe companies by various U.S. engine companies, numerically characterize an engine's performance as defined by the particular U.S. airframe manufacturer. Until recently, all numerical models were provided with a Fortran-compatible interface in compliance with the Society of Automotive Engineers (SAE) document AS681F, and data communication was performed via a standard, labeled common structure in compliance with AS681F. Recently, the SAE committee began to develop a new standard: AS681G. AS681G addresses multiple language requirements for customer decks along with alternative data communication techniques.

Along with the SAE committee, the NPSS Steady-State Cycle Deck project team developed a standard Application Program Interface (API) supported by a graphical user interface. This work will result in Aerospace Recommended Practice 4868 (ARP4868). The Steady-State Cycle Deck work was validated against the Energy Efficient Engine customer deck, which is publicly available. The Energy Efficient Engine wrapper was used not only to validate ARP4868 but also to demonstrate how to wrap an existing customer deck. The graphical user interface for the Steady-State Cycle Deck facilitates the use of the new standard and makes it easier to design and analyze a customer deck. This software was developed following I. Jacobson's Object-Oriented Design methodology and is implemented in C++.

The AS681G standard will establish a common generic interface for U.S. engine companies and airframe manufacturers. This will lead to more accurate cycle models, quicker model generation, and faster validation leading

to specifications. The standard will facilitate cooperative work between industry and NASA. The NPSS Steady-State Cycle Deck team released a batch version of the Steady-State Cycle Deck in March 1996. Version 1.1 was released in June 1996.

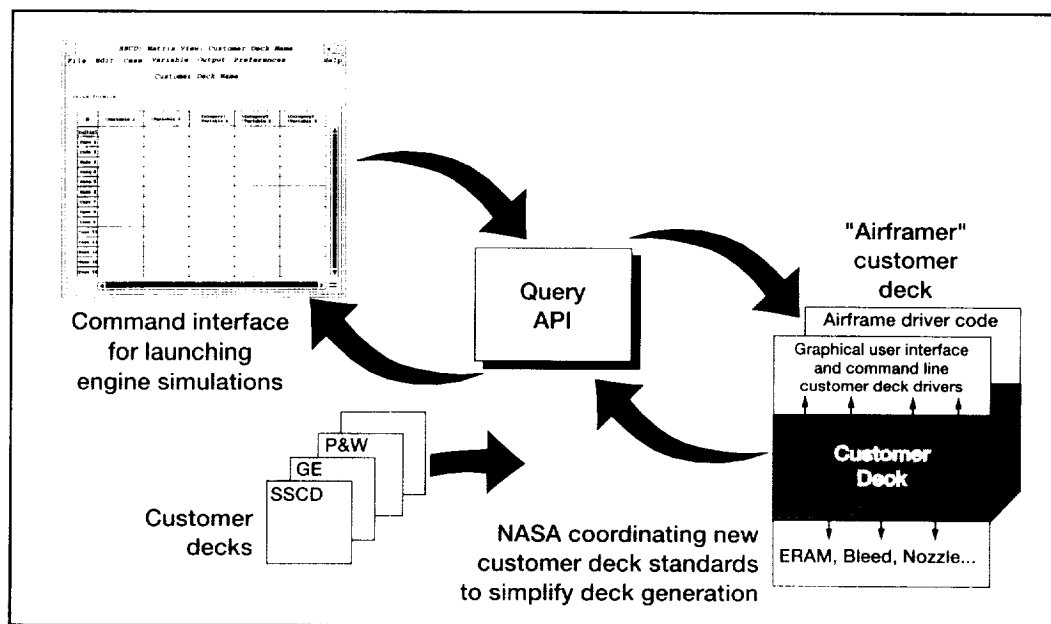
During fiscal 1997, NPSS accepted enhancements and modifications to the Steady-State Cycle Deck launcher. Consistent with NPSS' commercialization plan, these modifications will be done by a third party that can provide long-term software support.

#### Lewis contacts:

Donald E. Van Drei, (216) 433-9089, [dvandrei@lerc.nasa.gov](mailto:dvandrei@lerc.nasa.gov); and Gregory J. Follen, (216) 433-5193, [gfolen@lerc.nasa.gov](mailto:gfolen@lerc.nasa.gov)

**Author:** Donald E. Van Drei

**Headquarters program office:** OA (HPCCO)



*Steady-State Cycle Deck (SSCD) provides a mechanism to incorporate various customer decks.*



## Configuration Management File Manager Developed for Numerical Propulsion System Simulation

One of the objectives of the High Performance Computing and Communication Project's (HPCCP) Numerical Propulsion System Simulation (NPSS) is to provide a common and consistent way to manage applications, data, and engine simulations. The NPSS Configuration Management (CM) File Manager integrated with the Common Desktop Environment (CDE) window management system provides a common look and feel for the configuration management of data, applications, and engine simulations for U.S. engine companies. In addition, CM File Manager provides tools to manage a simulation. Features include managing input files, output files, textual notes, and any other material normally associated with simulation. The CM File Manager includes a generic configuration management Application Program Interface (API) that can be adapted for the configuration management repositories of any U.S. engine company.

Guided by emerging desktop standards, a team consisting of NASA Lewis Research Center personnel and representatives from U.S. engine and airframe companies defined, developed, and implemented a standard graphical user interface windowing system for launching and administering simulations with configuration management access functions and file management tools. The NPSS CM File Manager contains a common windowing system based on CDE that contains the necessary tools an engineer requires for designing and analyzing engines. The software was developed following I. Jacobson's Object-Oriented Design methodology and was implemented in C++.

In March and June of 1996, Lewis released beta versions of the NPSS CM File Manager. In September of 1996, Version 1.0, with documentation, was released to U.S. engine companies.

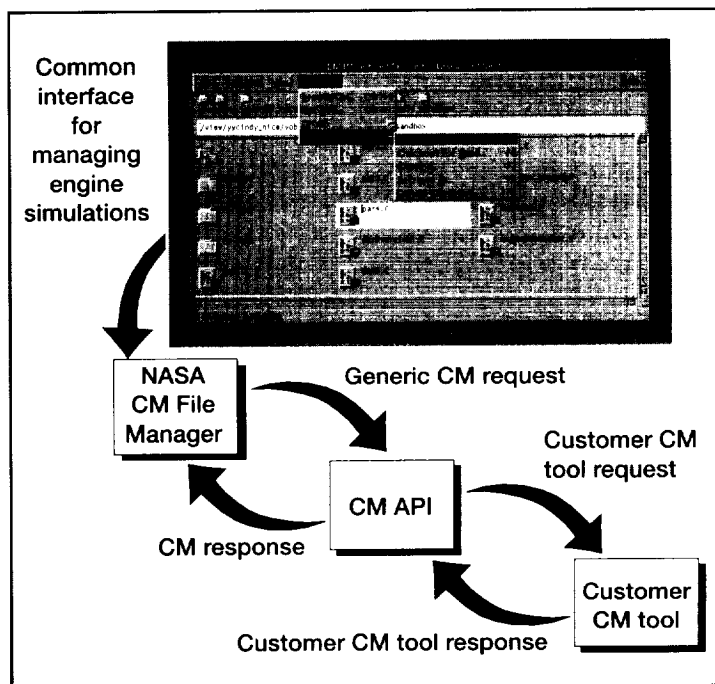
The development of the NPSS CM File Manager provides U.S. aeropropulsion companies a common tool for creating and modifying engine simulations. Since the CM File Manager was built on a desktop standard (CDE), it is easy for engine companies to use, accept, and manage. In addition, U.S. engine companies could save millions of dollars by using standard analysis and design tools in precompetitive areas.

During fiscal 1997, NPSS will accept enhancements and modifications to the CM File Manager. The modifications will be done by a third party that can provide long-term software support.

**Lewis contact:** Gregory J. Follen, (216) 433-5193, gfolle@lerc.nasa.gov

**Author:** Gregory J. Follen

**Headquarters program office:** OA (HPCCO)



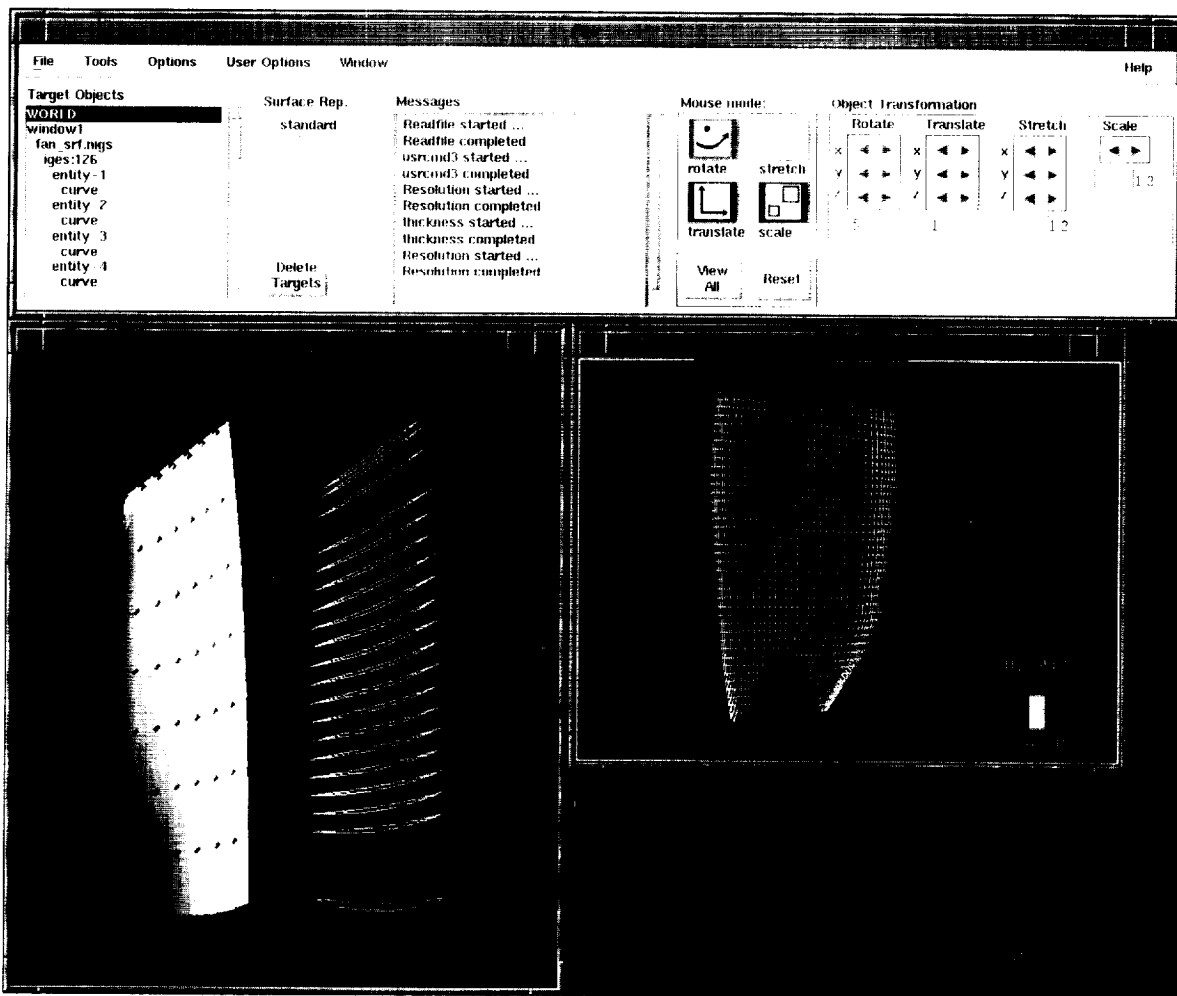
*Configuration Management (CM) File Manager. (Application Program Interface, API.)*

# Portable Extensible Viewer

The use of NURBS (Nonuniform Rational B-Splines) to represent geometry and data offers a standard way to facilitate the multidisciplinary analysis and design of aeropropulsion products. Using standard geometry defined by NURBS throughout design, analysis, part definition, manufacture, and test processes saves money and time. The Portable Extensible Viewer (PEV) offers engineers of different disciplines a means to view and manipulate NURBS geometry and associated data. Under the guidance of a team of Lewis, Boeing Company, and Navy personnel, PEV was developed by NASA Lewis Research Center's Computer Services Division for Lewis' Interdisciplinary Technology Office. The aeropropulsion industry provided input to the design requirements.

PEV software is designed to read, write, evaluate, display, manipulate, and analyze NURBS data. NURBS data can be stored in several predefined file formats (including the Initial Graphics Exchange Standard (IGES)) or in a file format that can be read in by a user-defined function. The data can be multidimensional, including not only geometry information, but also such data as temperature defined over multiple time steps and at various conditions.

A graphical user interface provides an easy, intuitive, and extensible interactive interface for users to perform geometric transformations (such as scaling, translating, stretching, and rotating objects), modify display attributes (such as the color, shading, visibility, and style), evaluate surfaces, annotate with text, create multiple view windows, save interactions in a journal file, invoke command scripts, and perform many other functions. PEV is extensible, allowing users to develop custom application codes with functions from the PEV library of routines.



Typical Portable Extensible Viewer (PEV) screen.

The PEV architecture was designed so that the graphical user interface remains active and responsive to users at all times, even when the application is busy processing requests or performing calculations. To achieve this goal, PEV runs as three distinct processes and communication is conducted through bidirectional interprocess communication channels. These channels allow commands of higher priority to interrupt the processing of lower priority commands.

PEV is written mostly in the ANSI C language, with a few Fortran routines. It has been compiled and run under the following operating systems: HP 9000/755, HPUX 9.05, SGI IRIX 5.3, SUN Sparc Solaris 2.4, and IBM RS6000 AIX 3.2. PEV requires the X-Window System, Motif, the DT\_NURBS library, and the HOOPS library. The DT\_NURBS library provides the mathematical tool kit to manipulate the NURBS-based representation of the data and geometry. HOOPS is the graphics library that provides three-dimensional capabilities for PEV to display and graphically manipulate NURBS.

In the example shown here (see the figure), a NASA IGES file was read in and the curves and surface were displayed. The surface was moved so that rather than being superimposed on the curves, it was placed next to them. The resolution of the surface was changed, and the appearance of the objects was modified. A second window was then created, and a four-dimensional NURBS object was read in. A script was executed that defined the variables used for the geometry as well as a variable assigned to the thickness of the geometry. Color coding of the thickness of the geometry was used to enhance understanding.

**More information about PEV can be found on the World Wide Web:**  
<http://www.lerc.nasa.gov/WWW/NPSS/PEV/pev.external.homepage.html>

**Lewis contact:** Gregory J. Follen, (216) 433-5193, [gfolle@lerc.nasa.gov](mailto:gfolle@lerc.nasa.gov)  
**Author:** Dr. Jay G. Horowitz  
**Headquarters program office:** OA (HPCCO)

# Visual Computing Environment

The Visual Computing Environment (VCE) is a NASA Lewis Research Center project to develop a framework for intercomponent and multidisciplinary computational simulations. Many current engineering analysis codes simulate various aspects of aircraft engine operation. For example, existing computational fluid dynamics (CFD) codes can model the airflow through individual engine components such as the inlet, compressor, combustor, turbine, or nozzle. Currently, these codes are run in isolation, making intercomponent and complete system simulations very difficult to perform. In addition, management and utilization of these engineering codes for coupled component simulations is a complex, laborious task, requiring substantial experience and effort. To facilitate multicomponent aircraft engine analysis, the CFD Research Corporation (CFDRC) is developing the VCE system. This system, which is part of NASA's Numerical Propulsion Simulation System (NPSS) program, can couple various engineering disciplines, such as CFD, structural analysis, and thermal analysis.

The objectives of VCE are to (1) develop a visual computing environment for controlling the execution of individual simulation codes that are running in parallel and are distributed on heterogeneous host machines in a networked environment, (2) develop numerical coupling algorithms for interchanging boundary conditions between codes with arbitrary grid matching and different levels of dimensionality, (3) provide a graphical interface for simulation setup and control, and (4) provide tools for online visualization and plotting.

VCE was designed to provide a distributed, object-oriented environment. Mechanisms are provided for creating and manipulating objects, such as grids, boundary conditions, and solution data. This environment includes parallel virtual machine (PVM) for distributed processing. Users can interactively select and couple any set of codes that have been modified to run in a parallel distributed fashion on a cluster of heterogeneous workstations. A scripting facility allows users to dictate the sequence of events that make up the particular simulation.

Several test simulations of differing complexity have been completed, validating the basic design and pointing out areas that need further improvements. NASA Lewis, Pratt & Whitney, and CFDRC are using VCE

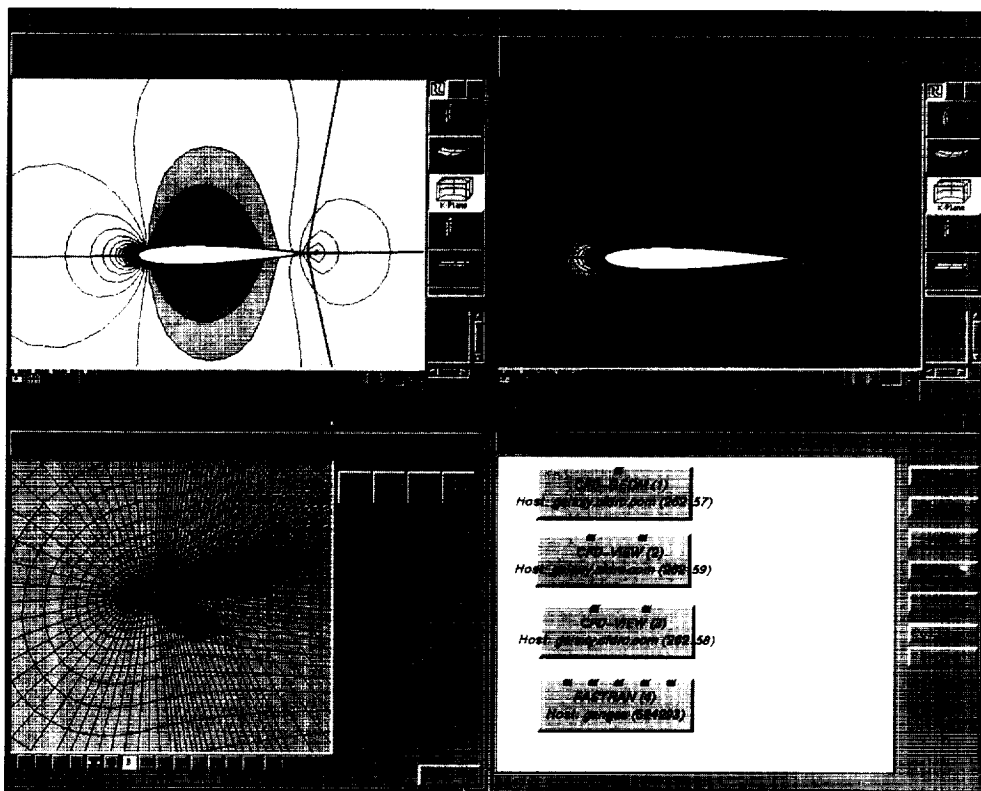
as part of the National Combustor Code for combining grid generator, flow solver, and visualization capabilities in one integrated environment. The NASA Ames Research Center is using VCE as an interface protocol and generic remeshing environment for deformable and moving-body simulations. NASA Lewis plans to continue to develop VCE for multidisciplinary and intercomponent simulations.

## Lewis contacts:

Dr. Charles Lawrence,  
(216) 433-6048,  
CLawrence@lerc.nasa.gov; and  
Charles W. Putt,  
(216) 433-5204,  
Cputt@lerc.nasa.gov

**Authors:** Dr. Charles Lawrence  
and Charles W. Putt

**Headquarters program office:**  
OA (HPCCO)

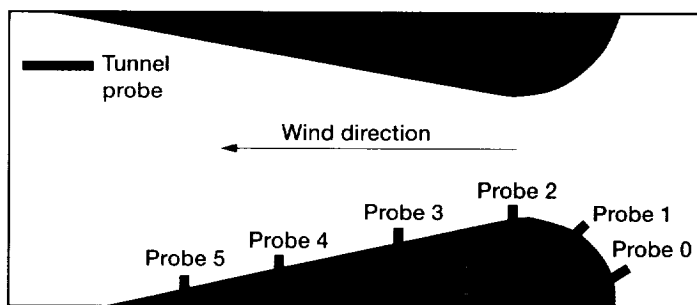


Typical Visual Computing Environment (VCE) screen.

## A Vision in Aeronautics—The K-12 Wind Tunnel Project

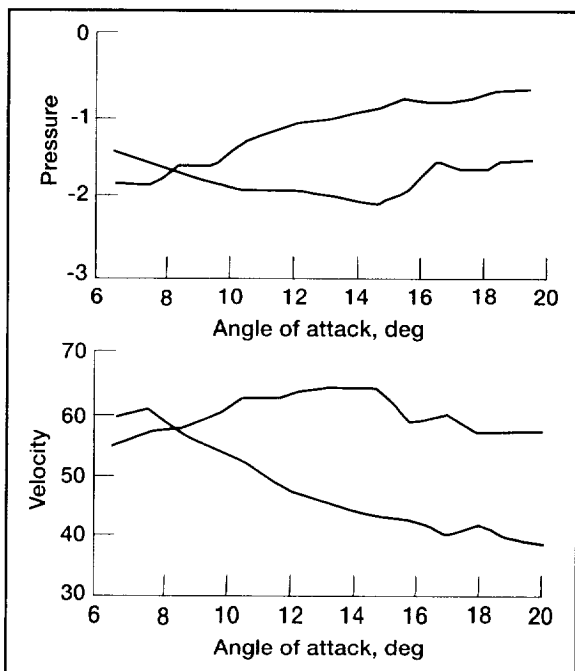
A Vision in Aeronautics, a project within the NASA Lewis Research Center's Information Infrastructure Technologies and Applications (IITA) K-12 Program, employs small-scale, subsonic wind tunnels to inspire students to explore the world of aeronautics and computers. Recently, two educational K-12 wind tunnels were built in the Cleveland area. During the 1995-1996 school year, preliminary testing occurred in both tunnels.

At General Benjamin O. Davis Jr. Aviation High School, the students conducted three wind tunnel experiments. In the first one, they analyzed a venturi (see the first figure). After collecting velocity and pressure data through the tunnel's instrumentation, the students used the data to create computer-generated graphs displaying the relationship of velocity and pressure.



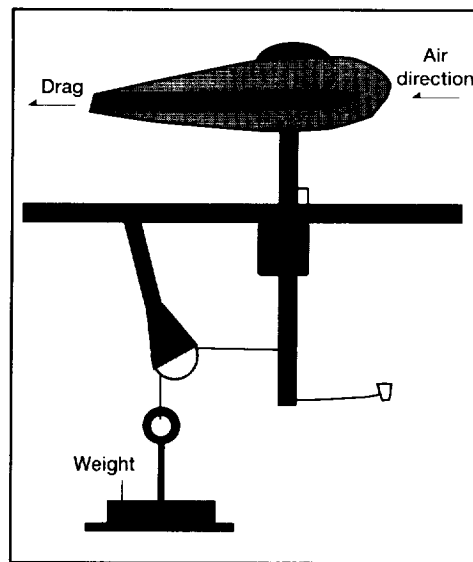
*Tunnel instrumentation.*

In the second experiment, the students observed an airfoil at various angles of attack. They visually observed the tufts on the airfoil as it was rotated from a horizontal position to a steep angle of attack. Then, they plotted the velocity and pressure readings at various angles (see figure below).



*Pressure and velocity differences at various angles of attack.*

By working with the students and using this educational tunnel, NASA researchers were able to expedite their research on this project instead of waiting for a schedule opening for the heavily used NASA wind tunnels.



*Wheel pant installation.*

Their third project was the wheel pant project, a research project conducted by NASA Lewis Research Center's Structural Systems Branch to design a more aerodynamic wheel cover for small aircraft. Helping out with this real-world research project, students performed initial tests of Lewis' wheel pant design in Aviation High School's K-12 wind tunnel. The tests indicated that the covered wheel will provide some additional drag reduction.

At Barberton High School, the wind tunnel was used for a pine car drag race. Students designed cars with features they believed would make their cars the fastest. Then the cars were tested in the tunnel to find the car with the least amount of drag.

At both schools, the student participants learned a great deal about aeronautics. They will have a head start on their college studies should they pursue aeronautics further.

During the 1996-1997 school year, these tunnels will be opened up to students in other schools through the use of the Internet. Students at remote schools will be able to build a test object and send it to the school with the tunnel it is to be tested in. While the test is being



*Students at General Benjamin O. Davis Aviation High School test an airfoil in the school's educational wind tunnel.*

conducted, desk-top video conferencing and electronic data transfer will allow students at the remote school to observe testing in real time.

**More information is available on the World Wide Web:**

**NASA IITA Program Office (NASA Ames):** <http://iita.ivv.nasa.gov>

**NASA Lewis K-12 Wind Tunnel:** <http://www.lerc.nasa.gov/WWW/K-12/windtunnel.html>

**Lewis contact:**

Beth Lewandowski, (216) 433-8873, [b.lewandowski@lerc.nasa.gov](mailto:b.lewandowski@lerc.nasa.gov)

**Author:** Beth Lewandowski

**Headquarters program office:** OA (HPCCO)

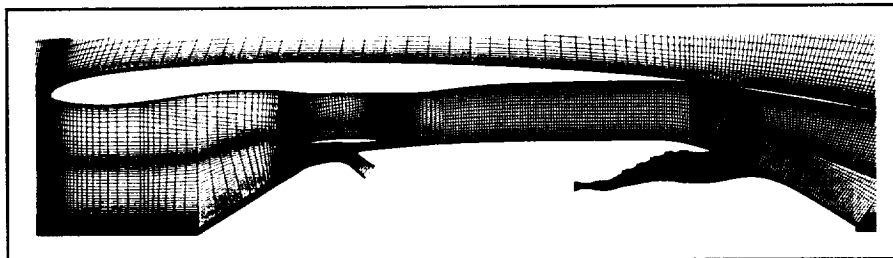
## Flow Analysis of a Gas Turbine Low-Pressure Subsystem

The NASA Lewis Research Center is coordinating a project to numerically simulate aerodynamic flow in the complete low-pressure subsystem (LPS) of a gas turbine engine. The numerical model solves the three-dimensional Navier-Stokes flow equations through all components within the low-pressure subsystem as well as the external flow around the engine nacelle. The Advanced Ducted Propfan Analysis Code (ADPAC), which is being developed jointly by Allison Engine Company and NASA, is the Navier-Stokes flow code being used for LPS simulation. The majority of the LPS project is being done under a NASA Lewis contract with Allison. Other contributors to the project are NYMA and the University of Toledo.

For this project, the Energy Efficient Engine designed by GE Aircraft Engines is being modeled. This engine includes a low-pressure system and a high-pressure system. An inlet, a fan, a booster stage, a bypass duct, a lobed mixer, a low-pressure turbine, and a jet nozzle comprise the low-pressure subsystem within this engine. The tightly coupled flow analysis evaluates aerodynamic interactions between all components of the LPS. The high-pressure core engine of this engine is simulated with a one-dimensional

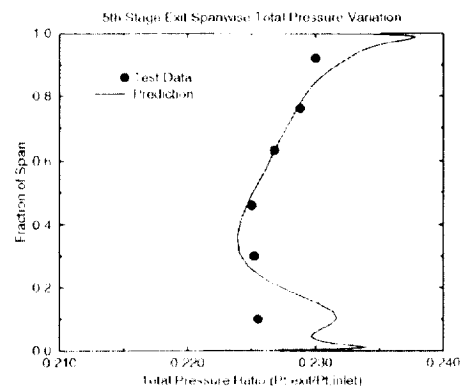
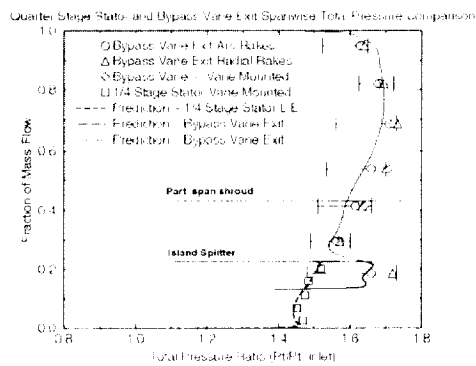
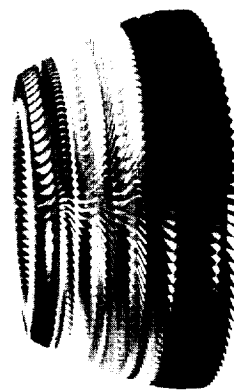
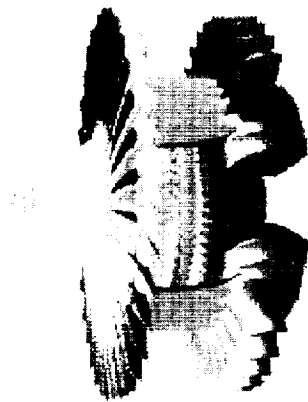
thermodynamic cycle code in order to provide boundary conditions to the detailed LPS model. This core engine consists of a high-pressure compressor, a combustor, and a high-pressure turbine.

The three-dimensional LPS flow model is coupled to the one-dimensional core engine model to provide a "hybrid" flow model of the complete gas turbine Energy Efficient Engine. The resulting hybrid engine model evaluates the detailed interaction between the LPS components at design and off-design engine operating conditions while considering the lumped-parameter performance of the core engine.



*Low-pressure subsystem computational mesh.*

The Navier-Stokes modeling of the large, low-pressure subsystem provides detailed knowledge of the interactions between its components. These interaction effects can be critical to engine performance, but they are usually not adequately accounted for in the early phases of



Cutaway view of the Energy Efficient Engine showing the fan and low-pressure turbine. The three-dimensional flow solution is superimposed onto the turbomachinery blades of the low-pressure subsystem and compared with test data.

a new engine design. Therefore, these interaction effects typically remain unknown until later in the design phase, after expensive hardware validation testing has been completed. A detailed LPS model provides the designer with a tool to reduce the unknowns due to engine component interaction effects early in the design process. Reduced risk associated with engine design reduces the number of hardware build and test iterations, and results in lowering the design cost.

The detailed LPS flow modeling capability will be integrated into the Numerical Propulsion System Simulator (NPSS), which serves as a numerical "test cell." This task demonstrates an important element within the NPSS project. The goal of the LPS modeling project, and NPSS, is to provide a tool that can significantly reduce the risks, uncertainty, and costs associated with designing advanced gas turbine engines. NPSS is supported by the High Performance Computing and Communication Program (HPCCP) and the Aeronautics R&T Base.

The LPS project is near completion. With an end date in September of 1997, the project is in the code-validation phase with component test data. A computer simulation of the fan and booster stage was created with the three-dimensional ADPAC numerical flow modeling code; then, a solution from the computer simulation was compared with test data obtained from the test rig. Likewise, a computer simulation of the five-stage, low-pressure turbine was created, and the solution was compared with test data obtained from the turbine test rig. In both cases, the solutions obtained from the computer models compared well with test data obtained from the test rig. A large computational mesh has been created for the complete LPS containing 6.7 million mesh points. A three-dimensional ADPAC flow simulation has been run on the complete LPS system at the engine design point operating condition. Computational time required for a converged solution is being reduced by running the large computer simulation of the complete LPS on networked workstations located at NASA Lewis and the NASA Ames Research Center.

**Find out more about this gas turbine research on the World Wide Web:**  
<http://www.lerc.nasa.gov/WWW/CISO/NPSS/projects/LPSubs/>

**Lewis contact:** Joseph P. Veres, (216) 433-2436, [jveres@lerc.nasa.gov](mailto:jveres@lerc.nasa.gov)  
**Author:** Joseph P. Veres  
**Headquarters program office:** OA (HPCCO)



# Aerospace Technology

## Materials

### Advanced High-Temperature Engine Materials Technology Progresses

The objective of the Advanced High Temperature Engine Materials Technology Program (HITEMP) at the NASA Lewis Research Center is to generate technology for advanced materials and structural analysis that will increase fuel economy, improve reliability, extend life, and reduce operating costs for 21st century civil propulsion systems. The primary focus is on fan and compressor materials (polymer-matrix composites—PMC's), compressor and turbine materials (superalloys, and metal-matrix and intermetallic-matrix composites—MMC's and IMC's), and turbine materials (ceramic-matrix composites—CMC's). These advanced materials are being developed in-house by Lewis researchers and on grants and contracts.

NASA considers this program to be a focused materials and structures research effort that builds on our basic research programs and supports component-development projects. HITEMP is coordinated with the Advanced Subsonic Technology (AST) Program and the Department of Defense/NASA Integrated High-Performance Turbine Engine Technology (IHPTET) Program. Advanced materials and structures technologies from HITEMP may be used in these future applications.

Recent technical accomplishments have not only improved the state of the art but have wide-ranging applications for industry. An oxidation-resistant coating was developed that is chemically compatible with a TiAl-base alloy. The coating, optimized for toughness and oxidation resistance, is being evaluated in a cooperative program with the Allison Engine Company for future turbine engine applications. Our patented "Single Transducer Ultrasonic Imaging Method That Eliminates the Effect of Plate Thickness Variation in the Image" won a 1996 R&D 100 Award. Another product of HITEMP research, the computer code CEMCAN (Ceramic Matrix Composite Analyzer), was released to COSMIC for commercialization, and several other developmental codes were released to industry via software release agreements. In the Lincoln Composites/AlliedSignal/Lewis cooperative program, a composite compressor case, which was manufactured with the Lewis-developed matrix VCAP, is currently being rig tested at AlliedSignal Inc. to demonstrate the

feasibility of VCAP in a high-temperature (500 °F) environment typical of jet engine applications.

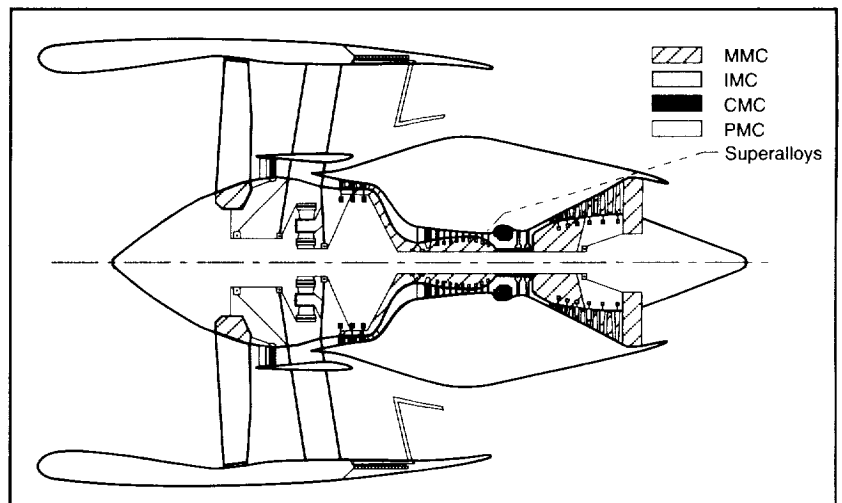
The next annual review of the HITEMP program will be held April 29–30, 1997. Details of research accomplishments will be published in a conference report that will be available at the conference, which is open to U.S. citizens only. (Permission to use this material was granted by Hugh R. Gray, January 1997.)

**Lewis contacts:**

Dr. Hugh R. Gray, (216) 433-3230, [Hugh.R.Gray@lerc.nasa.gov](mailto:Hugh.R.Gray@lerc.nasa.gov); and Carol A. Ginty, (216) 433-3335, [Carol.A.Ginty@lerc.nasa.gov](mailto:Carol.A.Ginty@lerc.nasa.gov)

**Authors:** Dr. Hugh R. Gray and Carol A. Ginty

**Headquarters program office:** OA



*Advanced materials for 21st century civil propulsion systems with greatly increased fuel economy, improved reliability, extended life, and reduced operating costs.*

# Natural Strain

Logarithmic strain is the preferred measure of strain used by materials scientists, who typically refer to it as the "true strain." It was Nadai (ref. 1) who gave it the name "natural strain," which seems more appropriate. This strain measure was proposed by Ludwik (ref. 2) for the one-dimensional extension of a rod with length  $l$ . It was defined via the integral of  $dl/l$  to which Ludwik gave the name "effective specific strain." Today, it is after Hencky (ref. 3), who extended Ludwik's measure to three-dimensional analysis by defining logarithmic strains for the three principal directions.

In their classic treatise in 1960, Truesdell and Toupin (ref. 4) pointed out that all applications of Hencky's logarithmic strain measure had had difficulties because it was complex to evaluate. As a consequence, applications were (up to that point in time) limited primarily to studies wherein the principal axes of strain did not rotate in the body of the structure. With computers now being readily available, this consideration (which was valid in 1960) is no longer a constraint.

In their treatise, Truesdell and Toupin went on to say, "Such simplicity for certain problems, as may result from a particular strain measure, is bought at the cost of complexity for other problems. In a Euclidean space, distances are measured by a quadratic form, and an attempt to elude this fact is unlikely to succeed." They advocate using the "topological," quadratic strain fields of Almansi (ref. 5) or Green (ref. 6) instead of the "physical," logarithmic strain field of Hencky (ref. 3).

For investigations at the NASA Lewis Research Center, this researcher based his definition for natural strain on the Riemannian, body-metric, tensor field of Lodge (ref. 7). There was no 'eluding' this fact. The outcome was an intuitive measure for strain.

A thorough and consistent development of the strain and strain-rate measures affiliated with Hencky was documented (ref. 8), and natural measures for strain and strain-rate were expressed in terms of the fundamental body-metric tensors of Lodge. These strain and strain-rate measures, which are mixed tensor fields, were mapped from the body to space<sup>1</sup> in both the Eulerian and Lagrangian configurations and were then transformed from general to Cartesian fields. Then, they were compared with the various strain and strain-rate measures found in the literature. A simple Cartesian description for the Hencky strain-rate in the Lagrangian state was obtained, but unfortunately, this Cartesian result cannot be integrated (a byproduct of nonunique mappings from general to Cartesian space). Nevertheless, this solution does point the way to obtaining other integrable solutions appropriate for using the Hencky strain to construct constitutive equations.

This investigator believes that physical, rather than topological, measures of strain, although more complex in evaluation, will ultimately lead to much simpler constitutive equations for describing material behavior, especially under the conditions of large deformations that are often present during material processing. Simpler constitutive equations mean quicker

characterization times, ultimately leading to faster turnaround times between the process design and final production.

**Find out more about this research on the World Wide Web:**

<http://sarah.lerc.nasa.gov/~al>

## References

1. Nadai, A.: Plastic Behavior of Metals in the Strain-Hardening Range. Part I. J. Appl. Phys., vol. 8, 1937, pp. 205-213.
2. Ludwik, P.: Elemente der Technologischen Mechanik. Applied Mechanics, Verlag von J. Springer, Berlin, 1909.
3. Hencky, H.: Über die Form des Elastizitätsgesetzes bei ideal elastischen Stoffen. Zeit. Tech. Phys., vol. 9, 1928, pp. 215-220, 457.
4. Truesdell, C.; and Toupin, R.: The Classical Field Theories. Encyclopedia of Physics, Vol. III/1, S. Flugge (ed), Springer-Verlag, Berlin, 1960, pp. 226-793.
5. Almansi, E.: Sulle deformazioni finite dei solidi elastici isotropi, I. Rendiconti della Reale Accademia dei Lincei, Classe di scienze fisiche, matematiche e naturali, v. 20, 1911, pp. 705-714.
6. Green, G.: On the Propagation of Light in Crystallized Media. Trans. Cambridge Phil. Society, vol. 7, 1841, pp. 121-140.
7. Lodge, A.S.: On the Use of Convected Coordinate Systems in the Mechanics of Continuous Media. Proc. Cambridge Phil. Soc., vol. 47, 1951, pp. 575-584.
8. Freed, A.D.: Natural Strain. J. Eng. Mater. Technol., vol. 117, Oct. 1995, pp. 379-385.

## Lewis contact:

Dr. Alan D. Freed, (216) 433-8747,  
[Alan.D.Freed@lerc.nasa.gov](mailto:Alan.D.Freed@lerc.nasa.gov)

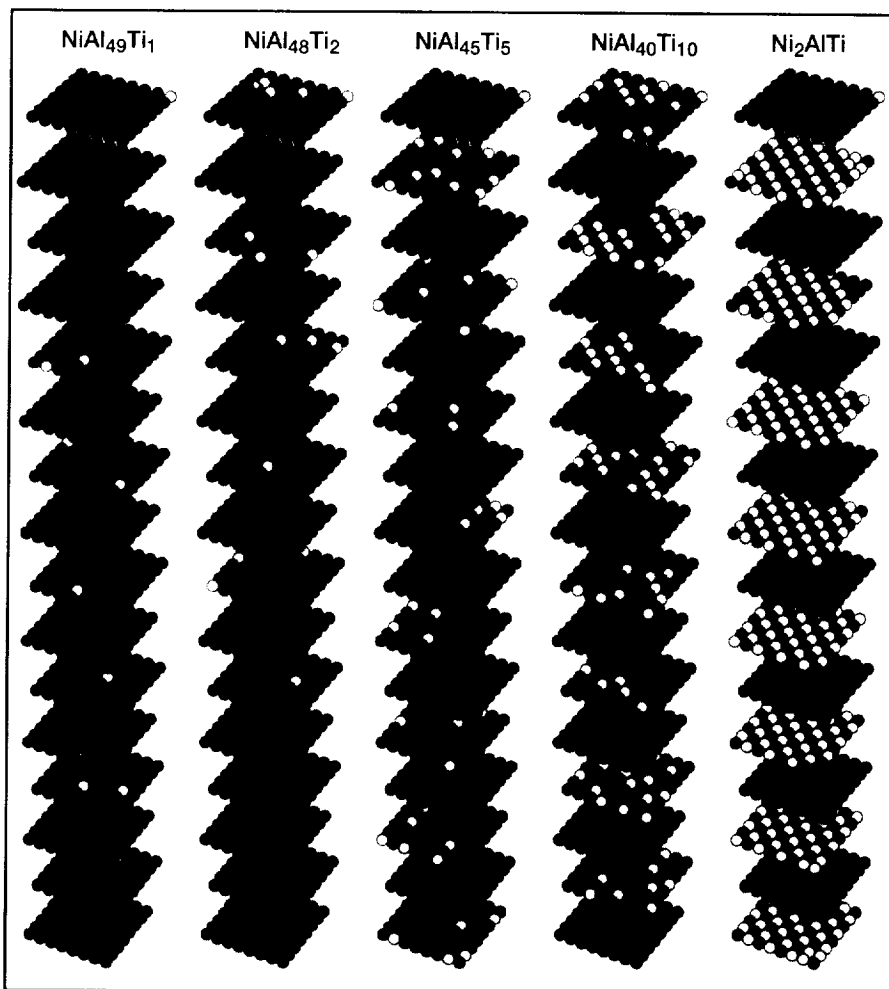
**Author:** Dr. Alan D. Freed

**Headquarters program office:** OA

<sup>1</sup>This is a one-to-one mapping (transformation law) between tensor fields defined on a body manifold to tensor fields defined on the spatial manifold.

# BFS Method for Alloys Optimized and Verified for the Study of Ordered Intermetallic Materials

The aerospace industry has a need for new metallic alloys that are light-weight and have high strength at elevated temperatures. However, the current design method for new materials is largely experimental, requiring substantial capital investment in processing the material and in determining the material's microstructure and properties. Theoretical methods that would narrow the field of promising candidate materials could substantially reduce cost and development time.



*Ni-Al-Ti alloys modeled with BFS, for different Ti concentrations. Above 5 at.% Ti, the formation of Heusler precipitates is seen. For 25 at.% Ti, the computational cell (1024 atoms) displays Heusler ordering with a few antistructural atoms.*

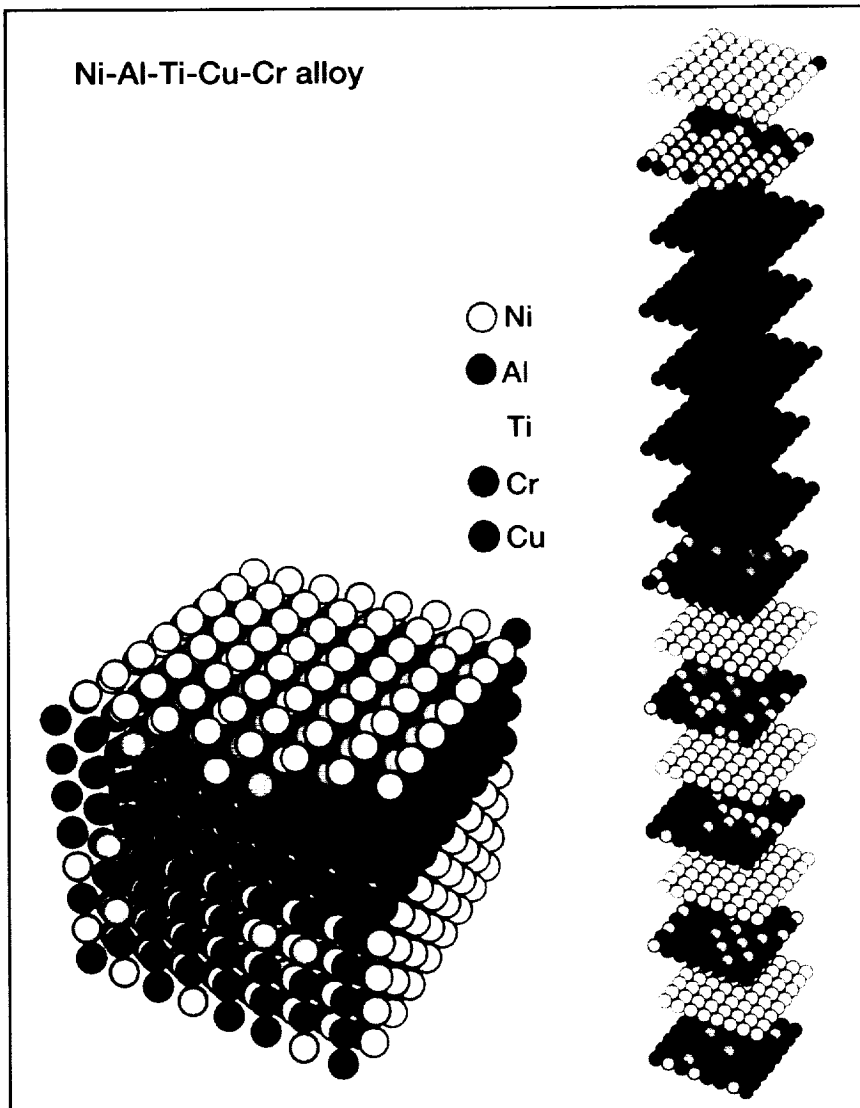
The BFS (Bozzolo, Ferrante, and Smith) method is a new, computationally efficient and physically sound quantum semi-perturbative approach for describing metals and their defects. Based on a simple interpretation of the alloy formation process that identifies strain and chemical contributions to the energy of the alloy, the method provides an atom-by-atom description of an alloy. Its implementation requires little more than algebra and the solution of transcendental equations.

In contrast, methods previous to BFS suffered from many limitations. The state-of-the-art nonatomistic approaches rely heavily on developing a substantial data base, then extrapolating to predict new properties. Although this approach has been successful, it leads to incremental rather than revolutionary improvements. Other approaches—such as first-principles, quantum mechanical methods, and other competing semi-empirical methods—suffer from more serious limitations. Quantum mechanical methods, although in principle the best, require so much CPU time as to make calculations on applied problems infeasible. Competing semi-empirical methods are limited to a few face-centered-cubic metals and are not successful in predicting most alloy properties.

At the NASA Lewis Research Center, we have demonstrated (ref. 1) that BFS can investigate the properties of a large number of alloys with a minimum computational effort on low-level computers. This screening allows the selection of the best alloy candidates for a particular application and, therefore, promises large cost savings over current approaches.

BFS has been tested in a variety of situations, consistently giving results in excellent agreement with experimental results. More recently, the method has been optimized for modeling ordered intermetallic alloys that are of interest in aeronautical applications, including the determination of the defect structure of FeAl alloys (ref. 2) and the characterization of ternary and quaternary  $\text{Ni}_3\text{Al}$ -based alloys (ref. 3). Much of the recent effort, however, has focused on

## Ni-Al-Ti-Cu-Cr alloy



*Ni-Al-Ti-Cu-Cr alloy modeled with BFS. The computational cell displays the formation of a Cr precipitate within the NiAl matrix. Also, the formation of the Heusler ( $\text{Ni}_2\text{AlTi}$ ) phase is observed. Cu atoms are found only in the interface between NiAl and the  $\alpha$ -Cr precipitate.*

alloy design of NiAl-based materials. The complexity of the systems modeled range from three-component, two-phase alloys (such as the Ni-Al-Ti alloys shown in the first figure) to five-component, three-phase alloys that exhibit solute enrichment at the interfaces (as shown in the figure above). Such complex structures cannot be modeled by alternative techniques, and the accuracy of the predictions has been verified by appropriate experimental studies.

The BFS method is not limited solely to high-temperature structural alloy design. It can be applied to the design of high-performance alloys for any application. In addition to the design function, it can be used in place of or in conjunction with experiments to analyze the poorly understood mechanical and thermal properties of existing alloys. The method also has shown potential to perform revolutionary analysis of alloy structures and thin films and to be applied in interface-related studies (ref. 4).

## References

1. Bozzolo, G.; Ferrante, J.; and Kobistek, R.: J. Computer-Aided Mater. Design, vol. 1, 1993, p. 305.
2. Bozzolo, G., et al.: Scripta Mater., 1996, in press.
3. Bozzolo, G.; Ferrante, J.J.: Computer-Aided Mater. Design, vol. 2, 1995, p. 113.
4. Bozzolo, G.; Ferrante, J.; and Noebe, R.D.: Surf. Sci., 1996, in press.

## Lewis contacts:

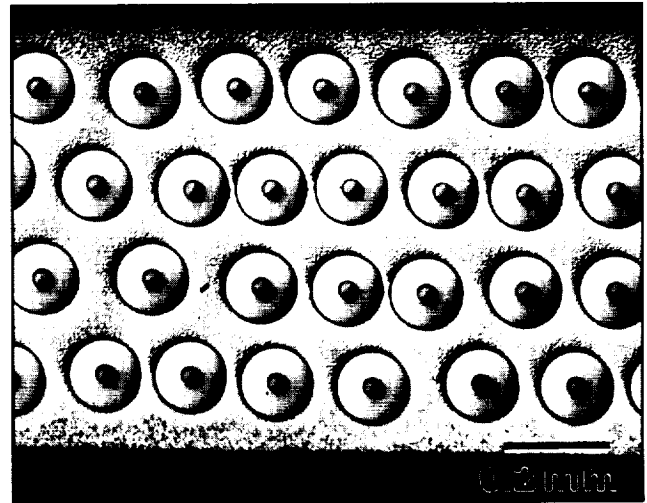
Dr. Guillermo H. Bozzolo,  
(216) 433-5824,  
Guillermo.H.Bozzolo@lerc.nasa.gov;  
Dr. Ronald D. Noebe, (216) 433-2093,  
Ronald.D.Noeb@lerc.nasa.gov; and  
Dr. John Ferrante, (216) 433-6069,  
John.Ferrante@lerc.nasa.gov

**Author:** Dr. Ronald D. Noebe

**Headquarters program office:** OA

# Orthorhombic Titanium Matrix Composite Subjected to Simulated Engine Mission Cycles

Titanium matrix composites (TMC's) are commonly made up of a titanium alloy matrix reinforced by silicon carbide fibers that are oriented parallel to the loading axis. These composites can provide high strength at lower densities than monolithic titanium alloys and superalloys in selected gas turbine engine applications. The use of TMC rings with unidirectional SiC fibers as reinforcing rings within compressor rotors could significantly reduce the weight of these components (ref. 1). In service, these TMC reinforcing rings would be subjected to complex service mission loading cycles, including fatigue and dwell excursions. Orthorhombic titanium aluminide alloys are of particular interest for such TMC applications because their tensile and creep strengths are high in comparison to those of other titanium alloys (ref. 2). The objective of this investigation was to assess, in simulated mission tests at the NASA Lewis Research Center, the durability of a SiC(SCS-6)/Ti-22Al-23Nb (at.%) TMC for compressor ring applications, in cooperation with the Allison Engine Company.

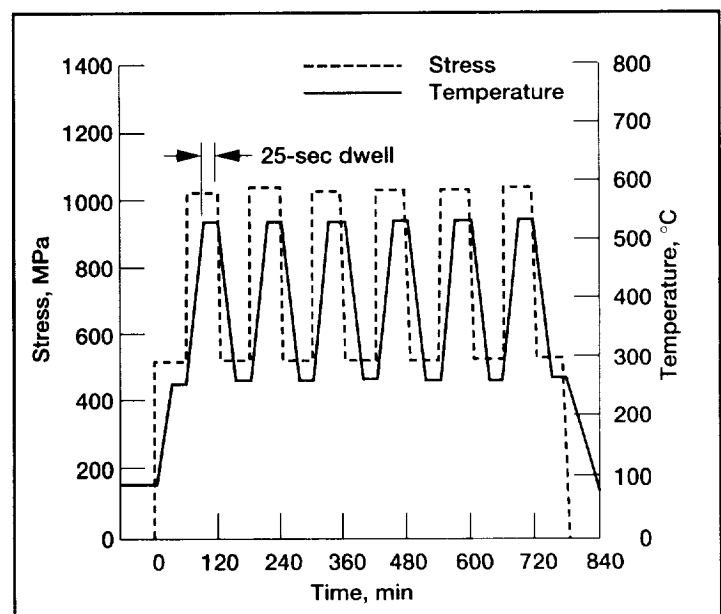


Typical cross section of an SCS-6/Ti-22Al-23Nb(at.%) composite panel.

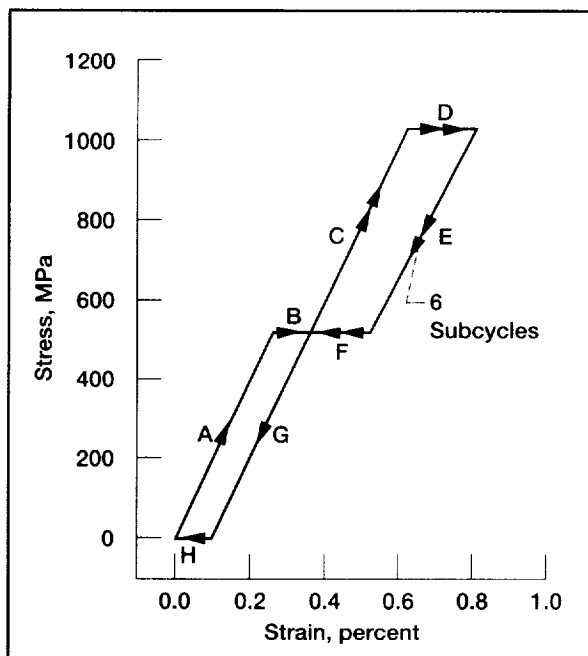
The composite consisted of Ti-22Al-23Nb (at.%) alloy reinforced by 41 vol % of unidirectional SCS-6 SiC fibers and consolidated by hot isostatic pressing. A typical specimen cross-section is shown in the photomicrograph. Specimens having a uniform reduced midsection with the fibers oriented parallel to the loading axis were machined and tested on a computer-controlled servohydraulic fatigue test system heated by a quartz lamp.

$R_\sigma = 0.5$ . One total mission cycle is composed of one Type I and six Type III subcycles. Baseline conditions of  $\sigma_{\max} = 1035$  MPa and  $T_{\max} = 538^\circ\text{C}$  were chosen for detailed evaluations.

Isothermal fatigue load-controlled tests were first performed at a frequency of 0.33 Hz, a temperature of  $538^\circ\text{C}$ , and a maximum applied stress ( $\sigma_{\max}$ ) of 1035 MPa. The effects of a more realistic simulated mission cycle were then assessed. The Allison baseline mission cycle was designed to simulate aircraft engine operation in a simplified manner. The mission, illustrated in the first graph, is made up of a "Type I" major cycle and "Type III" subcycles. The Type I cycle represents starting the engine, accelerating and stabilizing at maximum engine power at the beginning of an aircraft mission, and later shutting down the engine at the end of an aircraft mission. This cycle is simulated in the mechanical test specimen by an excursion from minimum temperature and zero stress through  $\sigma_{\max}$  and maximum temperature ( $T_{\max}$ ), with a cyclic stress ratio ( $R_\sigma$ ) of zero. Type III subcycles represent going from engine idle to maximum power, stabilizing at maximum power, then returning to idle at different times during a mission. This cycle is simulated in the mechanical test specimen by an excursion from intermediate stress and temperature through  $T_{\max}$  and  $\sigma_{\max}$ , with



Applied stress and temperature versus time in the Allison baseline mission cycle.



*Typical stabilized stress-strain hysteresis loop of the baseline mission cycle. A—load at 93 °C; B—heat to 260 °C; C—load at 260 °C; D—heat to 538 °C, then dwell at  $\sigma_{max}$ ,  $T_{max}$ ; E—unload at 538 °C; F—cool to 260 °C; G—unload at 260 °C; H—cool to 93 °C.*

#### **Lewis contacts:**

Timothy P. Gabb, (216) 433-3272,  
timothy.p.gabb@lerc.nasa.gov; and  
Dr. John Gayda, (216) 433-3273,  
John.Gayda@lerc.nasa.gov

**Author:** Timothy P. Gabb

**Headquarters program office:** OA

The second graph shows a typical stabilized stress-strain hysteresis loop with segment descriptions. The average mission life was 1235 cycles, significantly lower than the average isothermal life of 8149 cycles in duplicate tests with the same maximum temperature and stress. The mission test specimens had fatigue cracks initiating from damaged fibers along the machined specimen edges, as in isothermal specimens. However, the percentage of fatigue-cracked area in mission tests was significantly lower than in isothermal tests. This appeared to be associated with a process of enhanced cyclic stress relaxation of the matrix during the mission. The process encouraged load transfer from the matrix to the fibers, which suppressed fatigue cracking and induced fiber overload. In future work, mission tests will be performed on orthorhombic TMC's that contain fibers with greater inherent strength.

#### **References**

1. Larsen, J.M.; Revelos, W.C., and Gambone, M.L.: An Overview of Potential Titanium Aluminide Composites in Aerospace Applications. Intermetallic Matrix Composites II, Mat. Res. Soc. Symp. Proc., D.B. Miracle, D.L. Anton, and J.A. Graves, eds., Materials Research Society, Pittsburgh, PA, vol. 273, 1992, pp. 3-16.
2. Smith, P.R.; Graves, J.A.; and Rhodes, C.G.: Evaluation of an SCS-6/Ti-22Al-23Nb "Orthorhombic" Composite. Intermetallic Matrix Composites II, Mat. Res. Soc. Symp. Proc., D.B. Miracle, D.L. Anton, and J.A. Graves, eds., Materials Research Society, Pittsburgh, PA, vol. 273, 1992, pp. 43-52.

## Development of Creep-Resistant NiAl(Ti,Hf) Single-Crystal Alloys

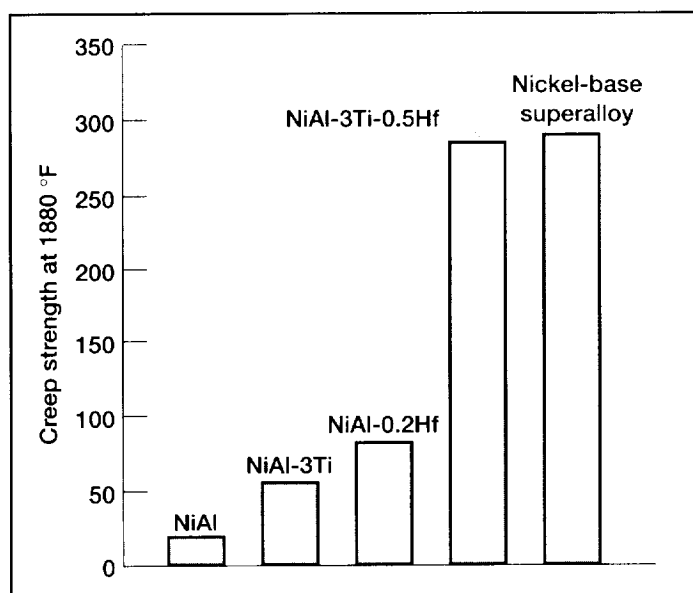
Nickel-base superalloys are the current choice for high-temperature jet engine applications such as turbine blades and vanes. However, after more than five decades of use, nickel-base superalloys have reached their limit, since the operating temperatures in gas turbine engines are now approaching the melting temperature of these alloys. Thus alternative materials, such as lightweight NiAl intermetallic alloys with superior properties, (e.g., high melting temperature, high thermal conductivity, and excellent chemical stability and oxidation resistance) are required for the next generation of high-temperature structural materials for more efficient 21st century civil transport systems.

The two major disadvantages that have historically prevented the application of NiAl as a high-temperature structural material are its poor creep resistance and low room-temperature ductility. Alloying strategies similar to those used for nickel-base superalloys are being used to improve the high-temperature strength via solid-solution and precipitate-hardening effects. This study highlights the potent role of Ti and Hf as potential solid-solution strengtheners in NiAl and also the added effect of second-phase particles when Ti and Hf are both used.

The high-temperature deformation behavior of  $\langle 001 \rangle$  NiAl-3Ti, NiAl-0.2Hf, and NiAl-3Ti-0.5Hf (at.%) single crystals was studied at the NASA Lewis Research Center in the temperature range  $\sim 800$  to  $1150^\circ\text{C}$ . The bar graph shows steady-state creep strengths of these alloys at  $1027^\circ\text{C}$  ( $1880^\circ\text{F}$ ) at a strain rate of  $\sim 10^{-6} \text{ sec}^{-1}$ . Comparison of these alloys with unalloyed NiAl and a first-generation single-crystal superalloy shows that the strengths of the NiAl alloys are higher than those of binary NiAl and that they approach

that of the superalloy. This increase in strength (to that of the superalloy) was accomplished with total alloying additions of less than four atomic percent. Furthermore, because the NiAl-3Ti-0.5Hf alloy is much lighter than the superalloy, it would exhibit about a 30-percent greater density-compensated creep strength in comparison to the superalloy under the test conditions described in the bar graph.

Transmission electron microscopy observations showed essentially no precipitation in the NiAl-3Ti and NiAl-0.2Hf alloys. Additional analysis revealed that strengthening in these alloys is due solely to solid-solution effects through a significant increase in the drag force on dislocations. When both Hf and Ti are added to the alloy, the individual solubility for each element decreases, resulting in significant precipitation. Consequently, the NiAl-3Ti-0.5Hf alloy contained a high density of very fine Heusler ( $\text{Ni}_2\text{AlTi}$ ) precipitates and a lower density of heterogeneously nucleated and somewhat coarser Heusler ( $\text{Ni}_2\text{Al}(\text{Hf,Ti})$ ) precipitates within the NiAl matrix, as shown in the photomicrograph. A higher level of strength was achieved in this precipitate-containing alloy because of the combined strengthening effects associated with solute drag on the dislocations plus impedance due to the presence of precipitate particles. The strength level of this alloy approaches that of the superalloy single crystal, whereas even higher levels of these alloying additions would increase the amount of precipitate phase and the strength of the NiAl even further.



Creep strength comparison of binary NiAl, alloyed NiAl single crystals, and a first-generation single-crystal nickel-base superalloy made at  $1880^\circ\text{F}$  and a strain rate of  $1 \times 10^{-6} \text{ sec}^{-1}$ .



*Microstructure of a creep-resistant NiAl-3Ti-0.5Hf single-crystal alloy.*

Consequently, through combined solid-solution and precipitation-strengthening mechanisms, NiAl alloys can be developed with creep strengths equivalent or superior to conventional nickel-base superalloys, while at the same time providing a 33-percent weight savings and higher temperature capability.

**Lewis contacts:** Dr. Ronald D. Noebe, (216) 433-2093, Ronald.D.Noebe@lerc.nasa.gov; Dr. Anita Garg, (216) 433-8908, Anita.Garg@lerc.nasa.gov; and Dr. J. Daniel Whittenberger, (216) 433-3196, jdwhittenberger@lerc.nasa.gov

**Author:** Dr. Ronald D. Noebe

**Headquarters Program Office:** OA

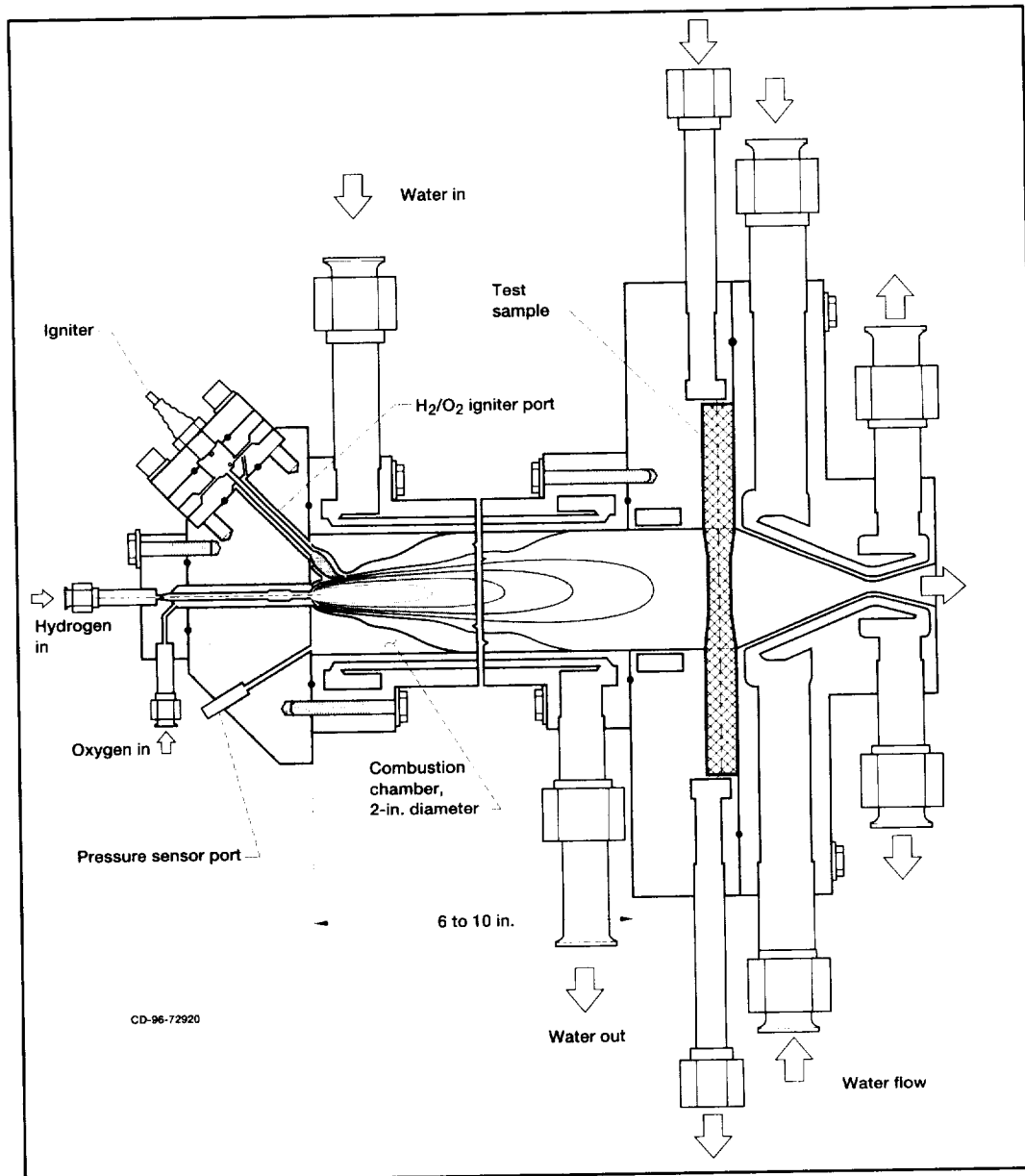
## Oxygen Compatibility Screening Tests in Oxygen-Rich Combustion Environment

The identification and characterization of oxygen-rich compatible materials enables full-flow, staged combustion designs. Although these oxygen-rich designs offer significant cost, performance, and reliability benefits over existing systems, they have never been used operationally by the United States. If these systems are to be realized, it is critical to understand the long-term oxidative stability in high-temperature, high-pressure, oxygen-rich combustion environments. A unique facility has been constructed at the NASA Lewis Research Center to conduct tests of small-scale rocket engine materials and subcomponents in an oxygen-rich combustion environment that closely approximates a full-scale rocket engine. Thus, a broad range of advanced materials and concepts can be screened in a timely manner and at a relatively low cost.

The test stand and corresponding tests are part of a national program to evaluate materials for use in oxygen-rich combustion environments. At the

onset of the program, a facility suitable for long-term oxygen-rich exposure testing did not exist. Cell 22 of Lewis' combustion research laboratory (CRL) could operate in oxygen-rich environments, but not at the desired oxygen-to-hydrogen ratio of >150:1. Modifications to the test stand allow operation of multiple full-design cycles (10 min each) at oxygen-to-hydrogen ratios of up to 175:1. In addition to revamping the oxygen-to-hydrogen ratio capability, the facility was modified to accommodate testing specimens





*Hydrogen/oxygen combustor test stand for advanced materials evaluation (internal test sample configuration).*

inside the combustion chamber (see the figure). Internal placement of the test specimens provides an environment with higher pressure and reduced flow in comparison to placement in the exhaust plume.

In summary, a new national facility was constructed for long exposures of advanced materials in high-temperature, high-pressure, oxygen-rich combustion environments. The facility demonstrated excellent temperature distribution and control across the test sample gage. Five materials, down-selected from data obtained by other tests, were exposed to more than 2130 min total in the new facility. All five materials survived multiple full-design cycle exposures, with only minimal surface oxidation visible afterwards.

**Lewis contacts:**

Andrew J. Eckel, (216) 433-8185,  
 Andrew.J.Eckel@lerc.nasa.gov;  
 Dr. Ali Sayir, (216) 433-6254,  
 Ali.Sayir@lerc.nasa.gov; and  
 Dr. Thomas P. Herbell, (216) 433-3246,  
 Thomas.P.Herbell@lerc.nasa.gov

**Author:** Andrew J. Eckel

**Headquarters program office:** OSAT

# Alternative Processing Method Leads to Stronger Sapphire-Reinforced Alumina Composites

The development of advanced engines for aerospace applications depends on the availability of strong, tough materials that can withstand increasingly higher temperatures under oxidizing conditions. The need for such materials led to the study of an oxide-based composite composed of an alumina matrix reinforced with zirconia-coated sapphire fibers. Because the nonbrittle behavior of this system depends on the interface and its ability to prevent fiber-to-matrix bonding and reduce interfacial shear stress, the microstructure of the zirconia must be carefully controlled during both coating application and composite processing. When it was both porous and unstabilized, zirconia (which does not react easily with alumina) was found to be the most effective material tested in reducing interfacial shear strength between the fiber and matrix.

From initial composite fabrication efforts, processing parameters to maintain the porosity of the interfacial coatings were determined at the NASA Lewis Research Center. Low temperatures and pressures were needed to avoid severe densification of the interfacial coating. Under these conditions, however, densification of the matrix was also limited. It was therefore necessary to alter the composite processing method to increase matrix densification while maintaining the porosity of the fiber coating.

By adding aluminum metal to the matrix and utilizing the conversion of aluminum to aluminum oxide in the initial processing stage of composite formation, it was possible to increase matrix density while maintaining a weak fiber/matrix interface in a sapphire-reinforced alumina matrix composite. The reaction formation of alumina led to an extremely fine grain size in the matrix that increased the sinterability and strength of the final ceramic. Without aluminum additions, the matrix density was approximately 62 percent of the theoretical density of alumina. Addition of aluminum increased matrix density up to 85 percent of the theoretical density. As anticipated, the composite strengths also increased with matrix density and aluminum content. Both first matrix cracking (the stress level at which matrix cracks first appear) and ultimate stress increased significantly.

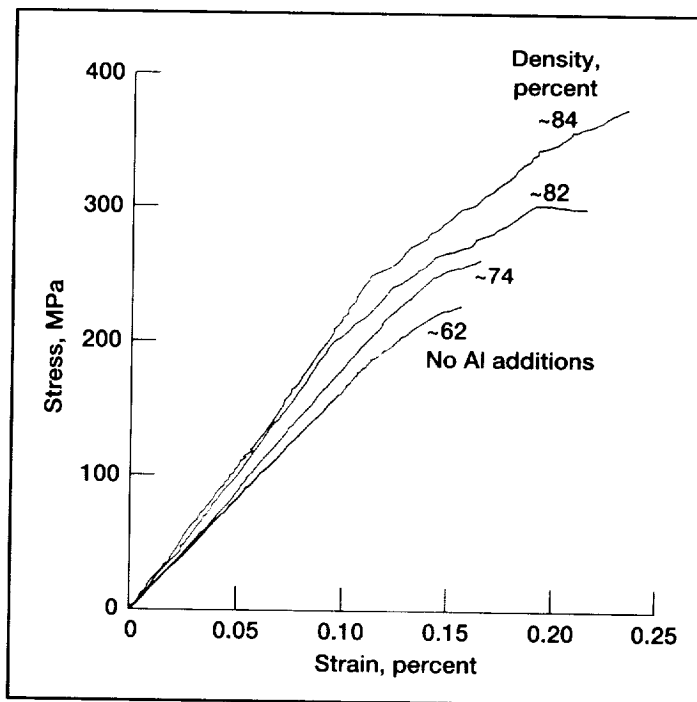
## Lewis contact:

Martha H. Jaskowiak, (216) 433-5515,

Martha.H.Jaskowiak@lerc.nasa.gov

Author: Martha H. Jaskowiak

Headquarters program office: OA



*Influence of increased matrix density on composite behavior.*

# Single-Tow Minicomposite Test Used to Determine the Stressed-Oxidation Durability of SiC/SiC Composites

SiC-fiber-reinforced SiC-matrix composites are considered future materials for high-temperature ( $>1200^{\circ}\text{C}$ ), air-breathing applications. For these materials to be successful, they must be able to maintain desirable mechanical properties at high temperatures while existing in highly corrosive environments. The critical constituent of a ceramic matrix composite is a thin interphase layer between the fiber and matrix which enables matrix cracks to deflect around the fibers, that is, to perform even when damaged. Unfortunately, the only interphase materials (to date) that offer the desired properties are carbon and boron nitride. Both of these materials react with oxidizing environments to form gaseous or liquid oxidation products that can lead to fiber-strength degradation or strong bonding between the fiber and the matrix at temperatures above  $\sim 600^{\circ}\text{C}$ .

Because it is important to understand the failure mechanisms and lifetimes expected for these composites under stressed-oxidative conditions, a single-tow minicomposite test was developed at the NASA Lewis Research Center to evaluate a number of different fiber/interphase combinations to determine which system has the best properties. The minicomposite consists of a single tow of SiC fibers (there are  $\sim 500$   $15\text{-}\mu\text{m}$ -diameter fibers in a tow), an interphase material ( $0.5\text{-}\mu\text{m}$ -thick C or BN), and a chemical-vapor-infiltrated SiC matrix.

A stress-rupture test was used to determine the stressed oxidative behavior of the minicomposite systems. Minicomposites were first precracked with a relatively high load to expose the interphases to the environment. Then, they were placed in a stress-rupture rig where a constant load and temperature ( $700$  to  $1200^{\circ}\text{C}$ ) were applied until the minicomposite failed.

We found that the carbon-interphase minicomposites had significantly poorer rupture properties than the BN-interphase minicomposites. These

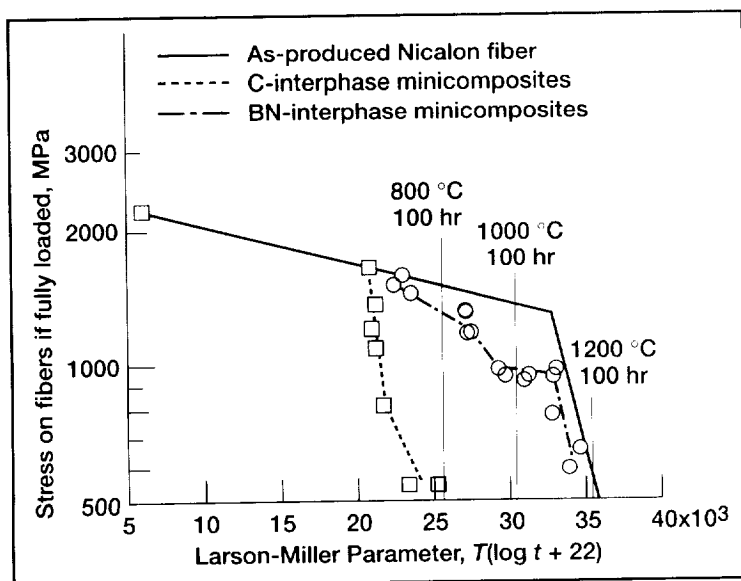
data were compared with what would be expected for individual fiber-rupture data with the same starting fiber strength (this is considered to be the best any composite could do with these fibers). Drastic degradation in rupture properties occurred at  $\sim 700^{\circ}\text{C}$  for carbon-interphase minicomposites. Microscopy showed that the carbon-interphase disappeared and the Nicalon fiber degraded to cause this behavior. For the BN-interphase minicomposites, only mild degradation in rupture properties occurred. In fact, the degradation in rupture properties for the BN-interphase minicomposites is about the same as that for the individual fibers, except for the data at  $\sim 950 \pm 100^{\circ}\text{C}$ . Microscopy showed that the BN-interphase also disappeared; however, glass layers were formed on the fiber surface and fiber/matrix bonding occurred for  $\geq 900^{\circ}\text{C}$  experiments. It is presumed that this intermediate temperature composite "embrittlement" was due to increased stress concentrations on the fibers as a result of the strong bonding. At  $1200^{\circ}\text{C}$ , glass filled the interphase region; however, the minicomposite rupture properties were the same as the fiber-rupture properties. It is evident that BN-interphase SiC/SiC composites are superior at high temperatures. This study is being advanced to understand cyclic loading conditions where the susceptibility to stress-concentrations are greater.

## Lewis contact:

Gregory N. Morscher, (216) 433-5512,  
Gregory.N.Morscher@lerc.nasa.gov

Author: Gregory N. Morscher

Headquarters program office: OA



Rupture properties for C-interphase and BN-interphase minicomposites in air. Temperature in degrees kelvin,  $T$ ; time in hours,  $t$ .

# First Single-Crystal Mullite Fibers

Ceramic-matrix composites strengthened by suitable fiber additions are being developed for high-temperature use, particularly for aerospace applications. New oxide-based fibers, such as mullite, are particularly desirable because of their resistance to high-temperature oxidative environments. Mullite is a candidate material in both fiber and matrix form. The primary objective of this work was to determine the growth characteristics of single-crystal mullite fibers produced by the laser-heated floating zone method.

Directionally solidified fibers with nominal mullite compositions of  $3\text{Al}_2\text{O}_3 \cdot 2\text{SiO}_2$  were grown by the laser-heated floating zone method at the NASA Lewis Research Center. SEM analysis revealed that the single-crystal fibers grown in this study were strongly faceted and that the facets act as critical flaws, limiting fiber strength. The average fiber tensile strength is 1.15 GPa at room temperature. The mullite fibers exhibit superior strength retention (80 percent of their room temperature tensile strength at 1450 °C). Examined by transmission electron microscopy, these mullite single crystals are free of dislocations, low-angle boundaries, and voids. In addition, they show a high degree of oxygen vacancy ordering.

## Bibliography

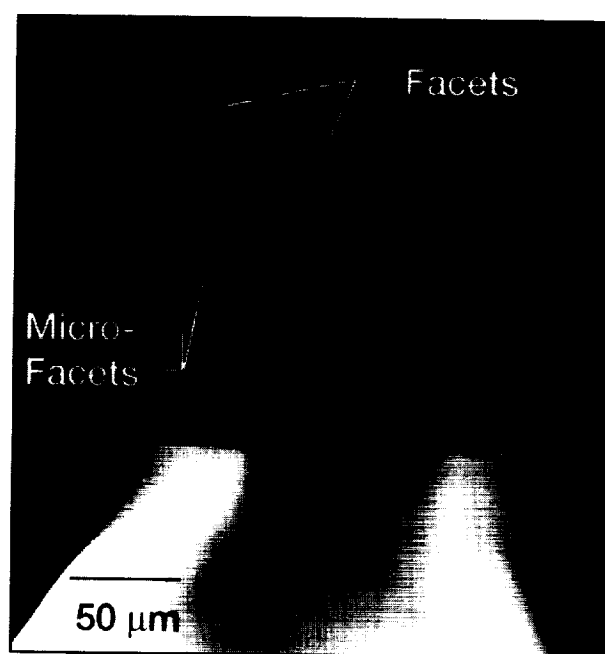
Sayir, A.; and Farmer, S.C.: Directionally Solidified Mullite Fibers. Ceramic Matrix Composites: Advanced High-Temperature Structural Materials, Mat. Res. Soc. Symp. Proc., R.A. Lowden, ed., Materials Research Society, Pittsburgh, PA, vol. 365, 1995, pp. 11-21.

## Lewis contacts:

Dr. Ali Sayir, (216) 433-6254, Ali.Sayir@lerc.nasa.gov; and Dr. Serene C. Farmer, (216) 433-3289, Serene.C.Farmer@lerc.nasa.gov

**Author:** Dr. Ali Sayir

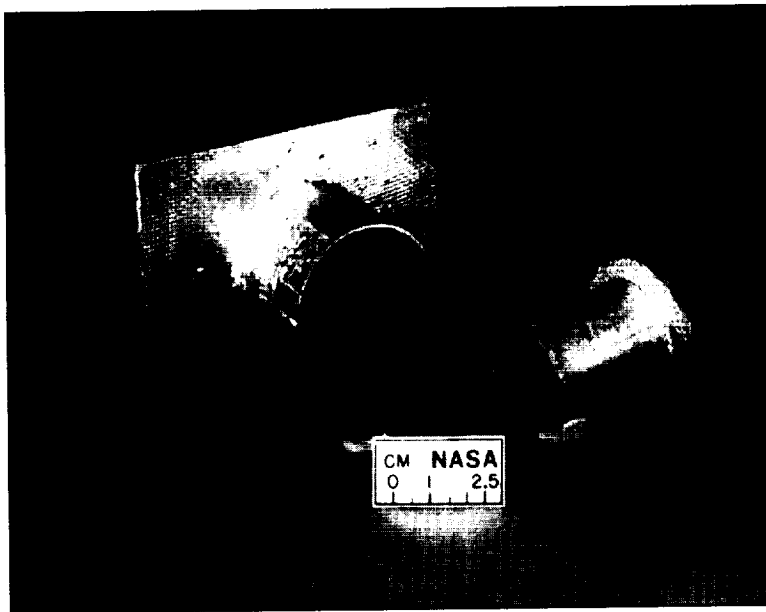
**Headquarters program office:** OA



*Strongly faceted single-crystal growth from planar interface (note loss of axial symmetry).*

High-resolution digital images from an optical microscope furnish evidence of the formation of a liquid-liquid miscibility gap during crystal growth. These images represent the first experimental evidence of liquid immiscibility for these compositions and temperatures. Continuing investigation with controlled seeding of mullite single crystals is planned.

## Method for Efficient Joining of Silicon-Carbide-Based Ceramic Materials Developed



*Joined SiC/SiC ceramic matrix composite (CMC) plates and cylinders.*

### **Lewis contacts:**

Dr. Mrityunjay Singh, (216) 433-8883,  
Mrityunjay.Singh@lerc.nasa.gov; and  
J. Douglas Kiser, (216) 433-3247,  
James.D.Kiser@lerc.nasa.gov

**Author:** J. Douglas Kiser

**Headquarters program office:** OA

An affordable and flexible method of joining silicon-carbide- (SiC-) based monolithic ceramics and fiber-reinforced ceramic matrix composites (CMC's) is being developed at the NASA Lewis Research Center. This technology will make it possible for ceramic and CMC components to be used for high-temperature applications in aeropropulsion, launch, and onboard space propulsion systems. Our goal is to develop a joining approach that can be scaled up to provide joints between SiC-based CMC or monolithic ceramic components or subcomponents.

In this joining process, which is based on the SiC reaction processing method, carbonaceous mixtures are applied to the joint area and subsequently infiltrated with molten silicon. The molten silicon reacts with carbon to form SiC joints that contain a controllable amount of silicon. This approach can be controlled via modification of the reactive constituents to yield joints with tailored microstructures and properties. The approach should be affordable because precision joint machining is unnecessary, the reactive constituents are inexpensive, and a pressureless melt infiltration process is used to introduce the molten silicon. The flexibility of the process makes it applicable to the joining of any SiC-based monolithic or composite material, and the ready availability of the required processing equipment to commercial materials suppliers facilitates technology transfer.

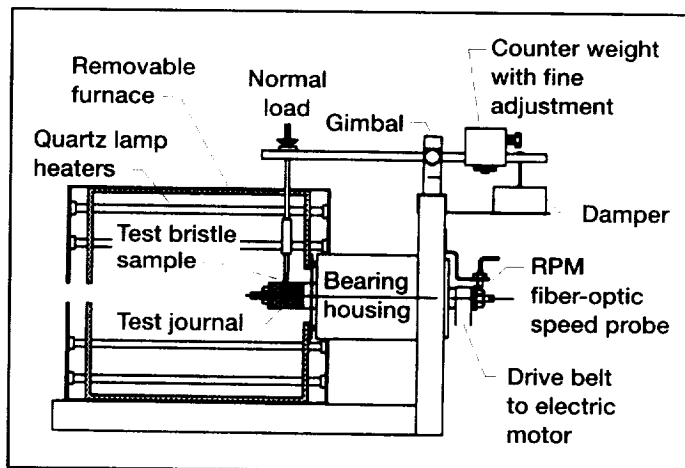
Thus far, several types of commercially available and NASA-processed SiC ceramics—including reaction bonded, reaction formed, and pressureless sintered SiC—have been joined. Joints having strengths that equaled or exceeded the strength of the base material were formed in reaction-bonded SiC. In addition, the ability to join CMC cylinders to CMC panels by using this reaction-joining approach has been demonstrated, as shown in the photo.

# Unique Tuft Test Facility Dramatically Reduces Brush Seal Development Costs

Brush seals have been incorporated in the latest turbine engines to reduce leakage and improve efficiency. However, the life of these seals is limited by wear. Studies have shown that optimal sealing characteristics for a brush seal occur before the interference fit between the brush and shaft is excessively worn. Research to develop improved tribopairs (brush and coating) with reduced wear and lower friction has been hindered by the lack of an accurate, low-cost, efficient test methodology. Estimated costs for evaluating a new material combination in an engine company seal test program are on the order of \$100,000.

To address this need, the NASA Lewis Research Center designed, built, and validated a unique, innovative brush seal tuft tester that slides a single tuft of brush seal wire against a rotating shaft under controlled loads, speeds, and temperatures comparable to those in turbine engines. As an initial screening tool, the brush seal tuft tester can tribologically evaluate candidate seal materials for *1/10th the cost of full-scale seal tests*.

Previous to the development of the brush seal tuft tester facility, most relevant tribological data had been obtained from full-scale seal tests conducted primarily to determine seal leakage characteristics. However, from

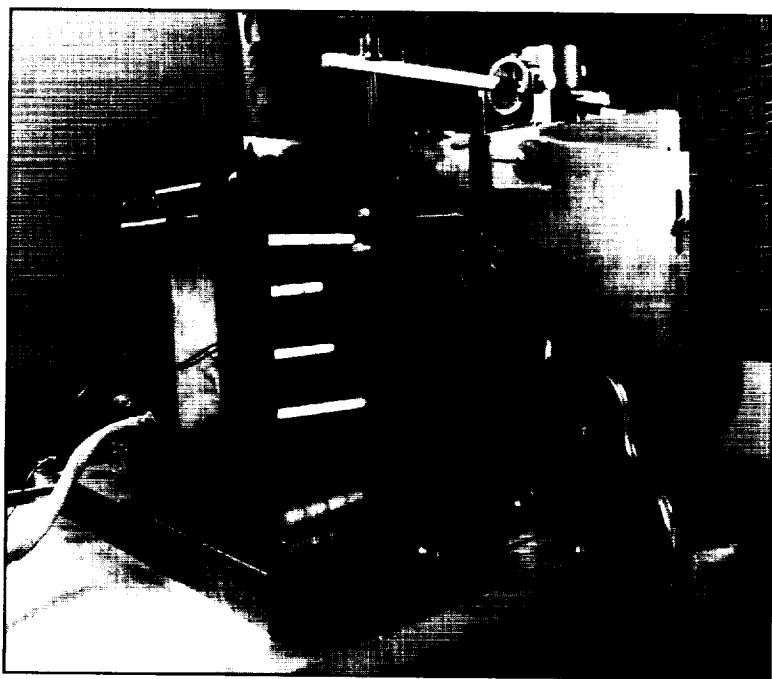


*Cross-section side view of the brush seal tuft tester.*

a tribological point of view, these tests included the confounding effects of varying contact pressures, bristle flaring, high-temperature oxidation, and varying bristle contact angles. These confounding effects are overcome in tuft testing. The interface contact pressures can be either constant or varying depending on the tuft mounting device, and bristle wear can be measured optically with inscribed witness marks.

In a recent cooperative program with a U.S. turbine engine manufacturer, five metallic wire candidates were tested against a plasma-sprayed Nichrome-bonded chrome carbide. The wire materials used during this collaboration were either nickel-chrome- or cobalt-chrome-based superalloys. These tests corroborated full-scale seal test results and provided insight into previously untested combinations.

As the cycle temperature for improved efficiency turbine engines increases, new brush seal materials combinations must be considered.



*NASA Lewis brush seal tuft tester in operation with half of the furnace shell removed.*

Future brush seal tuft testing will include both metallic and ceramic bristles versus commercial and NASA-developed shaft coatings. The ultimate goal of this work is to expand the current data base so that seal designers can tailor brush seal materials to specific applications.

### Bibliography

Fellenstein, J.A., et al.: High Temperature Brush Seal Tuft Testing of Metallic Bristles Versus Chrome Carbide. NASA TM-107238, 1996.

Fellenstein, J.A.; and DellaCorte, C.: A New Tribological Test for Candidate Brush Seal Materials Evaluation. NASA TM-106753, 1995.

**Lewis contact:** James A. Fellenstein, (216) 433-6065,  
James.Fellenstein@lerc.nasa.gov

**Author:** James A. Fellenstein

**Headquarters program office:** OA

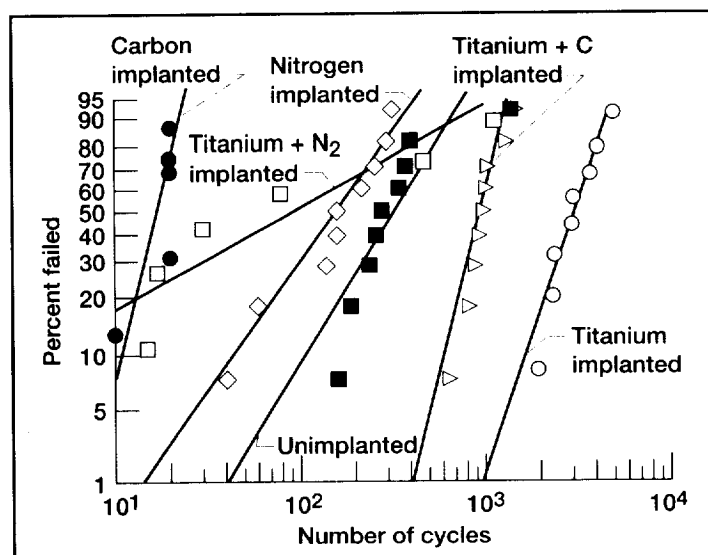
## Ion Implantation of Perfluoropolyether-Lubricated Surfaces for Improved Tribological Performance

For over 30 years, perfluoropolyethers (PFPE's) have been the liquid lubricants of choice for space applications because of their proven tribological performance and desirable properties, such as low vapor pressure and a wide liquid temperature range. These oils are used in such space mechanisms as gyroscopes, scanning mirrors, actuators, and filter wheels. In the past few years, there have been several incidents during which PFPE-lubricated space mechanisms have shown anomalous behavior. These anomalies are thought to be the result of PFPE degradation.

without affecting either the properties or dimensions of the bulk material beneath the treated layer. By introducing a foreign species into a submicron surface layer, ion implantation can induce unique surface microstructures.

Investigative research focused on understanding and modeling the degradation of PFPE lubricants has shown that PFPE's degrade and lose their desirable properties while under boundary-lubricated, sliding/rolling contacts and at elevated temperatures. These performance deficiencies are strongly dependent on the surface chemistry and reactivity of the lubricated contacts, which dictate the formation of harmful catalytic byproducts. One way to inhibit tribo-induced degradation may be to use passivated surfaces that do not promote the formation of harmful byproducts. Such a passivated surface would inhibit PFPE degradation and increase the lifetime of the lubricated mechanism.

Ion implantation is one such passivation technique. This surface-treatment technique can modify the surface properties of materials



Effect of ion implantation on Weibull distribution lifetimes for lubricated disks.

One notable study conducted by engineers from the NASA Lewis Research Center, Colorado State University, and Colorado School of Mines shows promise in enhancing PFPE-lubricating longevity by passivating the mating surfaces via ion implantation. In this study, thin films of a commercial PFPE lubricant were investigated in the presence of ion-implanted 440C steel. Stainless steel samples were implanted with either N<sub>2</sub>, C, Ti, Ti + N<sub>2</sub>, or Ti + C. The PFPE (60- to 400-Å thick) was applied uniformly across the surface; then, the steel was tested tribologically in an N<sub>2</sub> atmosphere.

Each of the ion-implantation conditions affected the lubricating longevity of the PFPE. Ranked from most to least effective in prolonging longevity, the implanted species were Ti, Ti + C, unimplanted, N<sub>2</sub>, and C  $\cong$  Ti + N<sub>2</sub>. In the mechanism postulated to explain these results, either a passivating or reactive layer was formed that either inhibited or facilitated, respectively, the production of harmful catalytic byproducts. The corresponding surface microstructures induced by ion implantation were obtained from x-ray diffraction and conversion electron Mössbauer spectroscopy. Ion implantation produced microstructures primarily consisting of amorphous structures. The amorphous Fe-Cr-Ti layer formed by implanting Ti ions was credited with increasing the lubricating longevity of the PFPE by an order of magnitude.

#### **Bibliography**

Shogrin, B., et al.: The Effects of Ion Implantation on the Tribology of Perfluoropolyether-Lubricated 440C Stainless Steel Couples. STLE Tribol. Trans. (Also NASA TM-106965), vol. 39, no. 3, 1996, pp. 507-516.

**Lewis contact:** Dr. William R. Jones, Jr., (216) 433-6051, William.R.Jones@lerc.nasa.gov

**Author:** Brad Shogrin

**Headquarters program office:** OSMA

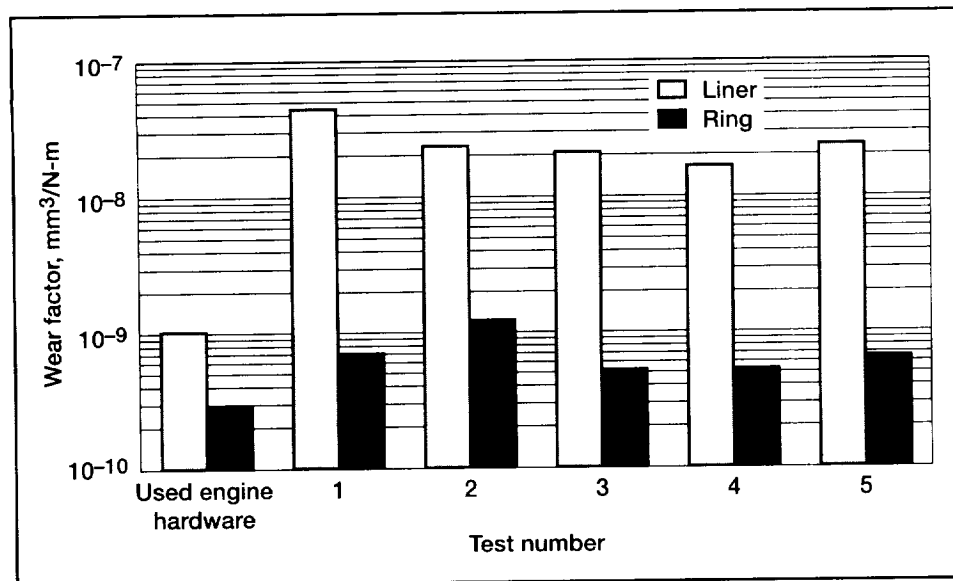
## **Test Method Designed to Evaluate Cylinder Liner-Piston Ring Coatings for Advanced Heat Engines**

Research on advanced heat engine concepts, such as the low-heat-rejection engine, have shown the potential for increased thermal efficiency, reduced emissions, lighter weight, simpler design, and longer life in comparison to current diesel engine designs. A major obstacle in the development of a functional advanced heat engine is overcoming the problems caused by the high combustion temperatures at the piston ring/cylinder liner interface, specifically at top ring reversal (TRR). TRR is the most critical part of the engine cycle because the ring and liner undergo a majority of their wear at this location. In a conventional engine, where TRR temperatures are near 200 °C, the cylinder kit materials consist of chrome-coated piston rings and cast-iron liners. These materials usually provide adequate service for about 500,000 miles before a major overhaul is needed. The TRR temperature in an advanced heat engine; however, has been predicted to be in excess of 300 °C, with some estimates as high as 650 °C. These high temperatures preclude the use of chrome-coated rings and cast-iron

liners because the extreme temperature severely degrades their wear life. Therefore, advanced cylinder liner and piston ring materials are needed that can survive under these extreme conditions.

To address this need, researchers at the NASA Lewis Research Center have designed a tribological test method to help evaluate candidate piston ring and cylinder liner materials for advanced diesel engines. The selected test method uses a commercially available,





*Wear factor results for used engine hardware and baseline tests.*

pin-on-plate, reciprocating wear test rig with specially modified specimens machined from conventional top compression piston rings and cast-iron liners. Loads, speeds, and temperatures are selected to approximate engine wear conditions present at the ring-liner interface at TRR. It is intended that this test setup be used as a screening tool to eliminate poor coating combinations before any effort is expended on costly engine tests.

As a way to validate the test method, repeated baseline tests were run with conventional chrome-coated ring and cast-iron cylinder liner specimens, and the results were compared with used engine hardware. On both the used and test specimens, the worn areas had a smooth glossy finish, which indicated the presence of a fine polishing wear mode. In addition, wear factors, which quantify the amount of wear produced over a given time, were calculated for the used hardware and test specimens. As shown in the figure, the baseline wear factors for both specimens were very repeatable from test to test. When individual components are compared, the ring specimen wear factors are very similar to that of the used ring. The baseline liner wear factors, on the other hand, are an order of magnitude greater than for the used liner, which suggests that the test conditions with respect to the liner are more severe than actual engine experience. Since studies have shown that ring wear is of greater concern, the corroboration exhibited between the wear factors of the used ring and the ring specimen suggests that the test rig and established procedures can be used to conveniently screen material candidates for advanced heat engine applications.

**Lewis contact:** Kevin C. Radil, (216) 433-5047, [Kevin.C.Radil@lerc.nasa.gov](mailto:Kevin.C.Radil@lerc.nasa.gov)

**Author:** Kevin C. Radil

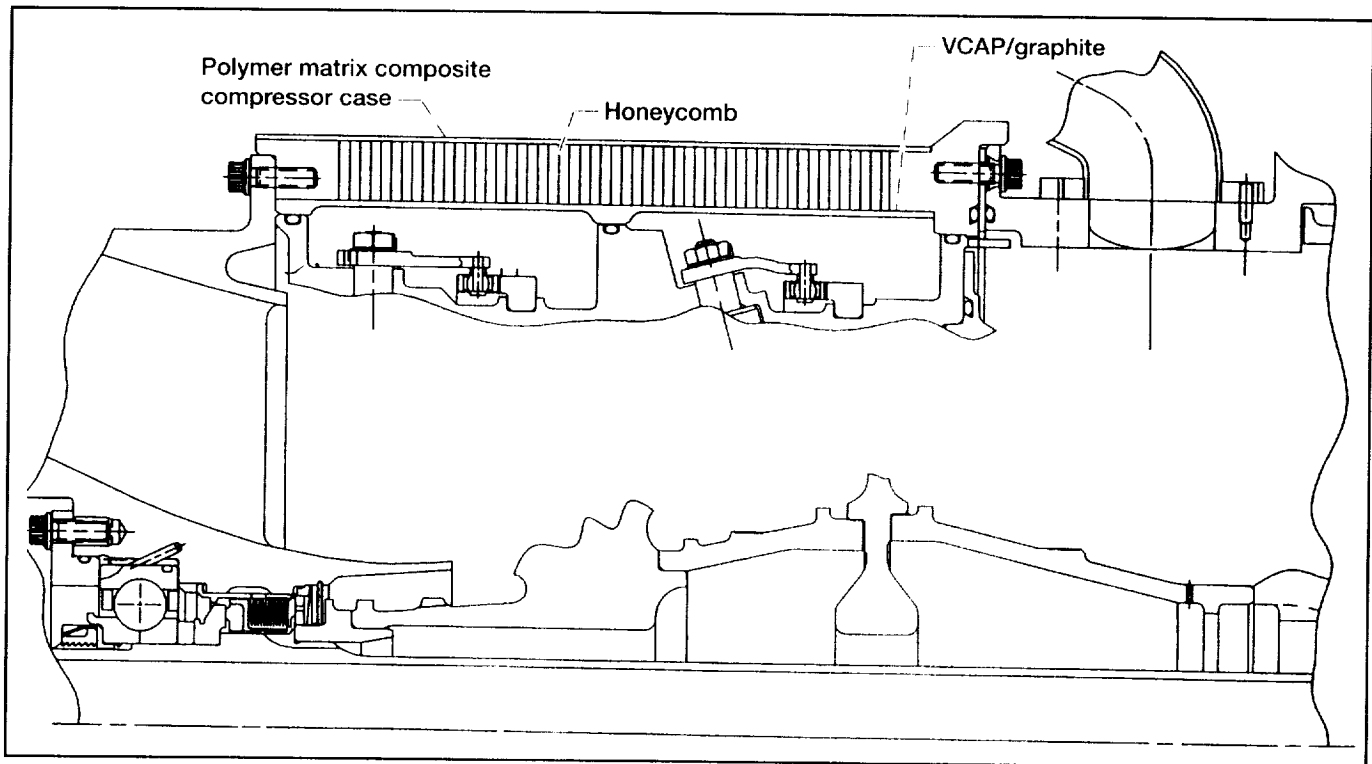
**Headquarters program office:** OA, Army

# Compressor Case Manufactured Using High-Temperature Polyimides

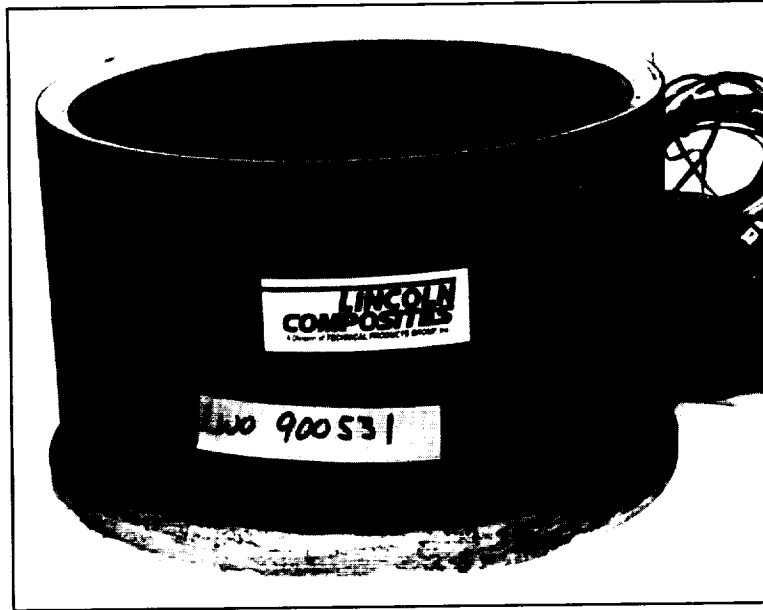
High-temperature polymer composites (PMC's) offer lighter weight and higher specific strengths than titanium alloys for advanced aircraft engine applications—especially in fan and compressor components, where temperatures do not exceed 550 °F (288 °C). VCAP, a polyimide resin developed at the NASA Lewis Research Center, was filament wound at Lincoln Composites in Lincoln, Nebraska, with graphite and glass fibers to produce a lightweight compressor case for an Integrated High Performance Turbine Engine Technology (IHPTET) engine. This engine application requires a PMC that can withstand air pressures (60 psi) and temperatures exceeding the degradation limits of other high-temperature polyimides, such as PMR-15.

In addition to increased performance characteristics, current commercial and military engine applications require low-cost fabrication methodologies. Two filament-winding processes were used to evaluate low-cost manufacturing techniques for the VCAP compressor case: "dry" powder tow and wet tow winding. In the dry tow process, a tow of graphite fibers (typically 3000 to 12,000 strands) is drawn through a bath of resin and then passed through a furnace to dry the solvent from the resin-soaked tow.

The product of this process, spools of graphite-fiber tow impregnated with a resin, can be shipped and handled without the safety concerns associated with hazardous residual solvents. Similar to the dry tow process, wet winding methods pass a tow of graphite fibers through a resin bath, but then the wet tow is placed on the tool used to shape the compressor case. Wet filament winding techniques are an established procedure for many aerospace fabricators, whereas dry tow winding is not. Four VCAP compressor cases have been produced, and the highest quality case was obtained when a wet filament winding method was used.



*Integrated High Performance Turbine Engine Technology (IHPTET) compressor cross section.*



*VCAP compressor case after thermal/pressure rig testing at AlliedSignal Engines.*

Finite element analysis modeling of the VCAP compressor case simplified the design and demonstrated the in situ mechanical and thermal loads for the compressor case. Static rig tests were performed by AlliedSignal Engines in Phoenix, Arizona, to verify the finite element analysis model and build a data base for further engine tests. Finally, the successful combination of NASA Lewis high-temperature polyimides, well-established manufacturing techniques, and the rigorous application of finite element analysis models enabled a 30-percent weight reduction for the PMC compressor case in comparison to the titanium case.

**Lewis contact:** Dr. James K. Sutter, (216) 433-3226, [James.K.Sutter@lerc.nasa.gov](mailto:James.K.Sutter@lerc.nasa.gov)

**Author:** Dr. James K. Sutter

**Headquarters program office:** OA

# Oxidation-Resistant Coating Alloy for Gamma Titanium Aluminides

Titanium aluminides based on the  $\gamma$ -phase (TiAl) offer the potential for component weight savings of up to 50 percent over conventional superalloys in 600 to 850 °C aerospace applications (ref. 1). Extensive development efforts over the past 10 years have led to the identification of "engineering"  $\gamma$ -alloys, which offer a balance of room-temperature mechanical properties and high-temperature strength retention (ref. 1). The  $\gamma$  class of titanium aluminides also offers oxidation and interstitial (oxygen and nitrogen) embrittlement resistance superior to that of the  $\alpha_2$  (Ti<sub>3</sub>Al) and orthorhombic (Ti<sub>2</sub>AlNb) classes of titanium aluminides. However, environmental durability is still a concern, especially at temperatures above 750 to 800 °C. Recent work at the NASA Lewis Research Center led to the development of an oxidation-resistant coating alloy that shows great promise for the protection of  $\gamma$  titanium aluminides.

Aluminizing treatments, conventional MCrAlY (M = Ni or Fe) coatings, and ceramic oxidation-resistant coatings for  $\gamma$ -based titanium aluminides have not proven successful because of poor mechanical properties, thermal expansion mismatch, and chemical incompatibility. Promising coating alloys have been identified in the Ti-Al-Cr system (ref. 2). These alloys exhibit excellent oxidation resistance and are generally compatible with the  $\gamma$  substrate alloys; however, they are brittle (ref. 2).

A Ti-Al-Cr oxidation-resistant coating alloy recently developed at NASA Lewis offers excellent substrate compatibility and some improvement in mechanical properties, without sacrificing oxidation resistance (refs. 3 and 4). The alloy composition, Ti-51Al-12Cr (in atomic percent), was selected so that the microstructure consists of the  $\gamma$ -phase and a minor volume of the oxidation-resistant Ti(Cr,Al)<sub>2</sub> Laves phase. By basing the coating alloy on the  $\gamma$ -phase, we can optimize the mechanical properties and substrate compatibility. The volume fraction of the Laves phase is kept to a minimum because it is extremely brittle.

The Ti-51Al-12Cr coating alloy was applied to the General Electric  $\gamma$ -alloy, Ti-48Al-2Cr-2Nb (in atomic percent), by low-pressure plasma spray. Oxidation tests at 800 and 1000 °C in air indicated that the coating alloy successfully protected the substrate from oxidation (see the figure). Evaluation of the isothermal fatigue behavior of coated Ti-48Al-2Cr-2Nb at elevated temperatures in air is in progress.

## References

1. Kim, Y.W.; and Froes, F.H.: Physical Metallurgy of Titanium Aluminides. High Temperature Aluminides and Intermetallics. S.H. Whang, et al., eds., The Minerals, Metals and Materials Society, Warrendale, PA, 1990, pp. 465-492.

2. McCarron, R.L., et al.: Protective Coatings for Titanium Aluminide Intermetallics. Proceedings of the Titanium 1992 Science and Technology Symposium. F.H. Froes and I. Caplan, eds., The Minerals, Metals and Materials Society, Warrendale, PA, 1993, pp. 1971-1978.

3. Brady, M.P.; Smialek, J.L.; and Brindley, W.J.: LEW 20,003-1 Invention Disclosure. Submitted to U.S. Patent Office, 1996.

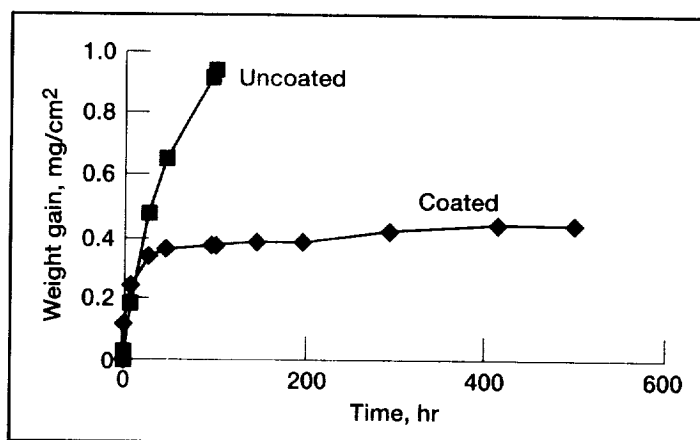
4. Brady, M.P., et al.: JOM, vol. 8, no. 11, 1996, pp. 46-50.

## Lewis contacts:

Dr. James L. Smialek, (216) 433-5500, James.L.Smialek@lerc.nasa.gov; and Dr. William J. Brindley, (216) 433-3274, William.J.Brindley@lerc.nasa.gov

**Authors:** Dr. Michael P. Brady, Dr. James L. Smialek, and Dr. William J. Brindley

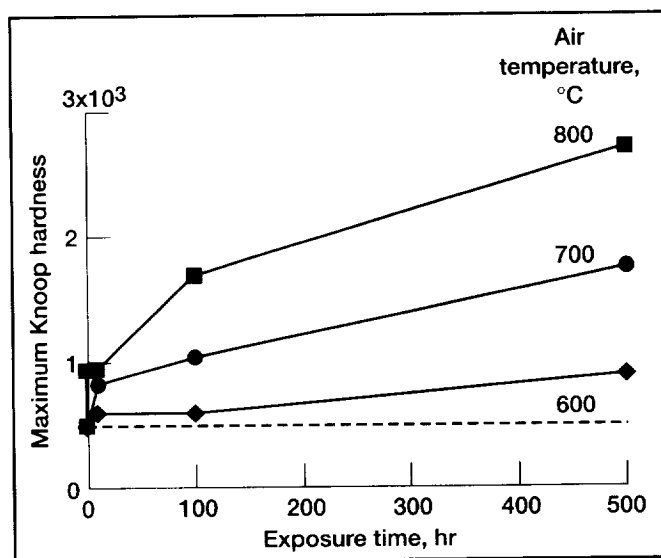
**Headquarters program office:** OA



Weight gain data for a low-pressure plasma spray Ti-51Al-12Cr coating on Ti-48Al-2Cr-2Nb exposed at 800 °C in air. At each data point, the sample was air cooled to room temperature, weighed, and returned to the test furnace. Data indicate that the coating successfully protected the substrate from oxidation.

# Environmental Studies on Titanium Aluminide Alloys

Titanium aluminides are attractive alternatives to superalloys in moderate temperature applications (600 to 850 °C) by virtue of their high strength-to-density ratio (high specific strength). These alloys are also more ductile than competing intermetallic systems. However, most Ti-based alloys tend to degrade through interstitial embrittlement and rapid oxidation during exposure to elevated temperatures. Therefore, their environmental behavior must be thoroughly investigated before they can be developed further. The goals of titanium aluminide environmental studies at the NASA Lewis Research Center are twofold: characterize the degradation mechanisms for advanced structural alloys and determine what means are available to minimize degradation. The studies to date have covered the  $\alpha_2$  ( $\text{Ti}_3\text{Al}$ ), orthorhombic ( $\text{Ti}_2\text{AlNb}$ ), and  $\gamma$  ( $\text{TiAl}$ ) classes of alloys.

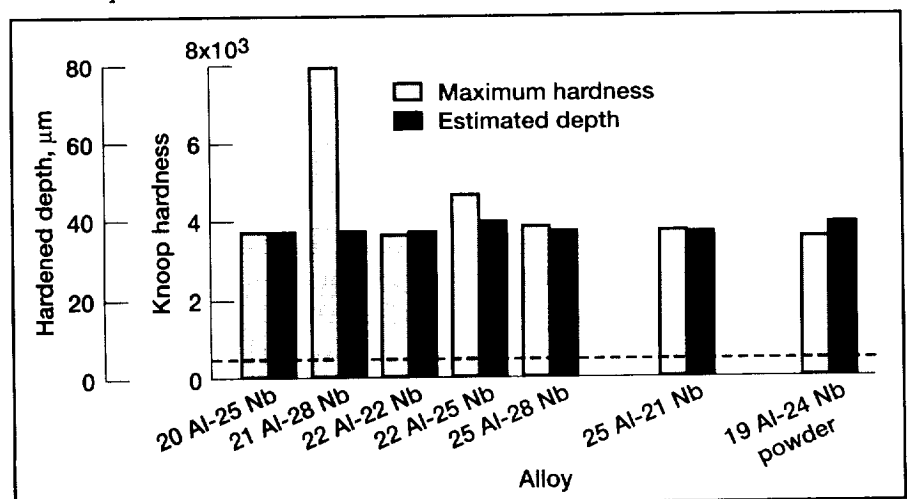


Near surface hardening of O-Ti as a function of air exposure duration at 600, 700, and 800 °C. The horizontal dashed line indicates the baseline hardness of the unexposed material.

The  $\alpha_2$  and orthorhombic (abbreviated here as O-Ti) alloys had high rates of oxidation at 800 °C, but the limiting environmental factor for both appears to be interstitial embrittlement during air exposure (refs. 1 and 2). Embrittlement, as measured by microhardness profiling, was significant for both the  $\alpha_2$  and O-Ti classes of alloys after exposure to 800 °C air for only 1 hr (see the top graph) and was measurable after 100 hr at 600 °C. In related studies at NASA Lewis, this level of embrittlement dramatically reduced the fatigue lives of  $\alpha_2$  and O-Ti alloys (refs. 3

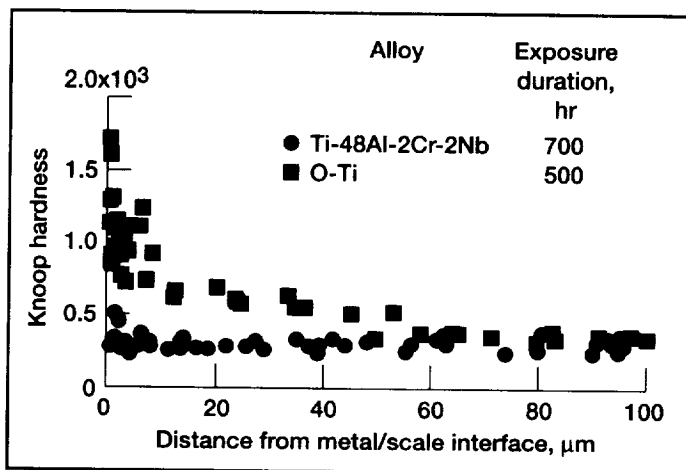
and 4). Examination of oxidation and embrittlement behavior as a function of composition showed that alloying was effective in reducing oxidation (as in the bottom graph), but was not effective in preventing or reducing embrittlement in any of 11 different O-Ti alloys examined (provided by the Materials Directorate at Wright Laboratory).

Coatings have been examined as a means to retard embrittlement in  $\alpha_2$  alloys and are under investigation for O-Ti alloys. For  $\alpha_2$  alloys, the coatings examined include those in the MCrAlY family, mixed ceramic-metallic coatings, and graded coatings. Silicide coatings have been examined for O-Ti alloys. Although all these coatings provide oxidation resistance and resistance to oxygen ingress, fatigue testing of coated coupons showed that all coatings induced a fatigue life debit that was more severe than the environmental embrittlement effect that the coating was supposed to prevent. This result is in general agreement with previous coating efforts on Ti-based alloys.



Depth of embrittlement after 500-hr exposure to 800 °C air does not correlate to O-Ti composition. The horizontal dashed line indicates the baseline hardness of the unexposed material.

Three different  $\gamma$  alloys were also evaluated in terms of their oxidation and embrittlement behavior: Ti-48Al-2Cr-2Nb (GE alloy, 48-2-2), Ti-46.5Al-3Nb-2Cr-0.2W (Universal Energy Systems alloy, K-5), and Ti-46Al-5Nb-1W (Allison alloy, Alloy 7). The 48-2-2 alloy had marginally acceptable oxidation kinetics at 800 °C, whereas both K-5 and Alloy 7 had acceptable oxidation rates to beyond 1000 hr at 800 °C.



*$\gamma$  TiAl has no detectable hardening after long-term exposure to 800 °C air, in contrast to O-Ti alloys that show extensive hardening under the same conditions.*

Eighth World Conference on Titanium. P.A. Blenkinson, et al., eds., vol. 620, pt. 1, Institute of Materials, London, 1996, pp. 113-120.

6. Brady, M.P.; Smialek, J.L.; and Brindley, W.J.: Oxidation-Resistant Coating Alloy for Gamma Titanium Aluminides. Research & Technology 1996. NASA TM-107350, 1997, pp. 66. Available WWW: <http://www.lerc.nasa.gov/RT1996/5000/5160ba.htm>

**Lewis contact :**

Dr. William J. Brindley, (216) 433-3274, [William.J.Brindley@lerc.nasa.gov](mailto:William.J.Brindley@lerc.nasa.gov)

**Authors:** Dr. William J. Brindley, Dr. Paul A. Bartolotta, Dr. James L. Smialek, and Dr. Michael P. Brady

**Headquarters program office:** OA

Microhardness profiling detected no evidence of embrittlement for any of the three  $\gamma$  alloys after a 1000-hr exposure to air at 800 °C. This is in stark contrast to the embrittlement behavior noted earlier for  $\alpha_2$  and O-Ti alloys (as shown in the graph above). However, data from other labs suggest that  $\gamma$  alloys do show a decrease in fatigue life when 600 °C vacuum and 600 °C air mechanical fatigue results are compared (ref. 5). Since the fatigue debit is relatively minor and the initial intent is to use these alloys in low-strain conditions, coatings may help extend the life of  $\gamma$  alloy components. A highly oxidation-resistant Ti-Al-Cr coating alloy, which combines excellent  $\gamma$  substrate compatibility with toughness, has been developed at NASA Lewis (ref. 6). This alloy is being evaluated as an oxidation and embrittlement resistant coating designed to enhance the life of structural  $\gamma$ -alloys.

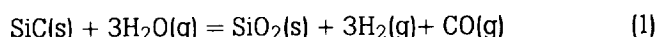
**References**

1. Brindley, W.J.; Smialek, J.L.; and Gedwill, M.A.: Oxidation Resistant Coatings for  $\text{Ti}_3\text{Al}+\text{Nb}$  and  $\text{SiC}/\text{Ti}_3\text{Al}+\text{Nb}$ . HITEMP Review 1992, NASA CP-10104, Vol. II, 1992, pp. 41-1 to 41-15.
2. Brindley, W.J., et al.: Oxidation and Embrittlement of Orthorhombic-Titanium Alloys. HITEMP Review 1994, NASA CP-10146, Vol. II, 1994, pp. 44-1 to 44-11.
3. Gabb, T.P.; and Gayda, J.: Fatigue Behavior of a Unidirectionally Reinforced Orthorhombic Matrix Composite. HITEMP Review 1993, NASA CP-19117, Vol. II, 1993, pp. 33-1 to 33-10.
4. Brindley, P.K.; and Bartolotta, P.A.: Isothermal Fatigue Behavior of  $\text{SiC}/\text{Ti}-24\text{Al}-11\text{Nb}$ . HITEMP Review 1991, NASA CP-10082, 1991, pp. 46-1 to 46-13.
5. Larsen, J.M., et al.: Reliability Issues Affecting the Implementation of Gamma Titanium Aluminides. Turbine Engine Applications. Institute of Materials 1996,

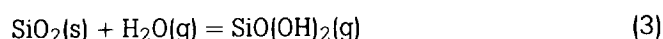
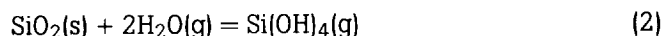
# Volatile Reaction Products From Silicon-Based Ceramics in Combustion Environments Identified

Silicon-based ceramics and composites are prime candidates for use as components in the hot sections of advanced aircraft engines. These materials must have long-term durability in the combustion environment. Because water vapor is always present as a major product of combustion in the engine environment, its effect on the durability of silicon-based ceramics must be understood. In combustion environments, silicon-based ceramics react with water vapor to form a surface silica ( $\text{SiO}_2$ ) scale. This  $\text{SiO}_2$  scale, in turn, has been found to react with water vapor to form volatile hydroxides. Studies to date have focused on how water vapor reacts with high-purity silicon carbide ( $\text{SiC}$ ) and  $\text{SiO}_2$  in model combustion environments.

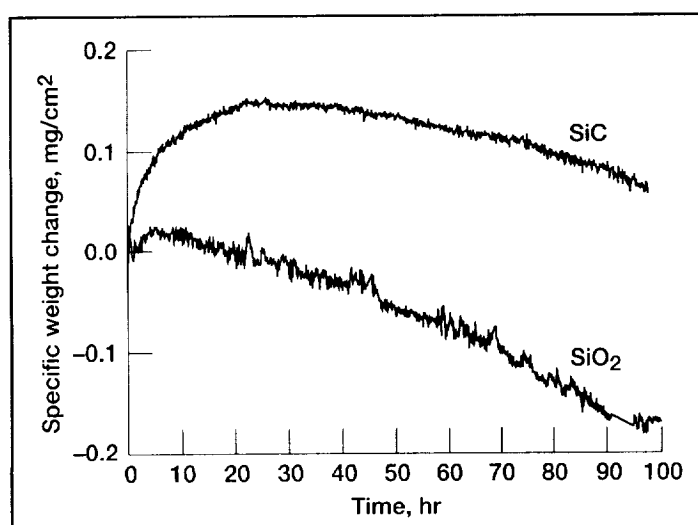
Because the combustion environment in advanced aircraft engines is expected to contain about 10-percent water vapor at 10-atm total pressure, the durability of  $\text{SiC}$  and  $\text{SiO}_2$  in gas mixtures containing 0.1- to 1-atm water vapor is of interest. The reactions of  $\text{SiC}$  and  $\text{SiO}_2$  with water vapor were monitored by measuring weight changes of sample coupons in a 0.5-atm water vapor/0.5-atm oxygen gas mixture with thermogravimetric analysis (ref. 1).  $\text{SiC}$  initially exhibited a weight gain due to  $\text{SiO}_2$  formation:



At longer durations, a weight loss attributed to the volatility of  $\text{SiO}_2$  in water vapor became apparent:



By testing  $\text{SiO}_2$  (rather than  $\text{SiC}$ ) in water vapor, a linear weight loss uncomplicated by the oxidation reaction (1) can be observed by thermogravimetric analysis.



Weight change kinetics for  $\text{SiC}$  and  $\text{SiO}_2$  in 0.5 atm  $\text{H}_2\text{O}$ /0.5 atm  $\text{O}_2$  at a temperature of 1200 °C and a velocity of 4.4 cm/sec.

The identities of the volatile species were established by using a specialized mass spectrometer that samples reactions at 1-atm total pressure (ref. 2).  $\text{SiO}_2$  samples with large surface areas were exposed to water vapor/oxygen mixtures at high temperatures. Molecules with masses corresponding to both  $\text{Si(OH)}_4$  and  $\text{SiO(OH)}_2$  were identified.

Because  $\text{SiO}_2$  is volatile in combustion environments, it no longer provides protection for  $\text{SiC}$ . Consumption of  $\text{SiC}$  thus occurs at more rapid rates in water-vapor-containing environments. The consumption rate of  $\text{SiC}$  increases with water vapor pressure as well as gas velocity. This is a concern when  $\text{SiC}$  is applied in the high-pressure, high-velocity aircraft engine environment. Current efforts are focused on coatings for  $\text{SiC}$  that prevent volatility of the surface  $\text{SiO}_2$ .

## References

1. Opila, E.J.; and Hann, R.E.: Paralineer Oxidation of CVD  $\text{SiC}$  in Water Vapor. To be published in J. Am. Ceram. Soc., vol. 80, no. 1, 1997.
2. Opila, E.J.; Fox, D.S.; and Jacobson, N.S.: Mass Spectrometric Identification of Si-O-H(g) Species From the Reaction of Silica With Water Vapor at Atmospheric Pressure. Submitted to J. Am. Ceram. Soc.

## Lewis contacts:

Dr. Elizabeth J. Opila, (216) 433-8904, opila@lerc.nasa.gov;  
 Dr. Nathan Jacobson, (216) 433-5498, Nathan.J.Jacobson@lerc.nasa.gov; and  
 Dennis Fox, (216) 433-3295, Dennis.S.Fox@lerc.nasa.gov

**Author:** Dr. Elizabeth J. Opila

**Headquarters program office:** OA

# Oxidation Resistance and Critical Sulfur Content of Single-Crystal Superalloys

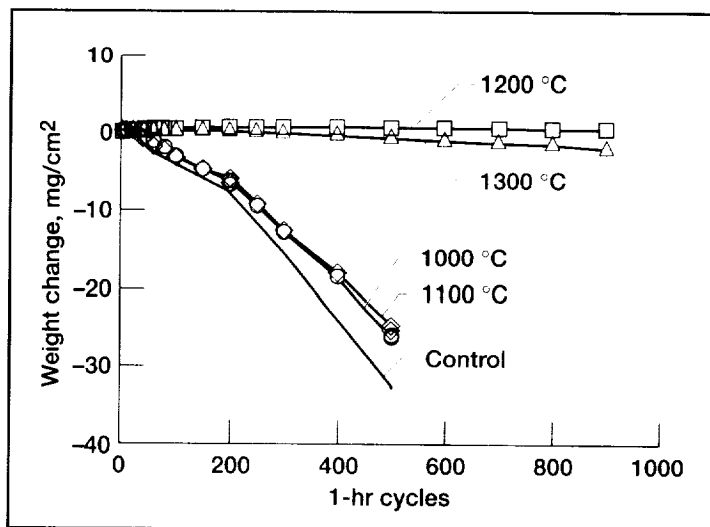
The high-temperature components of a jet turbine engine are made from nickel-base superalloys. These components must be able to withstand high stresses, fatigue, and corrosive reactions with high-temperature gases. Such oxidation resistance is associated with slow-growing  $\text{Al}_2\text{O}_3$  scales that remain adherent to superalloy components after many thermal cycles. Historically, good oxidation resistance has been obtained by coating these components with Ni-Cr-Al-Y coatings, where small additions of yttrium (Y) were necessary for scale adhesion. Subsequently, it was found that the Y aids scale adhesion by preventing sulfur from segregating to the scale metal interface and thus preventing the sulfur from weakening the oxide-metal bonds. Y is a difficult element to incorporate in single-crystal superalloy castings, but it was shown in early work at the NASA Lewis Research Center that good adhesion could be obtained for low-sulfur, uncoated, single-crystal superalloys, without Y additions (ref. 1).

Low sulfur contents for these uncoated superalloys were achieved in the laboratory by a high-temperature hydrogen annealing process. This process allows segregation and surface cleaning of sulfur monolayers in a reducing environment. (Annealing in air or oxygen simply traps the sulfur at the oxide-metal interface). Although this process has been pursued by industry (ref. 2), another approach is to remove sulfur from the alloy in the melting process. Both processes involve extra effort and costs that must be balanced against improved performance. The present study was designed to establish a guideline for the minimum level of desulfurization needed to achieve maximum performance (ref. 3).

Coupons of various thicknesses of the superalloy PWA 1480 were hydrogen annealed at various times (8 to 100 hr) and temperatures (1000 to 1300 °C), resulting in coupons with sulfur contents ranging from about 0.05 to 5 ppm. This variation occurs because sulfur removal is approximately controlled by diffusion and the parameter  $(Dt/L^2)$ , where  $D$  is the diffusion coefficient of sulfur,  $t$  is diffusion time, and  $L$  is the sample thickness.

Cyclic oxidation tests at 1100 °C were then used to assess adhesion and spalling. The weight change of one set of 20-mil (0.5-mm) samples, annealed for 20 hr at 1000, 1100, 1200, and 1300 °C, is shown in the figure to the right. Clearly, the effect of the annealing temperature is quite dramatic in that the higher temperatures produced scales that spalled very little, whereas the lower temperatures resulted in severe weight losses comparable to those for the as-received, unannealed sample.

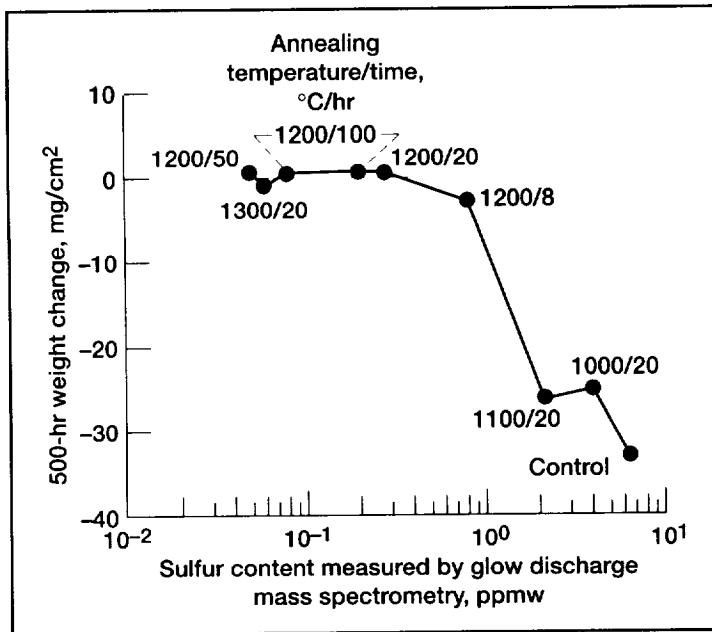
Similar effects were observed as a function of annealing time or sample thickness, because these parameters determine the final sulfur content from the hydrogen annealing process. Thus, spalling behavior can be related to a single parameter: sulfur content. This relationship is shown in the figure on the opposite page, where the weight change after 500 1-hr cycles for the 20-mil samples is plotted against the sulfur content, as measured by glow discharge mass spectrometry. (Individual points are identified by the annealing temperature and time.) There is a steep reduction in the degree of spallation as the sulfur content is reduced below the as-received value of ~6 ppmw (parts per million by weight). Furthermore, there is very little spallation for samples having less than 1 ppmw sulfur, with no further benefit for samples having less than about 0.3 ppmw sulfur. These values translate to 1 to 2 monolayers of total sulfur segregation



Effect of hydrogen annealing temperature on the 1100 °C cyclic oxidation weight change behavior of 0.5-mm (20 mil) PWA 1480 superalloy coupons annealed for 20 hr.



possible for a given sample geometry and sulfur level. A similar analysis of results, summarized from many published studies, produced the same sulfur dependencies for PWA 1484, René N5, René N6, René 142, and CMSX 4 superalloys (ref. 3).



*Correlation between sulfur content and cyclic oxidation performance for PWA 1480. Minimal scale spallation (weight loss) is shown for sulfur levels below 0.3 ppmw.*

Thus, for typical airfoil dimensions in advanced aeroengines, 0.5 ppmw sulfur would be a commendable target level and should result in excellent scale adhesion. Most advanced turbine blades are also thermal barrier coated with an insulating layer of plasma-sprayed  $\text{ZrO}_2$ . The integrity of this coating will also depend on good  $\text{Al}_2\text{O}_3$  scale adhesion, since the scale grows beneath the  $\text{ZrO}_2$ . These low-sulfur alloys will improve scale adhesion and, thus, should improve  $\text{ZrO}_2$  coating lives, even when NiCrAlY bond coats are employed.

## References

1. Tubbs, B.K.; and Smialek, J.L.: Corrosion and Particle Erosion at High Temperatures. Joint Symposium at the 116th Annual Meeting of the Minerals, Metals and Materials Society, V. Srinivasan and K. Vedula, eds., The Minerals, Metals and Materials Society, Warrendale, PA, 1989, pp. 459-487. (Also Smialek, J.L.; and Tubbs, B.K.: Metall. Mat. Trans., vol. 26A, Feb. 1995, pp. 427-435.)
2. Allen, W.P., et al.: Method for Removing Sulfur From Superalloy Articles to Improve Their Oxidation Resistance. U.S. Patent 5,346,563, Sept. 13, 1994.
3. Smialek, J.L.: Oxidation Resistance and Critical Sulfur Content of Single Crystal Superalloys. ASME Paper 96-GT-519, 1996.

**Lewis contact:** Dr. James L. Smialek, (216) 433-5500,  
James.L.Smialek@lerc.nasa.gov

**Author:** Dr. James L. Smialek

**Headquarters program office:** OA

# Structures

## Probabilistic Thermomechanical Fatigue of Polymer Matrix Composites

Traditional computational approaches for predicting the life and long-term behavior of materials rely on empirical data and are neither generic nor unique in nature. Also, those approaches are not easy to implement in a design procedure in an effective, integrated manner. The focus of ongoing research at the NASA Lewis Research Center has been to develop advanced integrated computational methods and related computer codes for a complete reliability-based assessment of composite structures. These methods—which account for uncertainties in all the constituent properties, fabrication process variables, and loads to predict probabilistic micromechanics, ply, laminate, and structural responses—have already been implemented in the Integrated Probabilistic Assessment of Composite Structures (IPACS) (ref. 1) computer code. The main objective of this evaluation is to illustrate the effectiveness of the methodology to predict the long-term behavior of composites under combined mechanical and thermal cyclic loading conditions.

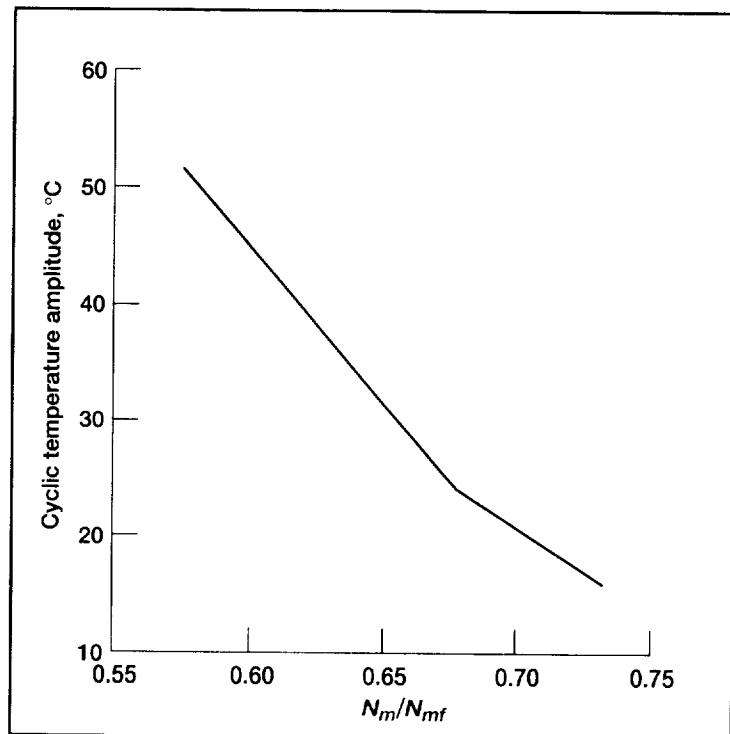
A unified time-, stress- and load-dependent Multifactor Interaction Equation (MFIE) model developed at NASA Lewis (ref. 2) has been used to simulate the long-term behavior of polymer matrix composites. The MFIE model evaluates the magnitude of degradation and properties of constituent materials (including possible impending failure modes) at every cycle step at the temperature that will be used for micromechanics and laminate analysis.

The deterministic part of the methodology has been implemented in the in-house computer code Integrated Composite Analyzer (ICAN) (ref. 3). NASA Lewis has demonstrated a methodology to compute the fatigue life for different applied-stress-to-laminate-strength ratios on the basis of first-ply failure criteria and thermal cyclic loads. (First-ply failure criteria assumes that a laminate has failed when any stress component in a ply exceeds its respective allowable.) Degradation effects due to long-term environmental exposure and thermomechanical cyclic loads are considered in the simulation process.

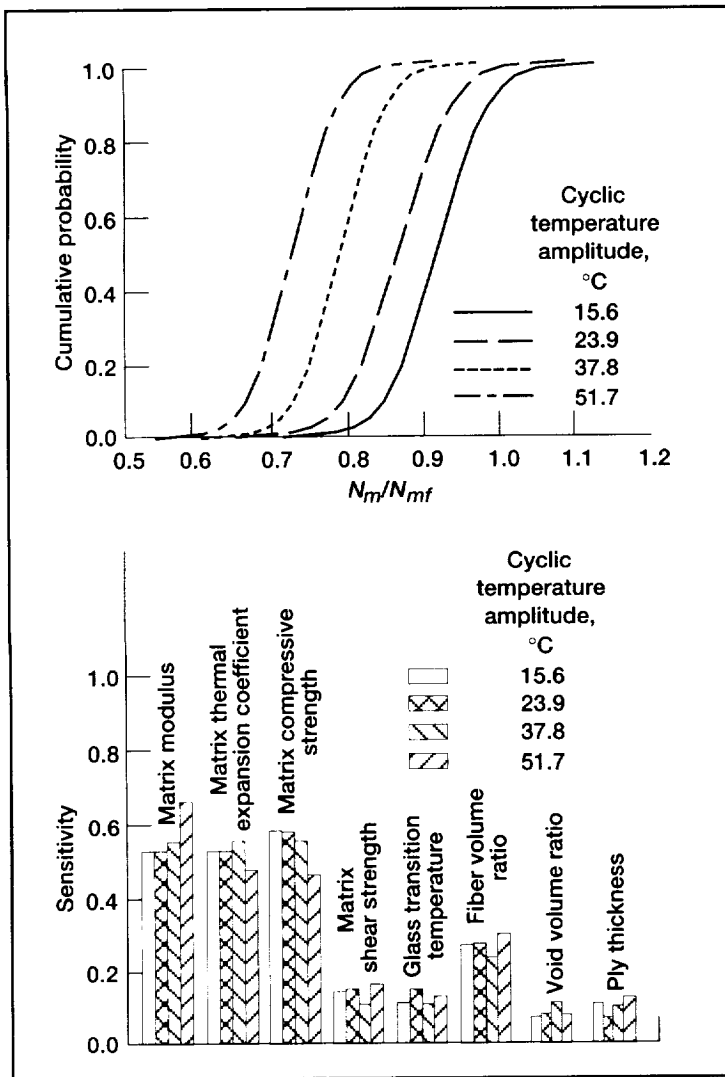
In reference 4, an application of MFIE is illustrated by considering a  $[0^\circ/\pm 45^\circ/90^\circ]_s$  graphite fiber epoxy matrix composite. The fatigue life cycles were computed for different thermal cycles and for different magnitudes of applied-stress-to-laminate-strength ratios,  $r$ , based on first-ply failure criteria (ref. 4). These curves can be used to assess the fatigue life of a component subjected to mechanical cyclic loading for a given reliability

(as in the figure below). Cumulative probability distribution functions for mechanical fatigue due to different cyclic stress magnitudes and the respective sensitivity factors are shown in the figure on the facing page.<sup>1</sup>

<sup>1</sup>Note that results similar to those in these figures can be developed for different stress ratios but constant temperatures (ref. 4).



Fatigue life variation for 0.999 reliability of  $[0^\circ/\pm 45^\circ/90^\circ]_s$  graphite/epoxy laminate. Ply thickness, 0.127 mm under thermal cyclic load; mean mechanical load, 0.5 static strength.



Cumulative distribution function and sensitivity of fatigue life for 0.999 reliability of  $[0^\circ/\pm 45^\circ/90^\circ]_s$  graphite/epoxy laminate. Ply thickness, 0.127 mm under thermal cyclic load; mean mechanical load, 0.5 static strength. Top: Cumulative distribution function. Bottom: Sensitivity of fatigue life for 0.999 reliability.

## References

1. Integrated Probabilistic Assessment of Composite Structures (IPACS) User's Manual: Ver. 1.0. NASA Contract No. NAS3-25266, Task Order No. 5209-02, Dec. 1991.
2. Boyce, L.; and Chamis, C.C.: Probabilistic Constitutive Relationships for Cyclic Material Strength Models. AIAA Paper 88-2376, 1988.
3. Murthy, P.L.N.; and Chamis, C.C.: Integrated Composite Analyzer (ICAN): Users and Programmers Manual. NASA TP-2515, 1986.
4. Shah, A.R.; Murthy, P.L.N.; and Chamis, C.C.: Effect of Cyclic Thermo-Mechanical Loads on Fatigue Reliability in Polymer Matrix Composites. NASA TM-107091, 1995.

## Lewis contact:

Dr. Christos C. Chamis, (216) 433-3252,  
smccc@popserve.lerc.nasa.gov

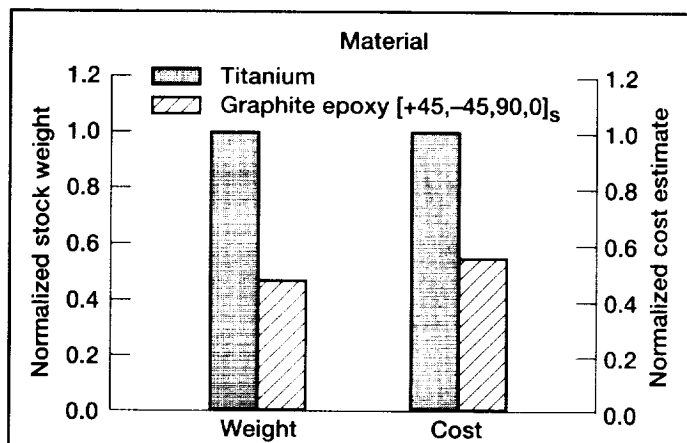
**Author:** Dr. Christos C. Chamis

**Headquarters program office:** OA

# T/Best: Technology Benefit Estimator for Composites and Applications to Engine Structures

Progress in the field of aerospace propulsion has heightened the need to combine advanced technologies. These benefits will provide guidelines for identifying and prioritizing high-payoff research areas, will help manage research with limited resources, and will show the link between advanced and basic concepts. An effort was undertaken at the NASA Lewis Research Center to develop a formal computational method, T/BEST (Technology Benefit Estimator), to assess advanced aerospace technologies, such as fibrous composites, and credibly communicate the benefits of research. Fibrous composites are ideal for structural applications such as high-performance aircraft engine blades where high strength-to-weight and stiffness-to-weight ratios are required. These factors—along with the flexibility to select the composite system and layup, and to favorably orient fiber directions—reduce the displacements and stresses caused by large rotational speeds in aircraft engines.

T/Best can readily evaluate typical blade manufacturing processes and the benefits of using composites to construct fan and compressor blades, as well as determine how to update blade geometry to maximize a rotor's efficiency. The bar graph compares these benefits with those of state-of-the-art titanium blades. The pie chart shows the cost required to manufacture composite fan blades as estimated with T/BEST.



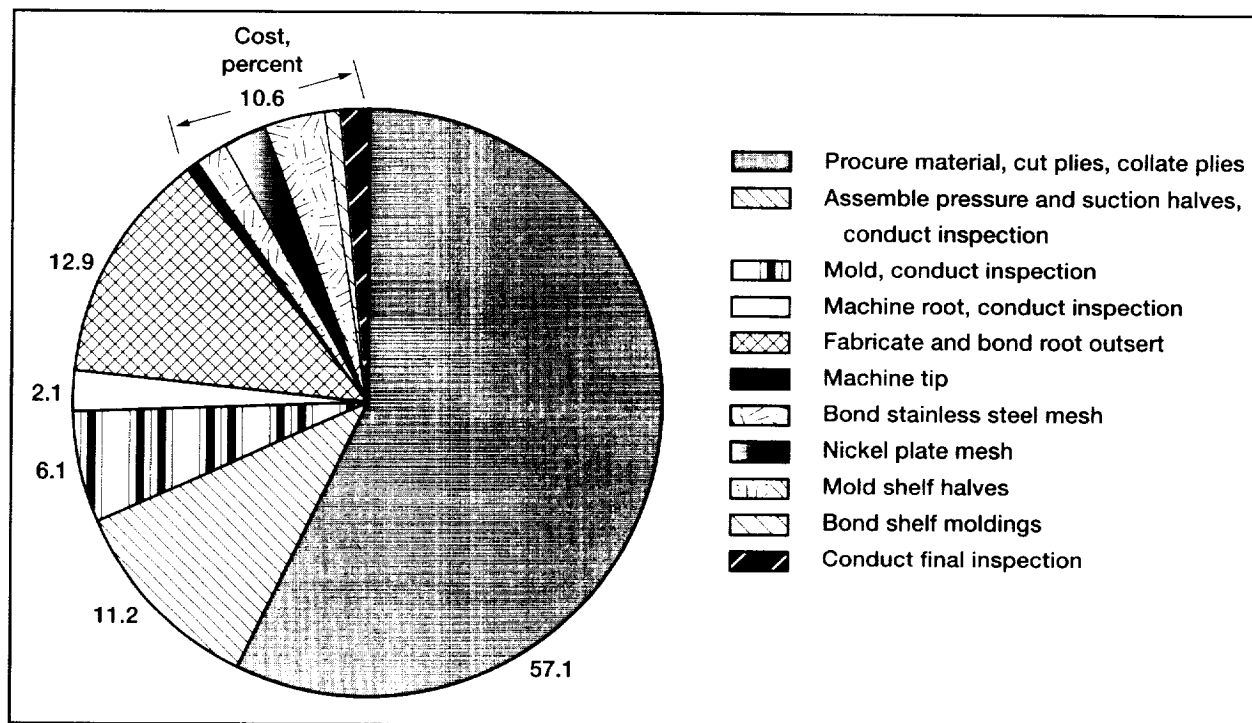
Maurer stock weight and cost estimation for manufacturing a fan blade.

## Lewis contact:

Dr. Christos C. Chamis, (216) 433-3252,  
smccc@popserve.lerc.nasa.gov

**Author:** Dr. Christos C. Chamis

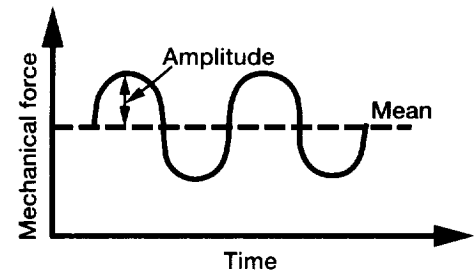
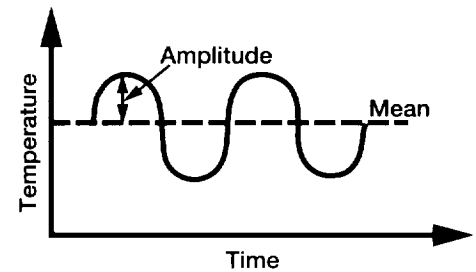
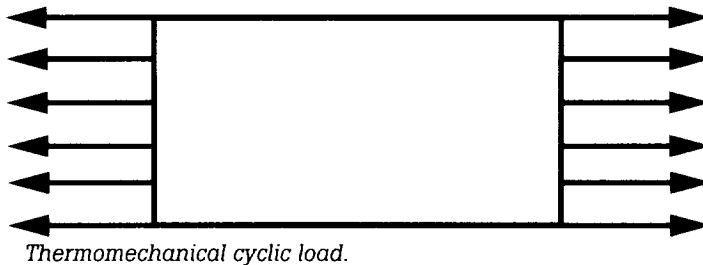
**Headquarters program office:** OA



Cost of a process for manufacturing resin matrix composite blades.

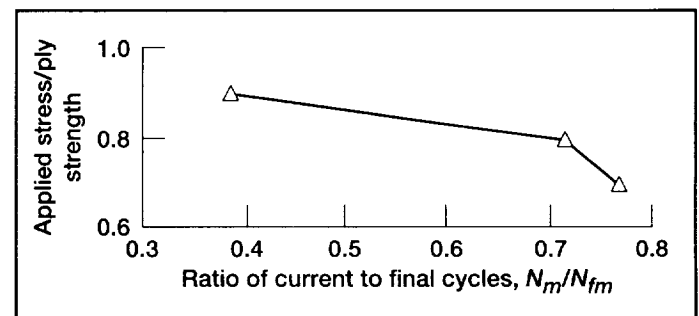
# Effect of Cyclic Thermal Loads on Fatigue Reliability in Polymer Matrix Composites

Technological solutions that will ensure the economic viability and environmental compatibility of a future High Speed Civil Transport plane are currently being sought. Lighter structural materials for both airframe primary structures and engine structure components are being investigated. We believe that such objectives can be achieved through the use of high-temperature composites as well as other conventional, lighter weight alloys. One of the prime issues for these structural components is assured long-term behavior with a specified reliability.



An investigation was conducted to describe a computational simulation methodology for predicting fatigue life (see the figure above), reliability, and probabilistic long-term behavior of polymer matrix composites. A unified time-, stress-, and load-dependent Multi-Factor Interaction Equation (MFIE) model developed at the NASA Lewis Research Center was used to simulate the long-term behavior of polymer matrix composites.

To illustrate the application of the methodology, we chose a typical composite system consisting of graphite fibers in an epoxy matrix with a layup of  $(0^\circ/\pm 45^\circ/90^\circ)_s$ . This methodology can be applied to other types of polymer matrix composites as well. The cumulative probability distribution functions for the fatigue life cycles were computed for different thermal cycle rates and constant applied stress. The laminate strength was evaluated on the basis of first-ply failure criteria (hereinafter referred to as laminate strength). First-ply failure criteria assumes that a laminate has failed when any stress component in a ply exceeds its respective allowable. Using these cumulative probability distribution functions, one obtains a fatigue life cycle curve for a reliability of 0.999 (as in the figure opposite). The results show that, at low mechanical cyclic loads and low thermal cyclic amplitudes, fatigue life for 0.999 reliability is most sensitive to the matrix compressive strength, matrix modulus, thermal expansion coefficient, and ply thickness. In contrast, at high mechanical cyclic loads and high thermal cyclic amplitudes, fatigue life at 0.999 reliability is more sensitive to the shear strength of the matrix, longitudinal fiber modulus, matrix modulus, and ply thickness.



*Fatigue life variation resulting from the thermomechanical cyclic load on 0.127-mm plies of graphite/epoxy in a  $(0^\circ/\pm 45^\circ/90^\circ)_s$  laminate configuration. Mean applied load, 50 percent of ply strength; mean temperature, 65.5 °C; and cyclic temperature, 51.7 °C.*

## Lewis contact:

Dr. Christos C. Chamis, (216) 433-3252,  
smccc@popserve.lerc.nasa.gov

**Author:** Dr. Christos C. Chamis

**Headquarters program office:** OA

# ICAN Computer Code Adapted for Building Materials

The NASA Lewis Research Center has been involved in developing composite micromechanics and macromechanics theories over the last three decades. These activities have resulted in several composite mechanics theories and structural analysis codes whose applications range from material behavior design and analysis to structural component response. One of these computer codes, the Integrated Composite Analyzer (ICAN), is designed primarily to address issues related to designing polymer matrix composites and predicting their properties—including hygral, thermal, and mechanical load effects. Recently, under a cost-sharing cooperative agreement with a Fortune 500 corporation, Master Builders Inc., ICAN was adapted to analyze building materials.

## **Lewis contact:**

Dr. Pappu L.N. Murthy, (216) 433-3332,  
pmurthy@lerc.nasa.gov

**Author:** Dr. Pappu L.N. Murthy

**Headquarters program office:** OA

The high costs and technical difficulties involved with the fabrication of continuous-fiber-reinforced composites sometimes limit their use. Particulate-reinforced composites can be thought of as a viable alternative. They are as easily processed to near-net shape as monolithic materials, yet have the improved stiffness, strength, and fracture toughness that is characteristic of continuous-fiber-reinforced composites. For example, particle-reinforced metal-matrix composites show great potential for a variety of automotive applications, such as disk brake rotors, connecting rods, cylinder liners, and other high-temperature applications. Building materials, such as concrete, can be thought of as one of the oldest materials in this category of multiphase, particle-reinforced materials. The adaptation of ICAN to analyze particle-reinforced composite materials involved the development of new micromechanics-based theories. A derivative of the ICAN code, ICAN/PART, was developed and delivered to Master Builders Inc. as a part of the cooperative activity.

ICAN/PART simulations help Master Builders Inc. early in the development of new particulate materials for specific needs. These simulations will expedite the development cycle by reducing extensive trial and error testing, thereby reducing the costs to bring new materials to market. The benchmark tests that will be needed can also be designed or guided as a part of this simulation activity.

Particulate-reinforced composites are prime candidates in many commercial applications, such as in the automotive and construction industries. Although our original intention for these NASA codes was to analyze materials of immediate interest to the aerospace community, they can easily be modified for nonaerospace, commercial applications.

## **Bibliography**

Murthy, P.L.N.; Goldberg, R.K.; and Mital, S.K.: Micromechanics for Particulate Reinforced Composites. NASA TM-107276, 1996.

Goldberg, R.K.; Murthy, P.L.N.; and Mital, S.K.: ICAN/PART: Particulate Composite Analyzer, User's Manual and Verification Studies. NASA TM-107297, 1996.

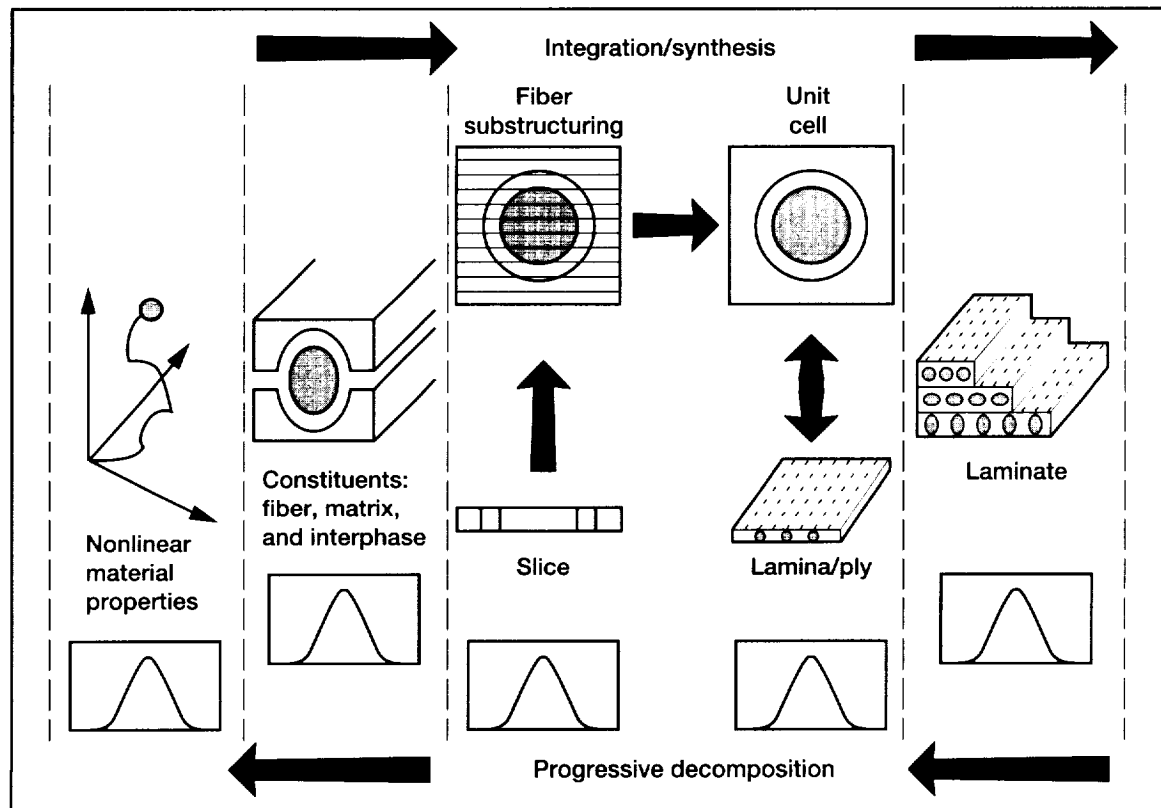
# Micromechanical Modeling Efforts for Advanced Composites

Over the past two decades, NASA Lewis Research Center's in-house efforts in analytical modeling for advanced composites have yielded several computational predictive tools. These are, in general, based on simplified micromechanics equations. During the last 3 years, our efforts have been directed primarily toward developing prediction tools for high-temperature ceramic matrix composite (CMC's) materials. These materials are being considered for High Speed Research program applications, specifically for combustor liners. In comparison to conventional materials, CMC's offer several advantages: high specific stiffness and strength, and higher toughness and nonbrittle failure in comparison to monolithic ceramics, as well as environmental stability and wear resistance for both room-temperature and elevated-temperature applications. Under the sponsorship of the High Temperature Engine Materials Program (HITEMP), CMC analytical modeling has resulted in the computational tool Ceramic Matrix Composites Analyzer (CEMCAN). This code was released through COSMIC (NASA's software distribution center, <http://www.cosmic.uga.edu> on the World Wide Web) recently.

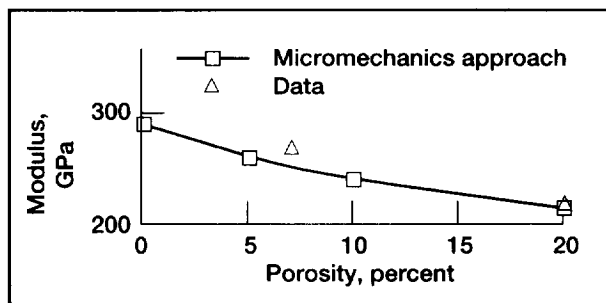
The analysis of CMC materials requires specialized modeling that considers their unique physical and mechanical behavior. Ceramic matrix composite materials are reinforced primarily to enhance toughness because the matrix material is quite brittle and fails at relatively low strain levels. The method-

ology incorporated in CEMCAN is based on micromechanics models in which, customarily, a representative volume element or unit cell is arranged in a square array pattern. However, the present approach employs a unique multilevel substructuring technique that allows the capture of greater local detail. The methodology also takes into account fracture initiation and progression, as well as nonlinear composite behavior due to temperature.

Unlike conventional materials, CMC's exhibit a considerable amount of scatter in the material properties. Since these materials must sustain a reliable life of several thousand hours in High Speed Civil Transport propulsion systems,



*Integrated probabilistic ceramic matrix composite mechanics approach.*



*In-plane modulus versus porosity (SiC/SiC composite; fiber volume ratio, 0.4).*

prediction tools must be developed to account for uncertainties in the material behavior and fabrication parameters. Currently, work is underway to incorporate probabilistic analysis in the micromechanics and macro-mechanics of CMC's. In addition to providing more formalism to the analysis as opposed to the conventional "safety factor approach," such procedures will enhance interpretation of experimentally measured properties that have a wide range of scatter. Furthermore, the procedure will help identify the variables that influence the response most, thereby providing guidelines for quality control during the fabrication process of these materials.

Another area of growing interest in the composite community is the use of woven or textile composites for a variety of structural applications. For example, plain- and satin-weave constructions are being considered for combustor liners in the Enabling Propulsion Materials program, and woven polymer matrix composites are being considered for lower temperature applications in the Advanced Subsonic Technology program. Woven composites are constructed by weaving two fiber tows together to form a layer. The interlacing of fiber bundles has several advantages, such as increasing the intralaminar and interlaminar strength, providing greater damage tolerance, and providing a possible way to produce near-net shapes for thick structural components. A micromechanics-based approach for analyzing plain-weave ceramic and polymer matrix composites, which was recently developed in-house, is being integrated into NASA Lewis' composite mechanics computer codes.

### **Bibliography**

Murthy, P.L.N.; Chamis, C.C.; and Mital, S.K.: Computational Simulation of Continuous Fiber-Reinforced Ceramic Matrix Composites Behavior. NASA TP-3602, 1996.

Mital, S.K.; Murthy, P.L.N.; and Chamis, C.C.: Simplified Micromechanics of Plain Weave Composites. NASA TM-107165, 1996.

Murthy, P.L.N.; Mital, S.K.; and Shah, A.R.: Probabilistic Micromechanics and Macromechanics for Ceramic Matrix Composites. NASA TM-4766, 1997.

**Lewis contact:** Dr. Pappu L.N. Murthy, (216) 433-3332, [smmurthy@maestro.lerc.nasa.gov](mailto:smmurthy@maestro.lerc.nasa.gov)

**Author:** Dr. Pappu L.N. Murthy

**Headquarters program office:** OA



# COMETBOARDS Can Optimize the Performance of a Wave-Rotor-Topped Gas Turbine Engine

A wave rotor, which acts as a high-technology topping spool in gas turbine engines, can increase the effective pressure ratio as well as the turbine inlet temperature in such engines. The wave rotor topping, in other words, may significantly enhance engine performance by increasing shaft horse power while reducing specific fuel consumption. This performance enhancement requires optimum selection of the wave rotor's adjustable parameters for speed, surge margin, and temperature constraints specified on different engine components. To examine the benefit of the wave rotor concept in engine design, researchers soft coupled NASA Lewis Research Center's multidisciplinary optimization tool COMETBOARDS and the NASA Engine Performance Program (NEPP) analyzer.

The COMETBOARDS-NEPP combined design tool has been successfully used to optimize wave-rotor-topped engines. For illustration, the design of a subsonic gas turbine wave-rotor-enhanced engine with four ports for 47 mission points (which are specified by Mach number, altitude, and power-setting combinations) is considered. The engine performance analysis, constraints, and objective formulations were carried out through NEPP, and COMETBOARDS was used for the design optimization. So that the benefits that accrue from wave rotor enhancement could be examined, most baseline variables and constraints were declared to be passive, whereas important parameters directly associated with the wave rotor were considered to be active for the design optimization. The engine thrust was considered as the merit function. The wave rotor engine design, which became a sequence of 47 optimization subproblems, was solved successfully by using a cascade strategy available in COMETBOARDS. The graph depicts the optimum COMETBOARDS solutions

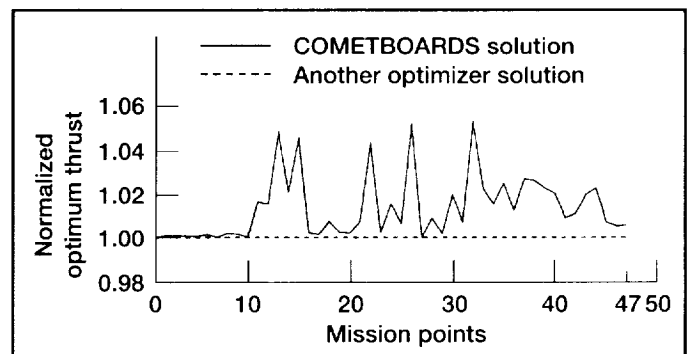
for the 47 mission points, which were normalized with respect to standard results. As shown, the combined tool produced higher thrust for all mission points than did the other solution, with maximum benefits around mission points 11, 25, and 31. Such improvements can become critical, especially when engines are sized for these specific mission points.

## Lewis contact:

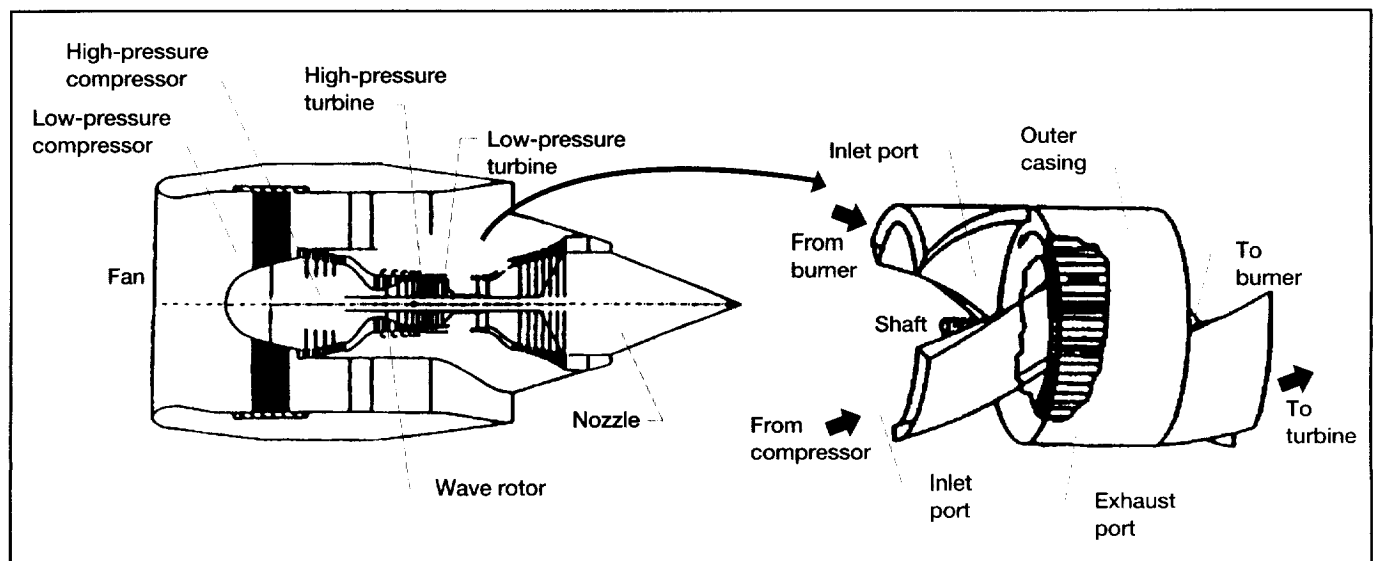
Dr. Surya N. Patnaik, (216) 962-3135,  
smsnp@hawaii.lerc.nasa.gov

**Author:** Dr. Surya N. Patnaik

**Headquarters program office:** OA



COMETBOARDS solution.



Subsonic gas turbine engine.

# Transient Finite Element Analyses Developed to Model Fan Containment Impact Events

Research is underway to establish an increased level of confidence in existing numerical techniques for predicting transient behavior when the fan of a jet engine is released and impacts the fan containment system. To evaluate the predictive accuracy that can currently be obtained, researchers at the NASA Lewis Research Center used the DYNA 3D computer code to simulate large-scale subcomponent impact tests that were conducted at the University of Dayton Research Institute (UDRI) Impact Physics Lab.

In these tests, 20- by 40-in. flat metal panels, contoured to the shape of a typical fan case, were impacted by the root section of a fan blade. The panels were oriented at an angle to the path of the projectile that would simulate the conditions in an actual blade-out event. The metal panels were modeled in DYNA 3D using a kinematic hardening model with the strain rate dependence of the yield stress governed by the Cowper-Simons rule. Failure was governed by the effective plastic strain criterion.

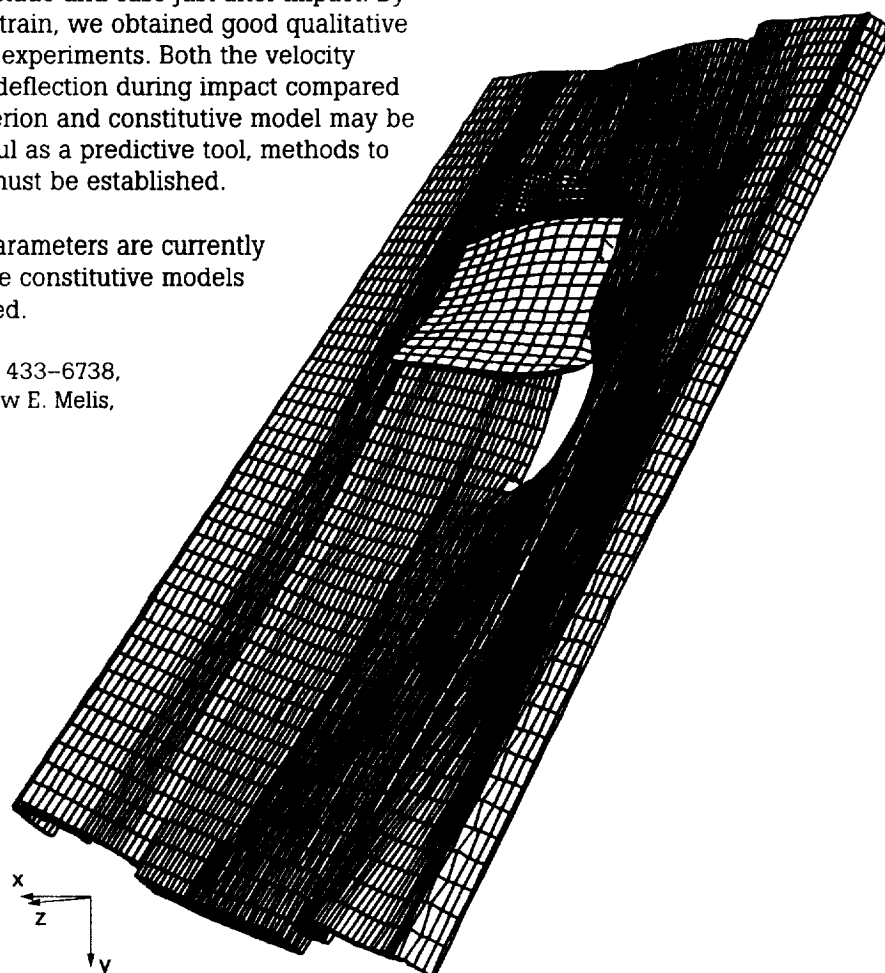
The figure shows the model of the fan blade and case just after impact. By varying the maximum effective plastic strain, we obtained good qualitative agreement between the model and the experiments. Both the velocity required to penetrate the case and the deflection during impact compared well. This indicates that the failure criterion and constitutive model may be appropriate, but for DYNA 3D to be useful as a predictive tool, methods to determine accurate model parameters must be established.

Simple methods for measuring model parameters are currently being developed. In addition, alternative constitutive models and failure criteria are being investigated.

**Lewis contacts:** Dr. J. Michael Pereira, (216) 433-6738, [smpere@popserve.lerc.nasa.gov](mailto:smpere@popserve.lerc.nasa.gov); and Mathew E. Melis, (216) 433-3322, [mmelis@lerc.nasa.gov](mailto:mmelis@lerc.nasa.gov)

**Author:** Dr. J. Michael Pereira

**Headquarters program office:** OA



*Third curved sector UDRI test 2.5 msec after impact.*

# High-Temperature Adhesive Strain Gage Developed

Researchers at the NASA Lewis Research Center have developed a unique strain gage and adhesive system for measuring the mechanical properties of polymers and polymer composites at elevated temperatures. This system overcomes some of the problems encountered in using commercial strain gages and adhesives. For example, typical commercial strain gage adhesives require a postcure at temperatures substantially higher than the maximum test temperature. The exposure of the specimen to this temperature may affect subsequent results, and in some cases may be higher than the glass-transition temperature of the polymer. In addition, although typical commercial strain gages can be used for short times at temperatures up to 370 °C, their long-term use is limited to 230 °C. This precludes their use for testing some high-temperature polyimides near their maximum temperature capability.

Lewis' strain gage and adhesive system consists of a nonencapsulated, unbacked gage grid that is bonded directly to the polymer after the specimen has been cured but prior to the normal postcure cycle. The gage is applied with an adhesive specially formulated to cure under the specimen postcure conditions. Special handling, mounting, and electrical connection procedures were developed, and a fixture was designed to calibrate each strain gage after it was applied to a specimen. A variety of tests was conducted to determine the performance characteristics of the gages at elevated temperatures on PMR-15 neat resin and titanium specimens. For these tests, which included static tension, thermal exposure, and creep tests, the gage and adhesive system performed within normal strain gage specifications at 315 °C. An example of the performance characteristics of the gage can be seen in the figure, which compares the strain gage measurement on a polyimide specimen at 315 °C with an extensometer measurement.

## Bibliography

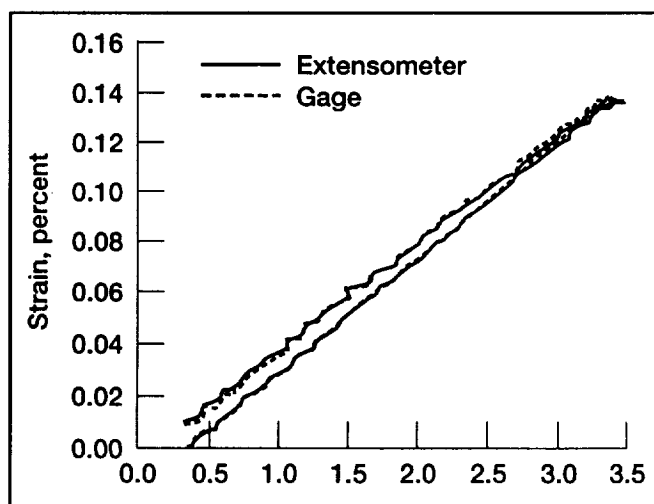
Rabzak, C.; Pereira, J.M.; and Roberts, G.D.: Adhesively Bonded Strain Gages for Extended Use at 315 °C on Polymers. ASTM Workshop on Strain Gages in Mechanical Testing, Orlando, FL, 1996.

Rabzak, C.; Pereira, J.M.; and Roberts, G.D.: Adhesively Bonded Strain Gages for Extended Use at 315 °C on Polymers. Submitted for publication in J. Testing Evaluation, 1996.

**Lewis contacts:** Dr. J. Michael Pereira, (216) 433-6738, [smpere@popserve.lerc.nasa.gov](mailto:smpere@popserve.lerc.nasa.gov); and Dr. Gary D. Roberts, (216) 433-3244, [G.D.Roberts@lerc.nasa.gov](mailto:G.D.Roberts@lerc.nasa.gov)

**Authors:** Dr. J. Michael Pereira and Dr. Gary D. Roberts

**Headquarters program office:** OA



Extensometer compared with gage at 315 °C on PMR-15.

# Novel Multidisciplinary Models Assess the Capabilities of Smart Structures to Manage Vibration, Sound, and Thermal Distortion in Aeropropulsion Components

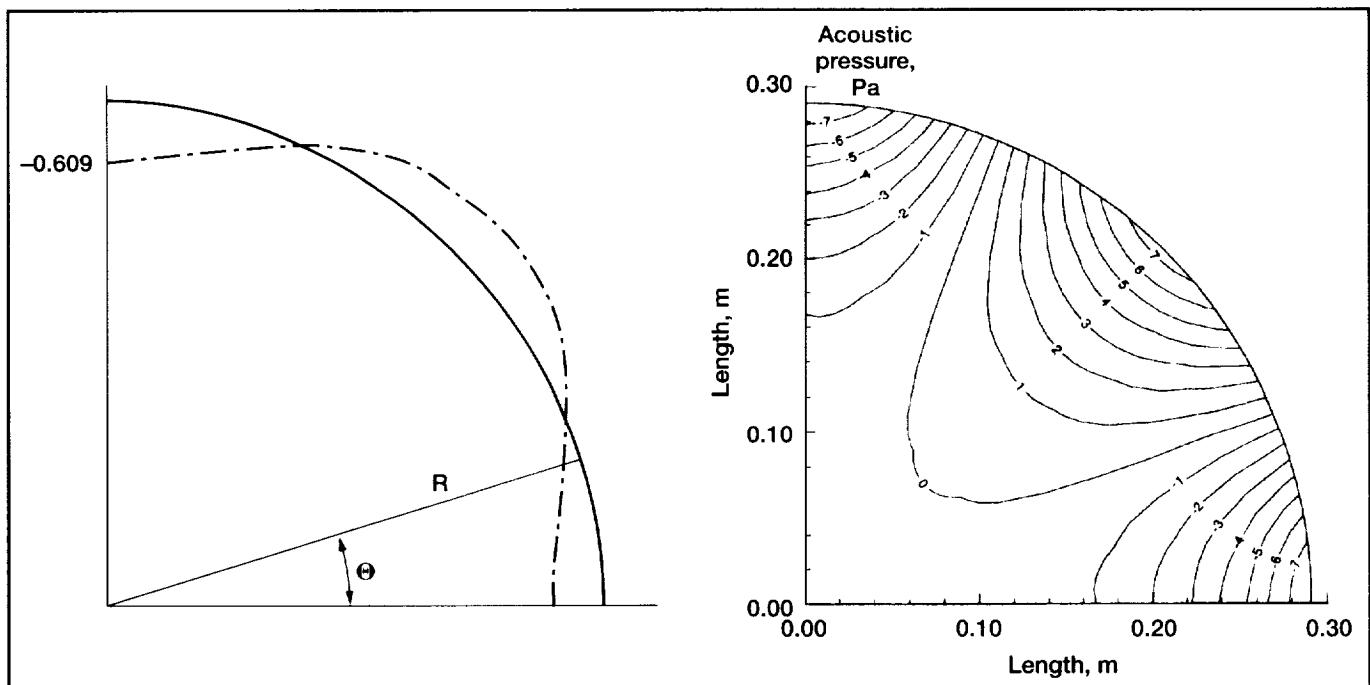
The development of aeropropulsion components that incorporate "smart" composite laminates with embedded piezoelectric actuators and sensors is expected to ameliorate critical problems in advanced aircraft engines related to vibration, noise emission, and thermal stability. To facilitate the analytical needs of this effort, the NASA Lewis Research Center has developed mechanics and multidisciplinary computational models to analyze the complicated electromechanical behavior of realistic smart-structure configurations operating in combined mechanical, thermal, and acoustic environments. The models have been developed to accommodate the particular geometries, environments, and technical challenges encountered in advanced aircraft engines, yet their unique analytical features are expected to facilitate application of this new technology in a variety of commercial applications.

This multidisciplinary effort encompasses analytical and computational developments in three disciplines. The first area involves a generalized curvilinear laminate theory and specialty finite elements for laminated composite shell structures with curved piezoelectric actuators and sensors (ref. 1). These novel curvilinear piezoelectric finite elements use different, yet adjustable, representations for the displacements and electric potential which can be adapted to capture the configuration of the laminate and the embedded piezoelectric devices. They enable efficient and accurate

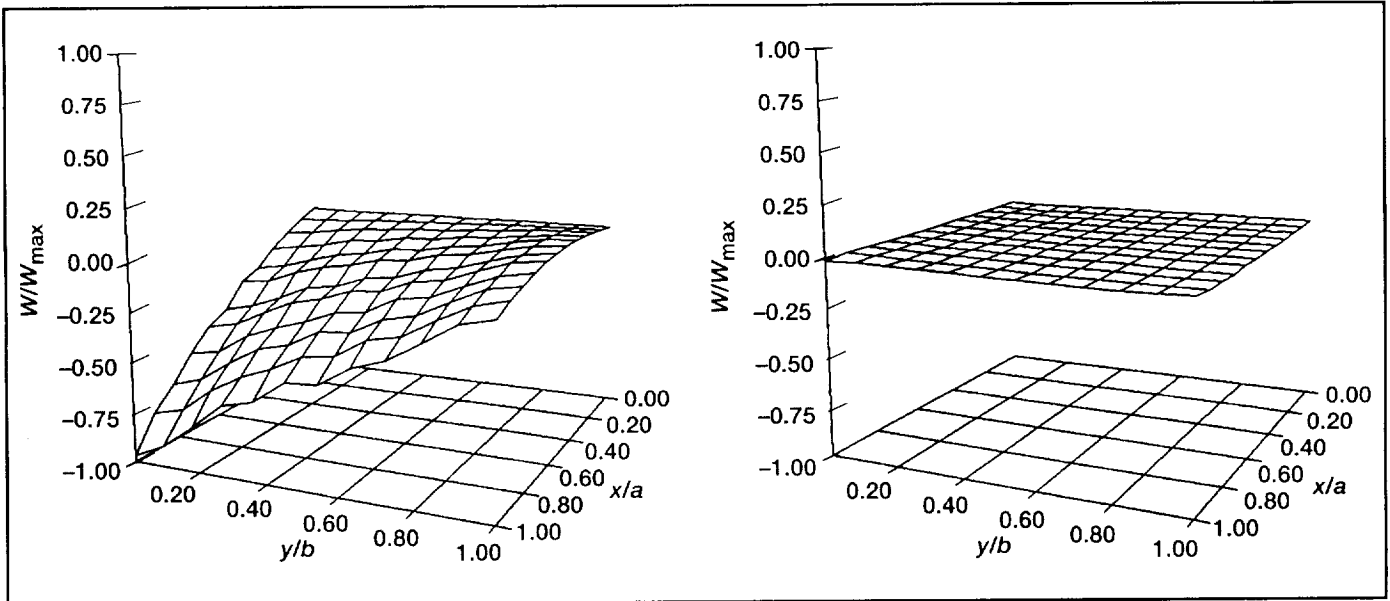
modeling of three-dimensional, smart composite shell structures of any shape, curvature, or laminate configuration.

The second area involves computational models for analyzing the coupled vibroacoustic response of smart shell structures that enclose acoustic fluids (ref. 2). These interdisciplinary models, which effectively provide coupled solutions by using the previously mentioned structural finite element models with acoustic boundary element methods, are a necessary step toward the development of smart structures that can control noise.

In the third area, admissible computational models have been developed to quantify the performance of



*Coupled steady-state response of a smart cylindrical containment structure (quarter model) with piezoceramic actuators attached on the outer surface excited at 200 Hz. Left: Induced dynamic deflections. Right: Induced acoustic pressure (in pascals) in the enclosed air.*



Active compensation of thermal bending and twisting of a cantilever  $[-45^\circ/45^\circ]$  plate of length,  $a$ , and width,  $b$ , with piezoceramic actuators and sensors attached on the free surfaces. Left: Thermal distortion,  $w$ , induced by thermal gradient. Right: Compensation of thermal distortion by simultaneous application of electric potential on actuators.

piezoelectric structures in thermal environments (ref. 3). Besides helping us to understand and quantify the effect of thermal loads on the performance and structural integrity of smart structures, this work has enabled us to formally study the feasibility of active thermal distortion management.

The successful development and coupling of these models has resulted in a multidisciplinary computational platform that can simulate the coupled mechanical, electrical, thermal, and acoustic response of a smart structure. Such simultaneous predictions of the dynamic deflections of the smart structure and the interior acoustic pressure field, both induced by piezoelectric actuators embedded in the smart structure, are shown in the figure to the left. The figures above show the effects of a thermal gradient applied on a cantilever plate with attached piezoceramic patches. These effects typically include thermal distortions (left figure) and changes in sensory electric signals, as well as the ability to enhance thermal stability and to use piezoceramic actuators to compensate for thermal distortions (right figure).

## References

1. Saravanan, D.A.: Coupled Mixed-Field Laminate Theory and Finite Element for Smart Piezoelectric Composite Shell Structures. NASA CR-198490, 1996.
2. Kaljevic, I.; and Saravanan, D.A.: Coupled Analysis of Smart Structures Surrounding Acoustic Enclosures. AIAA Paper 96-3996, 6th AIAA/USAF/NASA/ISSMO Symposium on Multidisciplinary Analysis and Optimization, Bellevue, WA, Sept. 4-6, 1996.
3. Saravanan, D.A.; and Lee, H.J.: Layerwise Finite Elements for Smart Piezoceramic Composite Plates in Thermal Environments. AIAA Paper 96-1277 (NASA TM-106990), 1996.

## Lewis contact:

Dimitris A. Saravanan, (216) 962-3211,  
dsaravanan@lerc.nasa.gov

Author: Dimitris A. Saravanan

Headquarters program office: OA

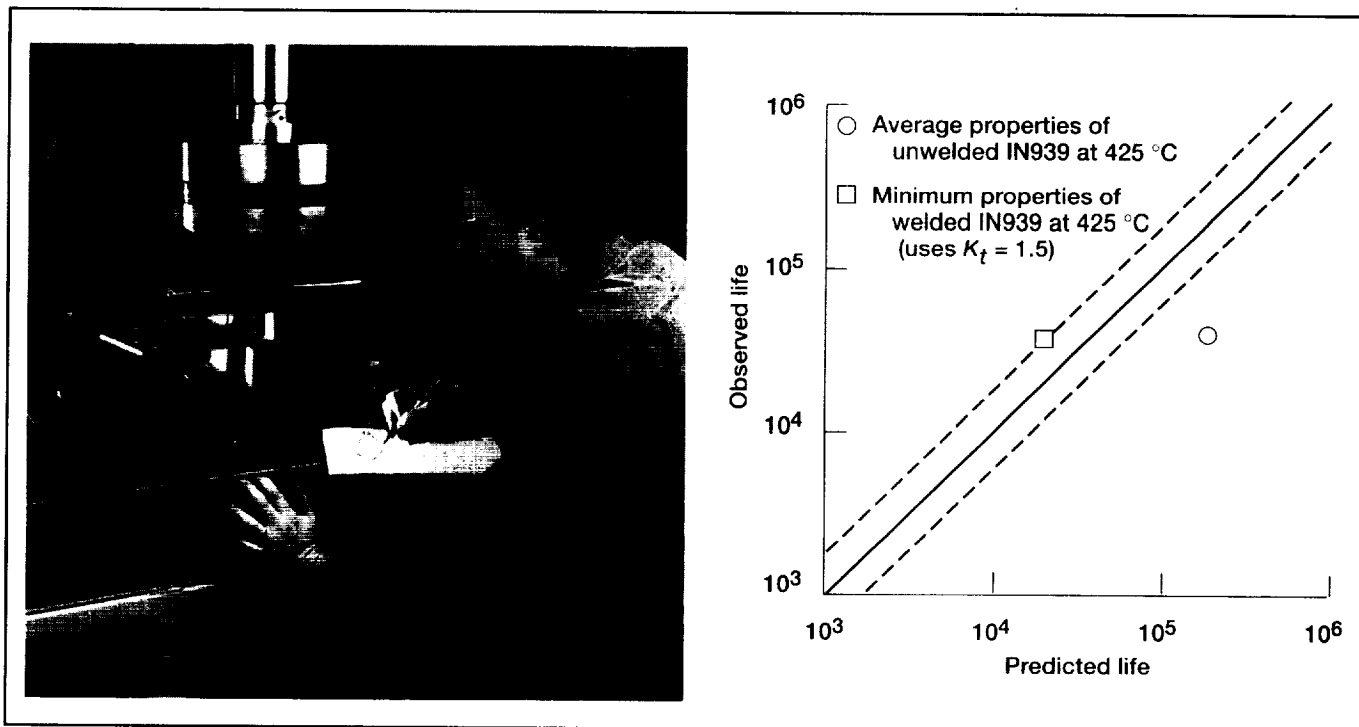
# Enabling Propulsion Materials (EPM) Structural Component Successfully Tested Under Pseudo-Operating Conditions\*

A fabrication feasibility demonstration component for the Enabling Propulsion Materials (EPM) program was evaluated under prototypical engine loading conditions at the Structural Benchmark Test Facility at the NASA Lewis Research Center. The purpose for this test was to verify EPM casting, joining, coating, and life-prediction methods. Electron beam welding techniques developed in the EPM program were used to join two large superalloy cast sections of an exhaust nozzle flap to fabricate the demonstration component. After the joints were inspected, the component was coated with an oxidation-resistant barrier coating and was sent to Lewis for testing.

The special test fixture shown in the photo (the Structural Benchmark Test Facility) was designed and built at Lewis to produce a biaxial bending condition similar to the loading condition this part would encounter during engine operation. Several finite element analyses were conducted to validate the mechanical test method. A floating furnace was then designed to provide prototypical thermal profiles in the component. An isothermal low-cycle fatigue test was used to evaluate the component at a cyclic load of 13 kN (maximum) to 1 kN (minimum) at a frequency of 1 Hz. Component failure was defined as a 30-percent increase in the component's compli-

ance. On the basis of this definition, the low-cycle fatigue life of this component would be 35,000 cycles.

As predicted, a fatigue crack began in the high stress location of the welded joint, and the local temperature at the failure site was 425 °C. On the basis of several lifing methods that were developed for conventional superalloys, the predicted life of the component was 18,000 cycles. As shown in the graph, using average material properties (see the circle on the graph) would give a very nonconservative (128,000 cycles) life prediction that is more representative of an unwelded component. To account



Left: Mechanical loading fixture with demo component, loading ram, universal support pivots, and sliding rockers. Failure initiated in the weld at the location of the highest stress. Local temperature, 425 °C; loading, -1 to -13 kN at 1 Hz; pressure equivalent, 110 kN/m<sup>2</sup> psi (maximum). Right: Life prediction of demo component showing predicted life for welded and unwelded component. Component life, 35,000 cycles; stress concentration factor  $K_t$ , 1.5.

\* Because of Limited Exclusive Rights restrictions, specifics on test conditions, material details, and engine operation conditions have been omitted.

for the welded joint and its unknown properties, minimum parent material properties and a  $K_t$  of 1.5 were used as knockdown factors. With these knockdown factors, the predicted life of the welded component was 18,000 cycles (see the square on the graph). Lewis' life prediction method was within a factor of 2 of the actual demo component life.

**Lewis contact:** Dr. Paul A. Bartolotta, (216) 433-3338,

SMBart@popserve.lerc.nasa.gov

**Author:** Dr. Paul A. Bartolotta

**Headquarters program office:** OA

## Retirement for Cause as an Alternate Means of Managing Component Lives

In the current budgetary environment, fielded equipment is often used beyond its design life. To avoid the large cost of replacing critical rotating parts as they reach their "safe-life" limits, a Retirement For Cause (RFC) program may prove to be a cost-effective, yet safe, alternative. Studies indicate that a full 80 percent of parts replaced at low-cycle fatigue calculated "safe life" limits have at least a full order of magnitude of remaining fatigue life. The Air Force has embraced RFC and currently uses it successfully to manage parts life for several of their gas turbine engines.

RFC involves periodic nondestructive evaluation to assess the damage state of components (whether or not detectable cracks exist). Those components with no detectable cracks are returned to service. This approach allows parts with low life to be detected and discarded before they can cause an incident and parts with high life to be used to their full potential. Although there are costs associated with procuring the inspection equipment and performing the inspections, they have been shown to be more than offset by the savings in replacement parts. Basic to an RFC program is the calculation of crack-growth rates under the expected service loads (mechanical and thermal). The results are used to define safe-use intervals between required (nondestructive evaluation) inspections. The starting crack size for the fracture mechanics analysis is a flaw that is just below the detection limit of the non-destructive evaluation technique employed. Crack growth in ductile materials is sensitive to loading sequence, in that large-amplitude load excursions in the early stages of crack formation can retard the crack growth rate, whereas in the later stages of crack growth these same overloads can lead to catastrophic failure. A population of components subjected to variable-amplitude loading will exhibit a distribution in crack-growth lives (greater than that observed in constant-amplitude loading). For an accurate assessment of component reliability, this variability must be characterized. A NASA Lewis Research Center/U.S.

Army Research Laboratory (ARL) team is providing analytical support to the U.S. Army Aviation and Troop Command (ATCOM) as they develop an RFC program for the T700-700 engine used in the Blackhawk helicopter. For this effort, the FASTRAN-II fracture mechanics analysis code, developed by NASA, is being employed to estimate crack growth lives.

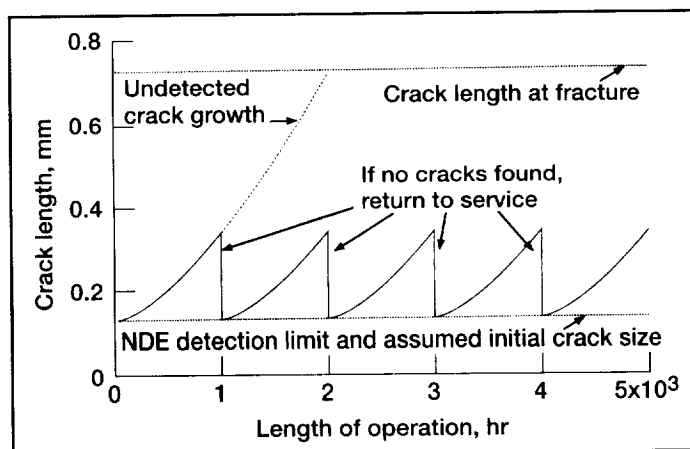
**Lewis contact:**

Peter J. Bonacuse, (216) 433-3309,

P.J.Bonacuse@lerc.nasa.gov

**Author:** Peter J. Bonacuse

**Headquarters program office:** OA



*Fatigue crack growth under RFC inspection regime (inspected every 1000 hr).*

# Model Determined for Predicting Fatigue Lives of Metal Matrix Composites Under Mean Stresses

Aircraft engine components invariably are subjected to mean stresses over and above the cyclic loads. In monolithic materials, it has been observed that tensile mean stresses are detrimental and compressive mean stresses are beneficial to fatigue life in comparison to a base of zero mean stress. Several mean stress models exist for monolithic metals, but each differ quantitatively in the extent to which detrimental or beneficial effects are ascribed. There have been limited attempts to apply these models to metal matrix composites. However, since most of the fatigue data have been limited to tension-tension loading, the range of mean stresses over which models could be assessed has been limited. In this work, a unidirectional, SiC/Ti-15-3 composite was tested with both tension and compressive stresses, thus extending the range of imposed mean stresses. It was shown that tensile mean stresses were detrimental and that compressive mean stresses were beneficial to the fatigue lives.

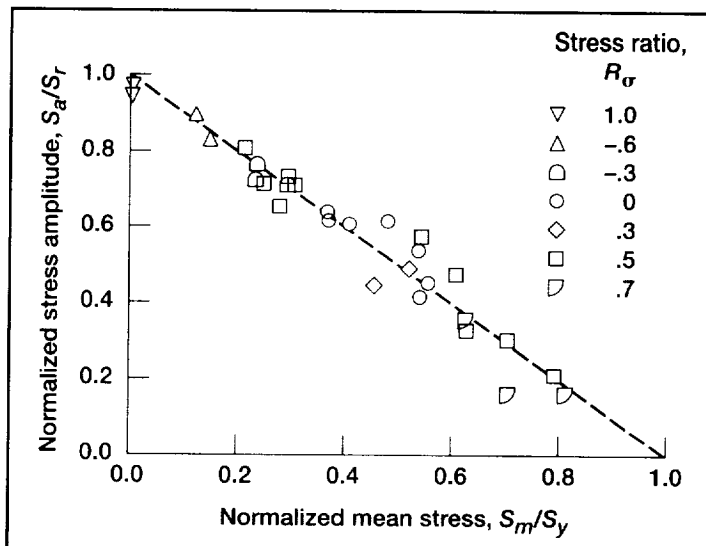
## Lewis contact:

Bradley A. Lerch, (216) 433-5522,  
SMLerch@popserve.lerc.nasa.gov

Author: Bradley A. Lerch

Headquarters program office: OA

At the NASA Lewis Research Center, several mean stress models—the Smith-Watson-Topper, Walker, Normalized Goodman, and Soderberg models—were examined for applicability to this class of composite materials. The Soderberg approach, which normalizes the mean stress to a 0.02-percent yield strength, was shown to best represent the effect of mean stresses over the range covered. The other models varied significantly in their predictability and often failed to predict the composite behavior at very high tensile mean stresses. This work is the first to systematically demonstrate the influence of mean stresses on metal matrix composites and model their effects. Attention also was given to fatigue-cracking mechanisms in the Ti-15-3 matrix and to micromechanics analyses of mean stress effects.

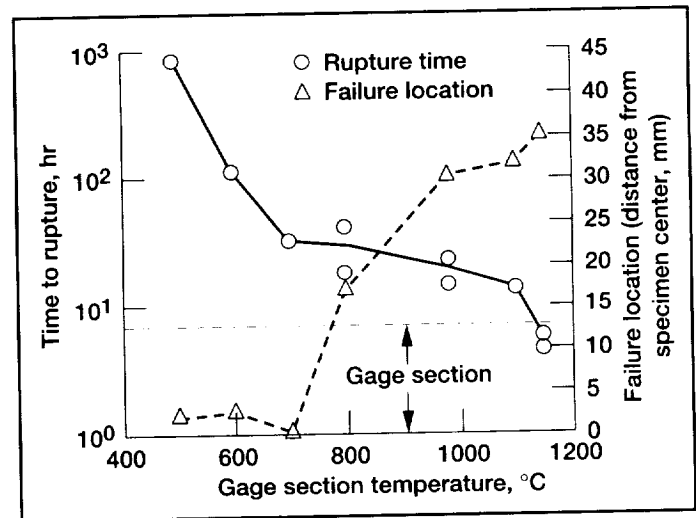


Prediction of mean stress effects on the fatigue lives of SiC/Ti-15-3 by using the Soderberg Approach.  $(S_a/S_r) + (S_m/S_y) = 1$ , where  $S_a$  is the stress amplitude under mean stress,  $S_r$  is the stress amplitude under fully reversed loading,  $S_m$  is the mean stress, and  $S_y$  is the 0.02-percent yield stress.



## Oxidation Embrittlement Observed in SiC/SiC Composites

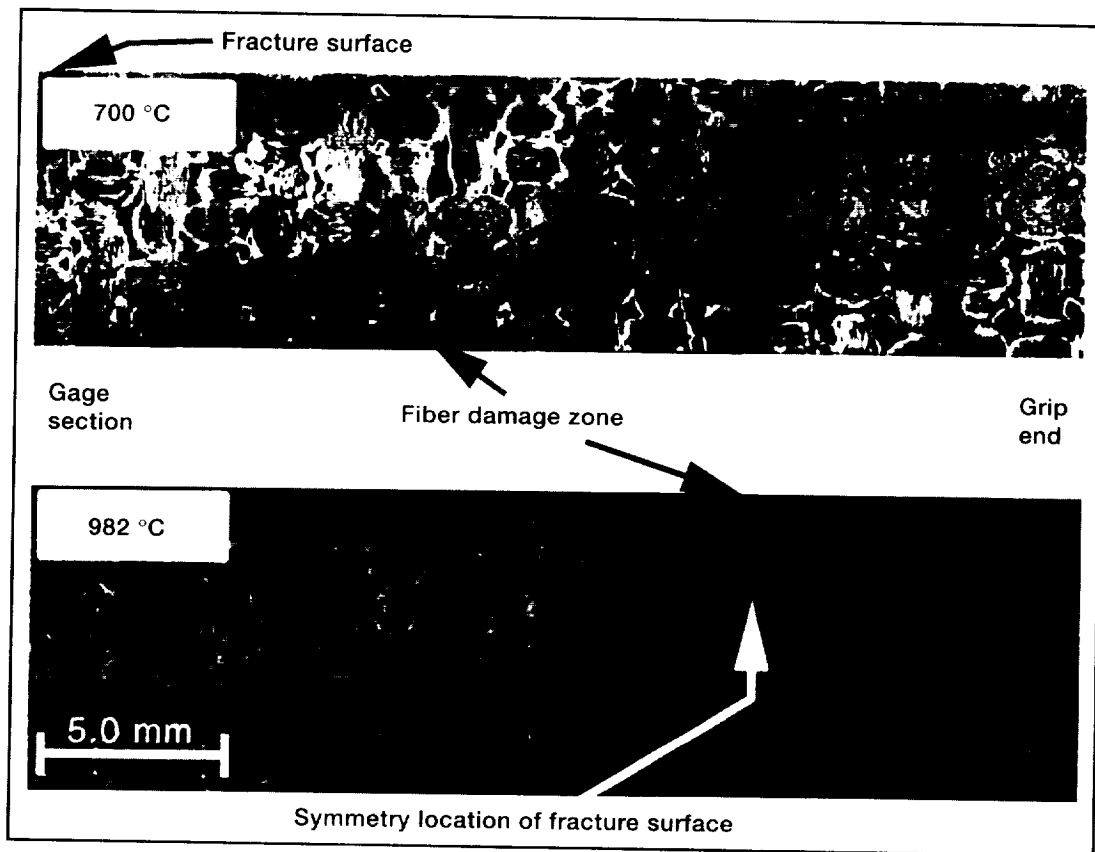
As part of a comprehensive materials characterization program at the NASA Lewis Research Center, tensile creep-rupture tests were performed on a SiC-fiber-reinforced SiC-matrix composite. The results of these tests and subsequent analysis revealed an oxidation embrittlement phenomena that occurs readily at a discreet temperature range below the maximum use temperature. The graph shows rupture lives for a creep stress of 83 MPa as a function of temperature. Note that the rupture time is constant at an intermediate temperature range of 700 to 982 °C. This graph also shows the failure location, as measured from the center of the specimen. Whereas for temperatures of 500 to 700 °C, failure occurred in the specimen gage section; at higher temperatures, the failure location migrated toward the cooled grip ends. Although the results initially suggested that the test procedure was influencing the measured creep rupture lives and driving the failure location out of the gage section, subsequent experiments and thermal stress analyses verified the robustness of the test method employed.



Stress rupture data for [0°/90°] DuPont enhanced chemical vapor infiltration SiC/Nicalon SiC composite as a function of gage section temperature at a creep stress of 83 MPa. Also shown is the failure location as a function of gage section temperature.

Metallurgical examination of failed specimens revealed an environmentally assisted material degradation operating in the 700 to 800 °C range. The photomicrographs show the distribution of damage in two specimens tested at the same stress but different gage section temperatures. In the views shown, the sections are polished in the thickness direction, showing the broad specimen face. The loading direction is horizontal. In the 700 °C specimen, creep damage is distributed throughout the uniformly heated test section. However, in the 982 °C specimen, damage is concentrated only at the point outside the gage section where the temperature was found to be 700 to 800 °C; less damage occurred within the hotter gage section. Both specimens failed because of an aggressive environmental attack of the SiC fibers at location where the temperature was in the 700 to 800 °C range.

SiC/SiC composites are candidates for a combustor liner application in the engine of the High Speed Civil Transport vehicle. During its service cycle, the combustor liner will experience a thermal gradient, being cooled near attachment regions and exposed to combustor gases on the inner wall. The existence of a minimum in creep rupture behavior over a discreet temperature range indicates that the kinetics of this process are unconventional. Thus, material properties must be well characterized over the temperature range of expected operation. Also, this behavior must be accounted for in designing and determining the life of components.



*Creep damage distribution of two [0°/90°] DuPont enhanced chemical vapor infiltration SiC/Nicalon SiC specimens tested at a stress of 83 MPa. The damaged fiber tows were found throughout the gage section of the 700 °C specimen. However, for the 982 °C specimen, the damage was concentrated at the point outside of the gage section where the temperature was 700 to 800 °C.*

## Reference

Verrilli, M.J.; Calomino, A.M.; and Brewer, D.N.: Creep Rupture Behavior of a SiC/SiC Composite. Thermal and Mechanical Test Methods and Behavior of Continuous Fiber Ceramic Composites, ASTM STP 1309, Michael G. Jenkins, Stephen T. Gonczy, Edgar Lara-Curzio, Noel E. Ashbaugh, and Larry P. Zawada, eds., American Society for Testing and Materials, in press.

**Lewis contact:** Michael J. Verrilli, (216) 433-3337, SMVeril@popserve.lerc.nasa.gov

**Author:** Michael J. Verrilli

**Headquarters program office:** OA

# TURBO-AE: An Aeroelastic Code for Propulsion Applications

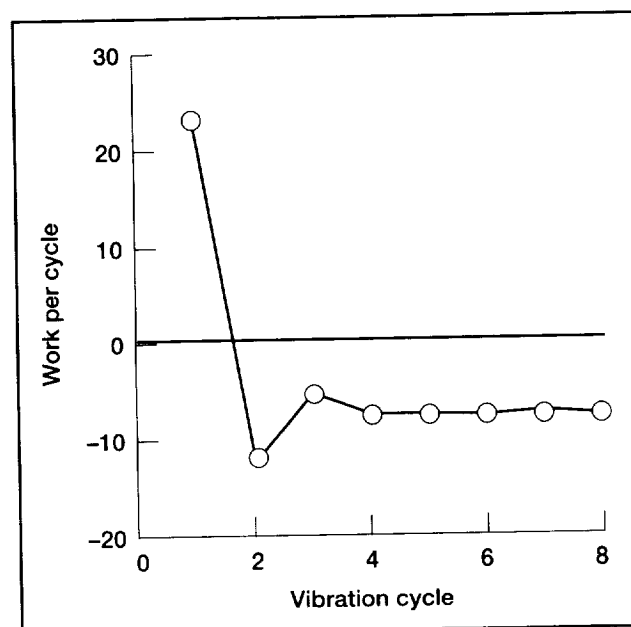
NASA's Advanced Subsonic Technology (AST) program is developing new technologies to increase the fuel efficiency of commercial aircraft engines, improve the safety of engine operation, and reduce engine emissions and noise. With the development of new designs for ducted fans, compressors, and turbines to achieve these goals, a basic aeroelastic requirement is that there should be no flutter or high resonant blade stresses in the operating regime. To verify the aeroelastic soundness of these designs, we need an accurate prediction and analysis code. Such a two-dimensional viscous propulsion aeroelastic code, named TURBO-AE, is being developed at the NASA Lewis Research Center.

The TURBO-AE aeroelastic code is based on a three-dimensional unsteady aerodynamic Euler/Navier-Stokes turbomachinery code TURBO, developed under a grant from NASA Lewis. TURBO-AE can model viscous flow effects that play an important role in certain aeroelastic problems, such as flutter with flow separation (or stall flutter) and flutter in the presence of shock and boundary-layer interaction. The structural dynamics representation of the blade in the TURBO-AE code is based on a normal mode representation. A finite-element analysis code, such as NASTRAN, is used to calculate in-vacuum vibration modes and the associated natural frequency.

A work-per-cycle approach is used to determine aeroelastic (flutter) stability. With this approach, the motion of the blade is prescribed to be a harmonic vibration in a specified in-vacuum normal mode. The aerodynamic forces acting on the vibrating blade and the work done by these forces on the vibrating blade during a cycle of vibration are calculated. If positive work is being done on the blade by the aerodynamic forces, the blade is dynamically unstable, since it will extract energy from the flow, leading to an increase in the amplitude of the blade's oscillation.

Initial calculations have been done for a configuration representative of the Energy Efficient Engine fan rotor. The accompanying figure shows the work-per-cycle after each cycle of vibration. It can be seen that the work-per-cycle does not vary much after the fourth cycle. The negative sign of the converged work-per-cycle shows that the fan blade is dynamically stable and will not flutter.

TURBO-AE will provide a useful aeroelastic prediction/analysis capability for engine manufacturers. It will reduce design cycle times by allowing new blade designs to be verified for aeroelastic soundness before blades are built and tested. With this prediction capability, it will be possible to build thinner, lighter, and faster rotating blades without encountering aeroelastic problems like stall flutter and high-cycle fatigue due to forced vibrations.



*Aeroelastic work-per-cycle for a blade vibrating in the first mode.*

## Bibliography

Bakhle, M.A., et al.: Development of an Aeroelastic Code Based on an Euler/Navier-Stokes Aerodynamic Solver. ASME Paper 96-GT-311, 1996.

## Lewis contact:

Milind A. Bakhle, (216) 433-6037, [smbakh@milind.lerc.nasa.gov](mailto:smbakh@milind.lerc.nasa.gov)

**Author:** Milind A. Bakhle

**Headquarters program office:** OA

# Rotordynamics on the PC: Transient Analysis With ARDS

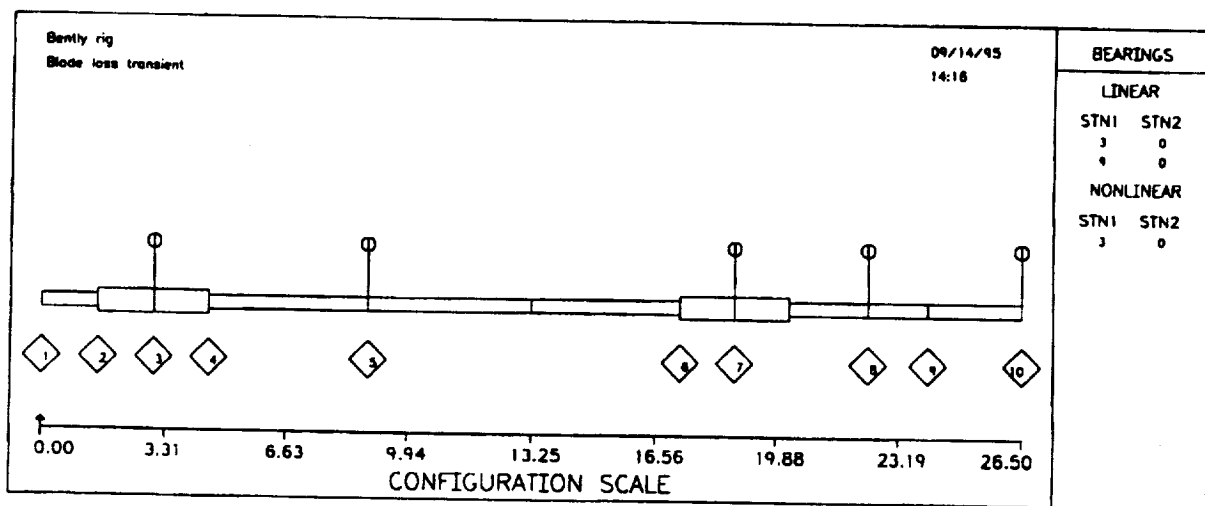
Personal computers can now do many jobs that formerly required a large mainframe computer. An example is NASA Lewis Research Center's program Analysis of RotorDynamic Systems (ARDS), which uses the component mode synthesis method to analyze the dynamic motion of up to five rotating shafts. As originally written in the early 1980's, this program was considered large for the mainframe computers of the time.

ARDS, which was written in Fortran 77, has been successfully ported to a 486 personal computer. Plots appear on the computer monitor via calls programmed for the original CALCOMP plotter; plots can also be output on a standard laser printer. The executable code, which uses the full array sizes of the mainframe version, easily fits on a high-density floppy disk. The program runs under DOS with an extended memory manager. In addition to transient analysis of blade loss, step turns, and base acceleration, with simulation of squeeze-film dampers and rubs, ARDS calculates natural frequencies and unbalance response.

ARDS-PC was used to analyze a magnetic-bearing-supported rotor (a small rotordynamics demonstrator rotor) as it experiences a sudden increase in imbalance or drops onto backup bearings. ARDS draws an outline of the rotor configuration, which appears in the following figure for the example rotor. This rotor was modeled with 9 elements, resulting in 10 rotor stations. Concentrated masses were attached to the shaft at 5 of the stations. An electromagnetic bearing was at station 3, and a bronze bushing supported the shaft at station 8. Magnetic bearings are customarily used with "back-up" bearings that can support the rotor if the magnetic bearing fails. For this example, a backup bearing in the form of a loose bushing was modeled in addition to the magnetic bearing at station 3. No contact occurred in the backup bearing during normal (magnetically suspended) operation; therefore, the backup bearing was nonlinear in that the stiffness was zero until the radial clearance was taken up. It was then assumed to have a constant

stiffness in the radial direction; the tangential force was calculated as the radial force times a friction coefficient. This bearing model was built into ARDS. Each computer run used 100 time steps per revolution. On the 50-MHz 486 computer used, 4000 time steps took slightly less than 2 min calculation time.

A blade loss in a turbine engine introduces a sudden imbalance that can be many times the normal operating imbalance. Under this condition, the magnetic bearing supporting the rotor can become overloaded to the point that the backup bearing comes into operation. As the bearing makes contact, the situation is similar to that of a turbine wheel contacting its outer shroud. The top figure on the facing page shows 10 revolutions of a blade loss transient with an active linear magnetic bearing and a friction coefficient of 0.4 assumed for the backup bearing. This figure is an orbital plot of the rotor at station 3, the magnetic bearing location. The imbalance is applied to the rotor at station 5. The plot



ARDS drawing of example rotor.

shows that the rotor flies out, hits the backup bearing, bounces off, and repeats this behavior for the entire time period plotted.

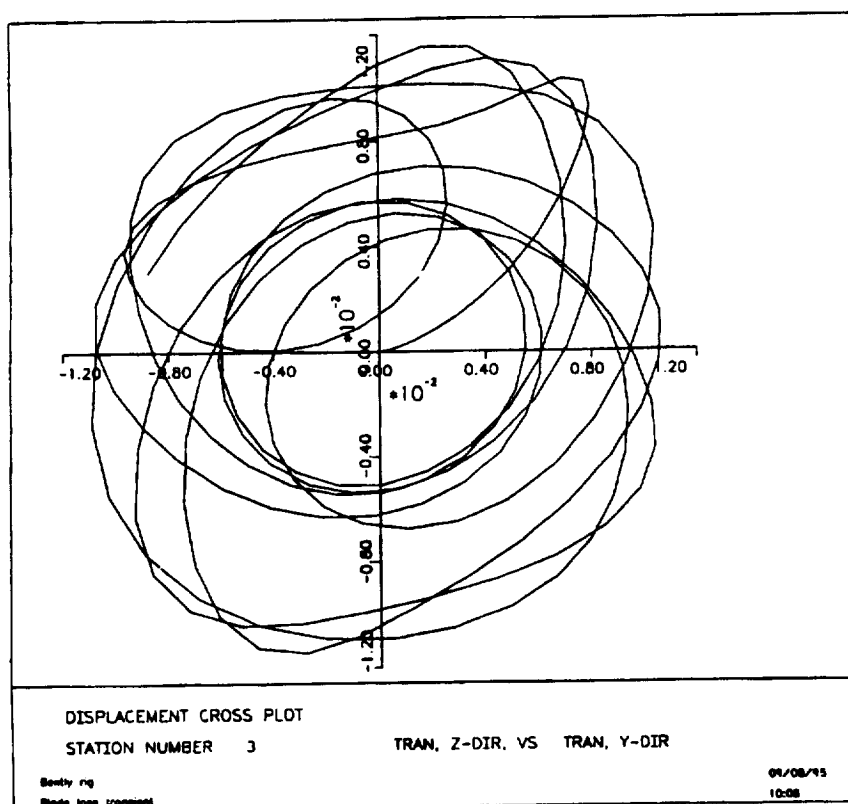
The bottom figure plots the dynamic behavior of the rotor when the magnetic support fails and the rotor drops onto the backup bearing. The rotor walks up the side of the bearing, although the more sensitive scale for the horizontal axis in this figure exaggerates this motion. The vibratory motion eventually dies down. Excitation forces can be combined: for example, a turn combined with blade loss and base acceleration.

**Lewis contact:**

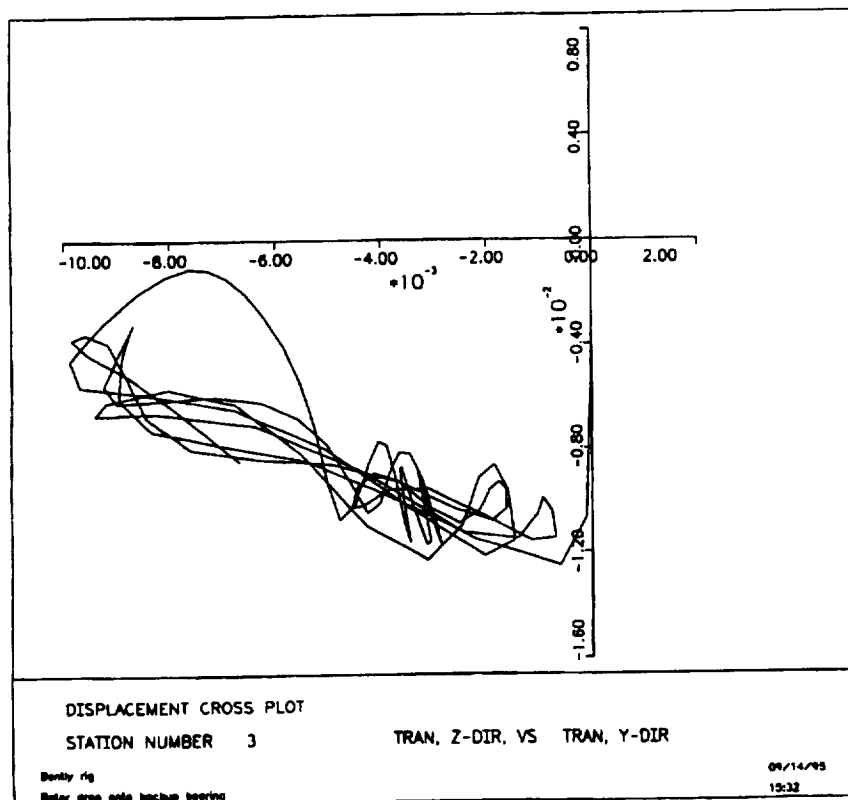
Dr. David P. Fleming, (216) 433-6013,  
smflemn@popserve.lerc.nasa.gov

**Author:** Dr. David P. Fleming

**Headquarters program office:** OA



Orbital motion of magnetic and backup bearing for sudden imbalance.



Rotor drop onto backup bearing.

# Space Mechanisms Lessons Learned and Accelerated Testing Studies

A number of mechanism (mechanical moving component) failures and anomalies have recently occurred on satellites. In addition, more demanding operating and life requirements have caused mechanism failures or anomalies to occur even before some satellites were launched (e.g., during the qualification testing of GOES-NEXT, CERES, and the Space Station Freedom Beta Joint Gimbal). For these reasons, it is imperative to determine which mechanisms worked in the past and which have failed so that the best selection of mechanically moving components can be made for future satellites. It is also important to know where the problem areas are so that timely decisions can be made on the initiation of research to develop future needed technology.

To chronicle the life and performance characteristics of mechanisms operating in a space environment, a Space Mechanisms Lessons Learned Study was conducted. The work was conducted by the NASA Lewis Research Center and by Mechanical Technologies Inc. (MTI) under contract NAS3-27086. The expectation of the study was to capture and retrieve information relating to the life and performance of mechanisms operating in the space environment to determine what components had operated successfully and what components had produced anomalies. The table on the facing page lists some mechanism anomalies found in spacecraft that are discussed in two publications on this subject (refs. 1 and 2).

The goal of building longer-life unmanned satellites and space probes has created a demand for meaningful accelerated test methods to simulate long-term service in space. This is particularly true for tribological components used in space—such as bearings, seals, and gears. In addition, there is an urgent need for lightweight, low-torque, durable mechanisms that can operate efficiently in a hard vacuum environment.

In response to this need, a study was conducted by Lewis and MTI (under contract NAS3-27086) to determine if any mechanisms (which operate in the space environment) would benefit from accelerated testing techniques (ref. 3). The study investigated the current types of accelerated testing techniques, their shortfalls, and the need to develop new techniques. An accelerated testing technology "roadmap" was developed for assessing the life and reliability of spacecraft mechanical systems by accelerated testing methods. The "roadmap" suggested that system components testing, analytical modeling, computer codes, and computer smart systems could be integrated into a methodology that could be used to predict or verify the life and reliability of a mechanical system. The study team suggested that a space mechanism mechanical system be tested to demonstrate that the methods developed could adequately predict the life and/or performance of a mechanism. Included in the "roadmap" are the experimental equipment needed, the test procedures, the time guidelines, and cost analysis.

## References

1. Shapiro, W., et al.: Space Mechanisms Lessons Learned Study, Volume I—Summary. NASA TM-107046, 1995.
2. Shapiro, W., et al.: Space Mechanisms Lessons Learned Study, Volume II—Literature Review. NASA TM-107047, 1995.
3. Murray, S.F.; and Heshmat, H.: Accelerated Testing of Space Mechanisms. NASA CR-198437, 1995.

## Lewis contact:

Robert L. Fusaro, (216) 433-6080,  
smfusro@popserve.lerc.gov

**Author:** Robert L. Fusaro

**Headquarters program office:** OA

## MECHANISM ANOMALIES IN SPACECRAFT

System	Conditions	Problem	Impact
Momentum wheel spin bearings	3600-rpm, grease-packed bearings; room temperature to 100 °F	Torque and spin temperature anomalies	Single-point mission failure; indication of failure
Sensor support bearing	Preloaded ball bearings oscillatory motion	Failure in test	>\$500,000 testing
Sensor launch clamp	Clamp located inside thermal blanketed craft	Seizure on launch pad	Single-point failure prohibited launch or mission failure
Harmonic drives	Very low speed; temperature <150 °F; fluorocarbon lubricant; boundary condition	Excessive wear; lube failure in test	Failure will degrade mission or possible mission failure; changed lubricant
Slip rings; brush contacts	MoS <sub>2</sub> /Ag/C brushes on Ag rings; numerous recurrences	Excessive electrical noise due to moisture and corrosion	Inability to point communications antennas; reduced mission objective
Potentiometer for ATP control	Low temperature; light-load fluid lubricant	Electrical noise lube thickening open circuit	Loss of pointing reduced mission ~\$500,000 testing
Control moment gyroscope	Oil injection on bearing land	Bearing failure lube design wrong	Premature mission failure
Control moment gyroscope	Very high torque for slewing	Bearing failure	Loss of mission; >\$1 million test and anneal
Momentum wheel	Grease lubricated	Torque and temperature anomalies	Possible mission failure
Propellant pump gearbox	High speed	Contractor switching lubricants	Possible launch failure with new lube
Slip rings; brush contacts	MoS <sub>2</sub> /Ag/C brushes on Ag rings	Excessive noise due to oxidation of MoS <sub>2</sub>	Rework brushes and rings; delivery delay
Gear mechanism	High loads; fluorocarbon grease; boundary conditions	Lube degradation	System failure
Synchronous motor assembly	Mineral oil grease-packed bearings	Motor failure due to increased bearing drag	Failure would degrade mission
Momentum wheel spin bearings	High speed; mineral oil grease	Possible lubricant degradation in testing	Single-point mission failure
Inertial guidance synchronous motor bearing	High speed; mineral oil grease	Possible chemical reaction between grease and iron surface during storage	Guidance failure
Harmonic drive	Low-temperature operation; fluoro-carbon grease	Low-temperature viscosity of grease causes excessive torque	Failure will degrade mission
Momentum wheel; active lubrication system	High-speed; long-life requirement	Inability to deliver adequate lubricant quantity	System will not meet lifetime requirement
SADM	Large launch loads on MoS <sub>2</sub> -lubricated bearings	Test of static loads	Possible single-point failure; passed test
Gimbal bearings on test; telescope	Low-temperature; dry (MoS <sub>2</sub> ) lubricant passed	Tested in air friction increase	Modified specification to do inert gas; passed
Spin bearing	Large diameter, thin cross section bearing	Humidity-induced dimensional instability of cotton-phenolic retainer	Possible target acquisition failure; changed to metal ball separator
Gas bearing; gyroscope	Alumina surfaces; stearate lubricant	Erratic friction on startup; uneven lube during test	Reliability problem for flight units; major rework if failure
Foil bearings for turbomachinery	High-strength alloy; CF <sub>x</sub> -polyamide lubricant; temperature extremes	High friction startup after standing	Potential system failure; inability to start turbine

# More-Electric Gas Turbine Engines

A new NASA Lewis Research Center and U.S. Army Research Laboratory (ARL) thrust, the more-electric commercial engine, is creating significant interest in industry. This engine would have an integral starter-generator on the gas generator shaft and would be fully supported by magnetic bearings. The NASA/Army emphasis is on a high-temperature magnetic bearing for future gas turbine engines. Magnetic bearings could increase the reliability and reduce the weight of such engines by eliminating the lubrication system. They could also increase the DN (diameter of the bearing times the rpm) limit on engine speed and allow active vibration cancellation systems to be used, resulting in a more efficient, more-electric engine.

The magnetic bearing, which is similar to an electric motor, has a laminated rotor and stator made of cobalt steel. Electrical wire coils wound around the stator form a series of electromagnets around the circumference that exert a force on the rotor. A probe senses the position of the rotor, and a feedback controller keeps it in the center of the cavity. The engine rotor, bearings, and case form a flexible structure with a large number of modes. The bearing feedback controller must be designed so that none of these modes become unstable. This controller could also be adapted to varying flight conditions so that seal rubs could be avoided. Lastly, this controller could be made to monitor the health of the system.

The cobalt steel used in this magnetic bearing has a curie point greater than 1700 °F, and the copper wire has a melting point beyond that. Practical limitations associated with the maximum magnetic field strength in cobalt steel and the stress in the rotating components limit the temperature to about 1200 °F.

The objective of this effort is to determine the limits in temperature and speed of a magnetic bearing operating in an engine environment. Our approach is to use our in-house experience in magnets, mechanical components, high-temperature materials, and surface lubrication to build and test a magnetic bearing in both a rig and an engine test either at Lewis or through cooperative programs in industrial facilities.

Last year, we made significant advances, and additional work is planned. We procured and tested a high-temperature capacitive displacement probe to 1200 °F. We built a high-temperature homopolar magnetic bearing. Our flexible casing rig is being converted to a high-temperature magnetic bearing rig, and testing should start next year. We plan to develop a high-temperature, compact wire insulation and to fiber reinforce the core lamination to operate at higher temperatures and at high speeds. In addition, we plan to modify our stability analysis and controller theory by including a nonlinear magnetic bearing model. We are developing a controller that has an expert system that can adapt the controller to changing flight conditions and diagnose the health of the system. Then, we will demonstrate the bearing on our rotordynamics rig and, finally, on an engine.

**Lewis contact:** Albert F. Kascak, (216) 433-6024, [smkascak@popserve.lerc.nasa.gov](mailto:smkascak@popserve.lerc.nasa.gov)

**Author:** Albert F. Kascak

**Headquarters program office:** OA

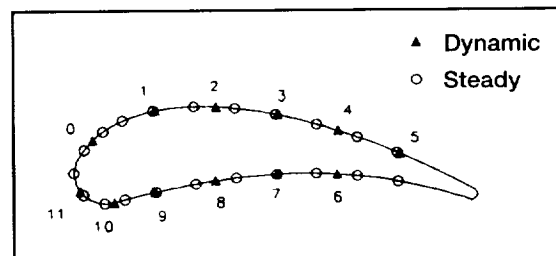


# Measurement of Gust Response on a Turbine Cascade

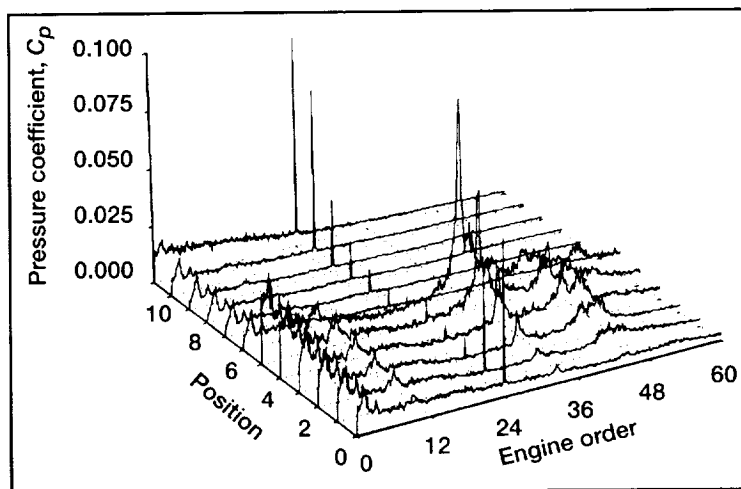
This in-house experiment on the gust response of an annular turbine cascade was particularly designed to provide data to compare with the results of a typical, linearized gust-response analysis. Reduced frequency, Mach number, and incidence were varied independently. Except for the lowest reduced frequency, the gust velocity distribution was nearly sinusoidal. For the high inlet-velocity series of tests, the cascade was near choking. The mean flow was documented by measuring blade surface pressures and the cascade exit flow, and high-response pressure transducers were used to measure the unsteady pressure distribution. Inlet-velocity components and turbulence parameters were measured using hot wire anemometry. In addition to the synchronous time-averaged pressure spectra, typical power spectra are included for several representative conditions.

The gusts were generated by a rotor consisting of 3.17- or 4.76-mm-diameter pins. Either 6, 12, or 24 pins were used, resulting in a gust reduced frequency of 2.5, 5, or 10. The annular turbine cascade had 24 blades, and it was positioned 3.9 axial chordlengths behind the rotor. The top figure illustrates the positions of instrumentation ports, and the bottom figure illustrates representative root-mean-square (rms) spectra. The synchronous peaks could have been obtained by linear phase-lock averaging; however, the rms-averaged spectra also include the nonsynchronous origin and the random pressure fluctuations. The frequency units are engine orders; thus, the synchronous peaks appear at the frequency equal to the number of rotor pins used to generate wakes. The position-axis units correspond to the blade port numbers in the first figure; thus, position 0 corresponds to the port nearest to the leading edge on the suction surface side, and position 11 corresponds to the port nearest to the leading edge on the pressure side.

The gust amplitude varied somewhat with the reduced frequency; however, it did not appear to have a dominant effect. Unsteady, synchronous-response blade pressures depend strongly on reduced frequency and incidence. Mach number dependence is weak for negative incidence and significant for positive incidence at lower reduced frequencies. The mean blade-pressure distribution depends, to some extent, on the reduced frequency, particularly for the negative incidence and the higher inlet Mach number. At a reduced frequency of 10, an inlet Mach number of 0.27, and a positive incidence, magnification of the turbulent pressure fluctuations on the suction side of the aft portion of the blade resulted in a significant excitation concentrated at an integral engine order much higher than the synchronous excitation frequency.



Instrumentation ports.



Root-mean-square pressure spectra showing the pressure coefficients,  $C_p$ , for a reduced frequency of 10, an inlet Mach number of 0.27, and a positive incidence.

## Lewis contact:

Dr. Anatole P. Kurkov, (216) 433-5695,  
Anatole.P.Kurkov@lerc.nasa.gov

**Author:** Dr. Anatole P. Kurkov

**Headquarters program office:** OA

# Fan Blade Deflection Measurement and Analyses Correlation

Steady deflection measurements were taken of two identical NASA/Pratt & Whitney-designed fan blades while they were rotating in a vacuum in NASA Lewis Research Center's Dynamic Spin Facility. The one-fifth-scale fan blades, which have a tip diameter of 22 in. and a pin-root retention, are of spar-shell construction and were unducted for this test. The purpose of the test was to measure the change of the radial deflection of the blade tip and blade angle at selected radial stations along the blade span with respect to rotational speed.

## Lewis contact:

Oral Mehmed, (216) 433-6036,  
oral.mehmed@lerc.nasa.gov

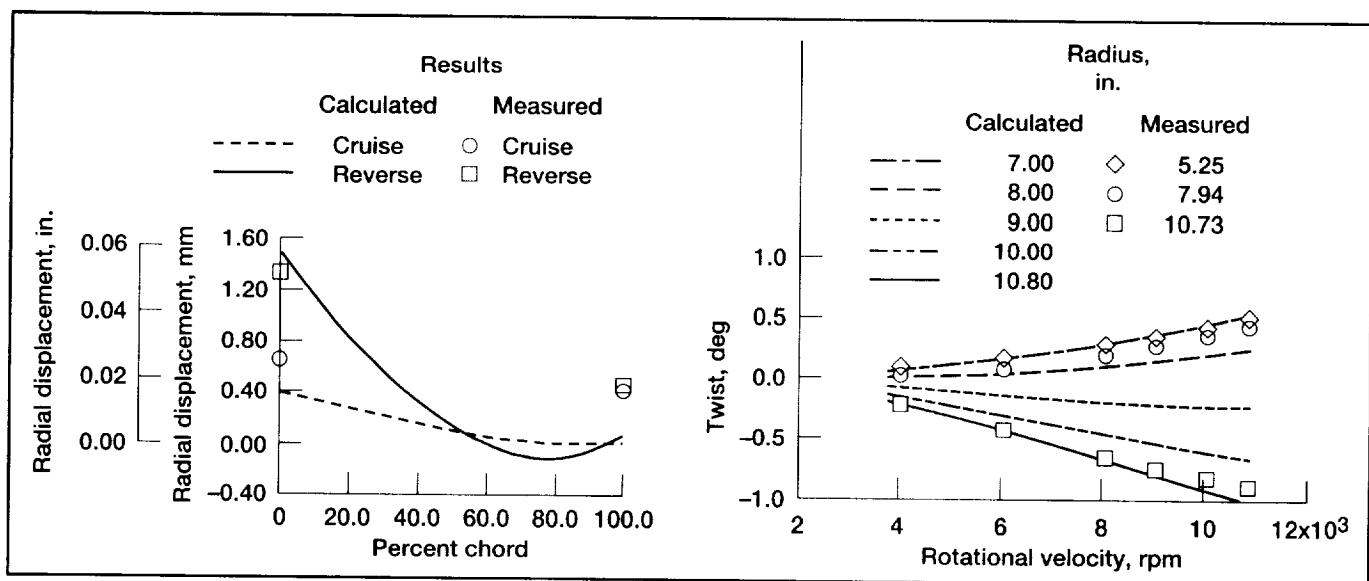
**Authors:** Oral Mehmed and  
David C. Janetzke

**Headquarters program office:** OA

The procedure for radial deflection measurement had no precedent and was newly developed for this test. Radial deflection measurements were made to assure adequate tip clearance existed between the fan blades and the duct for a follow-on wind tunnel test. Also, blade angle deflection measurements were desired before pitch-setting parts for the wind tunnel test were finish machined. During the test, laser beams were aimed across the blade path into photodiodes to give signals that were used to determine blade angle change or tip radial deflection. These laser beams were set parallel to the spin axis at selected radial stations.

For the figures, we compared results from the test with analytical predictions made at NASA. The figure on the left compares measured and calculated values for tip radial deflection at 10,000 rpm for cruise and reverse staggers.<sup>1</sup> The figure on the right shows the measured and calculated change in blade angle versus rotational speed for the cruise stagger measured at three radial stations.

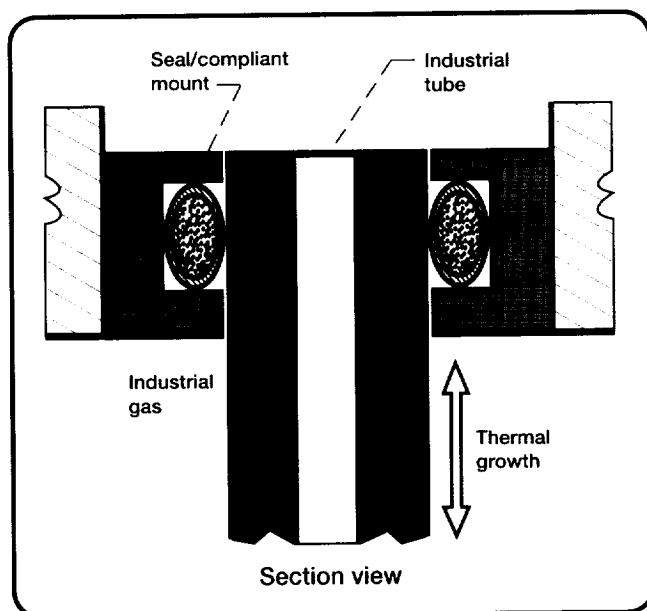
<sup>1</sup> Stagger refers to the pitch setting of the blade with respect to the axial flow direction.



Left: Measured and calculated blade tip radial displacements at 10,000 rpm. Right: Measured and calculated blade twist at cruise.

## Feasibility of Rope Seal Technology Demonstrated for an Industrial Application

As the operating temperatures of industrial systems and advanced gas turbines continue to rise, designers are facing increasingly more difficult challenges in implementing high-temperature structural materials and seals to meet system performance goals. To maximize efficiency, they are reducing seal purge flows to their practical minimum and are requiring low-leakage seals to be made of temperature-resistant superalloy and ceramic materials. Seals are being designed to both seal and serve as compliant mounts, allowing for relative thermal growths between high-temperature, but brittle, primary structures and the surrounding support structures (see figure).



*Technology transfer case study. Problem: An industrial application required a high-temperature, flexible seal/compliant mount to seal apparatus and prevent excessive structural loads. Solution: NASA demonstrated the feasibility of a compliant seal/mount arrangement that met the industrial customer's flow and durability goals—it operates hot (1500+ °F), exhibits low leakage, allows 0.3-in. relative thermal growth without binding or abrasion, and is chemically inert.*

Under a cooperative agreement with a major supplier of industrial gas products, the NASA Lewis Research Center has demonstrated the feasibility of all-ceramic and hybrid rope seals for a tube seal application. In this application, a seal is designed to serve as a seal and a compliant mount, allowing relative thermal growth between a high-temperature, low-expansion rate primary tube structure and a higher expansion rate structural support, thereby preventing excessive thermal strains and stresses. The all-ceramic seal consists of a tightly packed ceramic core (alumina-silica) overbraided with a ceramic sheath for low-leakage, low-scrubbing environments. The hybrid seal, which consists of a tightly packed ceramic (alumina-silica) core overbraided with a superalloy (cobalt base) wire sheath, was tested as an abrasion-resistant alternative.

High-temperature flow and durability were measured for both the all-ceramic and hybrid seals. Flow tests were performed in a unique NASA Lewis high-temperature test rig capable of 1500 °F. Compression tests in displacement control mode were used in conjunction with pressure-sensitive film to determine seal contact pressures and establish required groove-depths to set seal preload in the flow tests. (Braided seals exhibit hysteresis (i.e., non-recoverable displacement) during loading and have a memory of previous loading conditions.) The seal flows met the acceptable flow goal for the design preloads. Furthermore, sheath damage was minimal over the thermal cycles.

On the basis of these observations, which were made during Phase I, the braided seal was deemed feasible for the industrial tube seal application. As a result, NASA has entered into a Phase II Space Act Agreement with our industrial customer to transfer the seal technology to the actual industrial application. Lewis personnel will be helping the industrial customer insert these seals into their proprietary system. The industrial partner has expressed interest in licensing the rope seal technology from NASA after the seals have been qualified in the prototype system.

### Bibliography

Steinetz, B.M., et al.: High Temperature Braided Rope Seals for Static Sealing Applications. AIAA Paper 96-2910 (Also NASA TM-107233 Revised), 1996.

### Lewis contact:

Dr. Bruce M. Steinetz, (216) 433-3302, [Bruce.M.Steinetz@lerc.nasa.gov](mailto:Bruce.M.Steinetz@lerc.nasa.gov)

**Author:** Dr. Bruce M. Steinetz

**Headquarters program office:** OA

# X-Ray Computed Tomography Monitors Damage in Composites

A recent Presidential initiative in aeronautics and manufacturing technology identified critical technologies for solving key issues in materials and manufacturing. These technologies include high-quality processing of composites, rapid prototyping and reengineering, online sensors, and feedback controllers. The imperative is to reduce new-product development-cycle times and to integrate new technologies such as computed tomography (CT), smart materials with in situ sensors, and process controls. In this context, CT can provide rapid reengineering and cost-effective prototyping.

The NASA Lewis Research Center recently codeveloped a state-of-the-art x-ray CT facility (designated SMS SMARTSCAN model 100-112 CITA by Scientific Measurement Systems, Inc., Austin, Texas). This multipurpose, modularized, digital x-ray facility includes an imaging system for digital radiography, CT, and computed laminography. The system consists of a 160-kV microfocus x-ray source, a solid-state charge-coupled device (CCD) area detector, a five-axis object-positioning subassembly, and a Sun SPARC station-based computer system that controls data acquisition and image processing. The x-ray source provides a beam spot size down to 3  $\mu\text{m}$ . The area detector system consists of a 50- by 50- by 3-mm-thick terbium-doped glass fiber-optic scintillation screen, a right-angle mirror, and a scientific-grade, digital CCD camera with a resolution of 1000 by 1018 pixels and 10-bit digitization at ambient cooling. The digital output is recorded with a high-speed, 16-bit frame grabber that allows data to be binned. The detector can be configured to provide a small field-of-view, approximately 45 by 45 mm in cross section, or a larger field-of-view, approximately 60 by 60 mm in cross section. Whenever the highest spatial resolution is desired, the small field-of-view is used, and for larger samples with some reduction in spatial resolution, the larger field-of-view is used.

This CT system demonstrated excellent resolution<sup>1</sup> at 20 lp/mm (25  $\mu\text{m}$ ) with 20 to 40 percent modulation in the small field-of-view mode, and at 10 lp/mm (50  $\mu\text{m}$ ) with 50 to 70 percent modulation in the larger field-of-view mode. It detected fibers, fiber-matrix debonding, and fiber pullout in  $[\text{O}]_5$  SiC/RBSN (reaction-bonded silicon nitride), and it detected fiber-matrix debonding and the carbon core of oxidized SiC fibers in an engine vane tested at 1040 °C for 4 hr. Images are shown in the accompanying figure. CT evaluation of thermally cycled C/SiC revealed preexisting porosity, internal architecture, cracking, degra-

dation in coatings, and loss of SiC materials.

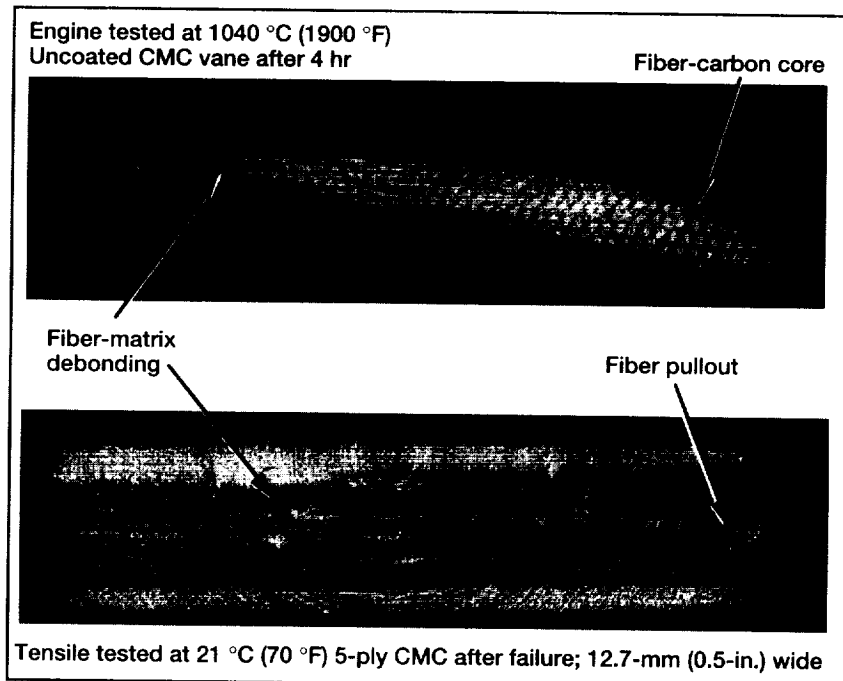
NASA Lewis' CT facility can characterize critical manufacturing problems and compare as-designed with as-built metal matrix composite engine subcomponents (rotors and rings). The facility was developed to provide rapid reengineering and to reduce new-product development-cycle times. Lewis is cooperating with industry to transform the CT technology from a nondestructive evaluation tool to a manufacturing and structural quality improvement tool for in-process modeling, structural modeling, and product safety assurance.

#### Lewis contact:

Dr. George Y. Baaklini, (216) 433-6016,  
Baaklini@lerc.nasa.gov

Author: Dr. George Y. Baaklini

Headquarters program office: OA



X-ray computed tomography (CT) at NASA Lewis monitors damage in CMC's. CT cross sections reveal fibers, fiber architecture, fiber-matrix debonding, and fiber pullout.

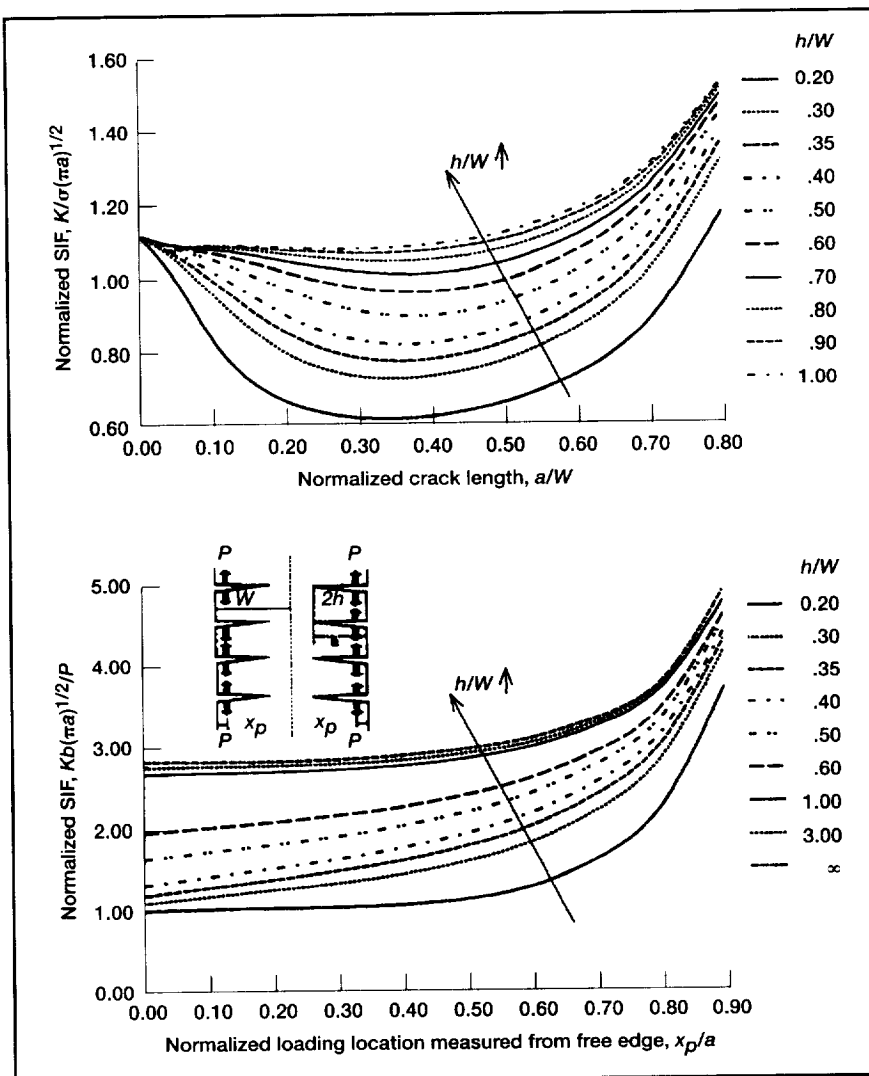
<sup>1</sup> Resolution is given in lines per millimeter (lp/mm) and micrometers (mm).

# Stress Intensity Factor Solutions for Multiple Edge Cracks in Ceramic Matrix Composites

Ceramic matrix composites (CMC's) are candidate materials for high-temperature aerospace applications where high-strength and low-weight are essential for more efficient engines. One advantage of fiber-reinforced ceramics over monolithic ceramics is an increase in fracture toughness because of the presence of unbroken fibers in the wake of advancing cracks. The unbroken fibers restrict the crack opening displacements, shield the crack tip, and reduce the crack driving forces. Extensive experimental studies of various CMC's have also shown the development of a periodic

array of matrix cracks bridged by unbroken fibers in unidirectional and two-dimensional woven systems.

Before these ceramic matrix composite systems can be used in actual engine applications, life-prediction methodologies have to be established on the basis of these observed failure mechanisms. Consequently, the NASA Lewis Research Center conducted a study to determine the stress intensity factor solutions for periodic arrays of bridged cracks for various crack spacings and crack lengths. Initially, the stress intensity factor of an array of unbridged multiple edge cracks was determined under constant global displacement as well as at a point load along the crack wake. These solutions are expected to contribute toward the development of a damage-based life-prediction methodology for CMC engine components.



Normalized stress intensity factor (SIF),  $K$ , for multiple double-edge notch specimens. Uniform stress,  $\sigma$ ; point load,  $P$ ; crack length,  $a$ ; half specimen width,  $W$ ; point loading location,  $x_p$ ; half crack spacing,  $h$ ; and specimen thickness,  $b$ . Top: Uniform remote load with no bridging. Bottom: Point load along the crack faces for  $a/W = 0.5$ .

## Bibliography

Ghosn, L.J.; and Worthem, D.W.: Damage Tolerance Based Life Prediction Methodology in Ceramic Matrix Composites. HITEMP Review 1995, NASA CP-10178, Vol. III, 1995, pp. 49-1 to 49-12.

## Lewis contact:

Dr. Louis Ghosn, (216) 433-3249, smghosn@lerc.nasa.gov

Author: Dr. Louis Ghosn

Headquarters program office: OA

# Award-Winning CARES/*Life* Ceramics Durability Evaluation Software Is Making Advanced Technology Accessible

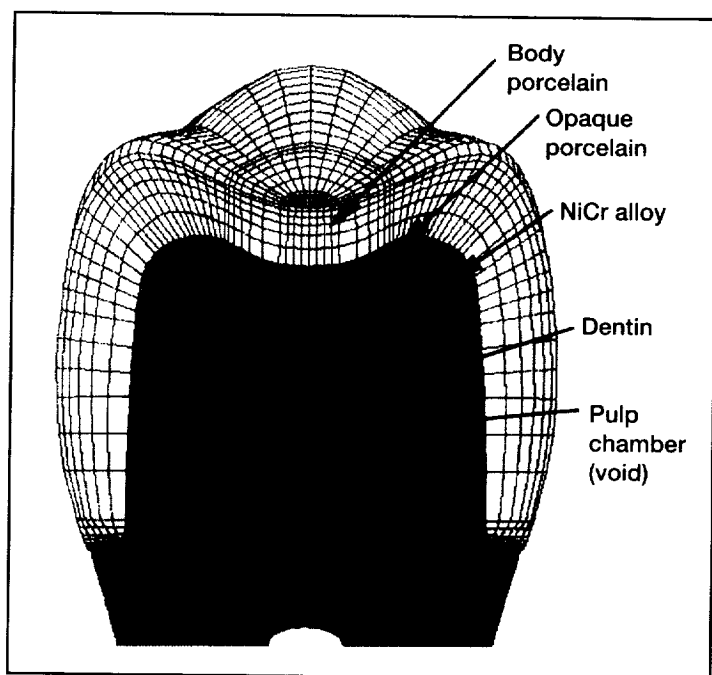
Products made from advanced ceramics show great promise for revolutionizing aerospace and terrestrial propulsion and power generation. However, ceramic components are difficult to design because brittle materials in general have widely varying strength values. The CARES/*Life* software developed at the NASA Lewis Research Center eases this by providing a tool that uses probabilistic reliability analysis techniques to optimize the design and manufacture of brittle material components.

CARES/*Life* is an integrated package that predicts the probability of a monolithic ceramic component's failure as a function of its time in service. It couples commercial finite element programs—which resolve a component's temperature and stress distribution—with reliability evaluation and fracture mechanics routines for modeling strength-limiting defects. These routines are based on calculations of the probabilistic nature of the brittle material's strength.

The program has many features and options for materials evaluation and component design, and the capability, flexibility, and uniqueness of CARES/*Life* has attracted much interest. To maintain this interest as well as keep abreast of fast-changing operating systems and applications software, we have upgraded CARES/*Life* with graphic templates for common business presentation software such as Lotus Freelance Graphics. In addition, an interactive input preparation program has been prepared to guide users through various program control options and specific data input formats. A grinding damage module has been added to account for flaws introduced

by finishing (grinding) operations and specimen rupture data. This grinding damage module, in conjunction with finite element analysis, can now be used to characterize the material fracture behavior.

CARES/*Life* has been in high demand world-wide, although present technology transfer efforts are entirely focused on U.S.-based organizations. Success stories can be cited in numerous industrial sectors, including aerospace, automotive, biomedical, electronic, glass, nuclear, and conventional power-generation industries. In 1995, R&D Magazine gave a prestigious R&D 100 Award jointly to the NASA Lewis Research Center for development of CARES/*Life* and to Philips Display Components Company for applying this software to the design and manufacture of an improved television picture tube for the U.S. consumer market. The exceptional technical accomplishments and efforts of the CARES/*Life* development team were also recognized with NASA Lewis' 1995 Steven V. Szabo Engineering Excellence Award.

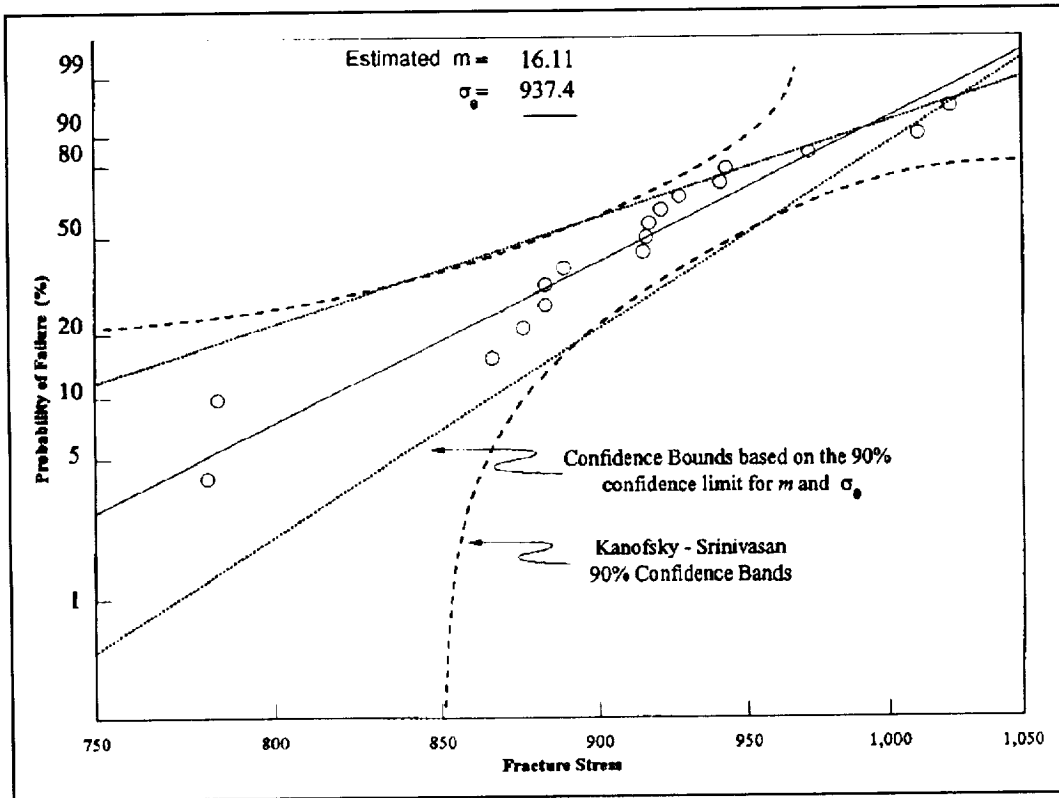


*Tilted view of a cross section and top of a finite element model of a porcelain-fused-to-metal molar crown analyzed with CARES/*Life*.*

## Bibliography

Nemeth, N.N., et al.: Time-Dependent Reliability Analysis of Monolithic Ceramic Components Using the CARES/*Life* Integrated Design Program. *Life Prediction Methodologies and Data for Ceramic Materials*, ASTM STP 1201, C.R. Brinkman, and S.F. Duffy, eds., American Society for Testing and Materials, Philadelphia, PA, 1994, pp. 390-408

Nemeth, N.N., et al.: Lifetime Reliability Evaluation of Structural Ceramic Parts With the CARES/*Life* Computer Program. AIAA Paper 93-1497, 1993.



Sample output from CARES/Graphics. The ability to depict specimen rupture data (two-parameter Weibull data) by using common business presentation graphics packages significantly enhances the utility of CARES/Life for the design engineer.

Powers, L.M., et al.: Lifetime Reliability Evaluation of Monolithic Ceramic Components Using the CARES/Life Integrated Design Program. Proceedings of the American Ceramic Society Meeting and Exposition, Cincinnati, OH, April 19-22, 1993.

Nemeth, N.N., et al.: Designing Ceramic Components for Durability. Am. Cer. Soc. Bul., vol. 72, no. 12, Dec. 1993, pp. 59-69.

Nemeth, N.N., et al.: Durability Evaluation of Ceramic Components Using CARES/Life. ASME Paper 94-GT-362, 1994.

Janosik, L.M.A., et al.: NASA/CARES Dual-Use Ceramic Technology Spinoff Applications. NASA TM-111694, 1994.

Salem, J.A., et al.: Reliability Analysis of Uniaxially Ground Brittle Materials. NASA TM-106852, 1995.

Anusavice, K.J., et al.: Stress and Reliability Analysis of a Metal-Ceramic Dental Crown. NASA TM-107178, 1996.

**Lewis contact:** Noel N. Nemeth, (216) 433-3215, noel.n.nemeth@lerc.nasa.gov

**Author:** Noel N. Nemeth

**Headquarters program office:** OA

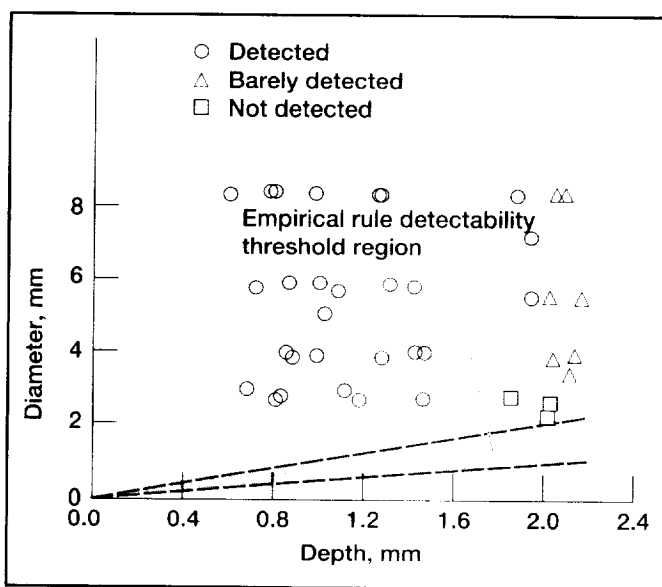
# Capability of Thermographic Imaging Defined for Detection in High-Temperature Composite Materials

Significant effort and resources are being expended to develop ceramic matrix (CMC), metal matrix (MMC), and polymer matrix (PMC) composites for high-temperature engine components and other parts in advanced aircraft. In addition, composite structural material development is being actively pursued in other industries, such as the automobile and sports equipment industries. A portion of the development effort assesses nondestructive evaluation (NDE) technologies for detecting flaws in these materials. Recent technological advancements in infrared camera technology and computer power have made thermographic (infrared) imaging systems worth reevaluating as a reliable NDE tool for advanced composites. Thermography offers the advantages of real-time inspection, no contact with the sample, non-ionizing radiation, complex-shape inspection capability, variable field-of-view size, and portability.

The objective of this NASA Lewis Research Center study was to evaluate the ability of a thermographic imaging technique for detecting artificially created defects (flat-bottom holes) of various diameters and depths in four composite systems (two CMC's, one MMC, and one PMC) of interest as high-temperature structural materials. In the thermographic imaging technique used, the heating source and camera were on the same side. The holes ranged from 1 to 13 mm in diameter and 0.1 to 2.5 mm in depth in samples approximately 2- to 3-mm thick. Limits of detectability based on the depth and diameter of the flat-bottom holes were observed for each composite material. This work was done in cooperation with Bales Scientific, Inc., a manufacturer of state-of-the-art thermography systems, via a Space Act Agreement. It was funded by the High Speed Research program, the Enabling Propulsion Materials (EPM) program, and the High Temperature Engine Materials Program (HITEMP) of which Pratt & Whitney and

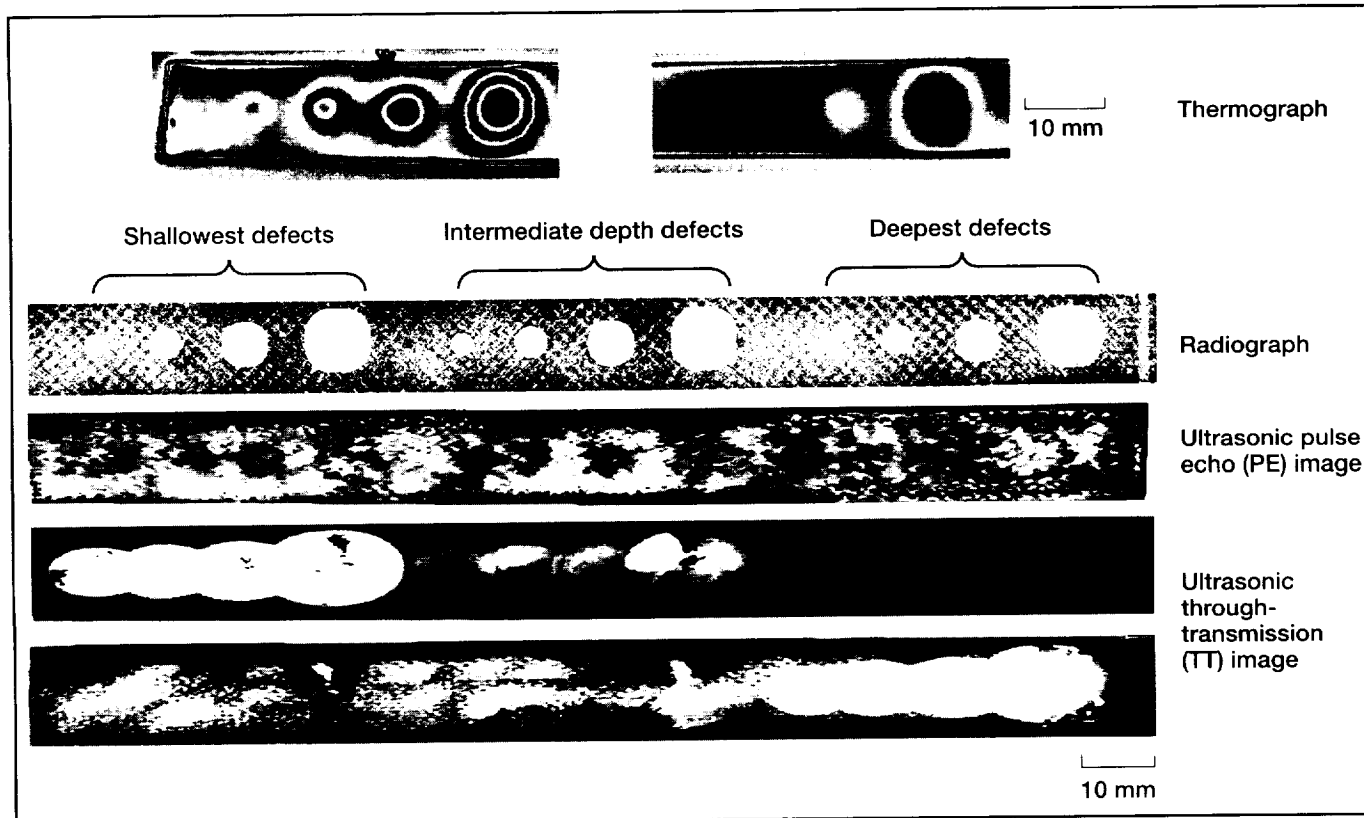
G.E. Aircraft engines are major partners and customers with NASA. This study was completed in 1996, with results reported at EPM, HITEMP, and Quantitative Nondestructive Evaluation (QNDE) technical meetings.

On the basis of the detectability results for the flat-bottom hole samples, the following conclusions were drawn. For the SiC/SiC CMC samples, defects with depths  $\leq 1.8$  mm and diameters  $\geq 2.6$  mm probably will be detected as shown in the graph. For the SiC/CAS CMC samples, defects with depths  $\leq 1.8$  mm and diameters  $\geq 1.6$  mm probably will be detected with the thermography methodology used in this study. For the SiC/Ti MMC samples, defects with depths  $\leq 1.6$  mm and diameters  $\geq 3.2$  mm probably will be detected. For the graphite/polyimide PMC samples, defects with diameters of  $\sim 3$  to 12 mm and  $\leq 1.8$  mm in depth probably will be detected. Depth appears to be the limiting variable with regards to detectability in the PMC system. The thermographic images were compared with ultrasonic and conventional film radiographic images (see the images in the figure on the facing page) for the SiC/SiC composite samples. For these SiC/SiC samples, radiography clearly shows all defects. The ultrasonic pulse echo (PE) image shows very diffuse indications of most defects because of the porous nature ( $\sim 15$  percent) of SiC/SiC. The ultrasonic through-transmission (TT) image shows clear indications of most defects. Thermography clearly shows shallow and intermediate depth defects.



SiC/SiC ceramic matrix composite defect distribution and thermography detectability data.





*Comparison of radiographic, ultrasonic, and thermographic imaging for a SiC/SiC CMC inspection method development.*

Probable detectability limits for the thermography method based on depth and diameter were defined for four composite systems that are of interest for use in high-temperature structural components. These baseline results allow material developers and component designers to determine whether this thermography method can detect a "critical" defect. Thermography images and detectability results were compared with those from conventional ultrasonic and radiographic imaging methods to highlight the relative strengths and weaknesses of the three imaging methods when applied to the composite systems used in this study.

#### **Bibliography**

Roth, D.J.; Bodis, J.R.; and Bishop, C.: Thermographic Imaging for High-Temperature Composite Materials—A Defect Detection Study. NASA TM-106950, 1995.

Roth, D.J.; Bodis, J.R.; and Bishop, C.: Capability of Single-Sided Transient Thermographic Imaging Method for Detection of Flat Bottom Hole Defects in High-Temperature Composite Materials. Proceedings From the 1996 Review of Progress in Quantitative NDE, Brunswick, ME, July 28–Aug. 1, 1996.

**Lewis contact:** Dr. Don J. Roth, (216) 433-6017, smroth@popserve.lerc.nasa.gov

**Author:** Dr. Don J. Roth

**Headquarters program office:** OA

# Space Propulsion Technology

## Rocket Engine Numerical Simulator (RENS)

Work is being done at three universities to help today's NASA engineers use the knowledge and experience of their Apollo-era predecessors in designing liquid rocket engines. Groundbreaking work is being done in important subject areas to create a prototype of the most important functions for the Rocket Engine Numerical Simulator (RENS). **Find out more about RENS on the World Wide Web** (<http://paris.lerc.nasa.gov/kdavidian/RENS/>).

The goal of RENS is to develop an interactive, real-time application that engineers can utilize for comprehensive preliminary propulsion system design functions. RENS will employ computer science and artificial intelligence research in knowledge acquisition, computer code parallelization and objectification, expert system architecture design, and object-oriented programming.

In 1995, a 3-year grant from the NASA Lewis Research Center was awarded to Dr. Douglas Moreman and Dr. John Dyer of Southern University at Baton Rouge, Louisiana, to begin acquiring knowledge in liquid rocket propulsion systems. Resources of the University of West Florida in Pensacola were enlisted to begin the process of enlisting knowledge from senior NASA engineers who are recognized experts in liquid rocket engine propulsion systems. Dr. John Coffey of the University of West Florida is utilizing his expertise in interviewing and concept mapping techniques to encode, classify, and integrate information obtained through personal interviews. The expertise extracted from the NASA engineers has been put into concept maps with supporting textual, audio, graphic, and video material. A fundamental concept map was delivered by the end of the first year of work and the development of maps containing increasing amounts of information is continuing. **For more information about this work, visit the Southern University/University of West Florida homepage on the World Wide Web** (<http://paris.lerc.nasa.gov/kdavidian/SUBR/>).

In 1996, the Southern University/University of West Florida team conducted a 4-day group interview with a panel of five experts to discuss failures of the RL-10 rocket engine in conjunction with the Centaur launch vehicle. The discussion was recorded on video and audio tape. Transcriptions of the entire proceedings and an abbreviated video presentation of the discussion highlights are under development. Also in 1996, two additional 3-year grants were awarded to conduct parallel efforts that would complement the work being done by Southern University and the University of West Florida.

Dr. Prem Bhalla of Jackson State University in Jackson, Mississippi, is developing the architectural framework for RENS. By employing the Rose Rational language and Booch Object Oriented Programming (OOP) technology, Dr. Bhalla is developing the basic structure of RENS by identifying and encoding propulsion system components, their individual characteristics, and cross-functionality and dependencies. **Find out more about the Jackson State University research on the World Wide Web** (<http://paris.lerc.nasa.gov/kdavidian/JSU/>).

Dr. Ruknet Cezzar of Hampton University, located in Hampton, Virginia, began working on the parallelization and objectification of rocket engine analysis and design codes. Dr. Cezzar will use the Turbo C++ OOP language to translate important liquid rocket engine computer codes from FORTRAN and permit their inclusion into the RENS framework being developed at Jackson State University. **More information about these Hampton University codes can be found on the World Wide Web** (<http://paris.lerc.nasa.gov/kdavidian/HU/>).

The Southern University/University of West Florida grant was extended by 1 year to coordinate the conclusion of all three efforts in 1999.

### Bibliography

Booch, G.: Object-Oriented Analysis and Design With Applications. Second edition, The Benjamin/Cummings Publishing Company, Inc., Redwood City, CA, 1994.

### Lewis contact:

Joseph A. Hemminger, (216) 977-7563,  
[Joseph.A.Hemminger@lerc.nasa.gov](mailto:Joseph.A.Hemminger@lerc.nasa.gov)

**Author:** Kenneth O. Davidian

## Ablative Material Testing at Lewis Rocket Lab

The increasing demand for a low-cost, reliable way to launch commercial payloads to low-Earth orbit has led to the need for inexpensive, expendable propulsion systems for new launch vehicles. This, in turn, has renewed interest in less complex, uncooled rocket engines that have combustion chambers and exhaust nozzles fabricated from ablative materials. A number of aerospace propulsion system manufacturers have utilized NASA Lewis Research Center's test facilities with a high degree of success to evaluate candidate materials for application to new propulsion devices.

Because of their knowledge of Lewis' extensive past experience in experimentally evaluating ablative materials (such as nozzle sections for rocket engines), TRW, Thiokol Corporation, and other companies submitted requests to evaluate new material compositions for Lewis. NASA Space Act Agreements were established to carry out these evaluations, utilizing samples supplied by the interested organizations, and the versatile rocket engine test facilities (Test Cell 22) at Lewis. A number of different composite materials were fabricated into nozzle inserts, with and without typical thrust chamber throats, and into as-throated disk samples. These samples were exposed to combustion gas temperatures of gaseous hydrogen and gaseous oxygen propellants from approximately 4400 °F to approximately 6000 °F at thrust chamber pressures from 500 to 900 psia.

Silica composite material samples provided by Thiokol were initially analyzed according to space shuttle experience, to predict the erosion of the nozzle liners to be tested. The primary goal was to minimize the ablative liner thickness and corresponding weight. The results of liner response from the rocket engine test stand show a wide range of erosion rates over test periods up to 341 sec, from negligible erosion for some ceramic composite materials to approximately  $3.4 \times 10^{-3}$  in./sec for some phenolic composites. These data provided key performance information for the application of low-cost, low-density materials. The test data from Cell 22 were also crucial to obtaining better "melt layer" models for silica composite materials.

The samples provided by TRW and others included phenolic and ceramic matrix composites, some with protective throat coatings. As expected, the evaluation resulted in a wide range of durabilities for the composites under these severe operating conditions: the results verified some analytical predictions, and experimentally showed the limitations of other compositions.

These experimental evaluations were conducted in an expeditious and very productive manner, with excellent cooperation between personnel from NASA Lewis and the other companies involved. Thiokol Corporation is currently under contract to the Rocketdyne Division of Rockwell, which is the rocket engine contractor to McDonnell Douglas. The rocket engine test stand, Cell 22, will provide continuing investigation of test

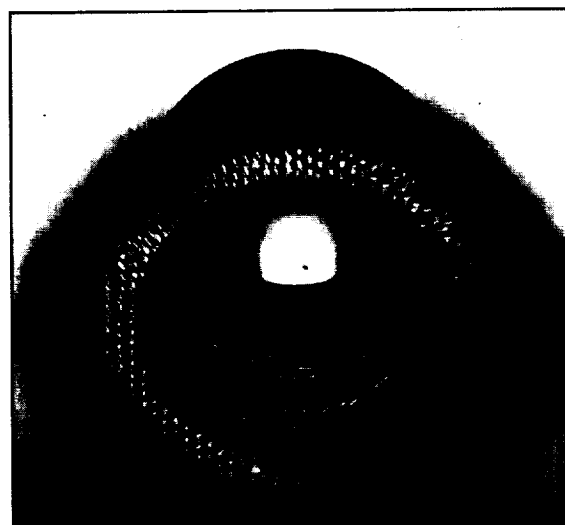
coupons, liners, and nozzles with a very cost effective, fast-paced schedule. The other companies involved have expressed interest in providing additional samples for evaluation in the near future.

### Lewis contacts:

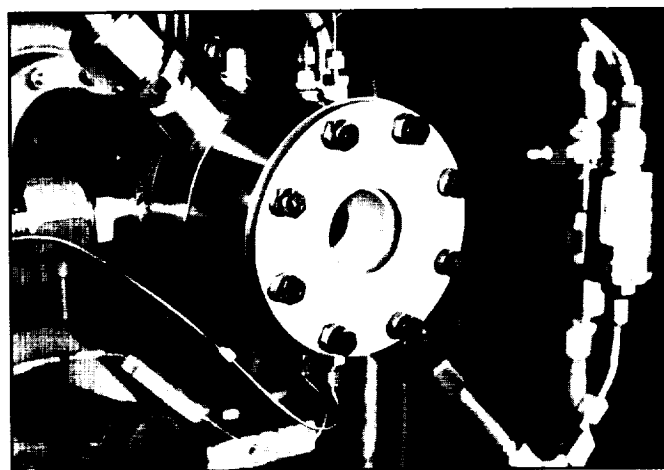
Andrew J. Eckel, (216) 433-8185,  
Andrew.J.Eckel@lerc.nasa.gov;  
Dr. Ali Sayir, (216) 433-6254,  
Ali.Sayir@lerc.nasa.gov; and  
G. Paul Richter, (216) 977-7537,  
G.P.Richter@lerc.nasa.gov

**Author:** G. Paul Richter

**Headquarters program office:** OSAT



*Ablative material sample prior to testing.*



*Test cell 22 rocket engine with sample in place.*

# Real-Time Sensor Validation System Developed for Reusable Launch Vehicle Testbed

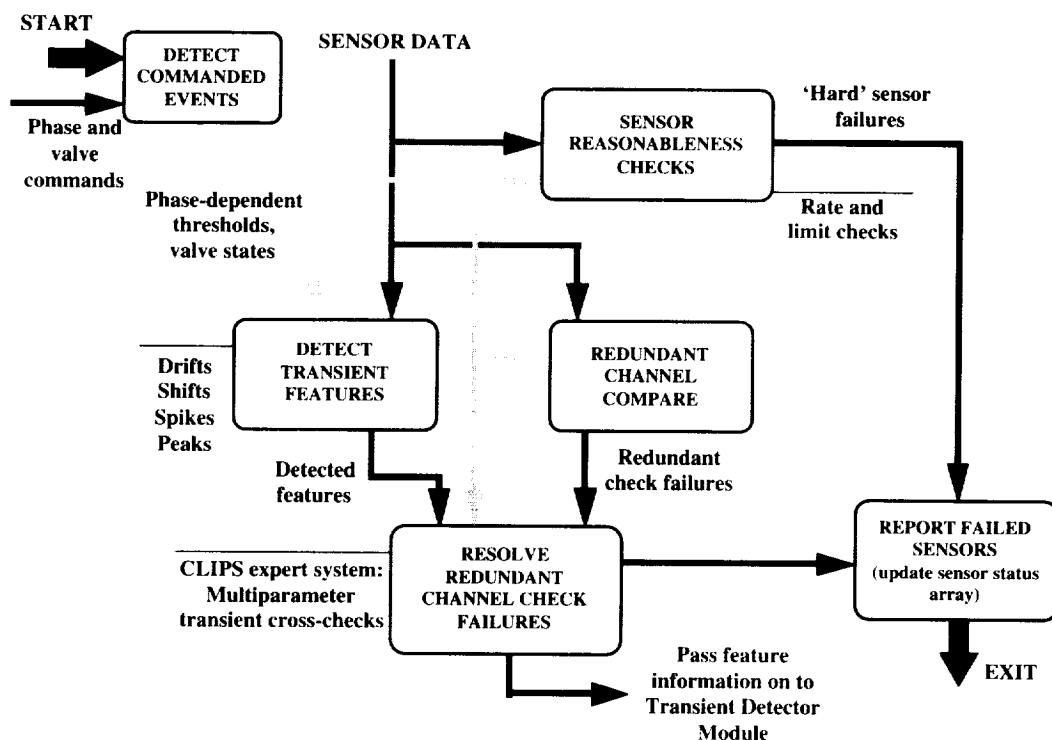
A real-time system for validating sensor health has been developed for the reusable launch vehicle (RLV) program. This system, which is part of the propulsion checkout and control system (PCCS), was designed for use in an integrated propulsion technology demonstrator testbed built by Rockwell International and located at the NASA Marshall Space Flight Center. Work on the sensor health validation system, a result of an industry-NASA partnership, was completed at the NASA Lewis Research Center, then delivered to Marshall for integration and testing.

The sensor validation software performs three basic functions: it identifies failed sensors, it provides reconstructed signals for failed sensors, and it identifies off-nominal system transient behavior that cannot be attributed to a failed sensor. The code is initiated by host software before the start of a propulsion system test, and it is called by the host program every control cycle. The output is posted to global memory for use by other PCCS modules. Output includes a list indicating the status of each sensor (i.e., failed, healthy, or reconstructed) and a list of features that are not due to a sensor failure. If a sensor failure is found, the system modifies that sensor's data array by substituting a reconstructed signal, when possible, for use by other PCCS modules.

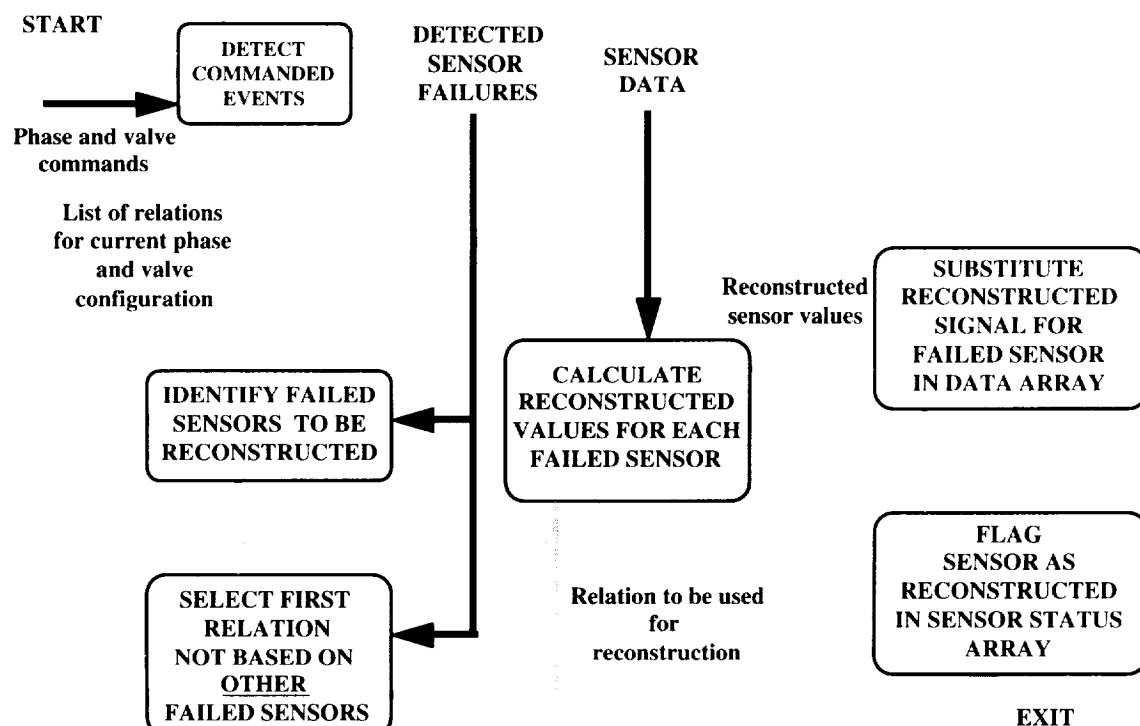
To determine whether a sensor has failed, the software first scans for hard failures by checking its range and rate of change against predetermined limits. The data are then processed to find any features such as drifts, shifts in level, peaks and spikes, and disagreement between redundant channels.

Any discrepancies found among redundant sensors during steady-state system operation are compared with features found in the data. This arbitration is performed by an expert system encoded by using an expert system shell. Any detected features that are not associated with a failed sensor are checked against planned system events, such as valve changes. Features that cannot be explained by a malfunctioning sensor or known system event are reported as transient behavior. This information is then used by other PCCS modules to determine the health of the remaining system components.

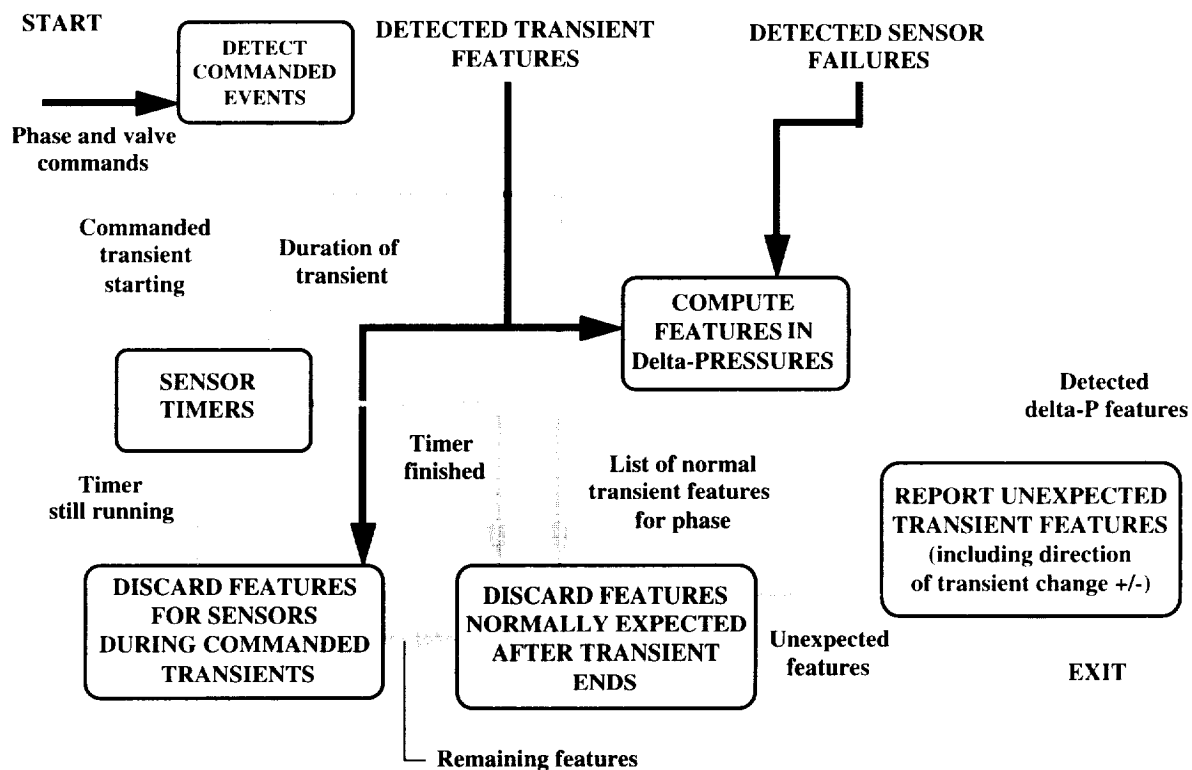
Review of test data from initial integration testing verified operation in real time. Tests were performed for both hard and soft sensor failures, and the sensor validation system was shown to work properly.



*Sensor validation function.*



Sensor reconstruction function.



System transient detector function.

**Lewis contact:** Amy L. Jankovsky, (216) 977-7498, amy@scotland.lerc.nasa.gov

**Author:** Amy L. Jankovsky

**Headquarters Program Office:** OSF

# Demonstration of Oxygen and Carbon Monoxide Propellants for Mars Missions

Currently, proposed planetary exploration missions must be small, with low costs and a short development time. Relatively high-risk technologies are being accepted for such missions if they meet these guidelines. For a Mars sample-return mission, one of the higher-risk technologies is the use of return propellants produced from indigenous materials such as the Martian atmosphere. This consists of 96 percent carbon dioxide, which can be processed into oxygen and carbon monoxide.

This year, the NASA Lewis Research Center completed the experimental evaluation and subscale technology development of an oxygen/carbon monoxide propellant combination. Previous research included ignition characterization, combustion performance, and heat transfer characterization with gaseous propellants at room temperature. In this year's tests, we studied the ignition characteristics and combustion of oxygen and carbon monoxide at near liquid temperatures.

The mixture ratio boundaries for oxygen and carbon monoxide were determined as a function of propellant temperature in a spark torch igniter. With both propellants at room temperature, the ignition range was between 0.50 and 1.44; and with both propellants chilled to near-liquid temperatures, it was between 2.4 and 3.1. Statistical analysis of the mean value of the ignition boundaries provided models that describe the combination of oxygen temperature, carbon monoxide temperature, and mixture ratio that resulted in ignition. This range is the larger boxed area shown in the figure. The smaller boxed area indicates the range at which there is a 90-percent confidence that ignition will occur. The relatively small range at only 90-percent confidence indicates that using the oxygen/carbon monoxide combination as its own ignition source may not be the best design for a remote engine operating on Mars.

Tests also were performed in a simulated small rocket engine that used oxygen/hydrogen combustion gases as the ignition source for oxygen/carbon monoxide. In these experiments, the oxygen/carbon monoxide was successfully ignited in eight of eight tests at a mixture ratio of 0.52. In addition, the oxygen/carbon monoxide maintained steady combustion after the oxygen/hydrogen ignition source was removed, verifying that the oxygen/carbon monoxide rocket engine should continue to be included in mission plans as return propulsion from Mars.

Using all of the previous experimental results, we designed a 500-lbf (Mars sea-level thrust) engine. This engine is the appropriate size for a Mars sample-return mission. Under a phase II

Small Business Innovation Research (SBIR) contract with Ultramet, Inc., the engine is being fabricated from a unique combination of lightweight ceramics for structure and high-temperature refractory metals for combustion-side protection. It will eventually be tested with liquid oxygen and liquid carbon monoxide propellants at NASA Lewis.

## Bibliography

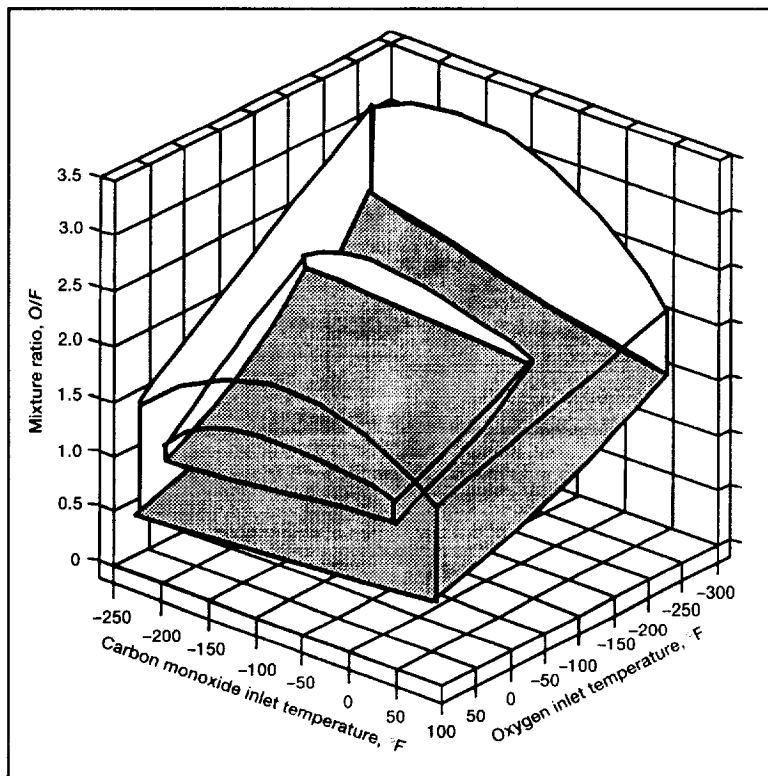
Linne, D.L., Experimental Evaluation of the Ignition Process of Carbon Monoxide and Oxygen in a Rocket Engine. AIAA 96-2943 (Also NASA TM-107267), 1996.

## Lewis contact:

Diane L. Linne, (216) 977-7512,  
Diane.Linne@lerc.nasa.gov

**Author:** Diane L. Linne

**Headquarters program office:** OSAT



Analytical model of the experimental ignition range of carbon monoxide/oxygen and a 90-percent confidence range.

# Metallized Gelled Propellant Heat Transfer Tests Analyzed

A series of rocket engine heat transfer experiments using metallized gelled liquid propellants was conducted at the NASA Lewis Research Center. These experiments used a small 20- to 40-lbf thrust engine composed of a modular injector, an igniter, a chamber, and a nozzle. The fuels used were traditional liquid RP-1 and gelled RP-1 with 0-, 5-, and 55-wt % loadings of aluminum particles. Gaseous oxygen was used as the oxidizer. Heat transfer measurements were made with a rocket engine calorimeter chamber and nozzle with a total of 31 cooling channels. Each channel used water flow to carry heat away from the chamber and the attached thermocouples; flow meters allowed heat flux estimates at each of the 31 stations.

Comparisons of the heat flux and temperature profiles of the RP-1 with those of the metallized gelled RP-1/Al fuels show that, with the metallized gelled  $O_2$ /RP-1/Al propellants, the peak nozzle heat fluxes are substantially higher (up to 2 times higher) than they are for the baseline  $O_2$ /RP-1. Analyses showed that for the RP-1/Al at 55 wt % the heat transfer to the wall differed significantly from its value for the RP-1 fuel. Also, a gellant and an aluminum combustion delay were inferred in the 0- and 5-wt % RP-1/Al cases because of the decrease in heat flux in the first part of the chamber. A large decrease in heat flux in the last half of the chamber was caused by fuel deposition in the chamber and nozzle. According to heat flux estimates from the temperature measurements, engine combustion occurred well downstream of the injector face.

Metallized gelled liquid fuels have the potential to increase the specific impulse, density, and safety of rocket propulsion systems. Although the benefits and military applications of Earth-storable (IRFNA/MMH) gelled and metallized gelled fuels and oxidizers are well established, some questions still exist regarding their application to NASA missions. Oxygen/RP-1/Al and cryogenic metallized gelled propellants show promise in design studies for NASA missions that have an engine efficiency comparable to that for traditional liquid fuels. Analysis of this work and planning for the future is ongoing at NASA Lewis.

The figure depicts the RP-1 and 5-wt % RP-1/Al heat flux profiles. The flux was slightly lower than the baseline RP-1 value near the injector face, reached a peak in the chamber at 5 cm from the face, dropped below the RP-1 flux in the last part of the chamber, and reached a final highest peak just before the nozzle throat. The peak flux in the nozzle was  $6.5 \text{ MW/m}^2$ . We can infer that the coating of partially consumed gel in the chamber reduced the heat flux in the second half of the chamber.

**For more information about this research, visit the Small Business Innovation Research Focused Topic Web Site:**

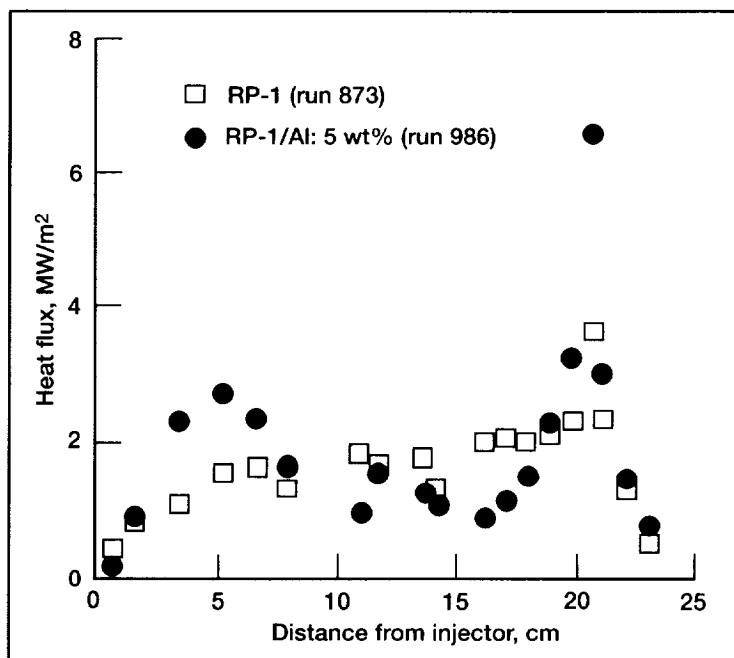
<http://www.lerc.nasa.gov/WWW/TU/launch/foctopsb.htm>

## Bibliography

Palaszewski, B.; and Zakany, J.: Metallized Gelled Propellants: Oxygen/RP-1/Aluminum Rocket Heat Transfer and Combustion Experiments. AIAA Paper 96-2622 (Also NASA TM-107309), 1996.

Palaszewski, B.; Starkovich, J.; Adams, S.: Nanoparticulate Gellants for Metallized Gelled Liquid Hydrogen With Aluminum: AIAA Paper 96-3234 (Also NASA TM-107280), 1996.

Palaszewski, B.: Metallized Gelled Propellant Experiences and Lessons Learned: Oxygen/RP-1/Aluminum Rocket Engine Testing. Presented at the Gel Propulsion Technology Symposium, Huntsville, AL, Sept. 1995. (Permission to use this material was granted by Dorothy L. Becker, January 1997.)



Metallized gelled propellant heat fluxes.

Palaszewski, B.; and Zakany, J.: Metallized Gelled Propellants: Oxygen/RP-1/Aluminum Rocket Combustion Experiments. AIAA Paper 95-2435 (Also NASA TM-107025), 1995.

Wong, W., et al.: Cryogenic Gellant and Fuel Formulation for Metallized Gelled Propellants: Hydrocarbons and Hydrogen with Aluminum. AIAA Paper 94-3175 (Also NASA TM-106698), 1994.

**Lewis contact:** Bryan A. Palaszewski, (216) 977-7493 (voice), (216) 977-7545 (fax), bryan.a.palaszewski@lerc.nasa.gov

**Author:** Bryan A. Palaszewski

**Headquarters program office:** OSAT

## Fuels and Space Propellants for Reusable Launch Vehicles: A Small Business Innovation Research Topic and Its Commercial Vision

Under its Small Business Innovation Research (SBIR) program (and with NASA Headquarters support), the NASA Lewis Research Center has initiated a topic entitled "Fuels and Space Propellants for Reusable Launch Vehicles." The aim of this project would be to assist in demonstrating and then commercializing new rocket propellants that are safer and more environmentally sound and that make space operations easier. Soon it will be possible to commercialize many new propellants and their related component technologies because of the large investments being made throughout the Government in rocket propellants and the technologies for using them. This article discusses the commercial vision for these fuels and propellants, the potential for these propellants to reduce space access costs, the options for commercial development, and the benefits to nonaerospace industries.

This SBIR topic is designed to foster the development of propellants that provide improved safety, less environmental impact, higher density, higher  $I_{sp}$ , and simpler vehicle operations. In the development of aeronautics and space technology, there have been limits to vehicle performance imposed by traditionally used propellants and fuels. Increases in performance are possible with either increased propellant specific impulse, increased density, or both. Flight system safety will also be increased by the use of denser, more viscous propellants and fuels.

Many challenges have been overcome recently by the discovery and synthesis of propellants that can have higher performance than traditional  $O_2/H_2$ ,  $O_2/RP-1$  and aircraft fuels. This SBIR topic provides a substantial infusion of resources so that these fuels and propellants can be commercialized for aeronautics and space applications.

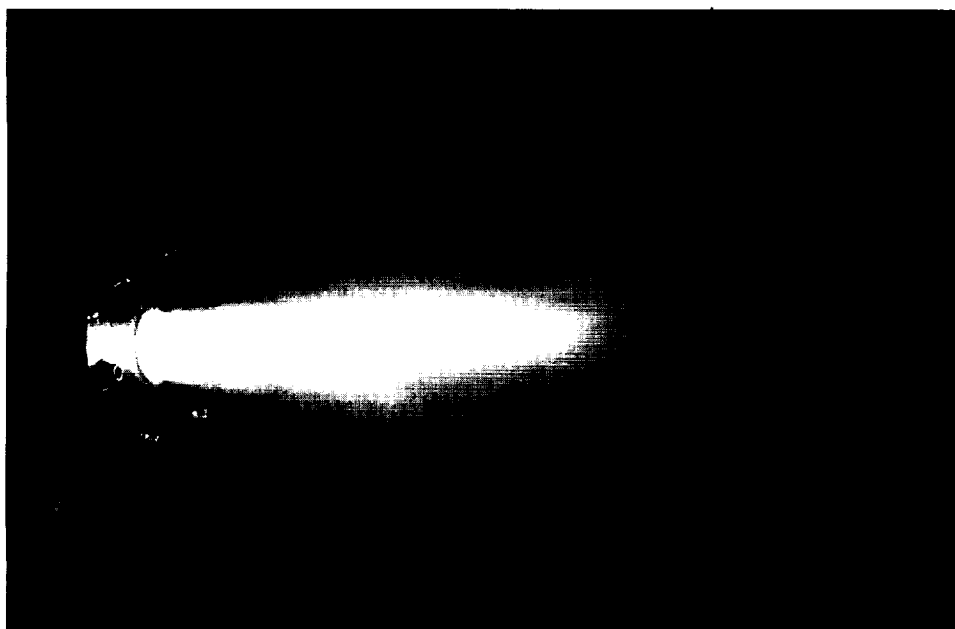
Space flight applications of higher performance propellants include high-density monopropellants for sounding rockets and upper stages, and

onboard propulsion for small spacecraft. Higher energy fuels, such as  $N_4$ ,  $N_6$ ,  $BH_4$ , and others, have a longer range development time and would be more applicable to future launch vehicles, such as next-generation Reusable Launch Vehicles. Aeronautical uses are directed toward improving the storage density over typical JP-type fuels and related research in endothermic fuels.

The commercialization of these propellants and fuels will be the major products of this SBIR topic. The development, commercialization, and marketing of these propellants will capitalize on the large investments made in the USAF High Energy Density Materials (HEDM) program, and in other extensive programs in the U.S. Navy, the U.S. Army, the Department of Energy, and NASA.

Our hope is that existing ideas for propellants can be used, and therefore, the development time will be shorter than for typical propellants.





*Gelled propellant engine test: 55-wt % RP-1/Al.*

Many of the stumbling blocks have been identified and can be avoided with the data from previous testing and research. Many nonaerospace applications also exist; see the following list:

#### **Applications**

- Particle formation
- Paint additives
- Reflective coatings
- Racing fuel additives
- Cryogenic liquid and solid storage systems
- Cryogenic coolers
- Combined solid-liquid-gas flow systems

#### **Benefits**

- Higher fuel performance
- Greater fuel safety
- Longer lived coatings
- Higher temperature coatings (for engines, etc.)
- Improved vibration isolation
- Longer cryogenic storage

**For more information, visit the Small Business Innovation Research Focused**

**Topic Web Site:** <http://www.lerc.nasa.gov/WWW/TU/launch/foctopsb.htm>

#### **Bibliography**

Naumann, W.: *Small Launchers in the Future: A Global Overview of Their Features and Prospects*. Acta Astronaut., vol. 37, Pergamon Press, 1995, pp. 471–486.

Griffin, M.D.; and Claybaugh, W.R.: *The Cost of Access to Space*. J. Brit. Interplanet. Soc., vol. 47, no. 3, Mar. 1994, pp. 119–122.

Carrick, P.; and Tam, S.: *Proceedings of the High Energy Density Matter (HEDM) Contractors' Conference*. USAF Phillips Laboratory Report Number PL-TR-95-3039, 1996.

Palaszewski, B.: *Atomic Hydrogen Propellants—Historical Perspectives and Future Possibilities*. AIAA Paper 93-0244, 1993.

Fleeter, R.; McLoughlin, F.; and Wanagas, J.: *Earth-to-Orbit Transportation Optimized for Small Low-Cost Satellites*. AAS 91-646, 1992, pp. 377–392.

Palaszewski, B.: *Fuels and Space Propellants for Reusable Launch Vehicles: A Small Business Innovation Research Focused Topic. Overview and Technical Briefing Packages*, 1996. Available WWW: <http://www.lerc.nasa.gov/WWW/TU/launch/foctopsb.htm>

#### **Lewis contact:**

Bryan A. Palaszewski,  
(216) 977-7493 (voice),  
(216) 977-7545 (fax),  
[bryan.a.palaszewski@lerc.nasa.gov](mailto:bryan.a.palaszewski@lerc.nasa.gov)

**Author:** Bryan A. Palaszewski

**Headquarters program office:**  
OSAT

# Electric Propulsion

NASA Lewis Research Center's electric propulsion technology program is developing and transferring new, innovative propulsion technologies to industry. Next-generation, high-performance arcjets are now operational on communications satellites. The improved fuel efficiency provided by this innovative, new arcjet technology was used both to reduce launch vehicle requirements and to extend satellite life.

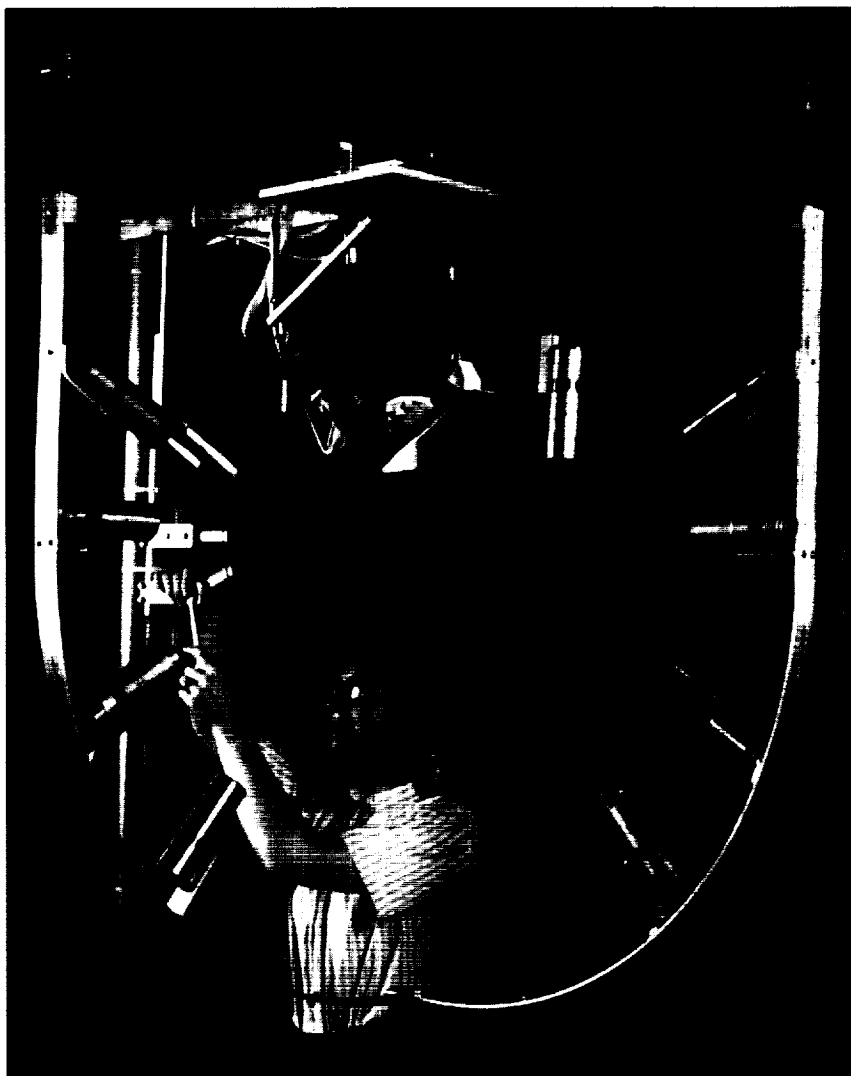
Ion propulsion technology pioneered by NASA Lewis has been selected as the primary propulsion system for the first New Millennium flight (DS-1). Development of this system is ongoing under the Lewis-supported NASA SEP (Solar Electric Propulsion) Technology Application Readiness (NSTAR) program. In the past year, a 2.5-kW engineering model 30-cm thruster and a breadboard power processor were fabricated at Lewis and delivered to the NASA Jet Propulsion Laboratory (JPL) for life verification. Multiple development tests were also performed at Lewis. Hughes Telecommunication and Space is developing the NSTAR flight system under contract to Lewis.

In support of the Department of Defense, a ground system test was completed on a 1.35-kW Hall thruster system under the first phase of the Russian Hall Electric Thruster Test program (RHETT1). A second phase to deliver and fly a hybrid U.S./Russian Hall system is the goal of the Lewis-managed RHETT2 program. In RHETT2, under sponsorship of the Ballistic Missile Defense Organization (BMDO), a system incorporating a Russian-manufactured Thruster with Anode Layer, a Lewis-developed cathode, and a power processor from U.S. industry will be demonstrated on a Naval Research Laboratory satellite.

Pulsed-plasma thrusters (PPT) are being developed under a joint Lewis/industry/university program for a broad range of applications. First-generation PPT technology is scheduled for demonstration for small satellite insertion in the Air Force's MightySat II.1 program and for propulsive attitude control in the New Millennium's first Earth Observer mission.

In addition to the technologies being readied for relatively near-term flight applications, Lewis' electric propulsion program continues to develop a broad range of technologies for mid- and far-

term missions. Many of these development efforts are aimed at future flight programs to be performed with small spacecraft and microspacecraft. The program is designed to take advantage of the synergy between advanced electric power and propulsion systems. For example, PPT's providing very low impulse bits have been identified as enabling for the high-resolution imaging missions projected for the 21st century. Work is being done in-house and with both the



*Setting up a pulsed plasma thruster impacts test in a specialized electric propulsion testbed.*

industrial and academic communities to find ways to minimize the mass and volume of PPT systems for critical NASA missions. Similarly, low-power electrostatic systems (ion and Hall) are being developed, and a direct-drive testbed for demonstrating very efficient, simple systems for the future has been installed under a joint NASA/Naval Research Laboratory program.

Finally, all of the programs mentioned require significant, high-fidelity testing of the components and systems to characterize performance, plasma plume/spacecraft interactions, thermal control, electromagnetic interactions, structural integrity, and other factors. The expertise and specialized, high-quality testbeds available at Lewis permit this critical testing to be done in a cost-effective, timely manner for NASA, industry, and other government agencies. These capabilities also provide a training ground for the next generation of engineers and scientists for the exciting, high-payoff area of electric propulsion.

#### **Lewis contact:**

John M. Sankovic, (216) 433-7429,  
John.M.Sankovic@lerc.nasa.gov

**Author:** John M. Sankovic

**Headquarters program office:** OSS

## On-Board Chemical Propulsion

NASA Lewis Research Center's On-Board Propulsion program (OBP) is developing low-thrust chemical propulsion technologies for both satellite and vehicle reaction control applications. There is a vigorous international competition to develop new, high-performance bipropellant engines. High-leverage bipropellant systems are critical to both commercial competitiveness in the international communications market and to cost-effective mission design in government sectors. To significantly improve bipropellant engine performance, we must increase the thermal margin of the chamber materials. Iridium-coated rhenium (Ir/Re) engines, developed and demonstrated under OBP programs, can operate at temperatures well above the constraints of state-of-practice systems, providing a sufficient margin to maximize performance with the hypergolic propellants used in most satellite propulsion systems.

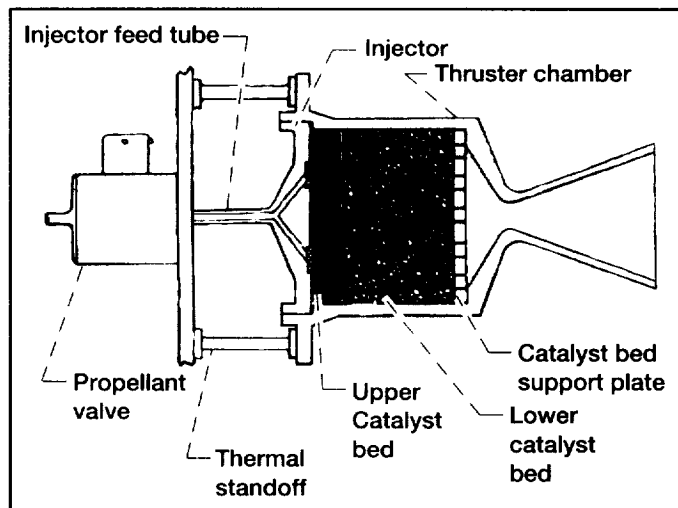
For the near term, the OBP program is focused on transferring Ir/Re technology to the user community. This effort includes the development of low-cost fabrication and joining technologies, the generation of Re mechanical properties, and critical technology demonstrations. Lightweight, low-volume, high-pressure bipropellant engine technology is also being developed for small-satellite applications requiring high thrust. This effort targets 200- to 500-kg satellites to be launched on inexpensive, volume-limited launch vehicles.

For the long term, the OBP program is developing chamber materials for long-life operation in combustion environments that are more energetic and oxidizing than hypergolic propellants. The long-range goal is to develop a material system that can run any propellant combination at any mixture ratio.

In addition to the bipropellant efforts, OBP is also developing high-performance, nontoxic, monopropellant systems to replace state-of-practice hydrazine ( $N_2H_4$ ) monopropellant thrusters. The monopropellants under consideration are based on liquid gun-propellant formulations, which are

environmentally friendly, have a high density, and have better thermal characteristics than hydrazine. The near-term goal is to transfer a "green" system to improve mission performance and greatly reduce ground operations costs. For the far-term, a very high performance (high specific impulse) system is being sought. The key to this goal is the development of a high-temperature catalyst; research in this area is underway.

For very small spacecraft and microspacecraft, several chemical propulsion technologies that provide performance and system benefits are being explored. Examples include (1) a warm gas propulsion system that uses a mixture of hydrogen, oxygen, and an inert gas (nitrogen or helium) and that offers a high specific impulse alternative to state-of-practice cold gas systems with a minimal increase in complexity; (2) exothermic decomposing solid and hybrid systems, which offer the high density and simplicity of solid propellants for low-thrust, quick-response applications; (3) a water electrolysis concept that can provide dual use as a



*Advanced monopropellant thruster.*

**Lewis contact:**

Dr. Steven J. Schneider,  
(216) 977-7484,

Steven.J.Schneider@lerc.nasa.gov

**Author:** Dr. Steven J. Schneider

**Headquarters program office:** OSS

combined propulsion/power system; and (4) a microturbomachinery-based bipropellant system for very high-performance applications which uses microelectromechanical system (MEMS) fabrication technology to provide propulsion systems "on-a-chip" similar to computer chips.

## Gas Wave Bearings: A Stable Alternative to Journal Bearings for High-Speed Oil-Free Machines

To run both smoothly and efficiently, high-speed machines need stable, low-friction bearings to support their rotors. In addition, an oil-free bearing system is a common requirement in today's designs. Therefore, self-acting gas film bearings are becoming the bearing of choice in high-performance rotating machinery, including that used in the machine tool industry. Although plain journal bearings carry more load and have superior lift and land characteristics, they suffer from instability problems.

Since 1992, a new type of fluid film bearing, the wave bearing, has been under development at the NASA Lewis Research Center in Cleveland, Ohio, by Dr. Florin Dimofte, a Senior Research Associate of the University of Toledo. One unique characteristic of the waved journal bearing that gives it improved capabilities over conventional journal bearings is the low-amplitude waves of its inner diameter surface. The radial clearance is on the order of one thousandth of the shaft radius, and the wave amplitude is nominally up to one-half the clearance. This bearing concept offers a load capacity which is very close to that of a plain journal bearing, but it runs more stably at nominal speeds.

Analyses reveal several important advantages of this type of bearing in comparison to other bearing designs (refs. 1 and 2). These advantages include higher stiffness, better stability, and lower friction with damping equal to that for a plain journal bearing. The wave bearing performance has also been evaluated experimentally. Both steady-state and dynamic

performance were evaluated with a tester built at NASA Lewis. The experimental results were found to agree very well with numerical predictions using an analytical code developed by Dr. Dimofte (refs. 3 to 6). This wave bearing technology can be successfully used in turbo-machines, auxiliary power units, fans and air cycling machines, pumps (including blood pumps), high-precision spindles (such as those used in laser copy machines and computers), and machine tools.

Since 1994 an effort has been underway with the Allison Engine Co. to install wave bearings in the auxiliary power units for a hybrid car. The bearing can be manufactured either as an integrated assembly ready to be installed inside the machine body (top figure) or as a two-piece assembly

consisting of a sleeve and a rotor (bottom figure). The sleeve needs to be supported inside the machine body. Ceramic/ceramic or ceramic/steel materials have been used for the sleeve/rotor assembly.

Furthermore, since 1995 several companies have become interested in this wave bearing technology, including Sundstrand, Teledyne, AlliedSignal Automotive and Aerospace Divisions, Hamilton Standard, and Pratt & Whitney. This advanced technology also has direct applications to NASA's aeronautical and space propulsion programs.

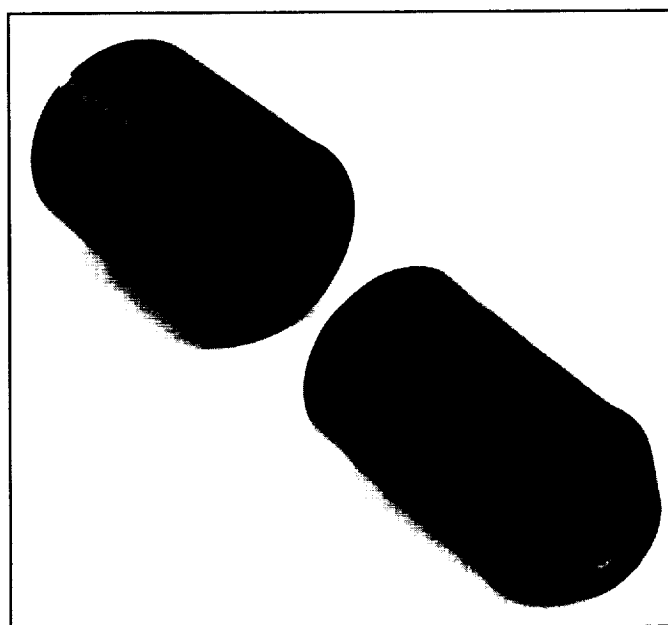
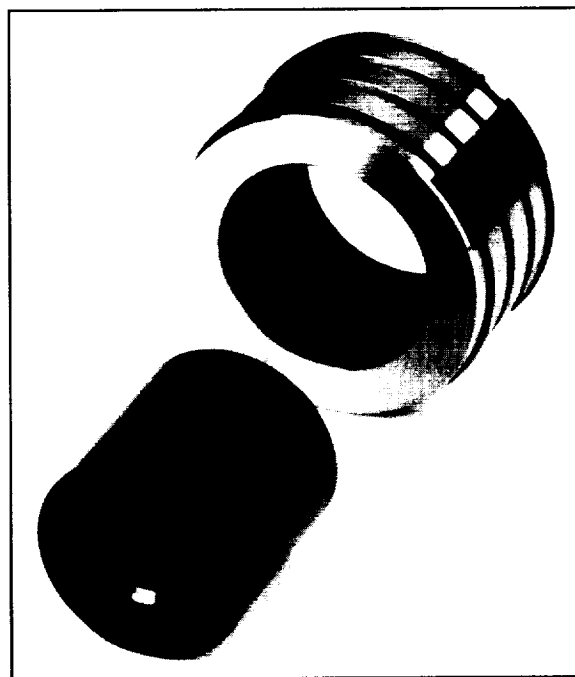
## References

1. Dimofte, F.: Wave Journal Bearing With Compressible Lubricant—Part I: The Wave Bearing Concept and a Comparison to the Plain Circular Bearing. *STLE Tribol. Trans.*, vol. 38, no. 1, 1995, pp. 153–160.
2. Dimofte, F.: Wave Journal Bearing With Compressible Lubricant—Part II: A Comparison of the Wave Bearing With a Wave Groove Bearing and Lobe Bearing. *STLE Tribol. Trans.*, vol. 38, no. 2, 1995, pp. 364–372.
3. Dimofte, F.; Addy, H.E.; and Walker, J.F.: Preliminary Experimental Results of a Three Wave Journal Air Bearing. *Advanced Earth-to-Orbit Propulsion Technology 1994*, NASA CP-3282, vol. II, 1994, pp. 375–384.
4. Dimofte, F.; and Hendricks, R.C.: Fractional Whirl Motion in Wave Journal Bearings. *Seals Code Development Workshop*, NASA CP-10181, 1995, pp. 337–352.
5. Dimofte, F.; and Hendricks, R.C.: Two- and Three-Wave Journal Bearing Fractional Whirl Motion. *Proceedings of the Society of Engineering Science 32nd Annual Technical Meeting held in New Orleans, LA, Oct. 29–Nov. 2, 1995*, pp. 773–774.
6. Dimofte, F.; and Hendricks, R.C.: Three-Wave Gas Bearing Behavior with Shaft Runout. *Proceedings of the Eighth Workshop on Rotordynamic Instability Problems in High-Performance Turbomachinery held at the Texas A&M University, College Station, TX, on May 6–8, 1996*, pp. 5–13.

**Lewis contacts:** Dr. Florin Dimofte, (216) 977-7468, [florin.dimofte@lerc.nasa.gov](mailto:florin.dimofte@lerc.nasa.gov); and Robert C. Hendricks, (216) 977-7507, [robert.hendricks@lerc.nasa.gov](mailto:robert.hendricks@lerc.nasa.gov)

**Author:** Dr. Florin Dimofte

**Headquarters program office:** OA



*Top: Wave journal bearing assembly. Bottom: Wave journal bearing sleeve and rotor.*

# Power Technology

## SCARLET Photovoltaic Concentrator Array Selected for Flight Under NASA's New Millennium Program

The NASA Lewis Research Center continues to demonstrate its expertise in the development and implementation of advanced space power systems. For example, during the past year, the NASA New Millennium Program selected the Solar Concentrator Array with Refractive Linear Element Technology (SCARLET) photovoltaic array as the power system for its Deep Space-1 (DS-1) mission. This Jet Propulsion Laboratory (JPL) managed DS-1 mission, which represents the first operational flight of a photovoltaic concentrator array, will provide a baseline for the use of this technology in a variety of future government and commercial applications.

SCARLET is a joint NASA Lewis/Ballistic Missile Defense Organization program to develop advanced photovoltaic array technology that uses a unique refractive concentrator design to focus sunlight onto a line of photovoltaic cells located below the optical element. The general concept is based on previous work conducted at Lewis under a Small Business Innovation Research (SBIR) contract with AEC-Able Engineering, Inc., for the Multiple Experiments to Earth Orbit and Return (METEOR) spacecraft. The SCARLET II design selected by the New Millennium Program is a direct adaptation of the smaller SCARLET I array built for METEOR. Even though SCARLET I was lost during a launch failure in October 1995, the hardware (designed, built, and flight qualified within 6 months) provided invaluable information and experience that led to the selection of this technology as the primary power source for DS-1.

The SCARLET II design is a 2.6-kW array that uses advanced multijunction photovoltaic cells and a variety of other improvements in the lens design and array-deployment mechanisms. The array will be used primarily to power the 2.5-kW electric propulsion thruster that will propel the DS-1 spacecraft on this comet/asteroid rendezvous mission. In addition to the first space flight demonstration of photovoltaic concentrator technology, the SCARLET II program will also help quantify the advantages of this technology for future applications: high array efficiency at low cost, inherent resistance to radiation degradation, and minimal space plasma interaction.

SCARLET II completed its critical design review in July 1996, and flight hardware fabrication is now underway. Delivery of the array is scheduled for August 1997, with a launch in July 1998. Whereas NASA Lewis managed the initial part of the SCARLET II program, flight hardware construction is now managed under a contract by the Ballistic Missile Defense Organization, the primary funding organization. NASA Lewis continues to play a vital role not

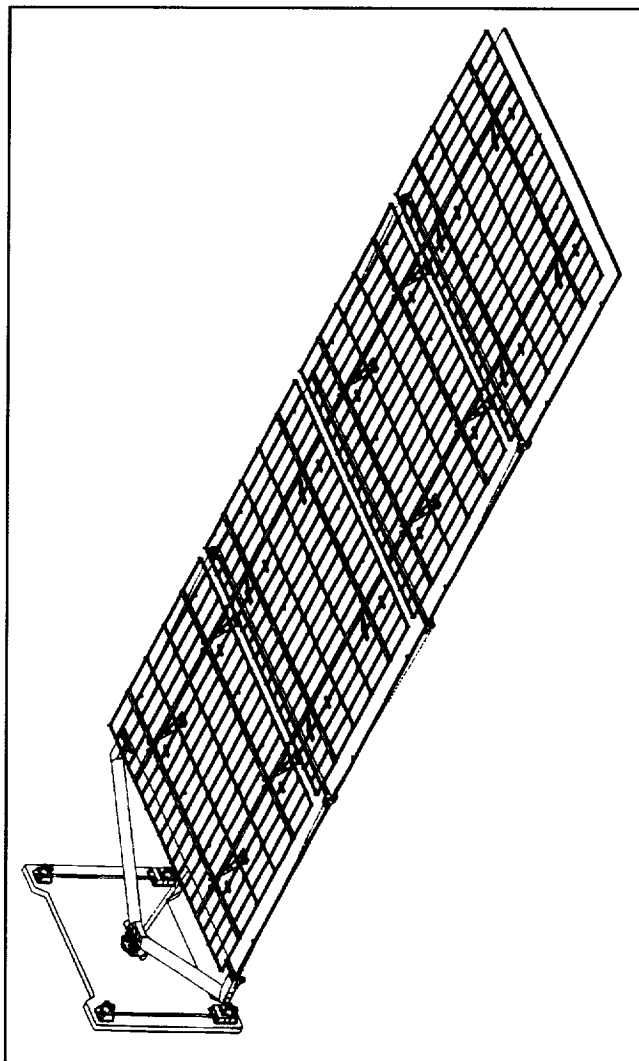
only in continued support of the SCARLET II/DS-1 mission, but in developing performance improvements and evaluating additional mission applications for advanced photovoltaic concentrator technology.

**Lewis contact:**

Michael F. Piszczor, Jr., (216) 433-2237,  
Michael.F.Piszczor@lerc.nasa.gov

**Author:** Michael F. Piszczor, Jr.

**Headquarters Program Office:** OSS



SCARLET II/New Millennium Deep Space-1 solar array.

## Thermophotovoltaic Cell Technology Transferred to the Department of Energy Laboratory and a Commercial Manufacturer

Researchers in the NASA Lewis Research Center's Photovoltaic Branch have developed a novel photovoltaic device, called a Monolithically Interconnected Module (MIM), for use in thermophotovoltaic (TPV) power systems. TPV power systems function by heating an emitter to produce light. This light is then converted into electricity by a photovoltaic device or a solar cell. Possible heat sources for the system include concentrated solar energy, the combustion of various fuels, and nuclear decay. NASA has an interest in TPV systems for deep space (nuclear-powered) and near-Sun (solar-powered) missions. There also are many commercial and military applications for TPV, given its potential for high efficiency, low noise, and reliable power.

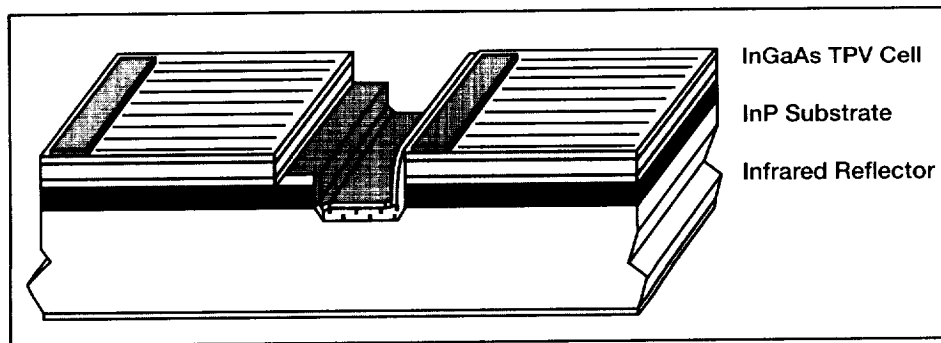
The Monolithically Interconnected Module consists of many small solar cells (two are shown in the figure) that are series-interconnected on a common substrate. The cells are fabricated from indium gallium arsenide (InGaAs), which can convert the near-infrared portion of the emitter output spectrum into electricity. The InGaAs devices are deposited on an indium phosphide (InP) substrate that provides electrical isolation. On the bottom of the InP substrate is an infrared reflector that returns all the photons that are not converted by the InGaAs device back to the emitter where they are absorbed. This process helps maintain the emitter temperature and dramatically improves the system efficiency.

Compared with conventional TPV cells, this TPV device has higher output voltages and lower resistive losses, higher output power density, simplified thermal management, improved reliability, and higher efficiency. The Monolithically Interconnected Module was initially developed under an internally funded effort (Director's Discretionary Fund). Development is now being funded by Bettis Atomic Power Laboratory, and prototype devices are being produced by a commercial solar cell manufacturer.

**Lewis contact:** David M. Wilt, (216) 433-6293 (voice), (216) 433-6106 (fax), david.wilt@lerc.nasa.gov

**Author:** David M. Wilt

**Headquarters program office:** OSS

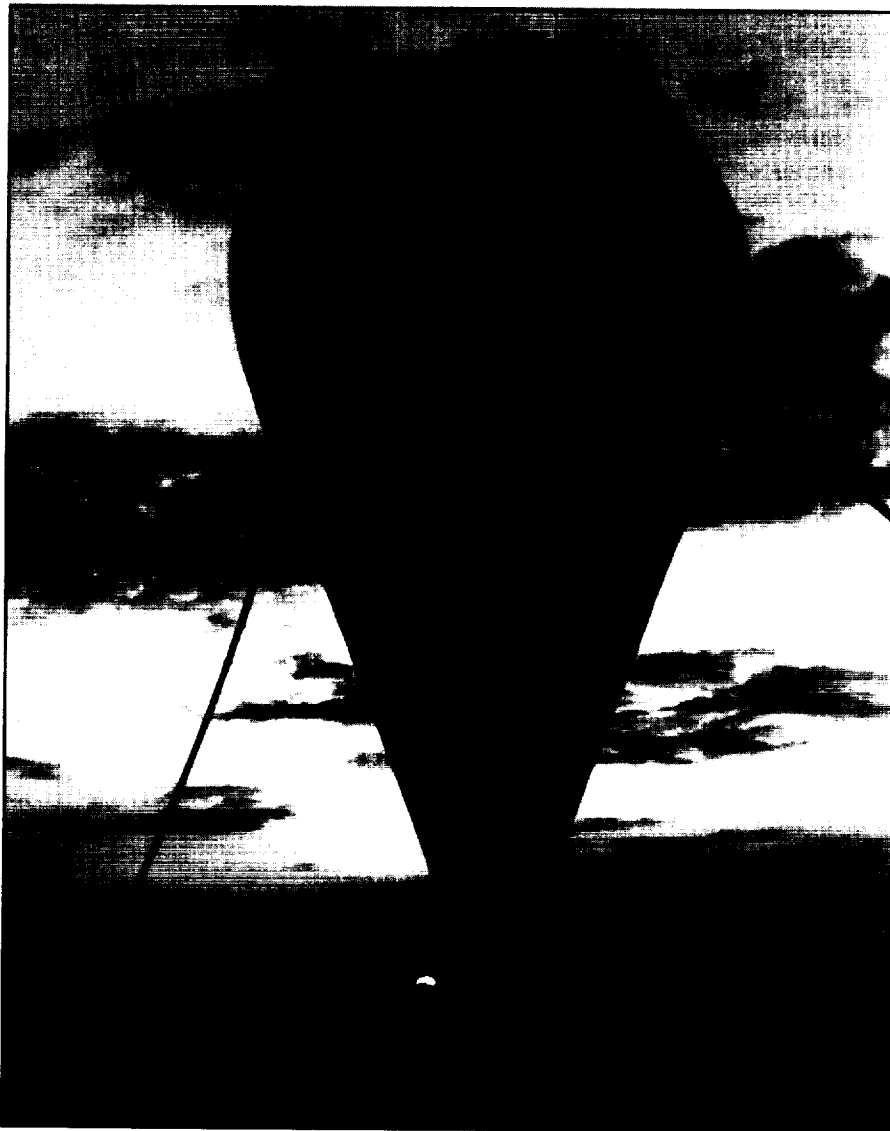


*Monolithically Interconnected Module InGaAs thermophotovoltaic cell developed by Lewis.*

# Balloon Fuel Cell Power System

NASA Lewis Research Center's Electrochemical Technology Branch has teamed with the NASA Wallops Flight Facility to demonstrate the operation of a hydrogen-oxygen proton exchange membrane (PEM) fuel cell for application in the upper atmosphere. NASA Wallops' Balloon Programs Branch has a requirement for a high-power, long-duration power system for use on a scientific balloon platform. The current power system will not meet these needs. The objective of this program is to deliver a 200-W (minimum) fuel cell system that can deliver approximately 10 kWh of electrical energy.

The Lewis team is responsible for designing, building, testing, and delivering a flight power system capable of meeting mission requirements. This power system will be based on a hydrogen/oxygen fuel cell developed as a result of a NASA Lewis Phase II Small Business Innovation Research (SBIR) PEM fuel cell program with ElectroChem, Inc.



*Scientific balloon.*

The remote system must deliver power continuously, in a safe, reliable manner. It must be able to accommodate extreme ambient conditions, including a temperature range of -70 to 100 °F and a pressure range of 14.7 to below 1 psia. Waste heat, which is normally rejected by fuel cell systems, will be used to maintain proper operating temperatures for the fuel cell and the accompanying ancillary components, including the electronic equipment. It will also be used to maintain the temperature of the product water and to aid in proper water storage and/or discharge.

In addition to the extreme environmental conditions, the fuel cell power system must be able to withstand the physical forces and accelerations that will be encountered over the course of the mission. These forces are expected to reach as high as 8 to 10g. The initial flight is scheduled for early Summer 1997, and pending successful operation, the system will be reused on subsequent experimental balloon flights. The next planned program phase is to scale-up the fuel cell power system to 96 kWh of electrical output.

**Lewis contact:**

Dr. Patricia L. Loyselle, (216) 433-2180,  
Patricia.L.Loyselle@lerc.nasa.gov

**Authors:** Dr. Patricia L. Loyselle and  
Dr. Thomas M. Maloney (NYMA)

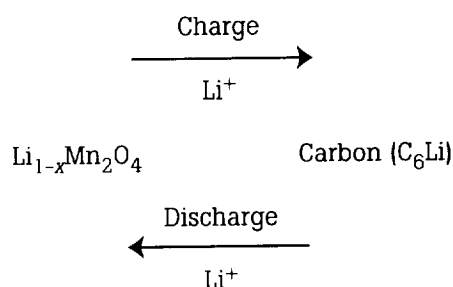
**Headquarters program office:** OSS



# Lithium Ion Batteries

Lithium ion batteries, which use a new battery chemistry, are being developed under cooperative agreements between Lockheed Martin, Ultralife Battery, and the NASA Lewis Research Center. The unit cells are made in flat (prismatic) shapes that can be connected in series and parallel to achieve desired voltages and capacities. These batteries will soon be marketed to commercial original-equipment manufacturers and thereafter will be available for military and space use. Current NiCd batteries offer about 35 W-hr/kg compared with 110 W-hr/kg for current lithium ion batteries. Our ultimate target for these batteries is 200 W-hr/kg.

This new system has charge/discharge characteristics very close to those of cells containing metallic lithium anodes, without the presence of lithium metal. In the following equations, it can be seen that only lithium ions are involved:

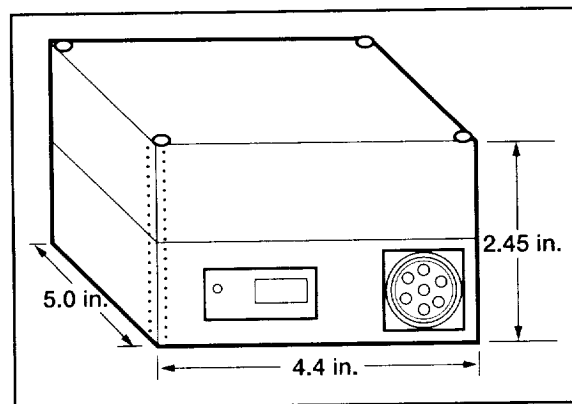


The absence of lithium metal, high energy density, and other factors lead to benefits for space, military, and commercial use. Lithium ion batteries are smaller and lighter than NiCd batteries, with no toxic materials, no free liquids (use a solid polymer electrolyte), no gas pressure, no thermal runaway, and no incineration problems. They produce no explosions when abuse tested by exposure to short circuits, nail punctures, water immersion, overcharge, overdischarge and reversal, and hydraulic pressures to 1500 psi. In addition to generating only low levels of heat, they operate at higher temperatures and are more powerful than conventional batteries (average discharge voltage is 3.7 V).

Some expected applications are given in the following table:

Nonmilitary uses	Military and space uses
Cellular phones	Backpack radio battery BB590L (see figure)
Laptop computers	Missile launch battery
Portable radios	Marine battery, swimmer <sup>a</sup>
Two-way radios	Satellite batteries
Electric vehicles	

<sup>a</sup>Submersible.



BB590L portable lithium-ion radio battery (capable of 15 V at 8 A-hr, or 30 V at 4 A-hr).

## Lewis contact:

Richard M. Wilson, (216) 433-5916  
(voice), (216) 433-6160 (fax),  
Richard.M.Wilson@lerc.nasa.gov

**Author:** Richard M. Wilson

**Headquarters program office:** OSAT

# High Capacity Battery Cell Flight Qualified

The High Capacity Battery Cell project is an effort equally funded by the NASA Lewis Research Center and Hughes Space and Communications Company (a unit of Hughes Aircraft Company) to develop and flight qualify a higher capacity nickel hydrogen battery for continuing use on commercial spacecraft. The larger diameter, individual pressure vessel cell will provide approximately twice the power, while occupying the same volume, as the current state-of-the-art nickel hydrogen cell. These cells are also anticipated to reduce battery cost by 20 percent. The battery is currently booked for use on 26 spacecraft, with the first flight scheduled in 1997.

A strong requirement for batteries with higher power levels (6 to 12 kW), long life, and reduced cost was identified in studies of the needs of commercial communications spacecraft. With the design developed in this effort, the higher power level was accommodated without having to modify the rest of the existing spacecraft bus. This design scaled-up the existing state-of-the-art nickel hydrogen battery cell from a 3.5-in., 50-Ahr cell to a 5.5-in., 350-Ahr cell. An improvement in cycle life was also achieved by

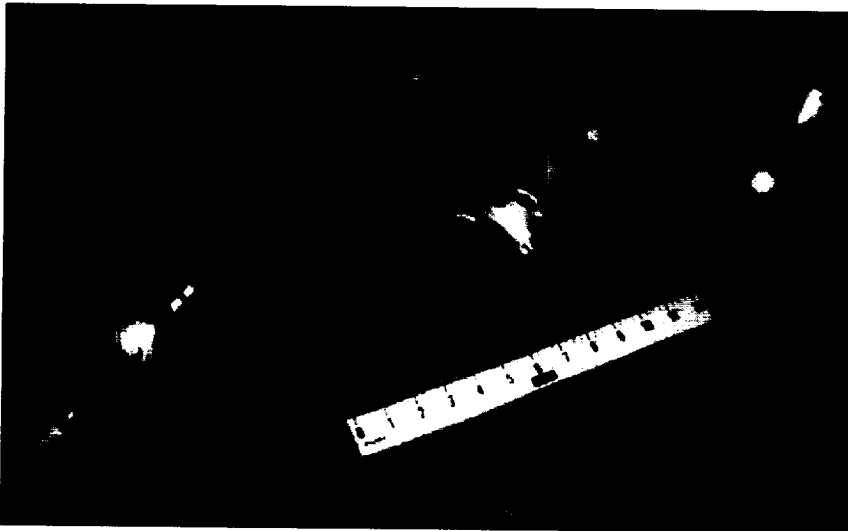
the use of the 26-percent KOH electrolyte design developed by NASA Lewis. The cell design was completed, and flight batteries were built and flight qualified by Hughes Space and Communications Company with input from NASA Lewis. Two batteries were shipped in September 1996 to undergo life cycle testing under the purview of NASA Lewis.

**Lewis contact:**

Barbara I. McKissock (216) 433-6102,  
barbara.mckissock@lerc.nasa.gov

**Author:** Barbara I. McKissock

**Headquarters Program Office:** OSAT



*Comparison of high-capacity cell with state-of-the-art cells.*

# NASA Flywheel Program

NASA Lewis Research Center's Electrical Systems Development Branch is leading a program to develop space flywheel energy storage with integrated attitude control systems. The objective of this effort is to develop a flywheel system that will reduce spacecraft infrastructure weight and improve power system efficiency. Additional potential benefits of these systems are their increased life and improved system operation. These potential advantages are due to a flywheel system's very large number of charge/recharge cycles and their known state of charge. Our multifaceted program consists of efforts to develop flywheels, and their components, as well as the facilities to test them.

Development of flywheels and components is being conducted jointly with industry. Currently, two systems are under development, one at SatCon Technology Corp. and the other at US Flywheels. Both of these systems are sized to store approximately 3 kW-hr of energy, which is appropriate for large spacecraft. When complete, the systems will be brought to NASA Lewis for evaluation and testing. To support the development of flywheels for small spacecraft, the Electrical Systems Development Branch has worked with the University of Maryland and small companies, such as Fare, Inc. This company has just completed a NASA Small Business Innovation Research (SBIR) Phase I project to design a very small, very high energy density flywheel that could provide 50 W at 100 Vdc. These flywheel systems provide the foundation for further flywheel development at NASA.

Flywheel component development, which is being performed by many organizations at NASA Lewis in concert with universities and industry, is being coordinated by Lewis' Electrical Systems Development Branch.

A flywheel test facility, which is designed to evaluate flywheel systems as part of an overall spacecraft electrical power system, is being constructed at NASA Lewis. It will be able to measure both electrical and mechanical parameters during the full-speed operation of a flywheel system. The first phase, which allows control and testing of an operating flywheel at a reduced speed (i.e., lower stored energy), has been completed. Later phases will add enhancements to the facility, such as life testing and attitude dynamics. When complete, this facility will be able to simulate a complete operational spacecraft electrical power system.

**Lewis contacts:** Raymond F. Beach, (216)433-5320, [raymond.beach@lerc.nasa.gov](mailto:raymond.beach@lerc.nasa.gov); and Bradford A. Kaufman, (216)433-5636, [bradford.kaufman@lerc.nasa.gov](mailto:bradford.kaufman@lerc.nasa.gov)

**Author:** Bradford A. Kaufman

**Headquarters program office:** OSAT

# Investigation of Teflon FEP Embrittlement on Spacecraft in Low-Earth Orbit

Teflon fluorinated ethylene propylene (FEP) (DuPont) is commonly used on exterior spacecraft surfaces for thermal control in the low-Earth orbit environment. Silverized or aluminized Teflon FEP is used for the outer layers of the thermal control blanket because of its high reflectance, low solar absorptance, and high thermal emittance. Teflon FEP is also desirable because, compared with other spacecraft polymers (such as Kapton), it has relatively high resistance to atomic oxygen erosion. Because of its comparably low atomic oxygen erosion yield, Teflon FEP has been used unprotected in the space environment.

Recent, long-term space exposures, such as on the Long Duration Exposure Facility (LDEF, 5.8 years in space) and the Hubble Space Telescope (after 3.6 years in space), have provided evidence of low-Earth orbit environmental degradation of Teflon FEP. These exposures provide unique opportunities for studying environmental degradation because of their long durations and different conditions (such as differences in altitude). Samples of Teflon FEP from LDEF and the Hubble Space Telescope (retrieved during its first servicing mission) were evaluated for solar-induced embrittlement and for synergistic effects of solar degradation and atomic oxygen. Surface hardness measurements were obtained with unique Nano Indenter (Nano Instruments, Inc., Oak Ridge, Tennessee) techniques for polymers, which can measure hardness versus depth. Samples were bend tested to induce surface cracking, and then the bend-tested samples were cross-sectioned to determine crack depth. Tensile testing was conducted on Hubble samples and compared with LDEF data. Surface morphologies of Hubble and LDEF Teflon FEP samples were compared by using scanning electron microscopy and atomic force microscopy.

Nano Indenter results indicate that the surface hardness increased as the ratio of atomic oxygen fluence to solar exposure fluence (in equivalent Sun hours) decreased for the LDEF samples. This occurred because the atomic oxygen eroded away part, or all, of the solar-embrittled layer. Teflon FEP multilayer insulation retrieved from Hubble provided evidence of severe embrittlement on solar-facing surfaces. Some areas were cracked through the thickness of the 5-mil film. Nano Indenter measurements indicated higher surface hardness values for these samples. Cracks induced during bend testing were significantly deeper for the Hubble samples with highest solar exposure than for LDEF samples with similar atomic oxygen/solar exposure.

These results underscore the need to conduct further studies and the necessity to consider causes for Teflon FEP embrittlement in addition to direct atomic oxygen/solar exposure, such as

the possible role of soft x-ray radiation, which is dependent on solar flares. Teflon FEP that was exposed to soft x-rays in a ground test facility showed similar embrittlement, which indicates that the observed differences between LDEF and Hubble Teflon might be due to varying soft x-ray fluences during these two missions.

## **Lewis contacts:**

Kim K. de Groh (216) 433-2297,  
Kim.K.DeGroh@lerc.nasa.gov; and  
Bruce A. Banks, (216) 433-2308,  
Bruce.A.Banks@lerc.nasa.gov

**Authors:** Kim K. de Groh  
and Bruce A. Banks

**Headquarters program office:** OSAT



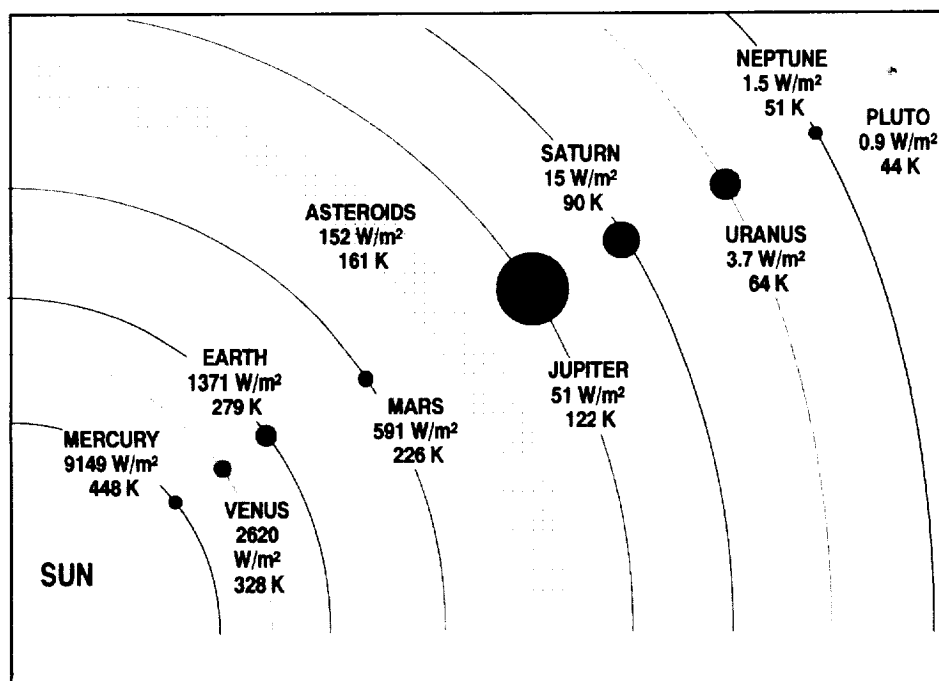
*Photograph of embrittled and cracked Teflon FEP retrieved from the Hubble Space Telescope.*

# Cryogenic Electronics in Support of Deep-Space Missions

Beyond the orbit of Mars, the average temperature seen by a spacecraft falls below the normal operating temperature range of the spacecraft's electronics. Presently, spacecraft operating in the cold environment of deep space carry onboard a large number of Radioisotope Heating Units to maintain an operating temperature for the electronics of approximately 300 K. This is not an ideal solution because the Radioisotope Heating Units are always producing heat, even when the spacecraft is already too hot, thus requiring an active thermal control system for the spacecraft. Those spacecraft with sufficient power reserves to use electrical heaters experience problems restarting after a hibernation period during which the electronics cool significantly below 70 K.

Another approach to problems associated with the cold operating environment of deep space is to use cryogenic electronics to operate the spacecraft at the ambient temperature. This approach has several advantages: semiconductor devices are more efficient at lower temperatures than at room temperature; high-temperature superconductors can be integrated with semiconductors to reduce losses; and a simpler (lighter and cheaper), passive, heat-rejection system can be employed. It has one significant challenge: cryogenic power generation and storage.

NASA Lewis Research Center is developing the enabling technologies for a cryogenic power system in conjunction with the NASA Jet Propulsion Laboratory (JPL) and universities. In addition, creative processes that could expand industrial participation in this program are being explored, such as the Small Business Innovation Research Program.



*Solar intensity and space probe temperature.*

Through a National Research Council Fellowship and a NASA Graduate Student Research Fellowship, demonstrations of two key technologies have been performed: high-temperature superconductor components and cryogenic compound semiconductor switch technology. A dc-dc converter for low-temperature operation was designed, built, and characterized with commercial, off-the-shelf components and a custom-built superconducting inductor. A High Electron Mobility Transistor switch was designed, fabricated, and characterized at low temperatures. High Electron Mobility Transistor structures have the potential to handle high current loads at cryogenic temperatures. Although many silicon power devices that operate from room temperature to liquid nitrogen temperature (77 K) were used at NASA Lewis to build dc/dc converters which successfully operated over that temperature range, none of the commercial silicon or germanium transistors tested operated successfully significantly below 77 K. Therefore, compound semiconductor devices with the potential to operate over the temperature range of interest to deep-space missions (30 to 60 K) are being investigated by NASA Lewis.

**Find out more about this research on the World Wide Web:**  
<http://www.lerc.nasa.gov/WWW/epbranch/lowtmpel.htm>

**Lewis contact:**  
 John Ellis Dickman,  
 (216) 433-6150,  
[John.E.Dickman@lerc.nasa.gov](mailto:John.E.Dickman@lerc.nasa.gov)  
**Author:** John Ellis Dickman  
**Headquarters program office:**  
 OSAT

# New Electromagnetic Interference Shielding Material Demonstrated

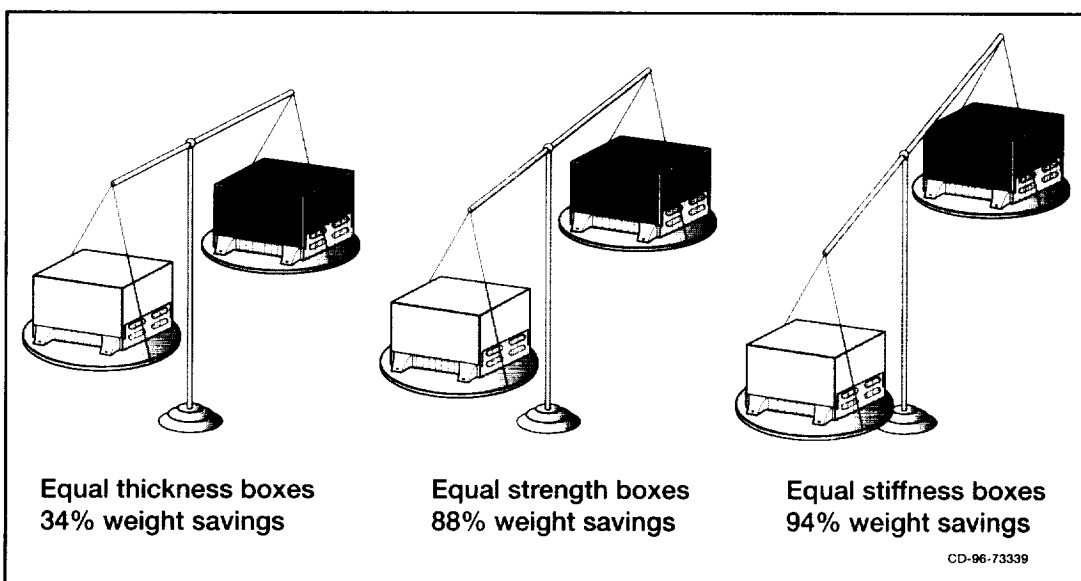
A demonstration electromagnetic interference (EMI) shielding cover that has a potential mass savings in excess of 80 percent over conventional aluminum has been fabricated and tested. It was the culmination of a 3-yr effort involving Hughes Space and Communications (Los Angeles), Applied Sciences, Inc. (Cedarville, Ohio), and the NASA Lewis Research Center. The cover was fabricated from a composite of polycyanate ester resin and graphite fibers that had been chemically modified by intercalation to enhance their electrical conductivity.

Intercalated graphite fibers are made by diffusing bromine between the carbon layers of the graphite fibers. The resulting material has mechanical and thermal characteristics that are virtually identical to pristine graphite fibers, but with a fivefold greater electrical conductivity. Although intercalates are available which increase the conductivity more, bromine forms intercalation compounds that are stable at high vacuum, high humidity, and temperatures as high as 200 °C. This enables the fibers to be handled at ambient conditions, and the resin to be cured at standard temperatures without decomposition. Flight tests on the space shuttle have confirmed the environmental stability of these fibers, and the enhancement in electrical conductivity makes composites made with these fibers more suitable for electromagnetic interference shielding applications.

The intercalated graphite technology was developed at NASA Lewis Research Center and transferred to Applied Sciences through a Space Act Agreement. With NASA's technical guidance, Applied Sciences intercalated the graphite fibers and then sent them to Hughes where, under a second Space Act Agreement, they were formed into composites with RS-3, a low-outgassing polycyanate ester resin. Three-foot-square composite sheets were fabricated along with a five-sided EMI shielding box (3 by 3 by 12 in.) with a standard mounting flange.

The shielding effectiveness of the composite box was tested over a frequency range of 100 kHz to 1 GHz. The box required no special treatment where it met the aluminum flange in order to electrically seal it. The shielding performance was acceptable over the entire frequency range, with the minimum shielding being 35 dB of the incident voltage (70 dB of incident power) in the 2- to 30-MHz range.

The potential for weight savings with this technology depends on which property of the cover is the limiting factor. If equal thickness covers are used, then the saving is about 34 percent because of the lower density of the composite. If shield strength is the limiting factor, then the superior strength of the composite allows the savings to be increased to about 88 percent. If stiffness is the limiting factor, then the savings can be as high as 94 percent.



#### Lewis contact:

Dr. James R. Gaier,  
(219) 982-5075 (during  
school year) or  
(216) 433-6686 (when  
school not in session),  
jrg@manchester.edu

#### Author:

Dr. James R. Gaier  
Headquarters program  
office: OSAT

*Mass savings of intercalated graphite composites over aluminum are significant.*

# High-Temperature Passive Power Electronics

In many future NASA missions—such as deep-space exploration, the National AeroSpace Plane, minisatellites, integrated engine electronics, and ion or arcjet thrusters—high-power electrical components and systems must operate reliably and efficiently in high-temperature environments. Such high-temperature electronics will not only provide tolerance to hostile environments, but will reduce system size and weight by eliminating radiators and thereby reducing launch costs, improving reliability and lifetime, and increasing energy densities. High-temperature electronic components will also have a great influence in terrestrial applications, such as well logging, the automotive industry, nuclear power, and industrial processing plants.

State-of-the-art power components are limited to a maximum operating temperature of 105 °C, with some devices functioning at temperatures to 150 °C. The high-temperature power electronics program at the NASA Lewis Research Center focuses on dielectric and insulating material research, the development and characterization of high-temperature components, and the integration of the developed components into a demonstrable 200 °C power system—such as an inverter.

NASA Lewis has developed high-temperature power components through collaborative efforts with the Air Force Wright Laboratory, Northrop Grumman, and the University of Wisconsin. Ceramic and film capacitors, molypermalloy powder inductors, and a coaxially wound transformer were designed, developed, and evaluated for high-temperature operation. Preliminary testing of these components has demonstrated stable operation from 20 to 200 °C in the frequency range of 50 Hz to 100 kHz. Limited life testing also has been performed on some of these components under simultaneous electrical and thermal stressing. The components will eventually be integrated into a power system that can operate at high temperatures, such as an inverter.

## Bibliography

Overton, E.; Baumann, E.D.; and Myers, I.T.: Thermal Aging Effects on the Electrical Properties of Film and Ceramic Capacitors. Presented at the Electrical/Electronics Insulation Conference, Chicago, IL, Oct. 1993.

Overton, E., et al: Effects of Combined Stressing on the Electrical Properties of Film and Ceramic Capacitors. IEEE International Symposium on Electrical Insulation, Pittsburgh, PA, June 1994.

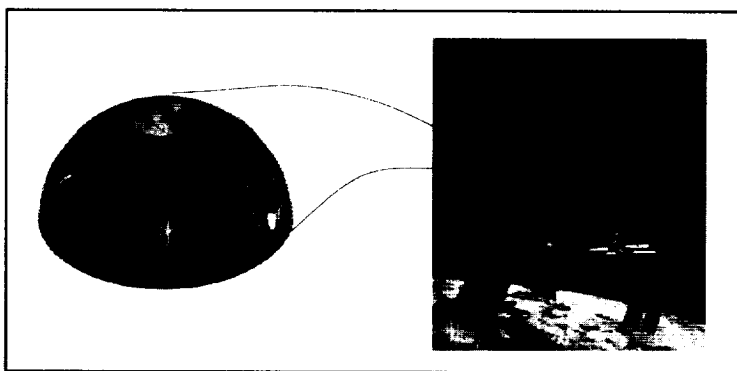
**Lewis contact:** Eric Overton, (216) 433-8189 (voice), (216) 433-8311 (fax), Eric.Overton@lerc.nasa.gov

**Author:** Eric Overton

**Headquarters program office:** OSAT

# Protective Coating Enhances the Durability of Retroreflectors for the International Space Station

Corner cube reflectors (retroreflectors) will be used on the International Space Station to aid in rendezvous and docking. They are designed to reflect light, such as that from a laser, directly back to the source. The resulting bright reflection from the surface can be used for critical alignment purposes. The housing for the reflectors is composed of polyoxymethylene, a polymer known as Delrin (DuPont), which is highly susceptible to erosion by the atomic oxygen environment that surrounds the station. Atomic oxygen is highly chemically reactive and will convert polymers such as Delrin into volatile oxidation products. This could cause the reflectors to detach from the housing, or could cause volatile products and other contamination to recondense onto the surface of the reflectors, causing them to darken.



*Fluoropolymer-filled silicon dioxide coated retroreflector for the International Space Station.*

The NASA Lewis Research Center is applying their patented fluoropolymer-filled silicon dioxide coating to the surface of the Delrin retroreflector to prevent degradation in performance caused by reactions with atomic oxygen. The fluoropolymer in the coating makes it slightly stretchy, which will help prevent thermal expansion from cracking the coating. The silicon dioxide provides a protective barrier that prevents atomic oxygen from attacking the Delrin. Several types of reflectors were coated at NASA Lewis at the request of the NASA Johnson Space Flight Center. Some test coupons were exposed to atomic oxygen in a ground-based atomic oxygen facility to verify performance, and the final coated reflectors were then sent to NASA Johnson for use on the International Space Station.

This coating has also been used on reflectors for the European Retrievable Carrier (EURECA) spacecraft, and the Japanese Space Flyer Unit. Thin-film coatings of this type also have potential commercial application as moisture and gas barriers in the packaging industry.

**Lewis contact:** Sharon K. Rutledge, (216) 433-2219,

Sharon.K.Rutledge@lerc.nasa.gov

**Author:** Sharon K. Rutledge

**Headquarters program office:** OSAT



# Space Electronics

## High-Power, High-Temperature Superconductor Technology Development

Since the first discovery of high-temperature superconductors (HTS) 10 years ago, the most promising areas for their applications in microwave systems have been as passive components for communication systems. Soon after the discovery, experiments showed that passive microwave circuits made from HTS material exceeded the performance of conventional devices for low-power applications and could be 10 times as small or smaller. However, for superconducting microwave components, high-power microwave applications have remained elusive until now.

In 1996, DuPont and Com Dev Ltd. developed high-power superconducting materials and components for communication applications under a NASA Lewis Research Center cooperative agreement, NCC3-344 "High Power High Temperature Superconductor (HTS) Technology Development." The agreement was cost shared between the Defense Advanced Research Projects Agency's (DARPA) Technology Reinvestment Program Office and the two industrial partners. It has the following objectives:

- (1) Material development and characterization for high-power HTS applications
- (2) Development and validation of generic high-power microwave components
- (3) Development of a proof-of-concept model for a high-power six-channel HTS output multiplexer

For the material development task, the essential factors that determine the losses in the films have been identified and their effects have been minimized by careful consideration and feedback to optimize the film growth conditions. These achievements have improved the power-handling capability of filters at 4 GHz by 2 orders of magnitude.

For the generic microwave components task, a three-pole filter that can handle more than 100 W of radiofrequency power with a 1-percent bandwidth has been demonstrated. Also, a method to measure calibrated S-parameters up to 35 W of radiofrequency power has been developed. The knowledge gained from designing and testing the microwave components implies HTS microwave circuits and filters could handle radiofrequency powers of 500 W or more with proper circuit designs and material.

For the last task, a high-power, six-channel HTS output multiplexer (see photo) has been successfully demonstrated at 4 GHz. The photo

compares the size of the conventional six-channel multiplexer (large one) to the HTS/dielectric multiplexer (small one), which can handle 20 W of power per channel when cooled to 77 K. It is 1/20th of the volume of a conventional multiplexer, and its performance in channel isolation and losses is better than that of a conventional multiplexer.

As part of the agreement, a thermal analysis of the system was done. The study determined, using the available technology data for HTS filter losses and cryocooler losses obtained during the first quarter of the 2-year agreement, that there was a 5- to 7-W dc-power penalty per channel for a high-power C-band multiplexer. However, with a factor of 2 improvement in the HTS filter losses, the dc-power



*Comparison of a conventional C-band output multiplexer with the HTS/dielectric multiplexer developed by ComDev and DuPont under a cooperative agreement with NASA Lewis, and the Defense Advanced Research Projects Agency (DARPA). Both multiplexers can handle 24W of microwave power per channel.*

losses were essentially zero. The needed improvement to achieve a zero dc-power penalty is readily achievable by using the techniques of improved film quality and circuit design that were demonstrated in the latter part of the agreement.

Recent improvements in cryocooler design have resulted in a threefold to fourfold increase in cooling power. This increase, coupled with the anticipated reduction of radiofrequency losses for a multiplexer, will result in a net gain of 3 to 6 W of dc-power per channel. For a typical 24-band C-band satellite, 72 to 144 W can be saved. As a follow-on, high-power and low-power hybrid superconductive and semiconductive microwave

circuits will be integrated with cryocoolers that use realistic communication payloads.

**Lewis contacts:**

Dr. Kul B. Bhasin, (216) 433-3676, Kul.B.Bhasin@lerc.nasa.gov; and Joseph D. Warner, (216) 433-3677, Joseph.D.Warner@lerc.nasa.gov

**Author:** Dr. Kul B. Bhasin

**Headquarters program office:** OSAT

## Digital Audio Radio Field Tests

Radio history continues to be made at the NASA Lewis Research Center with the beginning of phase two of Digital Audio Radio testing conducted by the Consumer Electronic Manufacturers Association (a sector of the Electronic Industries Association and the National Radio Systems Committee) and cosponsored by the Electronic Industries Association and the National Association of Broadcasters. The bulk of the field testing of the four systems should be complete by the end of October 1996, with results available soon thereafter.

Lewis hosted phase one of the testing process, which included laboratory testing of seven proposed digital audio radio systems and modes (see the following table). Two of the proposed systems operate in two modes, thus making a total of nine systems for testing. These nine systems are divided into the following types of transmission: in-band on channel (IBOC), in-band adjacent channel (IBAC), and new bands—the L-band (1452 to 1492 MHz) and the S-band (2310 to 2360 MHz).



*Digital Audio Radio field testing in San Francisco, California.*

System	Source coding	Data rate tested, kbs	System type	Proposed band, MHz
USA Digital FM-1	MUSICAM	256	IBOC <sup>1</sup>	88 to 108
USA Digital FM-2	MUSICAM	256	IBOC <sup>1</sup>	88 to 108
AT&T/AMATI	PAC <sup>2</sup>	128	IBOC <sup>1</sup>	88 to 108
AT&T/AMATI	PAC <sup>2</sup>	160	IBOC <sup>1</sup>	88 to 108
USA Digital AM	MUSICAM	92	IBOC <sup>1</sup>	525 to 1705
AT&T	PAC <sup>2</sup>	160	IBAC <sup>3</sup>	88 to 108
EUREKA 147	MUSICAM	224	New Band	1452 to 1492
EUREKA 147	MUSICAM	192	New Band	1452 to 1492
VOA/JPL	PAC <sup>2</sup>	160	New Band	2310 to 2360

<sup>1</sup>In-band on channel.

<sup>2</sup>An AT&T-developed source-coding scheme called Perceptual Audio Coding (PAC) is patterned after the distortion masking in the human auditory system, the phenomenon whereby one signal can completely mask a sufficiently weaker signal that is in its frequency or time vicinity.

<sup>3</sup>In-band Adjacent Channel.

Laboratory test results were announced by the Electronics Industry Association on September 24, 1995, in Monterey, California. The Digital Audio Radio Subcommittee indicated that these results were only one half of the picture. The second half of the picture will be the field testing to be conducted in San Francisco, California.

Lewis also supported the outfitting of the test vehicle that will be used in the field tests that are being conducted in San Francisco (see the

photograph). Proponent equipment and associated test equipment were loaded into the test vehicle prior to departure from Cleveland, Ohio. The systems included in this phase of the testing are outlined in the following table:

System	System type	Proposed band, MHz
AT&T	IBAC	88 to 108
EUREKA 147	L-Band	1452 to 1492
EUREKA 147	L-Band	452 to 1492
VOA/JPL	S-Band	2310 to 2360

The USA Digital Systems FM-1, FM-2, and AM will not be field tested because of unresolvable differences between USA Digital Radio and the Electronic Industries Association regarding the terms of the field test contract. The AT&T/AMATI Systems were withdrawn because of technical problems.

The field test portion of this activity will establish how each system would perform in a real world environment, under varying conditions, as opposed to a laboratory environment. San Francisco was selected as the preferred test site because of the challenging radiofrequency environment. This area provides a variety of mixed terrain, a dense urban environment, a large suburban area, extensive rural areas, mountains, and large bodies of water. There were three locations identified for the EUREKA 147 System terrestrial transmitter, one location for the AT&T IBAC System, and the use of NASA's Tracking and Data Relay Satellite (TDRS) for the JPL/VOA System.

The NASA Ames Research Center also played a role in the testing of the EUREKA 147 system. Since the EUREKA 147 System operates in the L-band (1452 to 1492 MHz) frequency, it was necessary to have very close coordination during the testing of this system. The U.S. aviation industry (commercial and military) uses the L-band for aeronautical telemetry, resulting in the requirement for close coordination of this band. If there had been any interference, this portion of the testing would have been shut down.

The field test task group selected six different routes to test all systems. Each route had different environmental and physical characteristics to transverse and different transmission times because of route distances. The qualitative characteristics of each route are summarized in the following table:

Qualitative characteristics	Route					
	1	2	3	4	5	6
Line-of-site conditions	X	X		X	X	X
Terrain shielding conditions exist	X	X	X	X	X	X
Significant shielding by buildings	X	X				X
Vertical shielding (tunnels/wire)	X	X		X		
Major over-water path	X	X		X		X
Travel along waterfront areas	X		X	X		X
Significant foliage along path	X	X	X	X	X	
Rural area(s) covered				X		
Primarily highway travel			X	X		X
Residential areas covered	X	X	X		X	

This comprehensive field test program currently in progress in the United States will add significantly to the already available information on the performance of Digital Audio Radio systems. The conclusion of the field tests, plus the information learned from the laboratory tests, will provide U.S. radio transmitter/receiver manufacturers with significant data on the operation of these new systems. It will also point out where additional work is needed to improve system reliability and performance.

**Lewis contact:**

James E. Hollansworth,

(216) 433-3458,

James.E. Hollansworth@lerc.nasa.gov

**Author:** James E. Hollansworth

**Headquarters program office:** OSAT

# Lewis Investigates Frequency Sharing Between Future NASA Space Systems and Local Multipoint Distribution Systems in the 27-GHz Band

At the request of the Federal Communications Commission (FCC), the NASA Lewis Research Center undertook an intensive study to examine the feasibility of frequency sharing between future NASA space services and proposed Local Multipoint Distribution Systems (LMDS) in the 25.25- to 27.5-GHz band. This follows NASA's earlier involvement in the FCC's 1994 Negotiated Rule Making Committee which studied frequency sharing between Ka-band Fixed Satellite Services and LMDS in the 27.5- to 29.5-GHz band (ref. 1).

LMDS is a terrestrial, cellular, wireless communication service primarily intended to provide television distribution from hub stations located within relatively small cells to fixed subscriber receivers. Some proposed systems, however, also plan to offer interactive services via subscriber-to-hub transmissions. LMDS providers anticipate that their systems will be a cost-effective alternative to cable television systems, especially in urban areas. LMDS proponents have expressed an interest in using frequencies below 27.5 GHz.

NASA, however, plans to operate three types of space systems below 27.5 GHz. The H, I, and J follow-on satellites for the Tracking and Data Relay Satellite System (TDRSS), which are planned for launch beginning in 1999, are designed to receive high-data-rate transmissions (up to 800 Mbps) from low-Earth orbiting "user" spacecraft in the 25.25- to 27.5-GHz band. In this case, the potential interference is the aggregate interference from LMDS transmitters (both hubs and subscribers) into the TDRSS tracking receive beams as they sweep over the Earth's surface while tracking lower altitude user spacecraft.

NASA is also developing the Proximity Operations Communications System (POCS) in the 25.25- to 25.55-GHz and 27.225- to 27.5-GHz bands for interorbit communications between the space station and robotic vehicles and astronauts. Again, there is the possibility of harmful interference from a collection of LMDS transmitters on the ground.

Finally, NASA is seeking a wideband allocation near 26 GHz to support future downlinks. Here, the concern is potential harmful interference from LMDS transmitters (both hubs and subscribers) into the Earth Exploration Satellite's Earth station receivers when they are located in an LMDS service area.

Interference into TDRSS and POCS was studied with LMDS characteristics from four proponents who plan to implement LMDS systems. System characteristics varied widely, since each of the proponents envisioned several different implementations that would allow certain types of service.

Results of the interference analysis showed that three of the four proposed LMDS systems would produce excessive interference into both TDRSS and POCS. Although LMDS interference into the Earth Exploration Satellite's

Earth station receivers was not analyzed in this study, earlier analysis results indicate that LMDS would also cause harmful interference in this case without proper coordination and site shielding. In light of the study results, NASA concluded that sharing between its future space services and LMDS is not feasible in the 27.5-GHz frequency band.

## Reference

1. Wayne A. Whyte, Jr.: Lewis Helps Examine Feasibility of Fixed Satellite Service and Local Multipoint Distribution Service Sharing the Same Frequency Band. Research & Technology 1995. NASA TM-107111, 1996, pp. 119-120. Available WWW: <http://www.lerc.nasa.gov/WWW/RT1995/5000/5610w.htm>

## Lewis contact:

Rodney L. Spence, (216) 433-3464, [rodney.spence@lerc.nasa.gov](mailto:rodney.spence@lerc.nasa.gov)

**Author:** Rodney L. Spence

**Headquarters program office:** OSAT

## Computer Simulation of Microwave Devices

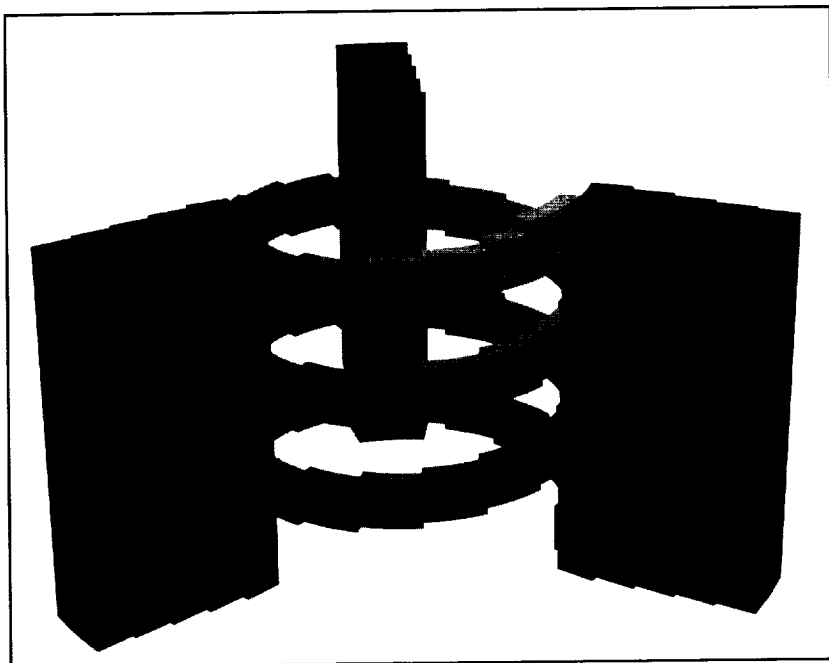
The accurate simulation of cold-test results including dispersion, on-axis beam interaction impedance, and attenuation of a helix traveling-wave tube (TWT) slow-wave circuit using the three-dimensional code MAFIA (Maxwell's Equations Solved by the Finite Integration Algorithm) was demonstrated for the first time (ref. 1). Obtaining these results is a critical step in the design of TWT's. A well-established procedure to acquire these parameters is to actually build and test a model or a scale model of the circuit. However, this procedure is time-consuming and expensive, and it limits freedom to examine new variations to the basic circuit. These limitations make the need for computational methods crucial since they can lower costs, reduce tube development time, and lessen limitations on novel designs.

Computer simulation has been used to accurately obtain cold-test parameters for several slow-wave circuits (refs. 2 and 3). Although the helix slow-wave circuit remains the mainstay of the TWT industry because of its exceptionally wide bandwidth, until recently it has been impossible to accurately analyze a helical TWT using its exact dimensions because of the complexity of its geometrical structure. A new computer modeling technique developed at the NASA Lewis Research Center overcomes these difficulties. The MAFIA three-dimensional mesh for a C-band helix slow-wave circuit is shown in the figure.

This unprecedented approach was employed by using MAFIA to model a 32-GHz helical TWT for the Cassini mission in an attempt to explain an anomaly observed in the spectrum analysis of one of the flight model tubes. To investigate whether this anomaly was a result of the electron beam coupling to the backward wave oscillation mode, we used MAFIA (for the first time) to accurately compute the dispersion relations for the fundamental amplification ( $n = 0$ ) and backward oscillation ( $n = -1$ ) modes of a helical TWT. Calculations of the gain at the point where the electron beam phase velocity line intersects the backward wave mode indicate that there is not enough interaction with the beam to produce spontaneous backward wave oscillation. Other computational efforts indicated that a strong second harmonic current exists only at the radiofrequency drive levels where the anomaly is observed. Since the effect is not observed within the range of parameters planned for use on the Cassini mission, even in the worst case analysis, this anomaly is not expected to appear. The 32-GHz TWT flight and engineering models for the Cassini mission have been packaged for flight, so it would have been virtually impossible to experiment with them to investigate the parameters of the anomaly. Thus, computer modeling was

crucial to the explanation of the anomaly and to predicting the changes that could be expected during the course of the Cassini mission.

Simulation of microwave tubes is becoming even more essential because of the substantial opportunity for growth in the commercial demand for TWT's. In particular, two types of systems are of interest: satellite communications and local multipoint distribution systems (LMDS)—a concept that would cover major metropolitan areas with a grid of cellular stations operating at the Ka band, transmitting programming in competition with cable television systems. U.S. industry is proposing to invest more than \$35 billion in commercial Ka-band satellite communications systems over the next 6 years, requiring more than 5000 Ka-Band TWT's. One estimate suggests that 5000 to 6000 highly linear Ka-Band TWT's would be required to implement



MAFIA three-dimensional mesh for a C-band traveling-wave tube helix slow-wave circuit.

LMDS in the continental United States (ref. 4). Because cost and reliability are paramount for TWT's, computer simulation becomes indispensable.

## References

1. Kory, C.L.: Three-Dimensional Simulation of Helix Traveling-Wave Tube Cold-Test Characteristics Using MAFIA. IEEE Trans. Electron Devices, vol. 43, no. 8, Aug. 1996, pp. 1317-1319.
2. Kory, C.L.; and Wilson, J.D.: Three-Dimensional Simulation of Traveling-Wave Tube Cold-Test Characteristics Using MAFIA. NASA TP-3513, 1995.
3. Kory, C.L.; and Wilson, J.D.: Novel High-Gain, Improved-Bandwidth, Finned-Ladder V-Band Traveling-Wave Tube Slow-Wave Circuit Design. IEEE Trans. on Electron Devices, vol. 42, no. 9, Sept. 1995, pp. 1686-1692.
4. Dayton, J.A., Jr. and Stevens, G.H.: Commercial Opportunities for Microwave Tubes. 1996 Crane Microwave Tube Conference, Nov. 13-14, Bloomington, IN, 1996.

## Lewis contact:

Dr. Vernon O. Heinen, (216) 433-3245,  
Vernon.O.Heinen@lerc.nasa.gov

**Author:** Carol L. Kory

**Headquarters program office:** OSAT

# High-Temperature Superconducting/Ferroelectric Structures for Tunable Microwave Components

At the NASA Lewis Research Center, ferroelectric films, such as  $\text{SrTiO}_3$  and  $\text{Ba}_x\text{Sr}_{1-x}\text{TiO}_3$ , are being used in conjunction with  $\text{YBa}_2\text{Cu}_3\text{O}_{7-\delta}$  high-temperature superconducting (HTS) thin films to fabricate tunable microwave components, such as filters, varactors, and local oscillators. These structures capitalize on the variation of the dielectric constant of the ferroelectric film upon the application of a dc electric field as well as on the low microwave losses exhibited by the high-temperature superconducting films relative to their conventional conductor counterparts. (For example, the surface resistance for a  $\text{YBa}_2\text{Cu}_3\text{O}_{7-\delta}$  thin film at 10 GHz and 77 K is more than two orders of magnitude lower than that of copper at the same frequency and temperature.)  $\text{SrTiO}_3$  and  $\text{Ba}_x\text{Sr}_{1-x}\text{TiO}_3$  films are used because their crystal structure and lattice parameters are similar to those of  $\text{YBa}_2\text{Cu}_3\text{O}_{7-\delta}$ , thus enabling the growth of highly textured  $\text{YBa}_2\text{Cu}_3\text{O}_{7-\delta}$  films with high critical current densities on the underlying ferroelectric film, or alternatively, of highly textured ferroelectric film on the underlying  $\text{YBa}_2\text{Cu}_3\text{O}_{7-\delta}$  film.

Our efforts have been concentrated so far in determining the deposition parameters required for optimal ferroelectric thin-film growth (i.e., maximum tunability and lowest loss) and in investigating different varactor configurations to determine which geometry is the most advantageous in terms of tunability, losses, and required bias for a given communication application. For example, we have observed that for optimized  $\text{SrTiO}_3$  films in a parallel plate capacitor, tunabilities of up to 47 percent and dissipation losses ( $\tan \delta$ ) of 0.05 are attainable at 1 MHz, 80 K, and within the 0- to 5-V bias range. In contrast, for an interdigital configuration, tunabilities of up to 70 percent and  $\tan \delta$  ranging from 0.015 to 0.001 (depending on bias) have been observed at 1 MHz and 77 K within the 0- to 100-V bias range.

Efforts are underway to use these results in developing tunable receiver front-end preselect filters as well as in low-phase noise, tunable local oscil-

lators for K-band applications. These components represent a hitherto unavailable technology to meet the stringent performance requirements of foreseeable satellite and wireless communication systems (e.g., bandwidth, in-band insertion losses, out-of-band rejection, and noise, amongst others) in a more advantageous fashion than with currently available technology (e.g., dielectric-filled cavity and waveguide filters, and dielectric resonator oscillators). Prototypes of high-temperature superconducting/ferroelectric tunable components such as a low-phase noise K-band local oscillator, a preselect C-band filter, and a low-loss K-band phase shifter are under development at NASA Lewis.

## Bibliography

Miranda, F.A., et al.: HTS/Ferroelectric Thin Films for Tunable Microwave Components. IEEE Trans. Appl. Supercond., vol. 5, no. 2, 1995, pp. 3191-3194.

Miranda, F.A., et al.: Electrical Response of Ferroelectric/Superconducting/Dielectric  $\text{Ba}_x\text{Sr}_{1-x}\text{TiO}_3/\text{YBa}_2\text{Cu}_3\text{O}_{7-\delta}/\text{LaAlO}_3$  Thin-Film Multilayer Structures. *Supercond. Sci. Technol.*, vol. 8, 1995, pp. 755-763.

Miranda, F.A.; et al.: Effect of  $\text{SrTiO}_3$  Deposition Temperature on the Dielectric Properties of  $\text{SrTiO}_3/\text{YBa}_2\text{Cu}_3\text{O}_{7-\delta}/\text{LaAlO}_3$  Structures. Presented at the 8th International Symposium on Integrated Ferroelectrics, Tempe, Arizona, Mar. 17-20, 1996. To be published in *Integrated Ferroelectrics*, 1997.

#### Lewis contacts:

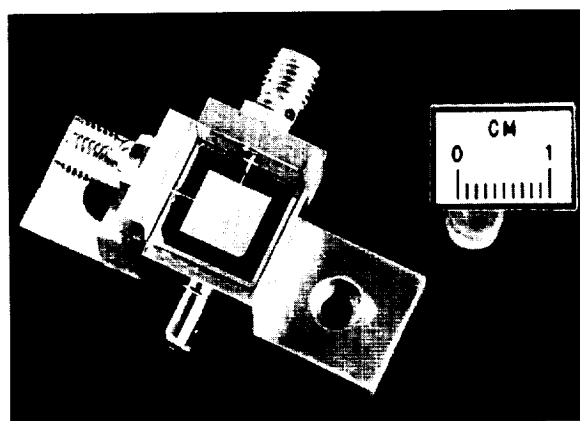
Dr. Félix A. Miranda, (216) 433-6589, felix.miranda@lerc.nasa.gov; and Robert R. Romanofsky, (216) 433-3507, Robert.R.Romanofsky@lerc.nasa.gov

**Authors:** Dr. Félix A. Miranda and Robert R. Romanofsky

**Headquarters Program Office:** OSAT

## Miniaturized High-Temperature Superconducting/Dielectric Multilayer Filters for Satellite Communications

Most communication satellites contain well over a hundred filters in their payload. Current technology in typical satellite multiplexers use dual-mode cavity or dielectric resonator filters that are large (~25 to 125 in.<sup>3</sup>) and heavy (up to 600 g). As the complexity of future advanced electronic systems for satellite communications increases, even more filters will be needed, requiring filter miniaturization without performance degradation. Such improvements in filter technology will enhance satellite performance. To reduce the size, weight, and cost of the multiplexers without compromising performance, the NASA Lewis Research Center is collaborating with industry to develop a new class of dual-mode multilayer filters consisting of  $\text{YBa}_2\text{Cu}_3\text{O}_{7-\delta}$  high-temperature superconducting (HTS) thin films on  $\text{LaAlO}_3$  substrates.

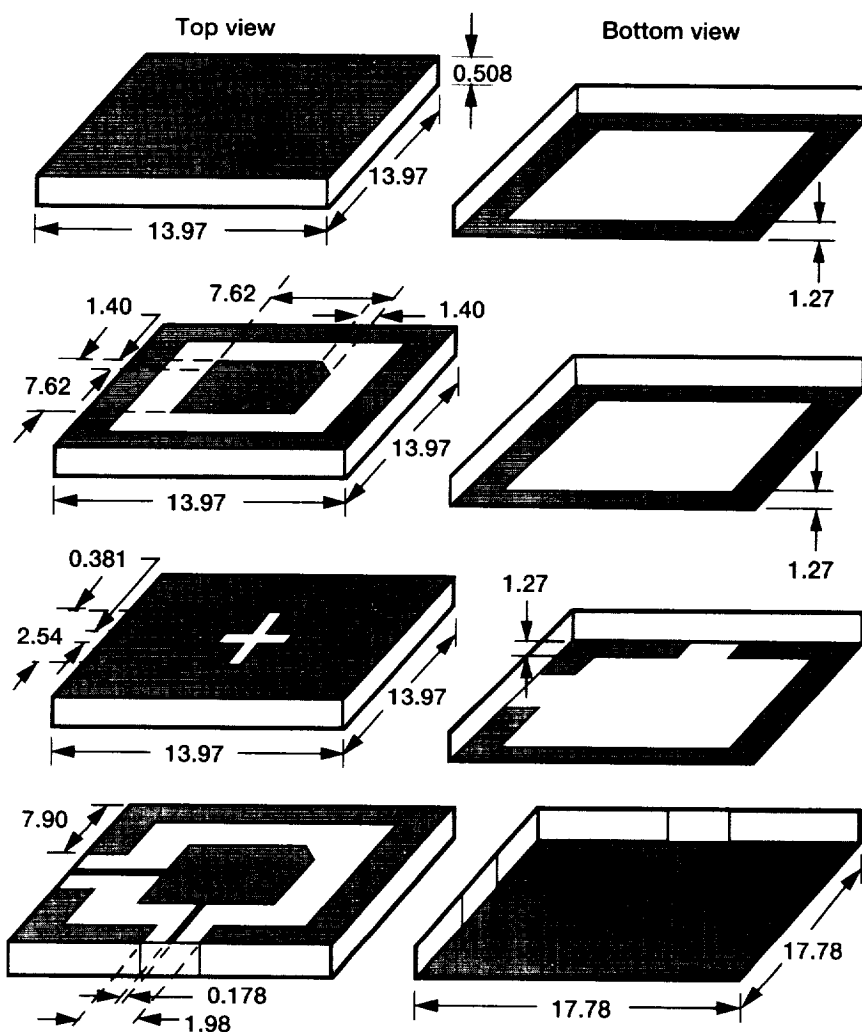


*Dual-mode proof-of-concept gold resonator with corner-cut.*

A major limiting factor in the continuing improvement of satellite communication systems is the unavailability of high-performance (i.e., high-Q) miniaturized filters that are compatible with monolithic microwave integrated circuits (MMIC) components. The poor Q factor of current miniature, planar components is due primarily to conductive loss, which can be significantly reduced by using HTS thin films (For example, at 77 K the surface resistance of  $\text{YBa}_2\text{Cu}_3\text{O}_{7-\delta}$  thin films at 10 GHz is more than 2 orders of magnitude

lower than that of copper at the same temperature and frequency). Therefore, it will be advantageous to replace dual-mode cavity and dielectric resonator filters with HTS thin-film-coated printed circuits that are dramatically smaller, lighter, and potentially less costly.

In this work, a new class of miniaturized filters based on a multilayered stack of dual-mode stripline or microstrip resonators coupled through irises, is being developed. These filters, which are extremely small in size and mass, can be fabricated of thin-film superconductors such as  $\text{YBa}_2\text{Cu}_3\text{O}_{7-\delta}$ . All current filter types that have dual-mode cavities or dielectric resonators can be replaced with those having this novel filter structure. For example, in the C-band this configuration will occupy only 1 percent of the volume of its dielectric resonator counterpart. Also, the multilayer configuration is smaller and lighter than the previously introduced dual-mode microstrip filters (ref. 1). The  $\text{YBa}_2\text{Cu}_3\text{O}_{7-\delta}/\text{LaAlO}_3$  multilayer filters being pursued in this work can be based on a variety of dual-mode, planar resonator structures similar to those used in dual-mode microstrip filters. These include square patches, circular disks, and rings (ref. 2). Coupling between the



Physical layout of a four-pole dual-mode multilayer filter. (Dimensions are in millimeters.)

## References

1. Curtis, J.A.; and Fiedziuszko, S.J.: Miniature Dual Mode Microstrip Filters. IEEE MTT-S International Microwave Symposium Digest, Vol. II, 1991, pp. 443-446.
2. Fiedziuszko, S.J., et al.: Low Loss Multiplexers With Planar Dual Mode HTS Resonators. IEEE Trans. Microwave Theory Tech., vol. 44, July 1996, pp. 1248-1257.
3. Kwok, R.S., et al.: Miniaturized HTS/Dielectric Multilayer Filters for Satellite Communications. Presented at the Applied Superconductivity Conference, Aug. 25-30, 1996, Pittsburgh, PA. To be published in the IEEE Trans. on Applied Superconductivity, 1997.

## Lewis contact:

Dr. Félix A. Miranda, (216) 433-6589,  
felix.miranda@lerc.nasa.gov

Author: Dr. Félix A. Miranda

Headquarters Program Office: OSAT

dual orthogonal modes supported by these resonators is achieved by introducing a perturbation to the symmetry of the previously single-mode resonator at a location that is offset  $45^\circ$  from the axes of coupling to and from the resonator. Proof-of-concept of these miniaturized multilayer filters has already been demonstrated in our laboratory (ref. 3), and work is underway to optimize their performance through more detailed analysis, fabrication, and testing.



# Root-Raised Cosine Filter Implementation That Uses Canonical Signed Digits for High-Speed Digital Filter Applications

NASA Lewis Research Center's Space Communications Division has been investigating high-speed digital filters that can operate at a higher speed than those in current use for a digital modulator and demodulator (modem). Using the Canonical Signed Digits (CSD) number representation for filter coefficients is a very effective way to increase the filter's speed while reducing complexity in the digital filter hardware design. This approach is a good alternative to using an expensive parallel-processing design technique or custom, application-specific integrated circuits. Such integrated circuits may not be suitable for applications that require filter speeds faster than what application-specific integrated circuits digital signal processors can offer for a dedicated channel. When a communication channel is a dedicated, multiplication process—a costly, time-consuming process—it can be greatly simplified by a replacement of the filter coefficients with CSD numbers. A computer code written with the MATLAB software package runs the program and generates CSD-represented filter coefficients that are based on minimizing minimum mean square errors. Also, the Alta Group of Cadence's Signal Processing Workstation is used to simulate and analyze the CSD filter responses.

The impulse response of the root-raised cosine filter that is used as a base model is defined in reference 1. From this filter, a set of coefficients is sampled and stored in a file. For the all coefficients, the optimal CSD number for each coefficient is searched on the basis of the minimum-mean-square-errors criterion. Because the distribution of CSD numbers is not uniform, quantization errors tend to be bigger for coefficients greater than  $\frac{1}{2}$ . To offset errors that occur in a region of coefficients between  $\frac{1}{2}$  to 1 and to better represent fractions with CSD numbers, an extra nonzero digit is allowed for any coefficients exceeding  $\frac{1}{2}$ . This will greatly improve frequency response as well as intersymbol interference at the receiver.

The frequency response of a set of collected CSD-represented filter coefficients was compared with the same filter that was conventionally implemented. Analyses show CSD-implemented filters perform as well as conventional filters. Comparison of eye diagrams and bit-error-rate curves between CSD filters and traditionally implemented filters are almost indistinguishable. However, filter complexity was reduced from almost 3.5 to 1 for CSD filters. Complete computer simulation results are available. In the near future, work will focus on building actual working digital filter hardware in a field programmable gate array (FPGA).

## Reference

1. Kim, H.: Computer Simulation Results and Analysis for a Root-Raised Cosine Filter Design Using Canonical Signed Digits. NASA TM-107327, 1996.

**Lewis contact:** Heechul Kim, (216)433-8698, heechul.kim@lerc.nasa.gov

**Author:** Heechul Kim

**Headquarters program office:** OSAT



# Space Flight Systems

## Space Experiments

### Shuttle Fire Tests Are Radiant

Flame spreading is a phenomenon familiar to everyone who has witnessed an accidental fire. Yet, because of the complexity of the physical and chemical processes that are involved, the theoretical understanding of fires and flame spreading is a relatively new science. Flames spread along solid materials in a process where heat from the flames vaporizes the fuel just ahead of the moving flame. The vaporized fuel mixes with oxygen from the air and reacts chemically with it, producing the flame. On Earth, the spread rate of the flame is directly affected by the rate at which the fuel and oxygen are mixed with the help of buoyant convection.

Fires in spacecraft pose significant dangers to the crew. Toxic products can quickly poison the atmosphere and be difficult to remove, production of gases at high temperatures can lead to rapid overpressurization and rupture of the spacecraft, and extinguishing systems can damage critical electrical systems. This suggests that momentary ignitions due to electrical shorts or overheating might be an acceptable and recoverable hazard, but a transition from the ignition to fire growth is an unacceptable risk. To stop this transition, the conditions that allow transition must be avoided. Unfortunately, these conditions are not yet well known.

Flown on the USMP-3 mission, the Radiative Ignition and Transition to Spread Investigation (RITSI) studied the ignition process and the transition from this momentary ignition to a fire spread situation. Heating of the sample and ignition was via radiative heat transfer and absorption with a subsequent transition to flame spread in low gravity in the presence of very low-speed airflows in two-dimensional (2D) and three-dimensional (3D) configurations. In the 2D tests, ignition occurred across the full width of the fuel sample to initiate planar 2D spread in the axial direction. In the 3D tests, ignition was isolated to a central spot, allowing spread to occur in all dimensions. The key aspect of this approach is that a flame may spread simultaneously both upstream and downstream, or it may split into two or more flames that propagate at different rates and extinguish at different times. The airstream, however, comes principally from one direction, at magnitudes from 1 to 15 cm/sec. This arrangement is both more realistic as a fire scenario in space and is also unachievable at these flow speeds on Earth.

RITSI hardware consists of a flow duct with screens at both ends and a fan that pulls air through the duct. Some samples are rectangular to allow for 2D flame spread, and some are square to allow for 3D flame spread. A radiant heater, and when needed, a hot wire, are used to ignite the samples. Some samples were doped with a smoldering promoter to study smoldering rather than flaming combustion. Six thermocouples and an ignitor wire were preinstalled on each sample holder. The thermocouple data were recorded along with radiant heater power, ignitor power, and flow velocity.

A total of 25 tests conducted with ashless filter paper produced many exciting surprises. The first surprise was that radiative ignition by the lamp followed by successful transition to flame spread occurred in all experiments except at zero external velocity. This has never been observed at normal gravity; that is, ignition in 1g always needed the assistance of a hot wire ignitor near the fuel surface. This finding indicates that the transition tends to be easier in microgravity than in normal gravity. Another interesting observation was that the flame did not spread downstream at all in air (along the direction of the external flow) following ignition at the middle part of a sample. The flame spread upstream, however, in the shape of a fan; the spread rate was most rapid directly in the direction of the incoming flow and gradually slowed down to zero in the direction normal to the incoming flow. With an increase in the incoming air flow velocity, the fan angle increased due to an increase in oxygen supply rate. These two trends are completely opposite to those observed in normal gravity, where spread is much more rapid downstream and the fan angle narrows with an increase in the incoming flow velocity.

Three narrow samples (4-cm-wide instead of the regular 10-cm-wide sample) with two open sides were used to examine flame spread characteristics along the open edges. The results show that once a flame reaches the edge of the sample, it spreads much faster than it does

along the center of the sample. With 2 cm/sec external air speed, a flame only spreads upstream along the edges; but at forced air speeds greater than 3.5 cm/sec flow, a flame spreads both upstream and downstream along the sample edges. At the downstream edge, the flame spread rate appears to be the highest. RITSI also studied the effects of a corner on flame spread, using a 90° bend at one side of the sample. Slowdown of the approaching flame toward the corner was observed, but a flame coming from the open corner side (270°) appeared and spread rapidly along the open corner. These results show that there are significant effects of the 3D

geometrical configuration on flame spread which cannot be observed by a 2D configuration. Since the flame spreads much faster than it does in the 2D configuration, these 3D flame spread configurations would be more relevant to fire safety in microgravity.

The development of a model and associated numerical codes are nearing completion, and experimental data are being compared with predicted results. From the comparison, the validity of our understanding of ignition and flame spread mechanisms can be assessed and any deficiencies pointed out.

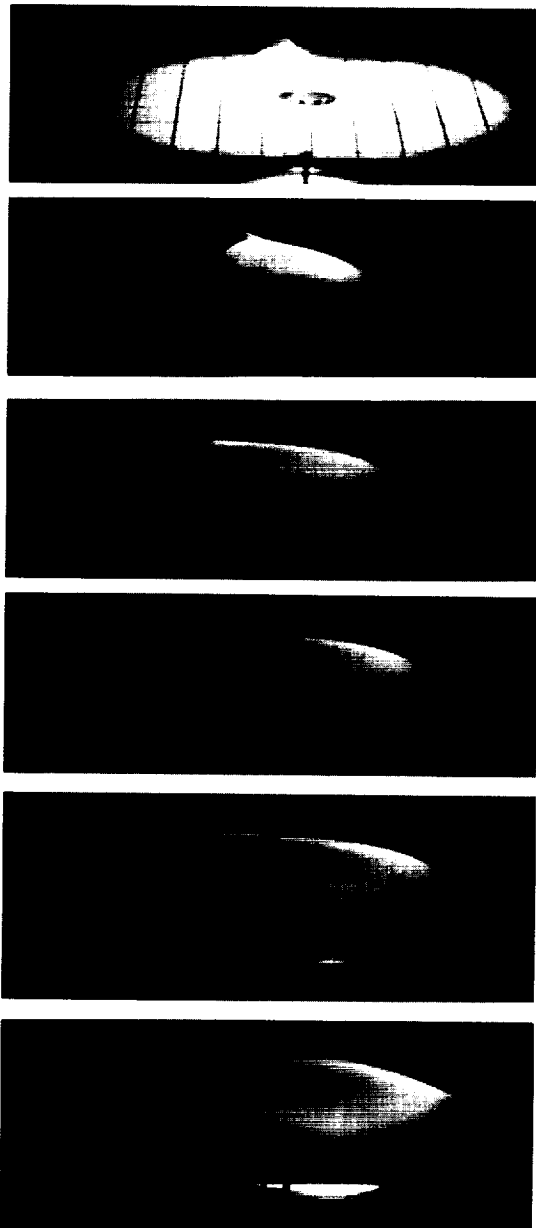
**For more information, visit RITSI on the World Wide Web:**  
<http://zeta.lerc.nasa.gov/expr/ritsi.htm>

**Lewis contact:**

Sandra L. Olson, (216) 433-2859,  
[sandra.olson@lerc.nasa.gov](mailto:sandra.olson@lerc.nasa.gov)

**Authors:** Sandra L. Olson (NASA Lewis)  
 and T. Kashiwagi (NIST)

**Headquarters program office:** OLMSA  
 (MSAD)



*USMP-3 Radiative Ignition and Transition to Spread Investigation (RITSI) smoldering sample with flow entering from the right. Bifurcating smolder fronts are the glowing tips of each char peninsula.*

## Comparative Soot Diagnostics Experiment Looks at the Smoky World of Microgravity Combustion

From an economic standpoint, soot is one of the most important combustion intermediates and products. It is a major industrial product and is the dominant medium for radiant heat transport in most flames used to generate heat and power. The nonbuoyant structure of most flames of practical interest (turbulent flames) makes the understanding of soot processes in microgravity flames important to our ability to predict fire behavior on Earth. In addition, fires in spacecraft are considered a credible possibility.

To respond to this risk, NASA has flown fire (or smoke) detectors on Skylab and the space shuttles and included them in the International Space Station design. The design of these detectors, however, was based entirely on normal gravity (1g) data. The detector used in the shuttle fleet is an ionization detector, whereas the system planned for the space station uses forward scattering of near-infrared light. The ionization detector, which is similar to smoke detectors used in homes, has a comparative advantage for submicron particulates. In fact, the space shuttle model uses a separation system that makes it blind to particles larger than a micron (believed to be dust). In the larger size range, the light-scattering detector is most sensitive.

Without microgravity smoke data, the difference in the particle size sensitivities of the two detectors cannot be evaluated. As part of the Comparative Soot Diagnostics (CSD) experiment, these systems were tested to determine their response to particulates generated during long periods of low gravity. This experiment provided the first such measurements toward understanding soot processes on Earth and for designing and implementing improved spacecraft smoke detection systems.

The objectives of CSD were to examine how particulates form from a variety of sources and to quantify the performance of several diagnostic techniques. The sources tested included four overheated materials (paper, silicone rubber, Teflon-coated (Dupont) wire, and Kapton-coated (Dupont) wires), each tested at three heating rates, and a candle tested at three air velocities. Paper, silicone rubber, and wire insulation, materials found in spacecraft crew cabins, were selected because of their different smoke properties. The candle yielded hydrocarbon soot typical of many 1g flames. Four diagnostic techniques were employed: thermophoretic sampling collected particulates for size analysis; laser light extinction measurements near the source tallied total particulate production; and laser light scattering and ionization detector measurements far from the particulate source provided data for evaluating the performance of smoke detection systems for these particulate sources.

The CSD experimental hardware consisted of two modules: the Near-Field Module and the Far-Field Box. The Near-Field Module contained the combustible sample and near-field diagnostics. The Far-Field Box contained two spacecraft smoke detectors, an exact copy of those currently used on the shuttles and a prototype International Space Station detector. Products (soot and gases) from the near-field tests were transported to the Far-Field Box and subsequently back through Teflon hoses, isolating the crew from the smoke. This project was a collaborative effort of the NASA Lewis Research Center, the NASA Marshall Space Flight Center, and the NASA Johnson Space Center.

For the majority of the samples, detectable smoke concentrations were produced and the smoke was detected by both detectors. Smoke



*Comparative Soot Diagnostics (CSD) hardware. The Far-Field Box contains space station and space shuttle smoke detectors. The Near-Field Module, which is placed in the Glovebox facility, contains the combustible samples.*

particulate samples were successfully collected for most of the tests. Smoke particle size distributions determined from Transmission Electron Microscope data are being evaluated. In general, the light-scattering detector detected the smoke from the majority of the tests, whereas the ionization detector was less sensitive to smoke from some of the tests. Both detectors responded very well to the smoke from these sources in preflight normal-gravity tests; this suggests that the particle size distribution shifted toward larger particles.

**Find out more about the Comparative Soot Diagnostic experiment on the World**

**Wide Web:** <http://einstein.lerc.nasa.gov/dlurban/csd/csdbrochure.html>

**Lewis contact:** Dr. David L. Urban, (216) 433-2835, [david.urban@lerc.nasa.gov](mailto:david.urban@lerc.nasa.gov)

**Authors:** Dr. David L. Urban, Dr. DeVon W. Griffin, and Melissa Y. Gard

**Headquarters program office:** OLMSA (MSAD), OSMA

## Pool Boiling Experiment Has Five Successful Flights

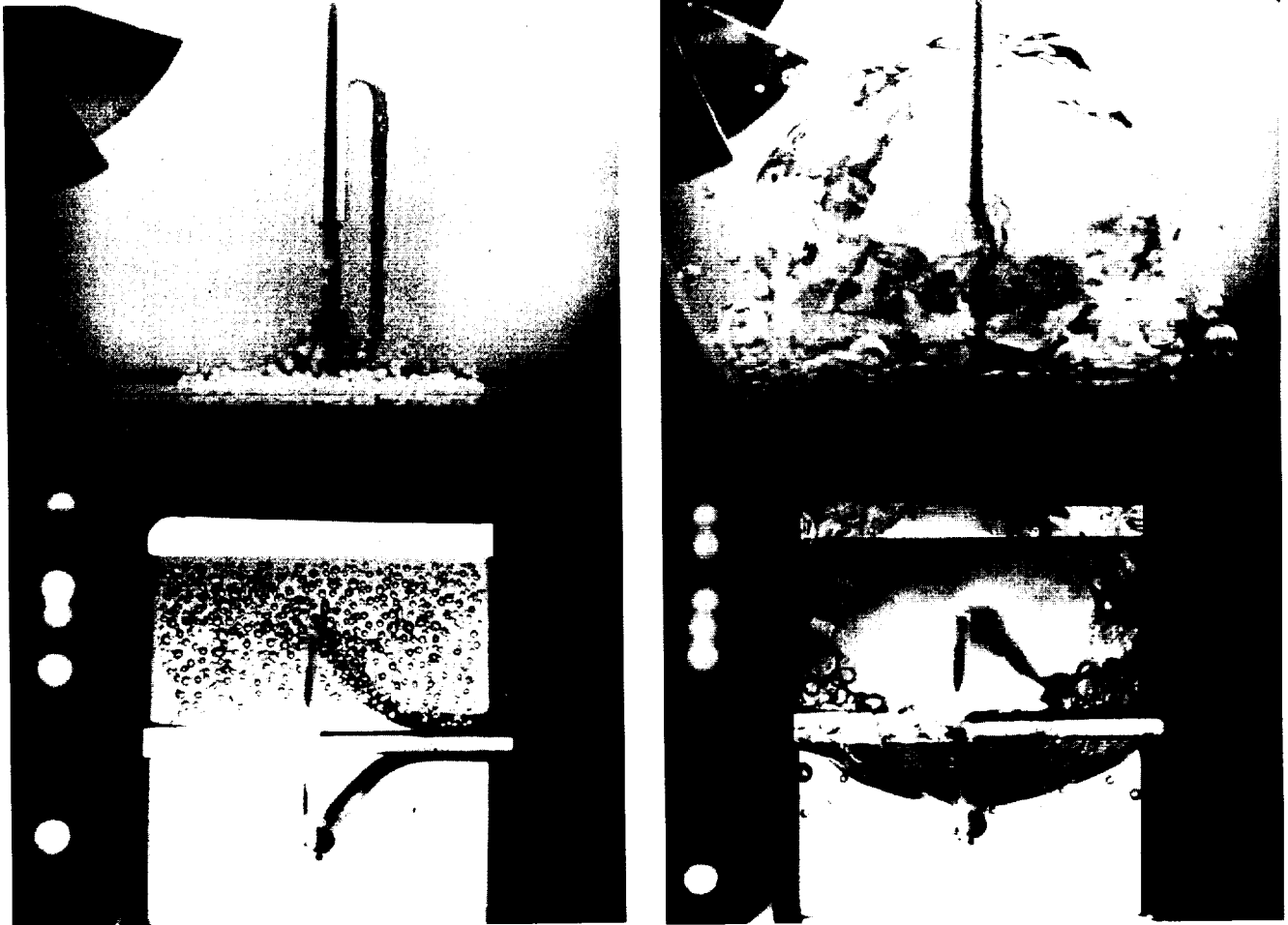
The Pool Boiling Experiment (PBE) is designed to improve understanding of the fundamental mechanisms that constitute nucleate pool boiling. Nucleate pool boiling is a process wherein a stagnant pool of liquid is in contact with a surface that can supply heat to the liquid. If the liquid absorbs enough heat, a vapor bubble can be formed. This process occurs when a pot of water boils. On Earth, gravity tends to remove the vapor bubble from the heating surface because it is dominated by buoyant convection. In the orbiting space shuttle, however, buoyant convection has much less of an effect because the forces of gravity are very small. The Pool Boiling Experiment was initiated to provide insight into this nucleate boiling process, which has many earthbound applications in steam-generation power plants, petroleum plants, and other chemical plants. In addition, by using the test fluid R-113, the Pool Boiling Experiment can provide some basic understanding of the boiling behavior of cryogenic fluids without the large cost of an experiment using an actual cryogen.

The experiment was conceived by Professor Herman Merte of the University of Michigan, was developed by the NASA Lewis Research Center, and is supported by NASA Headquarters' Microgravity Science and Applications Division. The pool boiling prototype system, which was initially flown on the STS-47 shuttle mission in September 1992, acquired a considerable amount of scientific data. The expected boiling pattern was observed in all high-heat-flux cases, but a different pattern was observed in the low-heat-flux cases. These differences appear to be caused by the rewetting of the heater surface. Photographic data indicate that the saturated cases experienced a more activated boiling process (more vapor than expected was generated).

Some minor modifications were made in the timing sequences in the test matrix on the next two experiments that were flown on space shuttle flights STS-57 and STS-60. This was done to increase the probability of observing

the initial dynamic vapor bubble growth while the camera was running at the higher speed and to observe the influence of a stirrer on the active boiling process. Currently, results appear to indicate the potential for quasi-steady nucleate pool boiling in long-term microgravity, with certain combinations of levels of heat flux and bulk liquid subcooling. These were the first experiments of nucleate boiling obtained for long periods of microgravity, and the matrix test conditions were selected in part to cover a reasonably broad range of test parameters.

The primary objective of the last two experiments, flown on STS-72 and STS-77, was to determine the factors governing the onset of dryout and/or rewetting on a flat heater surface. On the STS-72 mission, the subcooling levels were increased, whereas on the STS-77 mission, the heat flux levels were reduced. For high-heat-flux levels at all but the highest subcooling, dryout was observed. For lower levels of heat flux where dryout did



*Pool Boiling Experiment.*

not take place, it appeared that the excess surface energy associated with the coalescence of bubbles was sufficient to impel the resulting combined bubble away from the vicinity of the heater surface. This sufficiently stirred the liquid so as to bring the subcooled liquid to the heater surface.

**Find out more about the Pool Boiling Experiment, Lewis' fluids experiments, and other Lewis microgravity experiments at our PBE home page on the World Wide Web:**

<http://zeta.lerc.nasa.gov/expr/pbeinfo.htm>.

**Lewis contact:** Angel M. Otero, (216) 433-3878; [angel.otero@lerc.nasa.gov](mailto:angel.otero@lerc.nasa.gov)

**Author:** Dr. Fran Chiaramonte

**Headquarters program office:** OLMSA (MSAD)

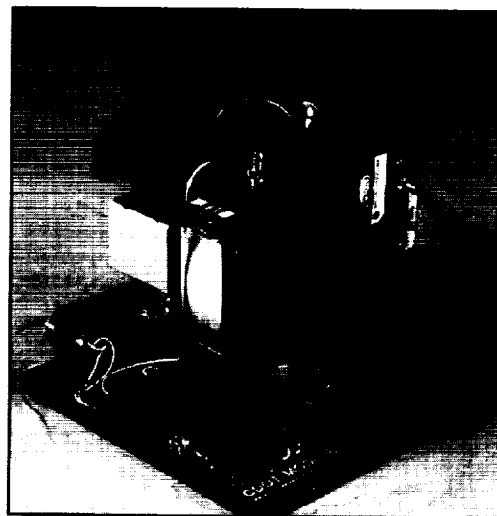
# Colloidal Disorder-Order Transition Experiment Probes Particle Interactions in Microgravity

Everything in the universe is made up of the same basic building blocks—atoms. All physical properties of matter such as weight, hardness, and color are determined by the kind of atoms present and the way they interact with each other. The Colloidal Disorder-Order Transition (CDOT) shuttle flight experiment tested fundamental theories that model atomic interactions. The experiment was part of the Second United States Microgravity Laboratory (USML-2) aboard the Space Shuttle Columbia, which flew from October 20 to November 5, 1995.

The CDOT experiment used colloidal suspensions of microscopic plastic spheres as a model of atomic interactions. A colloidal suspension, or colloid, is a system of fine particles suspended in a fluid. Paint, ink, and milk are examples of colloids found in everyday life. When the particles in a colloidal suspension are uniformly sized spheres that cannot penetrate each other (hard spheres), this system shares a very fundamental characteristic with atomic systems—both undergo a transition from a disordered liquid state to an ordered solid state under the proper conditions. The freezing of water to form ice crystals as temperature is lowered is a familiar example. With hard-sphere systems, the liquid-to-solid transition occurs as the average spacing between the spheres is varied. The gravitational effects of sedimentation and convection limit definitive colloidal experiments on Earth. By conducting hard-sphere experiments in the microgravity environment of space, we hope to gain a better understanding of the liquid-to-solid transition and, thereby, the structures and properties of solids.

During orbit, astronauts gathered data on 15 hard-sphere samples, including 35-mm and digital photographs, video images, and digital correlation data. The CDOT hardware operated in the Spacelab Glovebox Facility. This first set of hard-sphere data from microgravity yielded several interesting and valuable results. A number of the photographs revealed the first physical evidence of dendritic growth in hard-sphere crystals. Dendrites, snow-flakelike structures that are a common feature of atomic materials, are not observed in hard-sphere systems on Earth because of the effects of gravity. Laser-light-scattering video images indicate that the structure of the crystals formed in space were also different from the structure of crystals formed on Earth. On Earth, colloidal crystals are a mixture of face centered cubic and random hexagonal close-packed structures. In microgravity, it appears that crystals form only random hexagonal close-packed structures. Lastly, a high volume fraction sample that did not crystallize on Earth readily crystallized in microgravity. This suggests that the glassy state observed on Earth may be an artifact of gravity, not a thermodynamic state.

The CDOT experiment was conceived by Professors Paul M. Chaikin and William B. Russel of Princeton University and William V. Meyer of the Ohio Aerospace Institute. The experiment hardware was designed by Aerospace Design & Fabrication, Inc. (ADF) and was built and tested by the NASA Lewis Research Center under the direction of Richard B. Rogers of NASA, Dr. Jixiang Zhu of Princeton University, and the experiment originators. The CDOT instrument employed several laser-light-scattering techniques using state-of-the-art avalanche photodiodes and digital correlation hardware.



*Colloidal Disorder-Order Transition (CDOT) flight experiment module.*

Both of these components represent advances in commercially available products that were driven by NASA requirements for microgravity research.

CDOT is the first of a series of planned space shuttle and space station colloids experiments. The knowledge gained from these experiments will allow scientists to better understand basic atomic interactions and may eventually help to reduce the trial and error involved in developing new and better materials. Industries dealing with semiconductors, electro-optics, ceramics, and composites are just a few that may benefit from this knowledge.

**For more information, visit the CDOT homepage on the World Wide Web:**

<http://zeta.lerc.nasa.gov/expr2/cdot.htm>

**Lewis contacts:**

Richard B. Rogers, (216) 433-6512, [rrogers@sarah.lerc.nasa.gov](mailto:rrogers@sarah.lerc.nasa.gov); and William V. Meyer, (216) 433-5011, [bill@sarah.lerc.nasa.gov](mailto:bill@sarah.lerc.nasa.gov)

**Author:** Richard B. Rogers

**Headquarters program office:** OLMSA



# Surface Tension Driven Convection Experiment Completed

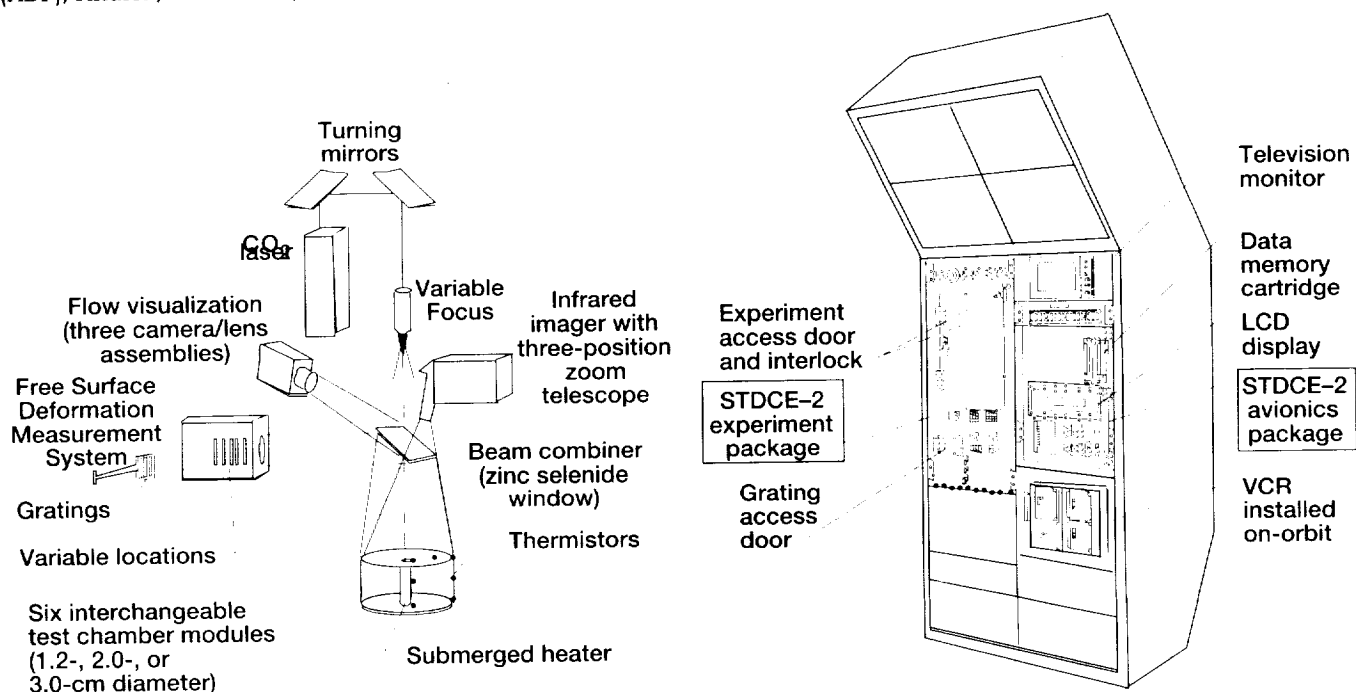
In the production of high-tech crystals, metals, alloys, and ceramics, materials are heated until they form a liquid or vaporize into a gas and then are cooled until they solidify. During this process, unwanted flows in the liquids and gases, created as the material heats and cools, often cause defects that can keep these materials from performing as predicted or designed. Advanced products, such as the crystals used to make computer chips and infrared detectors, require material that is as free from defects as possible.

In microgravity, defects due to buoyancy-driven flows are greatly reduced; however, other fluid motions that are difficult to study on Earth become more prominent in affecting crystal quality. Temperature variations along the surfaces that are not in contact with a container, called free surfaces, create fluid motions called thermocapillary flows. These flows are very difficult to measure accurately in Earth's gravity. Gravity also causes flat surfaces to form on liquids. In microgravity, investigators can study the different surface shapes that occur and how these shapes affect the thermocapillary flows.

The Surface Tension Driven Convection Experiment (STDCE) was designed to study basic fluid mechanics and heat transfer on thermocapillary flows generated by temperature variations along the free surfaces of liquids in microgravity. STDCE first flew on the USML-1 mission in July 1992 and was rebuilt for the USML-2 mission that was launched in October 1995. This was a collaborative project with principal investigators from Case Western Reserve University (CWRU), Professors Simon Ostrach and Yasuhiro Kamotani, along with a team from the NASA Lewis Research Center composed of civil servants and contractors from Aerospace Design & Fabrication, Inc. (ADF), Analex, and NYMA, Inc.

Oscillatory thermocapillary flows were studied under a variety of boundary conditions during the USML-2 mission—a total of 55 tests were conducted. STDCE-2 used 2-centistoke silicone oil and smaller test cells than were used for STDCE-1 (STDCE-2 cell diameters were 1.2, 2.0, and 3.0 cm) in six interchangeable test modules: three with laser heating (constant flux) and three with submerged heaters (constant temperature). New optics permitted laser heating of small zones (0.5 to 6 mm in diameter).

The Free Surface Deformation Measurement System, a single-channel Ronchi method that produced fringes in a video picture, was used to determine small deviations from the flat oil surface with slopes from 5 to 30  $\mu\text{m/ml}$ . Other video data were produced by the three-dimensional flow-visualization system and an infrared imager with an adjustable telescope. Three video pictures (infrared imager,



Left: Optical systems for STDCE-2. Right: STDCE-2 in Spacelab rack.

flow visualization, and free surface deformation) were recorded on a three-deck VCR and were downlinked, with the digital measurement data, to the Payload Operations Control Center at the Marshall Space Flight Center and to the Telescience Support Center at Lewis.

The hardware performed flawlessly, with all systems performing as designed. In addition, the ability to utilize telescience—both real-time telemetry/video and ground commanding—resulted in additional data. It was like “being there” to operate the experiment personally, allowing procedure changes to help in defining the transition point from steady flow to oscillatory flow in real time. Also, CWRU graduate students monitored the experiment at Lewis and provided additional feedback to the team at the Payload Operations Control Center.

In March 1996, results were shared with the USML-2 payload crew, whose hard, effective work made STDCE a success. The preliminary data supported the CWRU thermocapillary flow theories, which predict the importance of a second critical parameter. The transition to oscillatory flow occurred at a much lower point in low gravity and could be observed in the 3-cm test cell. As predicted by the CWRU theory, the transition point increased as the surface shape was made more concave or the aspect ratio decreased. Additional data, taken at heating levels well above the transition point, demonstrated some erratic flow and temperature patterns. Data analysis will be completed next year.

**For more information about STDCE, visit the following sites on the World Wide Web:**

**STDCE main page:** <http://zeta.lerc.nasa.gov/stdce/stdce.htm>

**STDCE-2 paper:** <http://zeta.lerc.nasa.gov/stdce2/iaf10906/iaf1096.htm>

### **Bibliography**

Ostrach, S.; and Kamotani, Y.: Surface Tension Driven Convection Experiment (STDCE). NASA CR-198476, 1996.

Pline, A.D., et al.: Hardware and Performance Summary of the Surface Tension Driven Convection Experiment-2 Aboard the USML-2 Spacelab Mission. IAF-96-J.5.01, presented at the 47th International Astronautical Congress, in Beijing, China, Oct. 7-11, 1996.

**Lewis contacts:** Thomas P. Jacobson, (216) 433-2872, [Thomas.P.Jacobson@lerc.nasa.gov](mailto:Thomas.P.Jacobson@lerc.nasa.gov); Robert L. Zurawski, (216) 433-3932, [Robert.L.Zurawski@lerc.nasa.gov](mailto:Robert.L.Zurawski@lerc.nasa.gov); Alexander D. Pline, (216) 433-6614, [Alexander.D.Pline@lerc.nasa.gov](mailto:Alexander.D.Pline@lerc.nasa.gov); and Nancy Rabel Hall, (216) 433-5643, [Nancy.R.Hall@lerc.nasa.gov](mailto:Nancy.R.Hall@lerc.nasa.gov)

**Authors:** Thomas P. Jacobson and Deborah A. Sedlak

**Headquarters program office:** OLMSA (MSAD)

## Isothermal Dendritic Growth Experiment (IDGE) Is the First United States Microgravity Experiment Controlled From the Principal Investigator's University

The scientific objective of the Isothermal Dendritic Growth Experiment (IDGE) is to test fundamental assumptions about dendritic solidification of molten materials. "Dendrites"—from the ancient Greek word for tree—are tiny branching structures that form inside molten metal alloys when they solidify during manufacturing. The size, shape, and orientation of the dendrites have a major effect on the strength, ductility (ability to be molded or shaped), and usefulness of an alloy. Nearly all cast-metal alloys used in everyday products, such as automobiles and airplanes, are composed of thousands to millions of tiny dendrites.

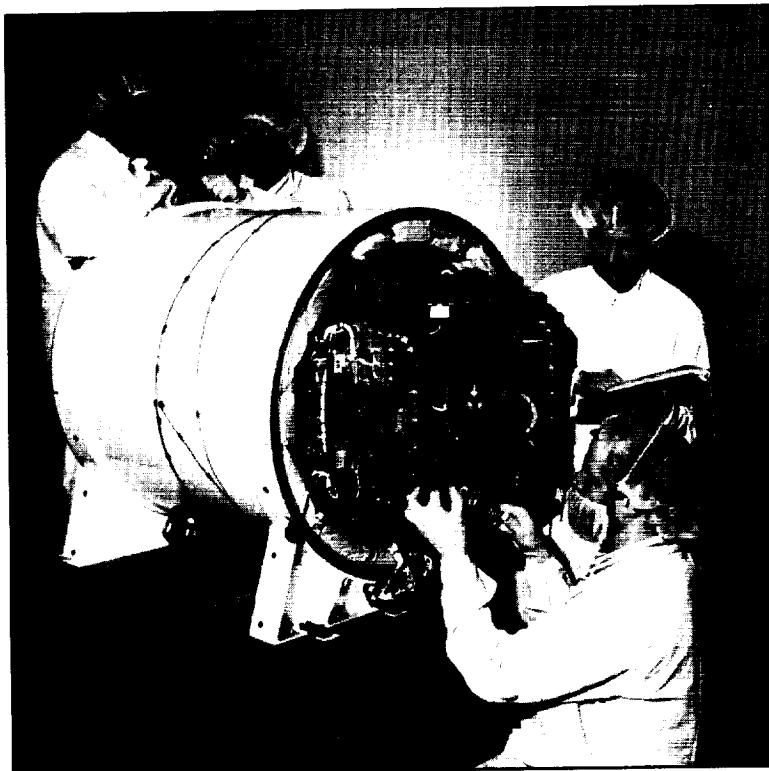
Gravity, present on Earth, causes convection currents in molten alloys that disturb dendritic solidification and make its precise study impossible. In space, the effects of gravity are negated by the orbit of the space shuttle. Consequently, IDGE enabled the acquisition of the first precise data regarding undisturbed dendritic solidification.

IDGE is a microgravity materials science experiment using apparatus that was designed, built, tested, and operated by people from the NASA Lewis

Research Center. The IDGE experiment was conceived by the principal investigator, Professor Martin E. Glicksman from Rensselaer Polytechnic Institute in Troy, New York. This experiment was a team effort of civil servants from the NASA Lewis Research Center, contractors from Aerospace Design & Fabrication, Inc. (ADF), and personnel at Rensselaer.

In February 1996, IDGE was launched for the second time aboard the Space Shuttle Columbia on the STS-75 mission, as part of the Third United States Microgravity Payload (USMP-3) series. This highly successful experiment became the first U.S. microgravity experiment to be commanded and controlled from an investigator's own control center at a university. The commanding of an experiment at an investigator's site is referred to as *telescience*. With the dawn of the Space Station Era, where experiments will be performed over a period of months rather than weeks, this is an important capability, since it is not feasible for investigators to spend that much time at NASA operations centers. In addition, *telescience* opens up new educational opportunities for students at universities to become intimately involved in the space program.

The flight objective was to acquire the large amounts of data required to make definitive determinations of the three-dimensional shape of dendrite tips. Data are currently being analyzed at Rensselaer. In addition, data were acquired that revealed that the residual microgravity environment of space does



*Members of the Lewis-based IDGE team assemble the flight unit. One of the IDGE 35-mm cameras and the Space Acceleration Measurement System (SAMS) sensor head are visible. IDGE is fully operable by remote control from Earth—a feature that contributed to its remarkable success on STS-62 and STS-75.*

not affect the direction and orientation of dendritic growth, as was previously theorized.

More than 120 dendrites were grown over the 15 days of operation—more than double the data returned from the first flight. These dendrites were solidified at over 20 different supercoolings, ranging from about 0.1 to 1.2 K. (Supercooling is the term used to describe the condition in which a dendrite solidifies at a temperature below its normal freezing point.) The data consisted of over 400 photographs and over 800 television images of dendrites solidifying in space, along with associated supercooling, pressure, and acceleration data. Photographs were possible because the test material was transparent succinonitrile, which mimics the behavior of iron when it solidifies.

Dendrite tip radii, tip solidification speed, and volumetric solidification rates have been determined from data gathered in space and on Earth. These were compared with predictions made by theorists over the last 50 years, which are currently used for metal production here on Earth. IDGE results indicate that these theories, although sound in some respects, are flawed in others. Consequently, corrected theories based on IDGE data should result in improved industrial metal production.

IDGE is scheduled to fly for the third time aboard the Space Shuttle Columbia on the STS-87 mission in October 1997. The IDGE apparatus will be modified to grow dendrites from a new sample material. This will allow a definitive test of the universality of both current and future dendritic solidification theories.

**Find out more about IDGE on the World Wide Web:**

<http://www.rpi.edu/locker/56/000756/>

**Lewis contact:** Diane C. Malarik, (216) 433-3203; [Diane.C.Malarik@lerc.nasa.gov](mailto:Diane.C.Malarik@lerc.nasa.gov)

**Author:** Diane C. Malarik

**Headquarters program office:** OLMSA (MSAD)

## Smoldering News From STS-77 Endeavour

The Microgravity Smoldering Combustion (MSC) experiment lifted off aboard the Space Shuttle Endeavour for its second flight in May 1996, as part of the STS-77 mission. This experiment is part of a series of studies focused on the smolder characteristics of porous combustible materials in a microgravity environment. Smoldering is a nonflaming form of combustion that takes place in the interior of combustible materials. Common examples of smoldering are nonflaming embers, charcoal briquettes, and cigarettes.

The objective of this study is to provide a better understanding of the controlling mechanisms of smoldering in microgravity and normal Earth gravity (1g). As with other forms of combustion, gravity affects the availability of air and transport of heat, and therefore, the rate of combustion. The results of the microgravity experiments will be compared with identical ones carried out in 1g. In addition, they will be used to verify present theories of smolder combustion and will provide new insights into the process of smoldering combustion, enhancing our fundamental understanding of this frequently encountered combustion process and guiding improvements in fire safety practices.

Two smoldering combustion tests with polyurethane foam were successfully accomplished during the STS-77 mission. The tests investigated smoldering combustion in a quiescent (no-flow) enriched oxygen environment, and in an air environment with a 2-mm/sec airflow through the fuel sample. The primary data from the tests are the ignition characteristics, spread rate, smolder reaction temperature, and products of combustion (solid and gas).

On both the first mission on STS-69 and the second mission on STS-77, a smolder front propagated the length of the forced-flow samples, with the spread rate between the corresponding upward and downward 1g smolder rates. Neither of the quiescent cases propagated combustion (the first case was due in part to a problem with the experiment electronics). These results show a dramatic difference from the normal gravity results, where

smolder propagation is very rapid and complete for both of these conditions.

The experiment was conceived by Prof. A. Carlos Fernandez-Pello at the University of California-Berkeley. The MSC hardware was designed and built at the NASA Lewis Research Center by a team of civil servants and contractors from NYMA, Inc., and Aerospace Design & Fabrication, Inc. (ADF). The hardware consists of two sealed aluminum combustion chambers (each being a half a cylinder). The chambers hold the MSC test section, data acquisition electronics, power distribution electronics, and instrumentation. The hardware is fitted into a 5-ft<sup>3</sup> Get-Away-Special (GAS) canister that is mounted in the shuttle cargo bay. The test section (shown in the figure) consists of a quartz cylinder that contains the polyurethane foam sample and an igniter. This igniter, which is an electrically heated wire sandwiched between two porous ceramic disks, is mounted in contact with the end of the foam sample. An array of 12 thermocouples placed axially and radially along the foam sample provide temperature histories, which are used to determine the rate of smolder propagation, and the characteristics of the reaction.

### Find out more about MSC on the World Wide Web:

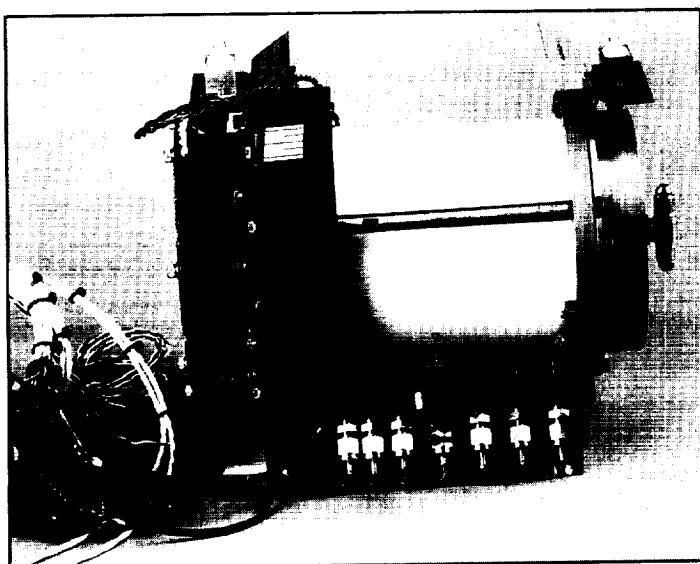
<http://einstein.lerc.nasa.gov/dlurban/msc/mscbrochure.html>

### Lewis contact:

John M. Koudelka, (216) 433-2852,  
John.Koudelka@lerc.nasa.gov

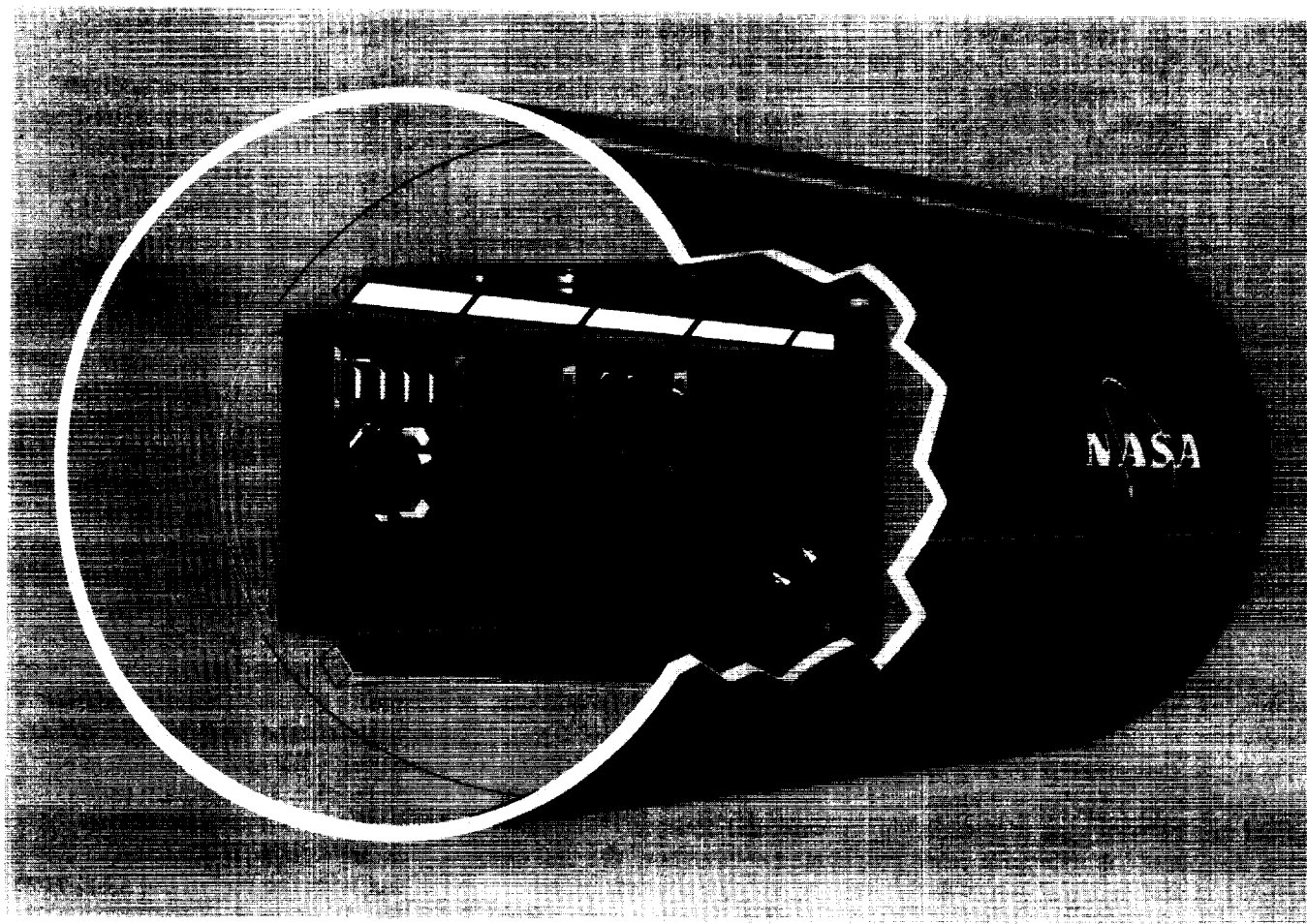
**Authors:** John M. Koudelka and  
Prof. A. Carlos Fernandez-Pello

**Headquarters program office:** OLMSA  
(MSAD)



*Microgravity Smoldering Combustion fuel sample and test section assembly.*

## Facilitating Science—The International Space Station Fluids and Combustion Facility



*International Space Station Fluids and Combustion Facility.*

Scientists in many fields would like to perform experiments on the International Space Station (ISS) to take advantage of the unique environment of microgravity (which is the near-absence of gravity). The ISS will provide the opportunity for scientists to perform microgravity tests over much longer time periods than previously available on the space shuttle—months rather than hours or days—providing more data that could lead to new discoveries. Many of the experiments on ISS will be conducted through the use of new microgravity science facilities. A microgravity science facility is a complete system of on-orbit and ground (on-Earth) hardware, software, operations, and plans that have been optimized to perform sustained microgravity research in one or two scientific disciplines.

The facility concept includes hardware that remains on-orbit (because of its general usefulness) and a small amount of unique hardware that is developed for each principal investigator. Such unique hardware customizes the facility to perform a given principal investigator's experiment effectively. Many facilities are planned for the ISS to accommodate scientists' needs.

While the quality and quantity of scientific data are being improved, per-experiment costs will be lowered relative to other ways of performing such experiments.

The NASA Lewis Research Center is developing a Fluids and Combustion Facility (FCF) to perform microgravity fluids and combustion experiments on the ISS. The FCF will be the lowest cost, most resource efficient approach to performing fluid physics and combustion science experiments on the ISS. Experiments performed in the FCF will be 3 to 9 times less

expensive than similar Spacelab experiments. Moreover, use of key ISS resources, such as upmass, power, cooling, and astronaut crew time, will be cut by the same factor.

Over its life cycle, FCF experimentation will be no more expensive than that on current low-cost carriers, such as sounding rockets, Get-Away-Special (GAS) canisters, and shuttle middeck lockers. However, it will be far more effective. In spite of its low cost, FCF will be more capable than the most sophisticated and expensive microgravity fluids or combustion hardware yet flown, and these capabilities will be broad and adaptable. Thus, other disciplines (besides fluids and combustion) may also be accommodated.

As the result of FCF concept development, many innovations have been invented at Lewis by a team of Lewis civil servants and contractors from Analex, Aerospace Design & Fabrication, Inc. (ADF), NYMA, Inc., and Sundstrand. The electrical power control units (EPCU) developed are considered "next-generation" in comparison to other power units designed for the ISS. Standardized drawers that house the principal-investor-specific hardware were designed that provide 50 percent more mass-carrying capacity than other ISS packaging concepts; a more rugged construction with greater containment of noise, vibration, electromagnetic interference, and thermal effects; and a reconfiguration setup that does not require any tools and saves astronaut time. Various structures and systems make use of commercial off-the-shelf hardware, saving time and cost. The most advanced video capability of any ISS facility will be available on the FCF; for example, video frame rates from still pictures to as high as 1000 frames/sec. Computers will be designed to allow for evolutionary upgrades to keep the data systems state-of-the-art. Bandwidths to send data back to Earth have been reduced through onboard data processing. A unique four-sided optics bench for fluids experiments was invented that will provide investigators real-time response to experiment data as it occurs, save astronaut time, and save hardware development cost and time. Digital imaging, laser lighting, onboard image analysis and compression, and other imaging innovations to support advanced technology will all be utilized on the FCF. The imaging system will use *Desert Storm* advanced technology to automatically track and zoom-in on moving "targets" of scientific interest, improving resolution and reducing communication bandwidth requirements.

The FCF will provide true telescience to investigators at NASA Centers and remote sites (such as the investigators' universities), and only the future can tell what scientific breakthroughs will result.

**For more information, visit the FCF homepage on the World Wide Web:**

<http://zeta.lerc.nasa.gov/fcfwww/index.htm>

**Lewis contact:** Edward A. Winsa, (216) 433-2861, [ewinsa@popserve.lerc.nasa.gov](mailto:ewinsa@popserve.lerc.nasa.gov)

**Authors:** Edward A. Winsa, Kathleen E. Schubert, and Deborah A. Sedlak

**Headquarters program office:** OLMSA (MSAD)

# Burning Candles in the Microgravity of Space

The Candle Flames in Microgravity (CFM) experiment was designed to study how long candle flames can be sustained in microgravity, how the flames behave prior to extinction, and how two closely spaced candle flames behave. The scientists hope that one day the results will help resolve age-old questions regarding the effects of gravity on certain types of flames (low momentum diffusion flames, or candle flames) and their ability to burn without the presence of gravity. This information will provide a better understanding of fires on spacecraft and could lead to advances in fire detection and extinction techniques.

Microgravity provides a nonconvecting, purely diffusive environment for this experiment. Under Earth's gravity, buoyant convection develops when hot, less-dense combustion products rise. The resulting flow draws oxygen into the flame and carries the combustion products (carbon dioxide and water vapor) away from the flame. This flow is the dominant transport mechanism in the flame. In microgravity, however, the process is not the same; there is no buoyant convection. Instead, the transport of combustion products and oxygen occurs by the much slower process of molecular diffusion that results when there is a concentration gradient in the candle flame zone. When there is a high concentration of combustion products and a low concentration of oxygen close to the flame, and there is a low concentration of combustion products and a high concentration of oxygen further away from the flame, the combustion products migrate away from the flame and oxygen migrates towards the flame. The diffusive transport rates in microgravity are much lower than the transport rates due to natural convection in normal gravity.

The CFM experiment was developed at the NASA Lewis Research Center to be used with the Microgravity Glovebox Facility in the Priroda Module of the Russian Space Station Mir. The experiment was launched aboard a Russian Proton rocket on April 23, 1996.

Astronaut Shannon Lucid began CFM operations aboard Mir on July 1. Dr. Lucid said that the data collected point to long-term flame survivability (which was anticipated by the investigators, but commonly postulated in the literature to be impossible) and show evidence of spontaneous and prolonged flame oscillations near extinction. Testing on Mir, which included 79 candle burns, was completed on July 26. The experiment hardware performed successfully, and data were returned to the investigators in October 1996, including photo-

graphs, video, temperature data, oxygen concentration data, gas samples, and radiometric data.

This project was designed, built, and tested by a team of civil servants from NASA Lewis, the contractors from Aerospace Design & Fabrication, Inc. (ADF), and university personnel. The principal investigator is Daniel Dietrich of Lewis and the co-investigators are Howard Ross of Lewis and Professor James T'ien of Case Western Reserve University. The project was managed by David Frate of Lewis.

**For more information, visit CFM on the World Wide Web:** <http://zeta.lerc.nasa.gov/expr/cfm.htm>

**Lewis contact:**

David T. Frate, (216) 433-8329,  
[david.frate@lerc.nasa.gov](mailto:david.frate@lerc.nasa.gov)

**Authors:** David T. Frate and  
Daniel L. Dietrich

**Headquarters program office:** OLMSA  
(MSAD)



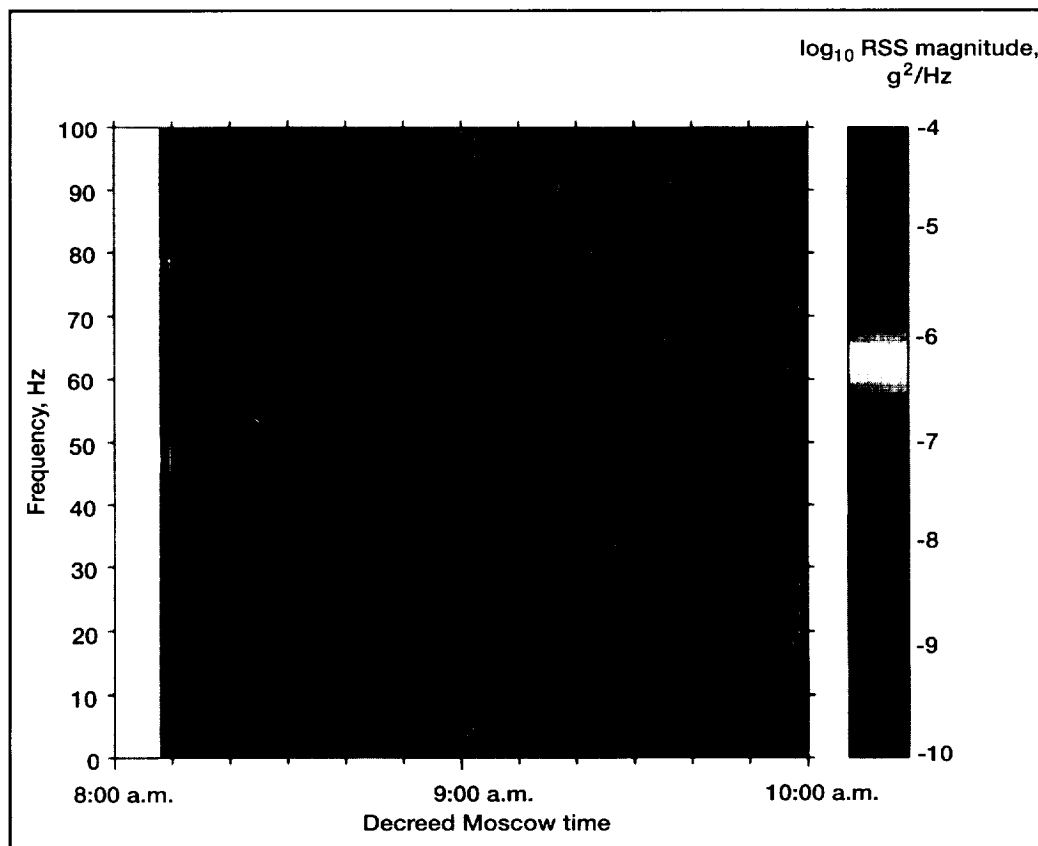
*David Frate (right) and Russian trainer Mikhail Bogdonov (left) train U.S. astronaut Shannon Lucid on the Candle Flames in Microgravity experiment at the Gagarin Cosmonaut Training Center in Star City, Russia.*



## Measured Success—The Microgravity Measurement and Analysis Project

The microgravity environment created by an orbiting spacecraft allows people to float effortlessly and events to occur as if there were no gravity present. Microgravity is not the absence of gravity, but is a state where the effects of gravity have been greatly reduced. It makes possible experiments that are normally limited by gravitational effects on Earth. However, whereas gravity is greatly reduced during orbit, vibrations and motions of the shuttle can affect experiment results. For example, the shuttle vibrates, accelerates, and decelerates when thrusters are fired, experiments are operated, and the crew performs various operations and exercises, among many other things. In microgravity, even minute forces can affect experiments: therefore, investigators need to know the precise strength of the gravitational levels and vibrations affecting their experiments to interpret results correctly and to develop an understanding of the effects caused by these forces.

The Microgravity Measurement and Analysis Project (MMA) at the NASA Lewis Research Center was established to provide a single source for measuring the microgravity environment on various orbiting spacecraft, providing support for scientists, and microgravity environment data. As part of this project, the Space Acceleration Measurement System (SAMS) and the Orbital Acceleration Research Experiment (OARE) have supported 15 shuttle missions. In addition, one



*Spectrogram produced by the Principal Investigator Microgravity Services project with data from the Space Acceleration Measurement System (SAMS) on the Mir Space Station in late 1995. Docking of the Orbiter Atlantis (on the STS-74 mission) to Mir on November 15, 1995, is indicated by the sudden appearance of a 17-Hz pair of vertical lines at about 8:47 a.m. Before docking, activity on Mir was relatively quiet, whereas after the docking many events occurred, such as leak checks and hatches opening and closing. (Root sum of squares, RSS.)*

SAMS unit has been operated on Russia's Mir Space Station since September 1994.

SAMS and OARE data were prepared and distributed to users after each mission. Specialized analyses were performed by the Principal Investigator Microgravity Services project in real time during missions, as well as before and after the missions for principal investigators. Reports summarizing the microgravity environment of the mission were prepared by the Principal Investigator Microgravity Services project and distributed to users after each shuttle mission and periodically from Mir operations.

Future microgravity science research on the International Space Station will be supported by a project called SAMS-II that will measure the microgravity environment near each science experiment and deliver the data to the investigators at their operations center on the ground.

Other future microgravity science experiments that require an extremely low level of microgravity may fly on a free flyer (unmanned) carrier. SAMS-FF, another MMAP project under development, will measure and record the microgravity environment encountered on such a satellite during a typical 2-week mission.

For both International Space Station and free flyer operations, the Principal Investigator Microgravity Services project will continue to provide scientists with data interpretation and summary reports.

**For more information, see our MMAP homepage on the World Wide Web:**

<http://www.lerc.nasa.gov/WWW/MMAP/>

### **Bibliography**

Rogers, M.J.B.; and DeLombard, R.: Summary Report of Mission Acceleration Measurements for STS-73. NASA TM-107269, 1996.

Ryaboukha, S., et al.: Further Analysis of the Microgravity Environment on Mir Space Station During Mir-16. NASA TM-107239, 1996.

DeLombard, R.: Compendium of Information for Interpreting the Microgravity Environment of the Orbiter Spacecraft. NASA TM-107032, 1996.

DeLombard, R., et al.: SAMS Acceleration Measurements on Mir From June to November 1995. NASA TM-107312, 1996.

**Lewis contact:** Pete Vrotsos, (216) 433-3560, [pvrotsos@lerc.nasa.gov](mailto:pvrotsos@lerc.nasa.gov)

**Authors:** Richard DeLombard and Deborah A. Sedlak

**Headquarters program office:** OLMSA (MSAD)

# Power Systems

## Mir Cooperative Solar Array

The Mir Cooperative Solar Array (MCSA), produced jointly by the United States and Russia, was deployed on the Mir Russian space station on May 25, 1996. The MCSA is a photovoltaic electrical power system that can generate up to 6 kW. The power from the MCSA is needed to extend Mir's lifetime and to support experiments conducted there by visiting U.S. astronauts. The MCSA was brought to Mir via the Space Shuttle Atlantis on the STS-74 mission, launched November 12, 1995.

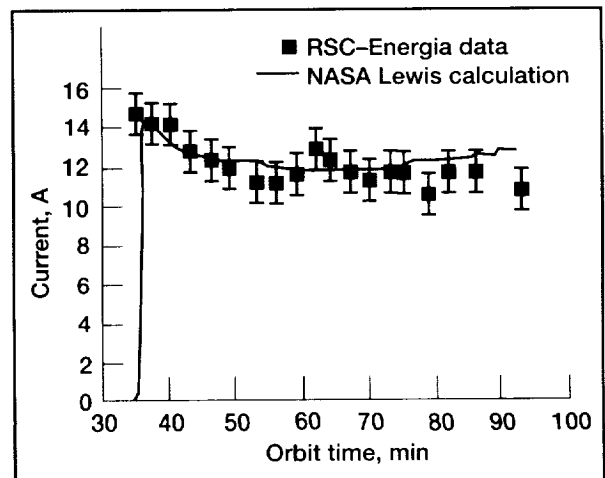
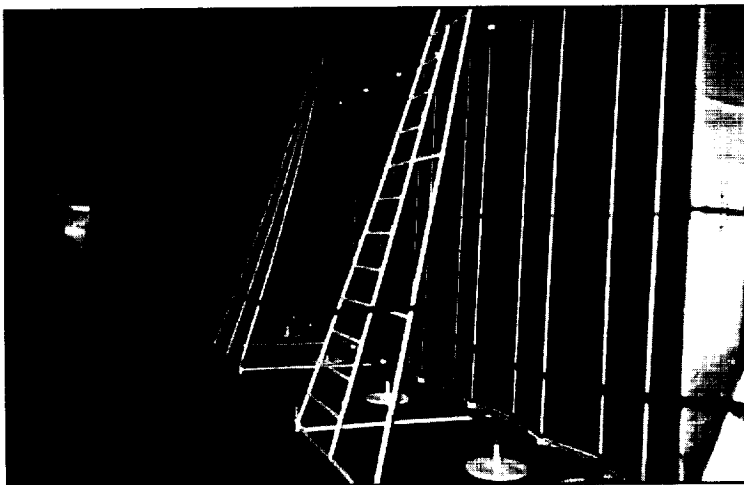
This cooperative venture combined the best technology of both countries: the United States provided high-efficiency, lightweight photovoltaic panel modules, whereas Russia provided the array structure and deployment mechanism. Technology developed in the Space Station Freedom Program, and now being used in the International Space Station, was used to develop MCSA's photovoltaic panel. Performance data obtained from MCSA operation on Mir will help engineers better understand the performance of the photovoltaic panel modules in orbit. This information will be used to more accurately predict the performance of the International Space Station solar arrays. Managed by the NASA Lewis Research Center for NASA's International Space Station Program Office in Houston, Texas, the MCSA Project was completed on time and under budget despite a very aggressive schedule.

The MCSA (see the photo) has 42 panels hinged like an accordion and is about 2.7-m (9-ft) wide and 18-m (59-ft) long when deployed. Each panel consists of two photovoltaic panel modules (PPM's) mounted side by side. A PPM is a collection of 80 large-area silicon solar cells in a 5- by 16-cell matrix. The entire solar array contains 6720 solar cells, which are mounted on a flexible film and wired in series via a flat printed copper circuit. Each PPM is secured to a Russian-built support structure at fastening points on the corner of each cell. To fit the PPM into existing frames, we shortened the row of cells at each end of the PPM by 0.5 cm (0.2 in.). A support ring

was placed on the back of each cell to increase the stiffness of the flexible solar cell substrate and help reduce the acceleration, or g-loads, experienced during their launch on the space shuttle.

To assure that no problems would occur when the U.S. PPM was integrated with the Russian composite frame, we performed an accelerated-life thermal cycle test. For this test, a U.S.-made 15-solar-cell coupon was integrated with a Russian-made structure frame to form a "minipanel" that was subjected to 24,000 temperature cycles alternating between 80 and -100 °C. At about 90 min per orbit, 24,000 such cycles correspond to a 4-year life.

Taking advantage of NASA Lewis' unique expertise in space photovoltaic power systems, a team from Lewis performed a "dark" electrical test on the MCSA's flight unit (ref. 1) while it was stowed and awaiting launch in the Space Station Processing Facility at the NASA Kennedy Space Center. The primary



Left: MCSA deployment test in Russia. Right: Comparison of NASA Lewis' electrical performance prediction with on-orbit measurements made by RSC-Energia for a segment of the MCSA known as "GS10."

objective of the test was to assess the overall electrical performance condition of the flight array, after handling and shipment from Russia to Kennedy, without having to deploy and illuminate it (hence, the "dark" test designation). The successful application of the dark test technique indicated that the MCSA's condition was nominal and was ready for launch.

The MCSA has been producing electrical power since its deployment on Space Station Mir. Currently, approximately half of the MCSA (38 of 84 PPM's) is providing electrical power to Mir. In June 1996, the Russians obtained estimates on a number of operating MCSA segments; they provided the preliminary MCSA performance data to NASA Lewis. This preliminary data compares well with Lewis' state-of-the-art space power computer model (see the graph).

The Russians will measure the MCSA's performance again in the fall of 1996, after the remainder of the MCSA is connected, and once more in the fall of 1997. In this way, the performance of the MCSA over time in the space environment can be measured and compared with analytical models. The models can then be refined on the basis of actual on-orbit data from a large space vehicle.

**Find out more about the Mir Cooperative Solar Array on the World Wide Web:**  
<http://godzilla.lerc.nasa.gov/ppo/csa.html>

#### **References**

Kerslake, T.W.; Scheiman, D.A.; and Hoffman, D.J.: Dark Forward Electrical Testing on the Mir Cooperative Solar Array. Research & Technology 1996. NASA TM-107350, 1997, pp. 157-158. Available on the WWW: <http://www.lerc.nasa.gov/RT1996/6000/6920k.htm>

**Lewis contacts:** Mike Skor, (216) 433-2286, [MSkor@lerc.nasa.gov](mailto:MSkor@lerc.nasa.gov) or [MSkor@lerc.nasa.gov](mailto:MSkor@lerc.nasa.gov), and Dave J. Hoffman, (216) 433-2445, [DJHoffman@lerc.nasa.gov](mailto:DJHoffman@lerc.nasa.gov)

**Authors:** Mike Skor and Dave J. Hoffman

**Headquarters program office:** OSF

## Advanced Power System Analysis Capabilities

As a continuing effort to assist in the design and characterization of space power systems, the NASA Lewis Research Center's Power and Propulsion Office developed a powerful computerized analysis tool called System Power Analysis for Capability Evaluation (SPACE). This year, SPACE was used extensively in analyzing detailed operational timelines for the International Space Station (ISS) program.

SPACE was developed to analyze the performance of space-based photovoltaic power systems such as that being developed for the ISS. It is a highly integrated tool that combines numerous factors in a single analysis, providing a comprehensive assessment of the power system's capability. Factors particularly critical to the ISS include the orientation of the solar arrays toward the Sun and the shadowing of the arrays by other portions of the station (refs. 1 and 2).

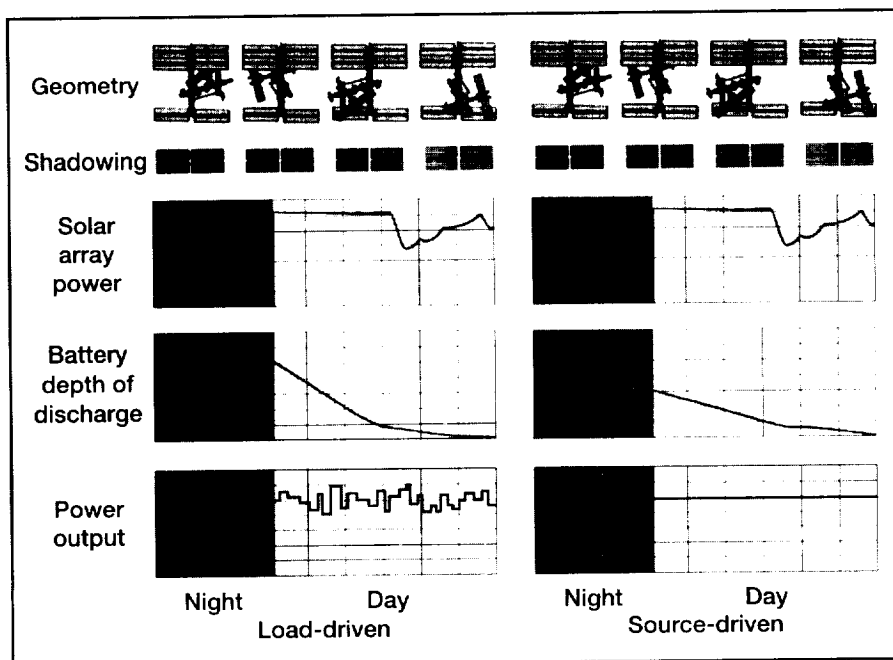
The figure below shows two types of analyses that can be performed with SPACE. A source-driven analysis (refs. 3 and 4) determines the highest power level that can be sustained over an orbit. This information is critical during the design phase for sizing system components and determining power available for experiments. A load-driven analysis (ref. 5) assesses the ability of the system to supply a specific time-varying power demand. This type of analysis is important in the operational phase for validating the interworkings of various systems.

The figure on the facing page, an example of the analysis currently being performed for the ISS program, shows part of a 2-week assembly mission. During this period (around shuttle separation), the orientation of the station is constantly changing. The dark bars show when the station is shadowed by the Earth. The three curves show the power demand, solar array power, and battery depth of discharge for one representative power channel. Battery depth of discharge is a measure of the energy removed from the batteries in comparison to their energy capacity. During the example analysis period, the solar array power drops, requiring more energy to be drawn from the batteries, resulting in a higher depth of discharge.

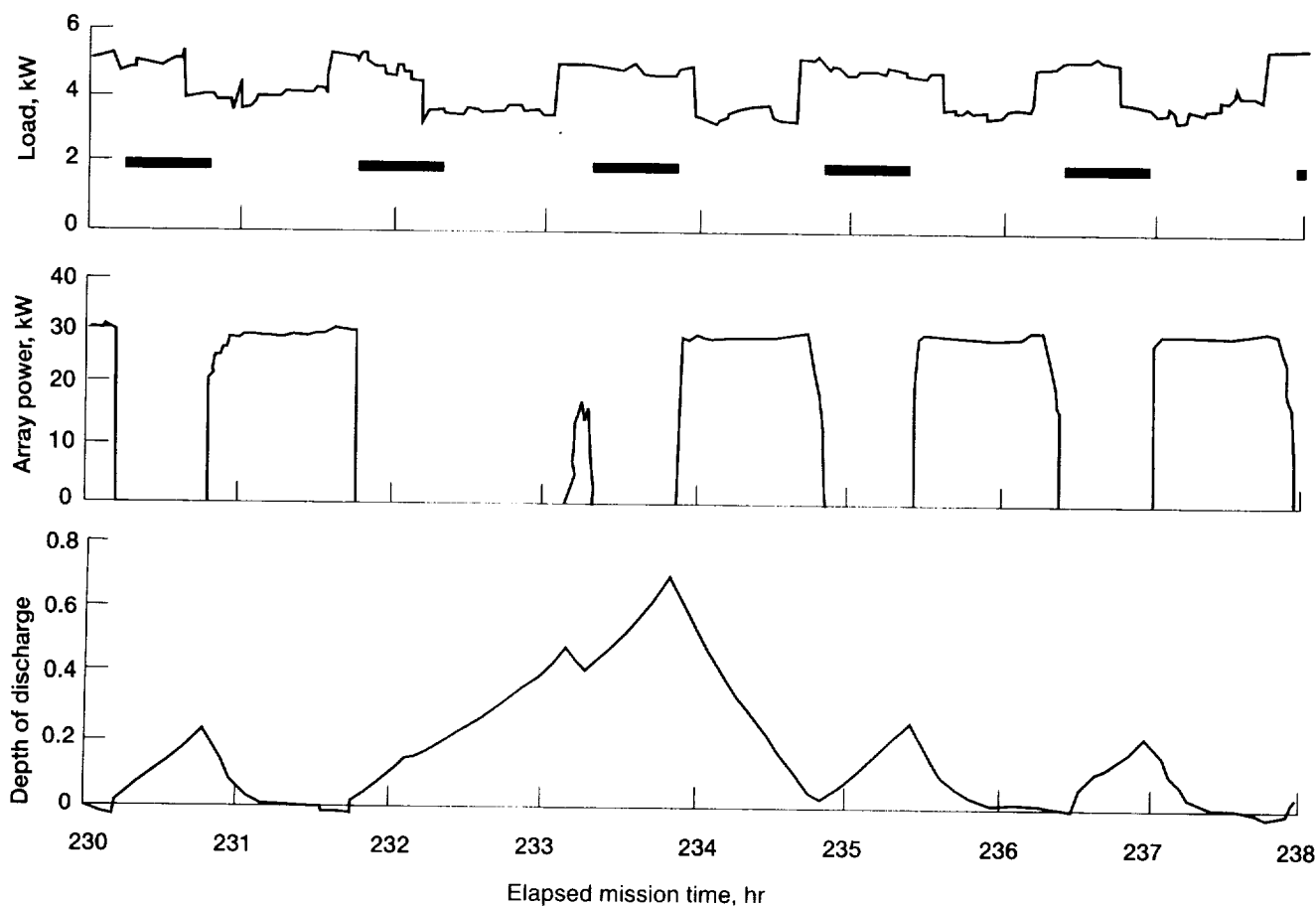
In this example, the depth of discharge reached a relatively high level. However, the mission was still viable, since no hardware limits were exceeded, and the batteries were not fully drained. However, this may not be true for all assessments. The model might detect hardware limit violations or predict that the battery depth of discharge reaches 100 percent.

At 100-percent depth of discharge, the battery is completely drained, and an unacceptable "blackout" occurs. Simpler power system models that do not account for all the factors that affect the power system would not be able to accurately predict these conditions.

Although its primary use has been to support the ISS program, SPACE has many other potential uses. It could be enhanced to analyze other power systems, including space- and ground-based systems. It could also be used as a basis for "smart" power systems with fault and failure prediction, diagnosis, and recovery tools or as an addition to other satellite analysis software. SPACE represents the synthesis of over 10 years of power system analysis expertise and software development, validation, and verification. It performs detailed, integrated performance analysis of power systems to determine optimum power capability and operation.



Two types of power system analysis capabilities.



*Typical analysis output for load-following case. Top: Load demand. Middle: Available array power. Bottom: Battery depth of discharge.*

**Find out more about this research on the World Wide Web:**

**Power and Propulsion Office:** <http://godzilla.lerc.nasa.gov/ppo/ppo.html>

**SPACE model:** <http://godzilla.lerc.nasa.gov/ppo/space.html>

**References**

1. Fincannon, J.: Analysis of Shadowing Effects on Spacecraft Power Systems. NASA TM-106994, 1995.
2. Fincannon, J.: Analysis of Shadowing Effects on Mir Photovoltaic and Solar Dynamic Power Systems. NASA TM-106940, 1995.
3. Hojnicky, J., et al.: Space Station Freedom Electrical Performance Model. NASA TM-106395, 1993.
4. Kerslake, T.W., et al.: System Performance Predictions for Space Station Freedom's Electrical Power System. NASA TM-106396, 1993.
5. Fincannon, J., et al.: Load-Following Power Timeline Analyses for the International Space Station. NASA TM-107263, 1996.

**Lewis contact:** Jeffrey S. Hojnicky, (216) 433-5393, [jhojnicky@lerc.nasa.gov](mailto:jhojnicky@lerc.nasa.gov)

**Authors:** Jeffrey S. Hojnicky and James Fincannon

**Headquarters program office:** OSF (Space Station)

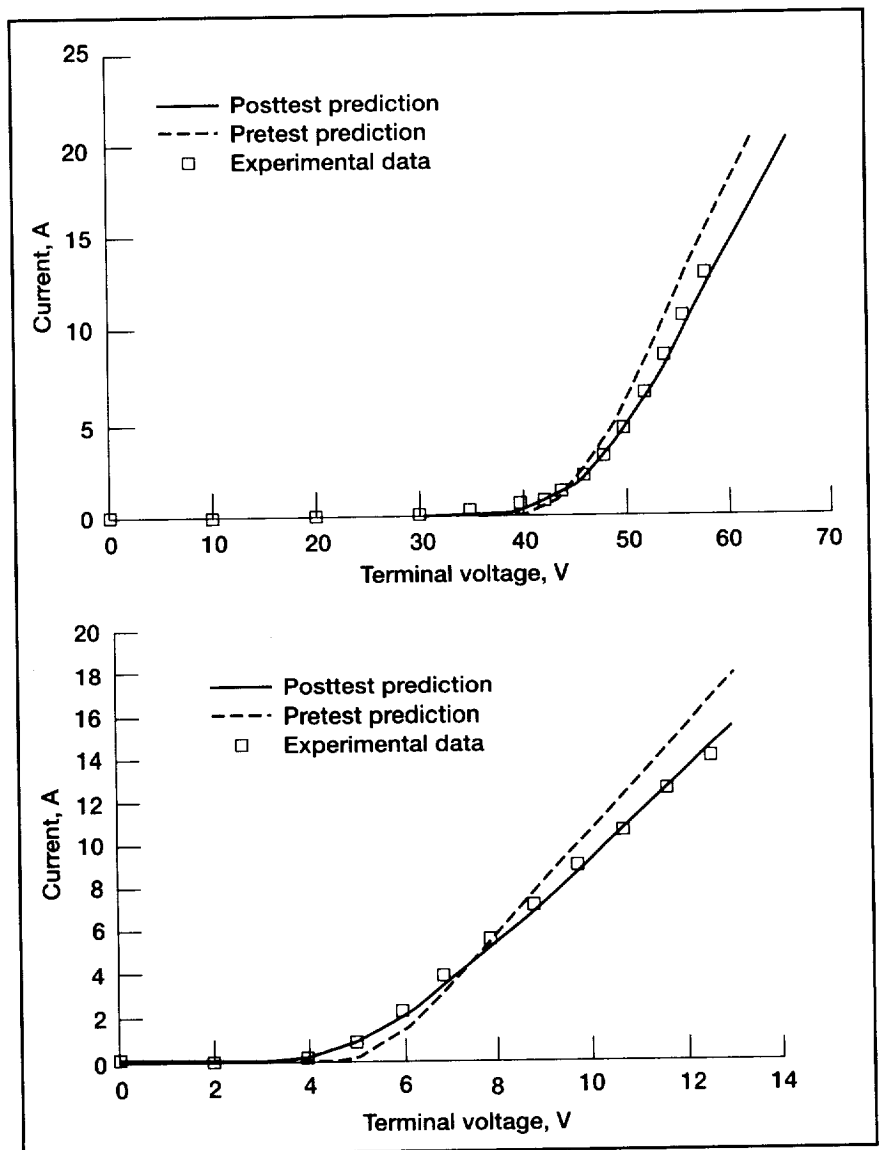
## Dark Forward Electrical Testing of the Mir Cooperative Solar Array

During July 11 to 13, 1995, a team from the NASA Lewis Research Center performed dark forward electrical testing on the Mir Cooperative Solar Array (MCSA) flight unit in the Space Station Processing Facility at the NASA Kennedy Space Center. The MCSA was jointly designed and built by the United States and Russia to supply approximately 6 kW of electricity to the Russian Mir space station (ref. 1). The primary objective of testing was to assess the overall electrical performance of the flight array after handling and shipment from Russia to NASA Kennedy. This objective was achieved without the high cost and difficulties of deploying and illuminating the MCSA as is usually done with large-area solar arrays. The data obtained provided U.S. and Russian program managers with a high level of confidence in the MCSA electrical performance prior to the array's launch on shuttle mission STS-74 in November 1995 and its deployment on Mir in May 1996.

NASA Lewis engineers developed the test hardware, test software, test procedures, and analytical software to support MCSA dark testing. The hardware and software were first verified by testing at Lewis with solar array strings available in-house. At Kennedy, MCSA dark forward testing was accomplished by applying a voltage and measuring the current. The resulting diode characteristic, or current-voltage curve, was then analyzed and compared with the nominal response expected. This procedure was repeated for each of the 12 MCSA generators. A generator consists of either 6 or 8 parallel circuits, each containing 80 solar cells connected in series. The dark forward current-voltage response of the solar cell bypass diodes was measured by reversing the polarity of the power supply. (There is one bypass diode for each group of 10 series-connected solar cells.)

The top and bottom graphs show measured and predicted dark-forward current-voltage curves for generator 7 solar cells and bypass diodes, respectively. These results, which are typical for all MCSA generators, show that pre-test predictions as well as refined post-test predictions compare very well with

the experimental data. This indicates that no substantial handling and shipment damage was sustained by the MCSA. Major differences in the current-voltage curves, if present, could have been attributed to various types of array hardware damage.



*Solar cell dark forward and bypass diode forward current-voltage response for generator 7 of the Mir Cooperative Solar Array. Top: Solar cell dark forward response. Bottom: Bypass diode forward response.*

Subsequently, we translated the measured MCSA dark current-voltage response into illuminated current-voltage response by factoring in solar cell series resistance and the voltage drop of test equipment and cabling. This enabled management to be fully aware, prior to launch, of the anticipated on-orbit MCSA electrical capability.

Because of the low cost of dark electrical testing and its significant mitigation of risks, NASA Lewis is supporting the International Space Station Program Office feasibility assessment of dark testing the International Space Station port-side preintegrated truss segment (P6) solar arrays.

**Find out more about the Mir Cooperative Solar Array on the World Wide Web:**  
<http://godzilla.lerc.nasa.gov/ppo/csa.html>

#### Reference

1. Skor, M.; and Hoffman, D.J.: Mir Cooperative Solar Array. Research & Technology 1996. NASA TM-107350, 1997, pp. 153-154. Available on the WWW: <http://www.lerc.nasa.gov/RT1996/6000/6910s.htm>

**Lewis contacts:** Thomas W. Kerslake, (216) 433-5373, [Thomas.W.Kerslake@lerc.nasa.gov](mailto:Thomas.W.Kerslake@lerc.nasa.gov); David A. Scheiman, (216) 433-6756, [David.A.Scheiman@lerc.nasa.gov](mailto:David.A.Scheiman@lerc.nasa.gov); Dave J. Hoffman, (216) 433-2445, [DJ.Hoffman@lerc.nasa.gov](mailto:DJ.Hoffman@lerc.nasa.gov)

**Authors:** Thomas W. Kerslake, David A. Scheiman, and Dave J. Hoffman  
**Headquarters program office:** OSF

## Stability of Large Direct-Current Power Systems That Use Switching Converters and the Application of Switching Converters to the International Space Station

As direct-current space power systems continue to grow in size, switching power converters are playing an ever larger role in power conditioning and control. When a large direct-current system that uses power converters of this type is being designed, special attention must be placed on the electrical stability of the system and of the individual loads on the system. In the design of the electric power system of the International Space Station (ISS), NASA and its contractor team led by the Boeing Defense & Space Group placed a great deal of emphasis on designing for system and load stability. To achieve this goal, the team expended considerable effort deriving a clear concept on defining system stability in both a general sense and specifically with respect to the space station.

The ISS power system presents numerous challenges with respect to system stability—such as high power, complex sources, and undefined loads. These were further complicated by source and load components being designed in parallel by three major subcontractors (the Boeing Company, Rocketdyne Division/Rockwell International, and McDonnell Douglas Corporation) with interfaces to both sources and loads being designed in different countries (Russia, Japan, Canada, Europe, and others). These issues, coupled with the program goal of limiting costs, have proven to be a significant challenge to the project.

As a result, the program derived an impedance specification approach for system stability. This approach is based on the significant relationship between source and load impedances and the effect of this relationship on system stability. The impedance specification approach is limited in its applicability by the theoretical and practical limits on component designs as presented by each system segment. Therefore, the overall approach to system stability implemented by the ISS program consists of specific hardware requirements coupled with extensive system analysis and hardware testing. The requirements for hardware integrators are that the system phase and gain margins must be 30° and 30 db, respectively.



In addition, wherever practical hardware elements will be tested together, end-to-end stability and functionality must be ensured. Following this approach, the ISS program plans to begin construction of the world's largest orbiting power system in 1997.

The impedance specification approach for system stability was accomplished as a result of cooperative work of the International Space Station program team, which consists of the NASA Lewis Research Center, the Boeing Company, and Rocketdyne Division/Rockwell International. In addition, major contributions were provided by the Virginia Polytechnic Institute and State University working under a grant to NASA Lewis.

**Find out more about this research on the World Wide Web:**

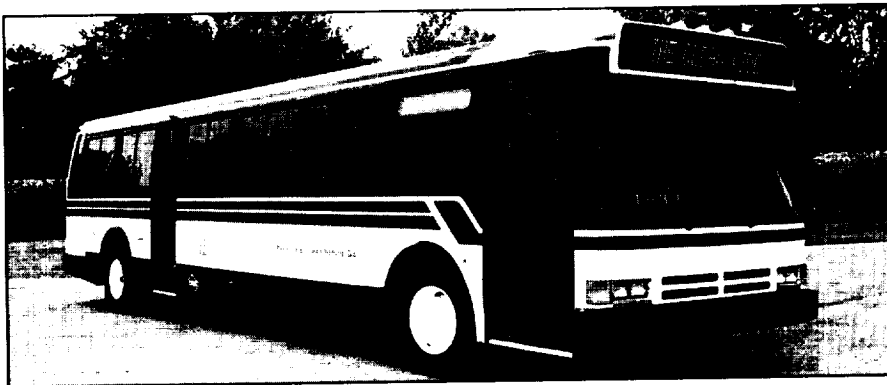
<http://godzilla.lerc.nasa.gov/ppo/ppo.html>

**Lewis contact:** Bruce A. Manners, (216) 433-8341, [Bruce.A.Manners@lerc.nasa.gov](mailto:Bruce.A.Manners@lerc.nasa.gov)

**Authors:** Bruce A. Manners (NASA Lewis), E.W. Gholdston (Rocketdyne Division/Rockwell International), K. Karimi (The Boeing Company), and F.C. Lee, J. Rajagopalan, and Y. Panov (Virginia Polytechnic Institute and State University)

**Headquarters program office:** OSF

## Hybrid Turbine Electric Vehicle

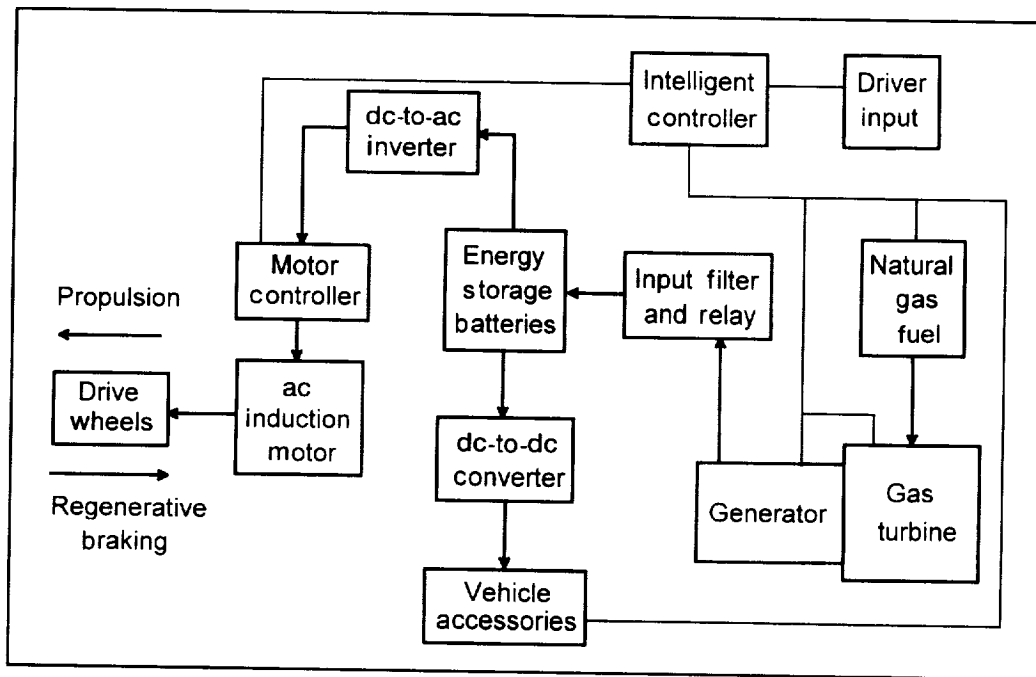


Hybrid electric power trains may revolutionize today's ground passenger vehicles by significantly improving fuel economy and decreasing emissions. The NASA Lewis Research Center is working with industry, universities, and Government to develop and demonstrate a hybrid electric vehicle. Our partners include Bowling Green State University, the Cleveland Regional Transit Authority, Lincoln Electric Motor Division, the State of Ohio's Department of Development, and Teledyne Ryan Aeronautical.

The vehicle will be a heavy class urban transit bus offering double the fuel economy of today's buses and emissions that are reduced to 1/10th of the Environmental Protection Agency's standards. At the heart of the vehicle's drive train is a natural-gas-fueled engine. Initially, a small automotive engine will be tested as a baseline. This will be followed by the introduction of an advanced gas turbine developed from an aircraft jet engine. The

engine turns a high-speed generator, producing electricity. Power from both the generator and an onboard energy storage system is then provided to a variable-speed electric motor attached to the rear drive axle. An intelligent power-control system determines the most efficient operation of the engine and energy storage system.

Hybrid electric power trains offer several advantages for vehicle performance and emissions. First, the load seen by the engine is decoupled from the short-term power requirements of the vehicle. With constant load, the engine can be designed to operate nearly continuously at its highest efficiency point. In addition, the size of the engine can be reduced significantly in most vehicles to the long-term average value of power. The electric drive train provides additional benefits by eliminating losses in the fluid couplings of conventional automatic transmissions. Finally,



Power and control diagram.

electric drive trains can recover energy as the vehicle brakes, further improving fuel economy. Gas turbines offer the additional benefits of being lightweight, using multiple fuels, and having high reliability and very low emissions.

In addition to initiating and coordinating the overall project, the NASA Lewis Research Center is performing much of the system engineering for the vehicle's electrical power system. A computer program called Hybrid Electric Vehicle Analysis (HEVA) has been developed to calculate vehicle performance and power requirements. Lewis is also developing the power control software and integrating an advanced capacitor system for energy storage. In addition, Lewis combustion test facilities are being used to support the gas turbine engine development. Initial operation of the prototype vehicle is scheduled for the First Quarter of 1997.

Potential markets for this vehicle include regional transit authorities in both the Northeast and California, who have already shown a great interest in fuel-efficient, low-emission transit buses. In addition to city transit buses, this technology has applications for many other ground vehicles, including automobiles, delivery vehicles, municipal waste trucks, school buses, and shuttle buses. Manufacturing methods developed for these markets will also return benefits to the aerospace industry through lower cost engines for small aircraft.

**Find out more about the Hybrid Turbine Electric Vehicle on the World Wide**

**Web:** <http://godzilla.lerc.nasa.gov/ppo/busprj.html>

**Lewis contact:** Dr. Larry A. Viterna, (216) 433-5398, [viterna@lerc.nasa.gov](mailto:viterna@lerc.nasa.gov),

**Author:** Dr. Larry A. Viterna

**Headquarters program office:** OSF (Space Station)

## Computational Support

### Integrated Digital Video and Experimental Data Analysis for Microgravity Combustion Experiment

The purpose of the Diffusive and Radiative Transport in Fires (DARTFire) Project is to study various mechanisms of energy transport in the ignition and growth of flames in microgravity. This sounding rocket experiment incorporates two multispectral video cameras, two 8-mm video recorders, and several temperature and pressure probes that record information on two separate flames, burning under different oxygen concentrations and flow rates. Mirrors allow each camera to view side-by-side images of both flames.

In support of this Space Experiments Division (SED) project, the Computer Services Division (CSD) at the NASA Lewis Research Center developed several programs and techniques for digitizing and analyzing video images, integrating the video with other experimental data, and providing postflight analysis of engineering mission performance.

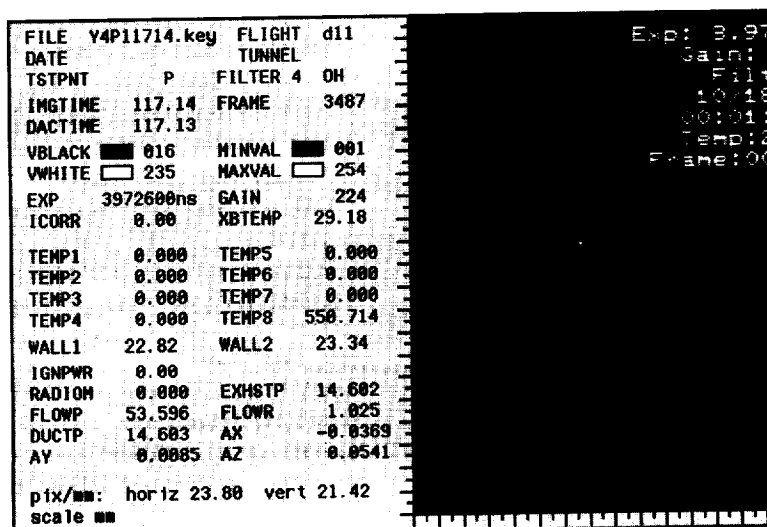
Both onboard video cameras are black-and-white, with a rotating, six-element filter wheel that provides images of the flames for various spectral ranges. One of the cameras operates in the visible-light spectrum, and its filter wheel is synchronized with the standard video frame rate (29.97 frames/sec); exposure time is automatically varied for each frame in response to flame brightness. Filter and exposure data are encoded in barcodes superimposed on each image. The other camera operates in the infrared spectrum at a nonstandard video rate (60 half-frame images/sec);

its filter wheel yields only 1 image/filter/sec; filter identity is again bar-coded on the image. The onboard data acquisition control system (DACS) sampled pressure, temperature, and status information 20 times/sec. This information was stored in 1 MB of RAM and transferred to a diskette after the flight.

All video from the 6-min experiment was digitized to an industry-standard format that generates 8-bit 720- by 486-pixel images with a broadcast-quality digital video animation system that allows real-time sampling and storage of 50 sec of video at a time. Each experiment generates over 10 GB of data, which are made available to the researchers online.

To meet the mission's imaging requirements, programs were developed for

- Analyzing video levels and background noise, and barcoding black-and-white levels for accurate image intensity calibrations
- Tagging each image with filter and frame-accurate timing information by using bar-codes, the camera-specific frame rate, the video frame count, and DACS-generated synchronization marks on the video
- Annotating each image with synchronized, calibrated DACS data and x- and y-axis millimeter scales (see the figure)



Video image showing annotations for DACS data and x- and y-axis millimeter scales.

- Correcting the intensity of the autoexposure images to provide consistent assessment of flame intensity and size
- Generating exposure-corrected, white-balanced full-color animation of the flames from red, green, blue images and neutral-density images filtered from the visible-light camera

Programs were also developed to graphically analyze DACS information for postflight analysis of system performance at the launch site.

The video animation system used to digitize the video was also used to animate preprocessed and postprocessed image data. Techniques are currently being developed to use the Computer Services Division's 1935- by 1120-pixel High Definition Television (HDTV) scientific animation testbed to

visualize flame shape and motion simultaneously for all filter images with no loss of resolution.

**Lewis contacts:**

Dr. Jay G. Horowitz (CSD), (216) 433-5194, Jay.G.Horowitz@lerc.nasa.gov; and Jeffrey A. Jones (SED), (216) 433-2870, Jeffrey.A.Jones@lerc.nasa.gov

**Author:** Dr. Jay G. Horowitz

**Headquarters program office:** OA (HPCCO)

## Automated Status Notification System

NASA Lewis Research Center's Automated Status Notification System (ASNS) was born out of need. To prevent "hacker attacks," Lewis' telephone system needed to monitor communications activities 24 hr a day, 7 days a week. With decreasing staff resources, this continuous monitoring had to be automated. By utilizing existing communications hardware, a UNIX workstation, and NAWK (a pattern scanning and processing language), we implemented a continuous monitoring system. The system is based on statistical analysis of our telephone call records (about 18 months worth), comprising mean call levels (traffic patterns) based on calls per time of day, calls per day of the week, and type of calls—Federal Telephone Service (FTS), Direct Out Dial, and Direct Inward Dialed calls. From these statistics, we programmed thresholds for alert levels into the system software.

Now that this ad hoc tool monitors our telephone activity, if telephone traffic in the Fujitsu 9600 exceeds the call traffic threshold set in the monitoring program, pocket pagers are called and special codes are sent that indicate the type of traffic and the number of calls exceeding the threshold. If the person who receives the page deems it necessary, they have a response team investigate the anomaly, and if warranted, they shut down the calling path.

ASNS runs 24 hr a day, 7 days a week, and it reports every hour that the threshold for the previous hour is exceeded. Thus, we know, in real time, what our telephones systems are doing, and we can react as necessary.

We have extended the same concept to our data networks. We currently monitor 15 critical network devices on a 24-hr, 7-day basis. Every 5 min, each device is queried; if less than 90 percent of the packets are transmitted, a pager notification is sent and logged. Since we developed this process, other devices that do similar types of monitoring have become commercially available.

### Resources Needed for ASNS

- Access to a Unix workstation attached to the network
- Minimal programming and statistical knowledge of normal operations
- Dial-out capabilities (pagers and modems)
- Pocket pager (can be local or nationwide)

### Applications of ASNS

- Continuous monitoring of voice and data networks
- Alerting during nonworking hours of significant events pertaining to the health of networks
- Automated repair calls during nonworking hours
- Greater visibility of high-profile resources
- Continuous monitoring of subsystems attached to networks
- High-profile monitoring of network devices undergoing upgrades and repairs
- SNMP (Simple Network Management Protocol) E-mail alerts of significant network connectivity events or loss of connectivity
- 24-hr, 7-day notification of hacker attempts on voice mail and telephone systems
- Facility and environmental monitoring (using some additional PC cards)
- Intrusion alerting and security for network communications rooms.

**Lewis contact:**

Joseph P. McMillen, (216) 433-5199, Joseph.P.McMillen@lerc.nasa.gov

**Author:** Joseph P. McMillen

**Headquarters program office:** OA

# Engineering Support

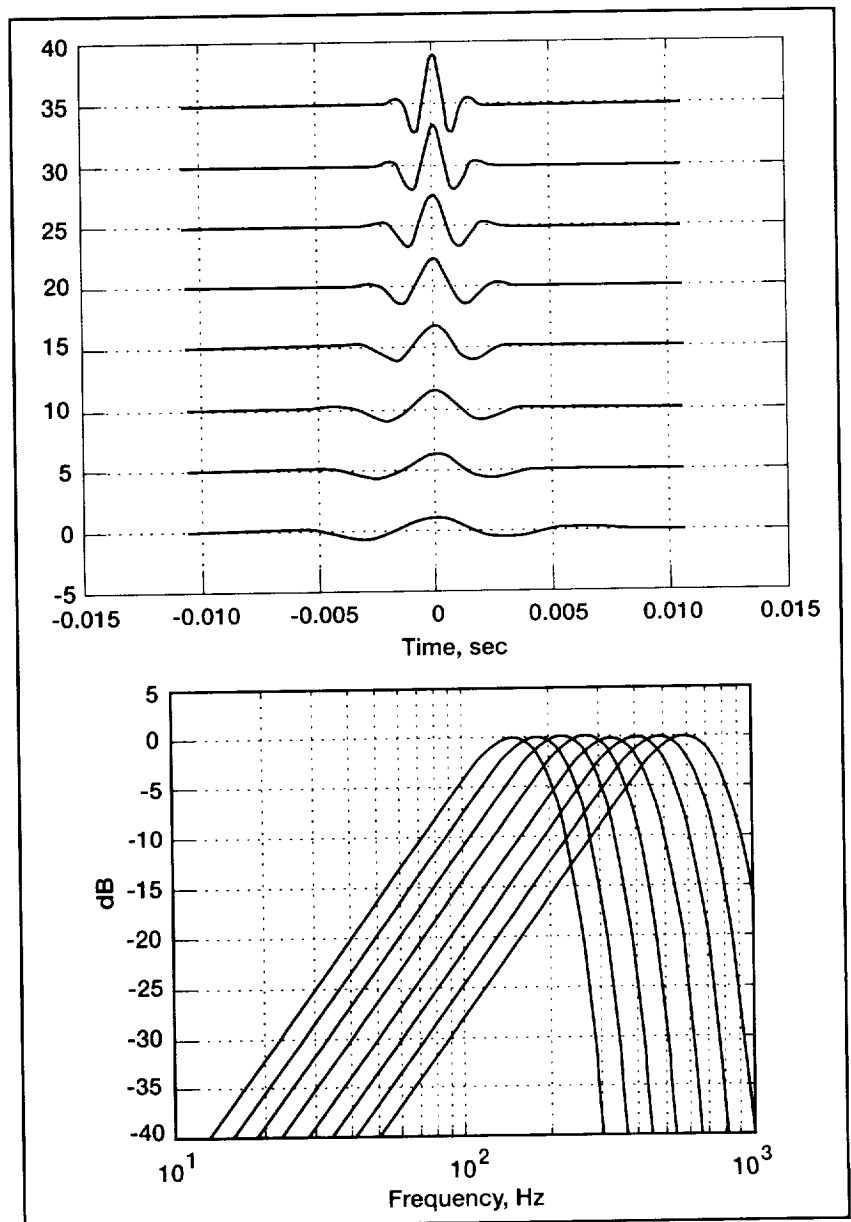
## Wavelet Methods Developed to Detect and Control Compressor Stall

A "wavelet" is, by definition, an amplitude-varying, short waveform with a finite bandwidth (e.g., that shown in the figures below). Naturally, wavelets are more effective than the sinusoids of Fourier analysis for matching and reconstructing signal features. In wavelet transformation and inversion (ref. 1), all transient or periodic data features (as in compressor-inlet pressures) can be detected and reconstructed by stretching or contracting a single wavelet to generate the matching building blocks. Consequently, wavelet analysis provides many flexible and effective ways to reduce noise and extract signals which surpass classical techniques—making it very attractive for data analysis, modeling, and active control of stall and surge in high-speed turbojet compressors. Therefore, fast and practical wavelet methods are being developed in-house at the NASA Lewis Research Center to assist in these tasks. This includes establishing user-friendly links between some fundamental wavelet analysis ideas and the classical theories (or practices) of system identification, data analysis, and processing (ref. 2).

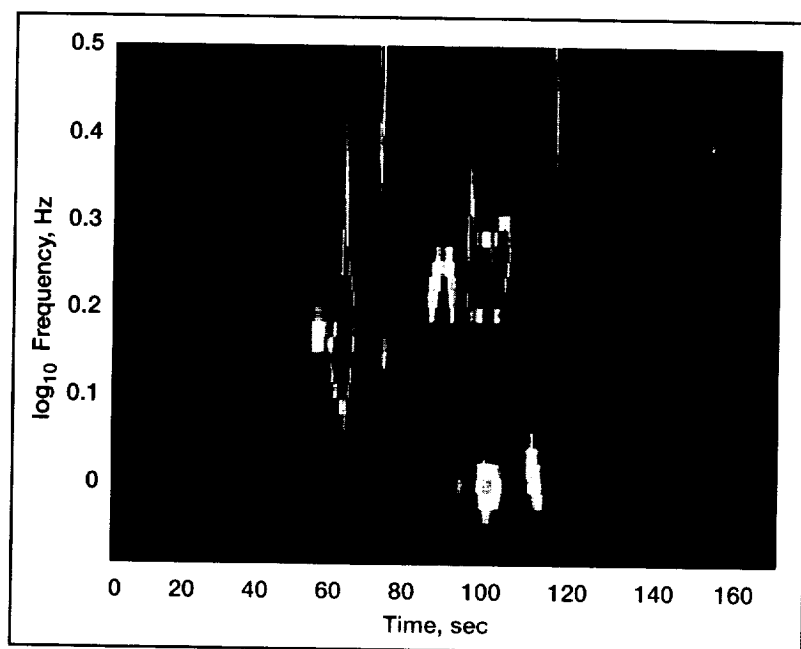
NASA Lewis' Fast Wavelet Transform/Reconstruction software—which features a unique wavelet algorithm that uses compact, harmonic-like waveforms of arbitrarily sharp frequency bands—can reconstruct signal components very quickly. This double feat was not possible in earlier wavelet literature. The figure on the facing page illustrates the use of mouse-clicks in this software to reconstruct signal components of any region on the wavelet scalogram.

Via this ongoing wavelet research, Lewis has made substantial progress recently in the detection and control of compressor stall and surge. In particular, a wavelet-based, real-time processing scheme for inlet-pressures in high-speed compressors has been designed. This scheme can detect precursors and provide reliable feedback for active control of stall and surge (ref. 3). The stall-inducing power estimated by this algorithm using eight shroud-mounted and nearly equally

spaced pressure sensors in front of the first stage showed clearly the incipient instabilities in compressor flows for more than 300 rotor revolutions before any stall or surge event. This is demonstrated in



Top: Filter bank of "compact harmonic wavelets." Bottom: Power spectra of the wavelets shown in top figure.



*One region of the scalogram is isolated by a polygon (dashed lines) for signal reconstruction.*

reference 3 for both the rig (AlliedSignal) and engine tests (NASA Lewis) of the axi-centrifugal turbojet T55-L-712. This scheme is being implemented on fast digital signal processing boards for the T55 Program to demonstrate in 1998 an active control technique for improving compressor performance.

The wavelet-enhanced pressure data (ref. 3) also highlight both the underdamped linear dynamics and the overdamped nonlinear dynamics of the prestall rotating waves and their interactions with low-frequency axial waves. Thus, this wavelet processing scheme is a valuable tool for empirical estimations of both linear model parameters and unmodeled, nonlinear uncertainties of compressor dynamics. These modeling data are important for robust control design.

## References

1. Rioul, O.; and Vetterli, M.: Wavelets and Signal Processing. IEEE Signal Processing Magazine, vol. 8, Oct. 1991, pp. 14-38.
2. Le, D.K.: Multiscale System Identification and Estimation. Advanced Signal Processing Algorithms, Proceedings of SPIE-The International Society for Optical Engineering, F.T. Luk, ed., vol. 2563, 1995, pp. 470-481.
3. Le, D.K.; Owen A.K.; and Mattern D.L.: Multiscale Analysis of Stall Inception and Instabilities in an Axi-Centrifugal Turboshift Engine. AIAA Paper 96-3174, 1996.

**Lewis contacts:** Dr. Dzu K. Le (Electronics and Control Systems Division), (216) 433-5640, scdle@ariel.lerc.nasa.gov; and Dr. Albert K. Owen (Army Vehicle Technology Center), (216) 433-5895, fsako@lerc.nasa.gov

**Author:** Dr. Dzu K. Le

**Headquarters program office:** OA

# Manipulating Liquids With Acoustic Radiation Pressure

At the NASA Lewis Research Center, high-intensity ultrasound is being used to create acoustic radiation pressure (ARP) on objects in liquids. It is also being used to create liquid currents or jets called acoustic streaming.

## Lewis contact:

Richard C. Oefftering, (216) 433-2285,  
Richard.C.Oefftering@lerc.nasa.gov

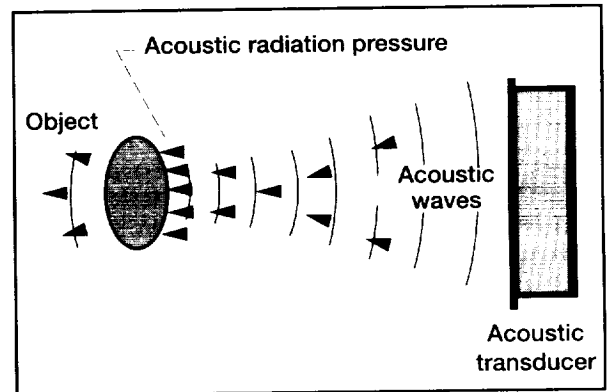
**Author:** Richard C. Oefftering

NASA's interest in ARP includes remote-control agitation of liquid systems in space, such as in liquid space experiments and liquid propellant tanks. It can be used to eject or deploy droplets for droplet physics or droplet combustion experiments. It can also be used to manipulate bubbles, drops, and surfaces suspended in liquid experiments and propellant systems.

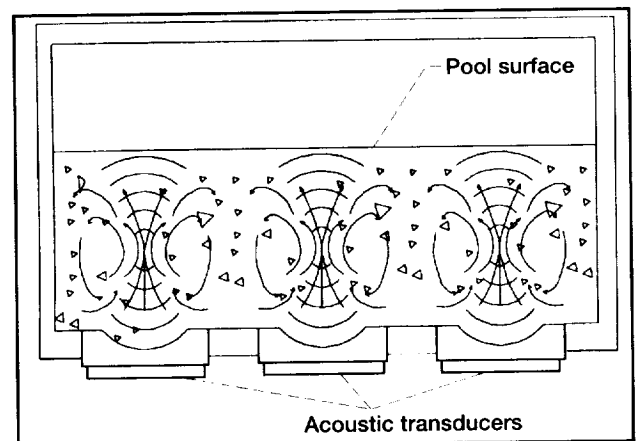
ARP agitation employs focus transducers to create agitating streams. The acoustic streaming can be used to suspend particles, mix liquids, and obliterate nonuniformities in temperature or concentration. Unlike conventional approaches, ARP agitation is nonintrusive, so there are no mechanical propellers, shafts, seals, or motors. Furthermore, it can be used to agitate sealed containers without external plumbing. Agitation can even be done without disturbing a liquid pool's surface.

By introducing high-intensity sound waves into a syringe needle, one can use ARP to dispense a droplet on demand. This increases the reliability and repeatability for liquid-dispensing devices. The speed of the separation can be tightly controlled for space experiments. The device also can enhance the dispensing of coatings, adhesives, and solder pastes for the electronics industry.

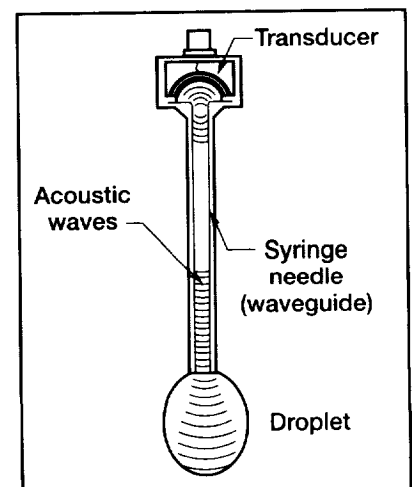
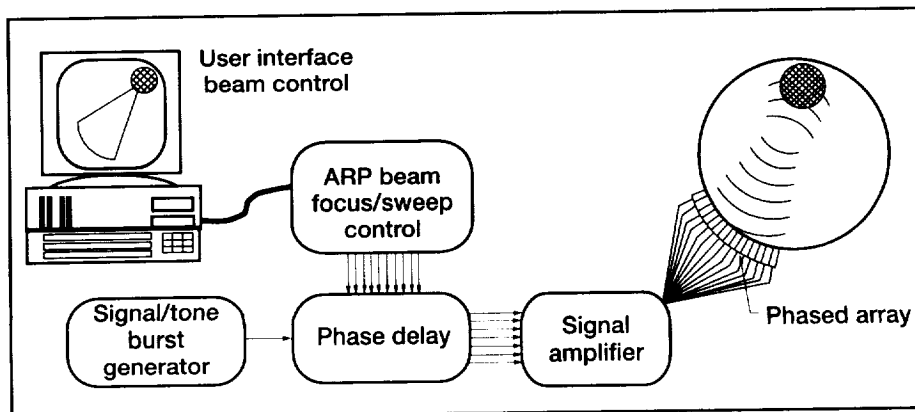
The ultimate in flexibility is to use a high-power acoustic phased array to generate and direct ARP. The sound beam direction and focus is controlled electronically. An interactive, real-time system lets experimenters manipulate objects anywhere in a test volume. Because the acoustic phased array can emulate simpler acoustic devices, it can serve as a general purpose system fulfilling multiple roles. This approach can also be used to control the location of bubbles and voids in spacecraft propellant tanks. In addition, ARP has potential uses in medicine, such as in repositioning detached retinas.



*Acoustic streaming.*



*ARP agitation with focused acoustic transducers.*



*Left: ARP liquid manipulation by acoustic phased arrays. Right: ARP droplet deployment.*

# Nonlinear Dynamic Behavior in the Cassini Spacecraft Modal Survey

In October 1997, the 6 $\frac{1}{2}$ -ton robotic spacecraft, Cassini, will lift off from Cape Canaveral atop a Titan IV B rocket, beginning a 7-year journey to Saturn. Upon completion of that voyage, Cassini will send the Huygens probe into the atmosphere of Saturn's largest moon, Titan. Cassini will then spend years studying Saturn's vast realm of rings, icy moons, and magnetic fields.

The size and complexity of this endeavor mandates the involvement of many organizations. The Jet Propulsion Laboratory (JPL) manages the project for NASA and is responsible for the spacecraft design, development, and assembly. The NASA Lewis Research Center is the launch system integrator. As is typical for such a spacecraft, a test-verified finite element model is required for loads analysis. JPL had responsibility for the Cassini modal survey and the development of the spacecraft test-verified finite element model. Test verification is a complex and sometimes subjective process. Because of this, NASA Lewis independently verified and validated the Cassini spacecraft modal survey.

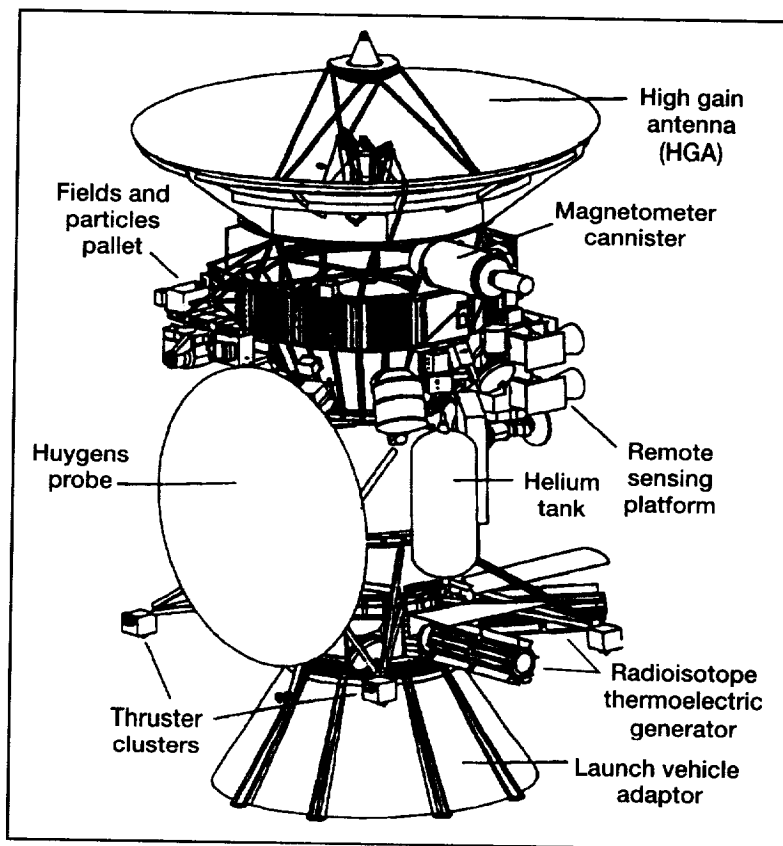
The Cassini modal survey was conducted in August 1995. Although the test was successful by standard measures, the Cassini spacecraft exhibited significant localized nonlinear behavior during testing. Loads predicted with worst-case assumptions would have necessitated a potentially unnecessary and expensive requalification of the Huygens probe, and perhaps even an unnecessary partial redesign.

The nonlinearities discovered during the Cassini modal survey manifested themselves primarily in the longitudinal mode of the Huygens probe. It had been previously known that a 15-percent reduction in the frequency of this mode would cause accelerations that exceeded the design specifications of the Huygens probe by almost 50 percent. This sensitivity occurs because the probe longitudinal mode tunes into the Titan IV B stage-two ignition-forcing event, which is primarily longitudinal.

Because of this extreme sensitivity to a potential drop in the frequency of the probe bounce mode, it was quite distressing to find that, as force levels increased in the August 1995 modal survey, the frequency for this mode decreased and kept decreasing until the load limits set for the modal survey were reached. At approximately 10 percent of the flight limit load, the frequency of this mode had decreased 5 percent, with no sign of the frequency drop leveling off. Planning began for

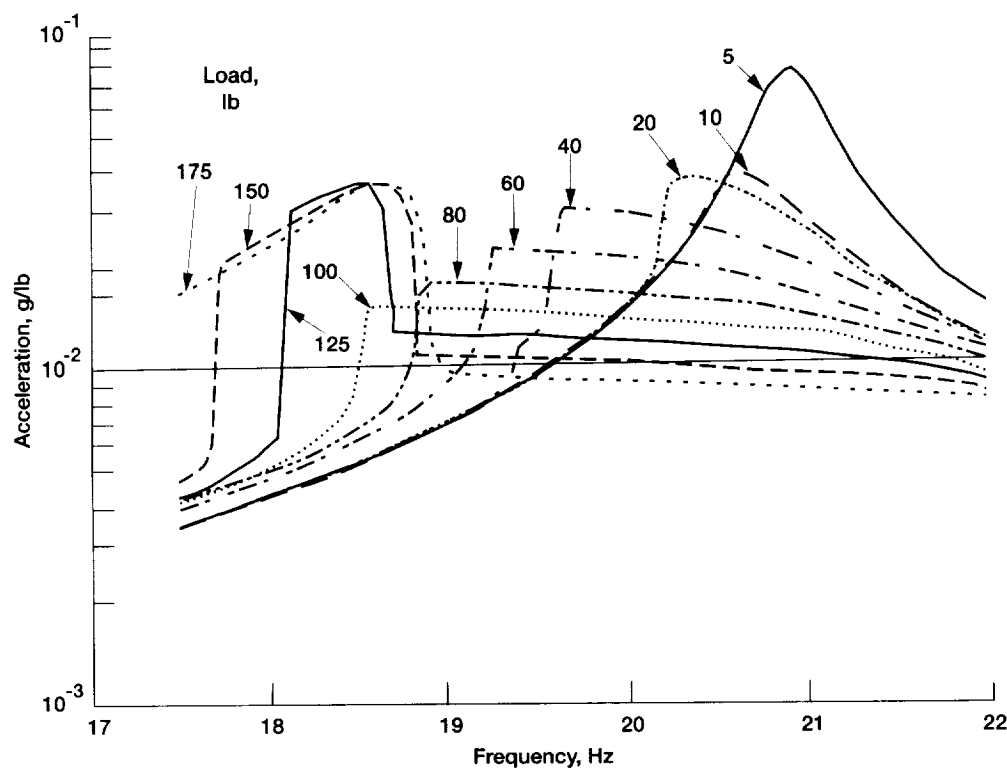
retesting the Cassini test article, this time taking the probe to almost 50 percent of the load limit levels, determining behavior at high load levels. Nonlinear dynamic analysis had shown that offset gapping was the cause of the probe nonlinearity. At higher load levels, this type of nonlinearity moderates.

In January of 1996, a high-force-level dynamic test of the Cassini spacecraft was performed. This test targeted the probe bounce mode exclusively. We discovered that, indeed, at higher load levels the probe longitudinal mode linearized somewhat (its frequency stopped decreasing) and that the nonlinear dynamic model with offset gapping matched the test data very well.



*Cassini spacecraft.*





*Nonlinear response of the probe. If this were a linear system, all of the curves would lie on the 5-lb line. The distortion of the curves is caused by the nonlinearity of the offset gapping.*

A linearized representation of this mode was included in the JPL-test-verified dynamic model. Subsequently, Lewis certification of the dynamic model was completed successfully.

#### References

1. Smith; and Peng: Cassini Spacecraft Modal Survey Report, JPL D-13300, Jan. 22, 1996.
2. Smith; and Coleman: Cassini Spacecraft Model Correlation Report, JPL D-13610, June 15, 1996.
3. Yunis; and Carney: Cassini: Spacecraft Independent Verification and Validation Final Modal Correlation Report. NASA Lewis Research Center, July 31, 1996.
4. Carney; Yunis; Smith; and Peng: Nonlinear Dynamic Behavior in the Cassini Spacecraft Modal Survey. 15<sup>th</sup> International Modal Analysis Conference, Feb. 1997.

**Lewis contact:** Kelly S. Carney, (216) 433-2386, Kelly.S.Carney@lerc.nasa.gov

**Author:** Kelly S. Carney

**Headquarters program office:** OA

# Aircraft Anti-Icing and Deicing Protection Using Ultrasound Technology

Ultrasonic devices are powerful enough to melt plastics, boil water, break up kidney stones, and weld metal. Research is currently being performed by the Engineering Directorate at the NASA Lewis Research Center to obtain an understanding of how ultrasonic sound waves can be used to protect aircraft from airframe icing. Three types of ultrasonic sound waves are being investigated: longitudinal waves, transverse waves, and surface waves. To date, ice has been removed from the surface of a 0.032-in.-thick aluminum sheet. In the application of these waveforms, a cost-effective, energy-efficient, lightweight ice-protection system is the end goal.

This technology could also be used in the automotive or marine industry, or any other industry that wants to break the adhesive bond between two materials. Some other uses for the ultrasonic system would include

- Ice buildup protection for automobile windshields
- Ice buildup protection for marine vessels
- Removal of frost from refrigerators and freezers
- Removal of mussels and other ocean life from marine vessels
- Elimination of material buildup in crucibles

**Video footage of ice being removed from an aluminum plate through the use of ultrasonic stress waves can be found on the World Wide Web:**

[http://www.lerc.nasa.gov/WWW/Photo\\_Lab/scigallery.html](http://www.lerc.nasa.gov/WWW/Photo_Lab/scigallery.html)

**Some still photos of icing research are also available on the web:**

<http://zeno.lerc.nasa.gov/htmls/general/archive.html>

**Lewis contact:** Damian R. Ludwiczak, (216) 433-2383,  
[damian.ludwiczak@lerc.nasa.gov](mailto:damian.ludwiczak@lerc.nasa.gov)

**Author:** Damian R. Ludwiczak

**Headquarters program office:** OA

# Lewis Research Academy

## Turbomachinery Flows Modeled

Last year, researchers at the NASA Lewis Research Center used the average passage code APNASA to complete the largest three-dimensional simulation of a multistage axial flow compressor to date. Consisting of 29 blade rows, the configuration is typical of those found in aeroengines today. The simulation, which was executed on the High Performance Computing and Communications (HPCC) Program IBM SP2 parallel computer located at the NASA Ames Research Center, took nearly 90 hr to complete.

Since the completion of this activity, a fine-grain, parallel version of APNASA has been written by a team of researchers from General Electric, NASA Lewis, and NYMA. Timing studies performed on the SP2 have shown that, with eight processors assigned to each blade row, the simulation time is reduced by a factor of six. For this configuration, the simulation time would be 15 hr. The reduction in computing time indicates that an overnight turnaround of a multistage configuration simulation is feasible.

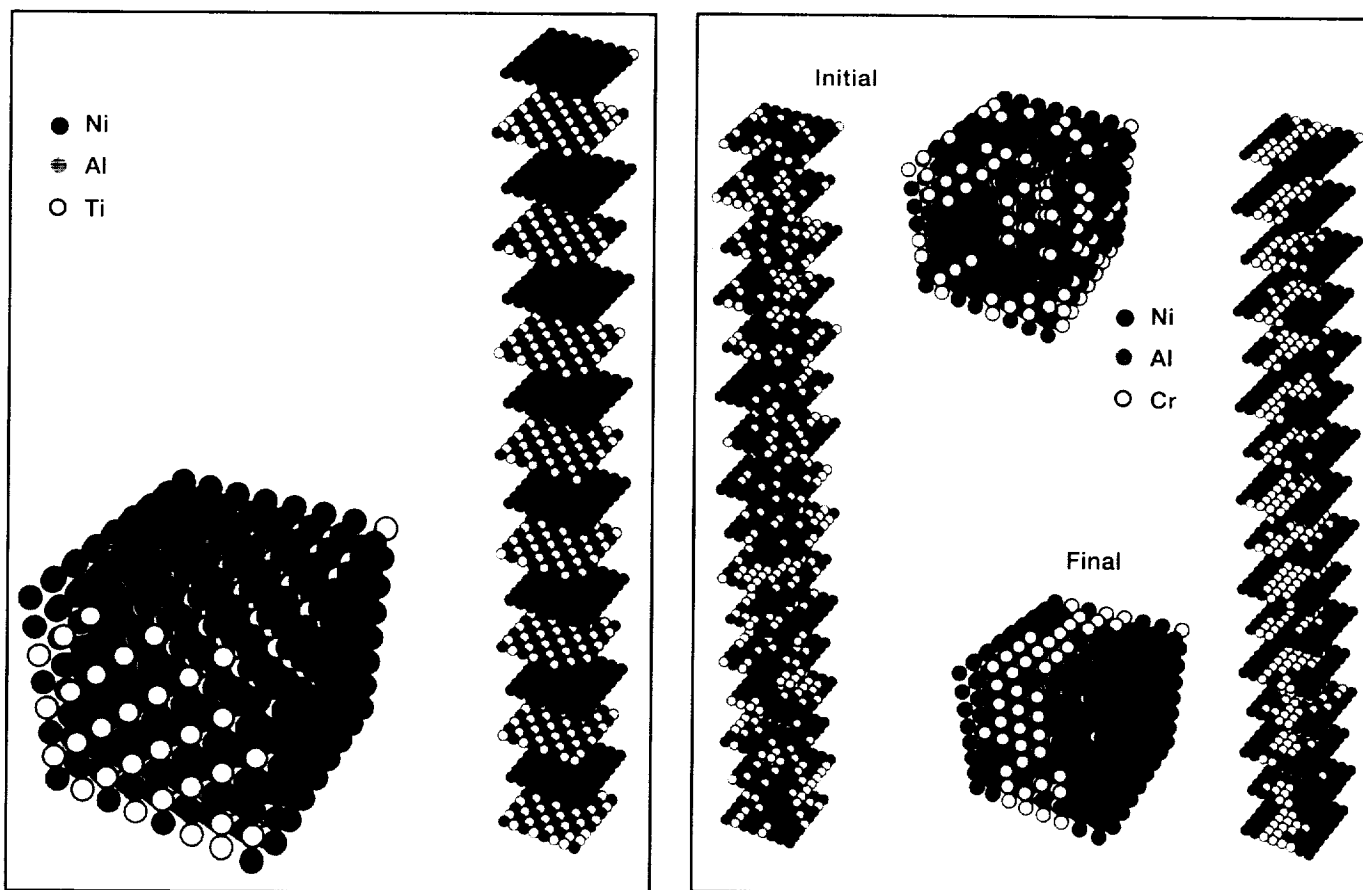
In addition, average passage forms of two-equation turbulence models were formulated. These models are currently being incorporated into APNASA.

**Lewis contact:** Dr. John J. Adamczyk, (216) 433-5829,  
john.j.adamczyk@lerc.nasa.gov

**Author:** Dr. John J. Adamczyk

**Headquarters program office:** OA

# New Theoretical Technique for Alloy Design



Left:  $Ni_{50}Al_{25}Ti_{25}$ ; final temperature, 100 K. Right:  $Ni_{33}Al_{34}Cr$ . (Elongated views; stretched computational cells are included for the ease of observing these structures.)

During the last 2 years, there has been a breakthrough in alloy design at the NASA Lewis Research Center. A new semi-empirical theoretical technique for alloys, the BFS Theory (Bozzolo, Ferrante, and Smith), has been used to design alloys on a computer. BFS was used, along with Monte Carlo techniques, to predict the phases of ternary alloys of NiAl with Ti or Cr additions. High concentrations of each additive were used to demonstrate the resulting structures.

The computer simulations showed very different behavior for these two alloy systems. NiAl-Ti condensed into the Heusler phase at 25 percent Ti, as shown in the figure on the left. In contrast, Cr additions resulted in very different behavior predictions (figure on the right), where we see phase separation of the Cr to regions between the NiAl crystals. Both computations were started at high temperatures with a random distribution of elements that were then Monte Carlo "annealed" to low temperatures, giving the phases shown. These theoretical predictions were verified experimentally by Ronald Noebe et al. Results indicate that it may now be possible to design alloys on a computer, which would greatly aid in narrowing the field of potential alloy candidates for a given application.

## Bibliography

Bozzolo, G.; Ferrante, J.; and Kobistek, R.J.: Modeling of Surfaces 2. Metallic Alloy Surfaces Using the BFS Method. *J. Computer-Aided Mater. Des.*, vol. 1, 1994, p. 305.

Bozzolo, G.; Ferrante, J.; and Noebe, R.D.: Energetics of Ternary and Quaternary Alloy Surfaces. *Surf. Sci.* (in press).

Bozzolo, G.; Good, B.; and Ferrante, J.: Cu-Au Alloys Using Monte Carlo Simulations and the BFS Method for Alloys. Fall 1995 Meeting of the Materials Research Society (in press).

**Lewis contact:** Dr. John Ferrante,  
(216) 433-6069,  
John.Ferrante@lerc.nasa.gov

**Author:** Dr. John Ferrante

**Headquarters program office:** OA

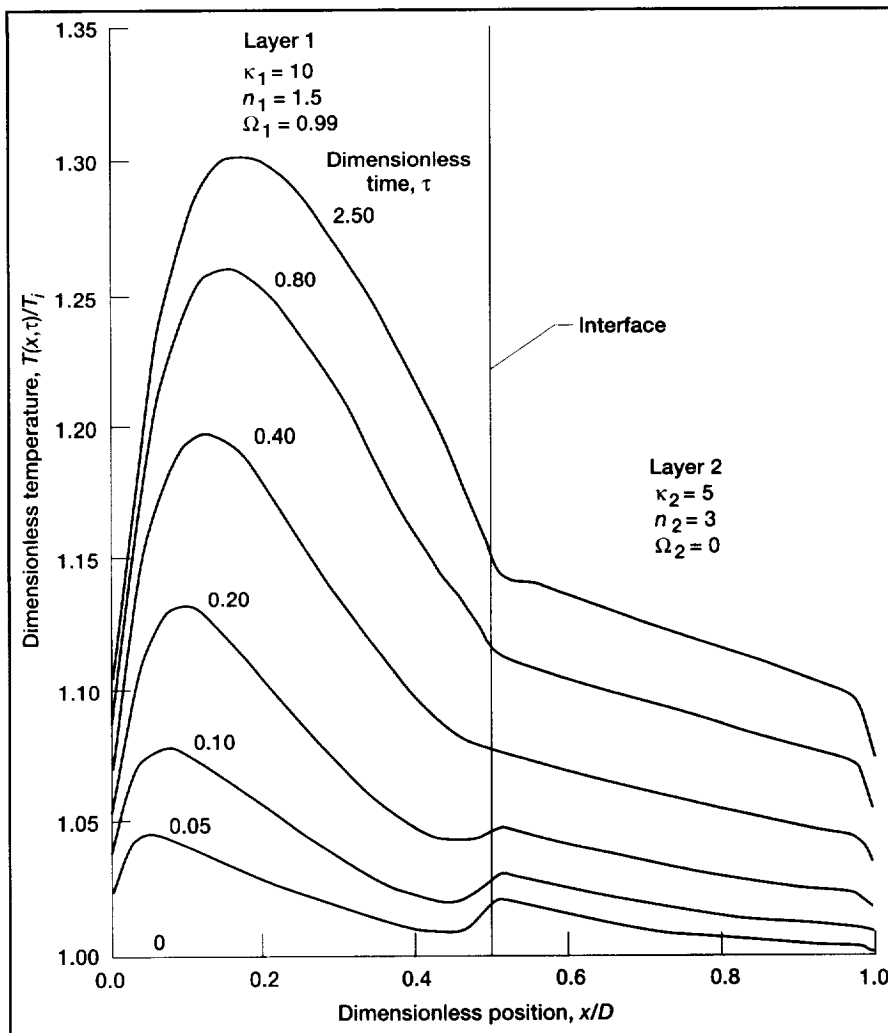
# Thermal Radiation Effects Analyzed in Translucent Composite and Thermal Barrier Coating

Ceramic parts and coatings are needed to withstand high temperatures in advanced aircraft engines. In hot environments, such as in the combustion chambers of these engines, infrared and visible radiation can penetrate into some ceramics and heat them internally. The internal temperatures depend on radiative effects combined with heat conduction, and on convection and radiation at the material boundaries. Since engine temperatures are high, radiant emission can be large from within translucent parts and coatings, and this must be included in the analysis. Transient and steady-state behavior are both important. During a transient, radiant penetration provides more rapid internal heating than conduction alone, and the temperature distributions are usually considerably different than for steady-state conditions; this can produce transient thermal stresses.

Analytical and numerical methods are being used at the NASA Lewis Research Center to predict transient temperatures and heat flows in translucent materials. A transient analysis was done for a composite of two translucent layers. The layer refractive indices were larger than 1, producing internal reflections at the boundaries and at the internal interface. In addition, steady-state results were computed for a two-layer composite with one layer opaque. The results were used to assess the importance of internal radiation in a zirconia thermal barrier coating on a cooled metal wall.

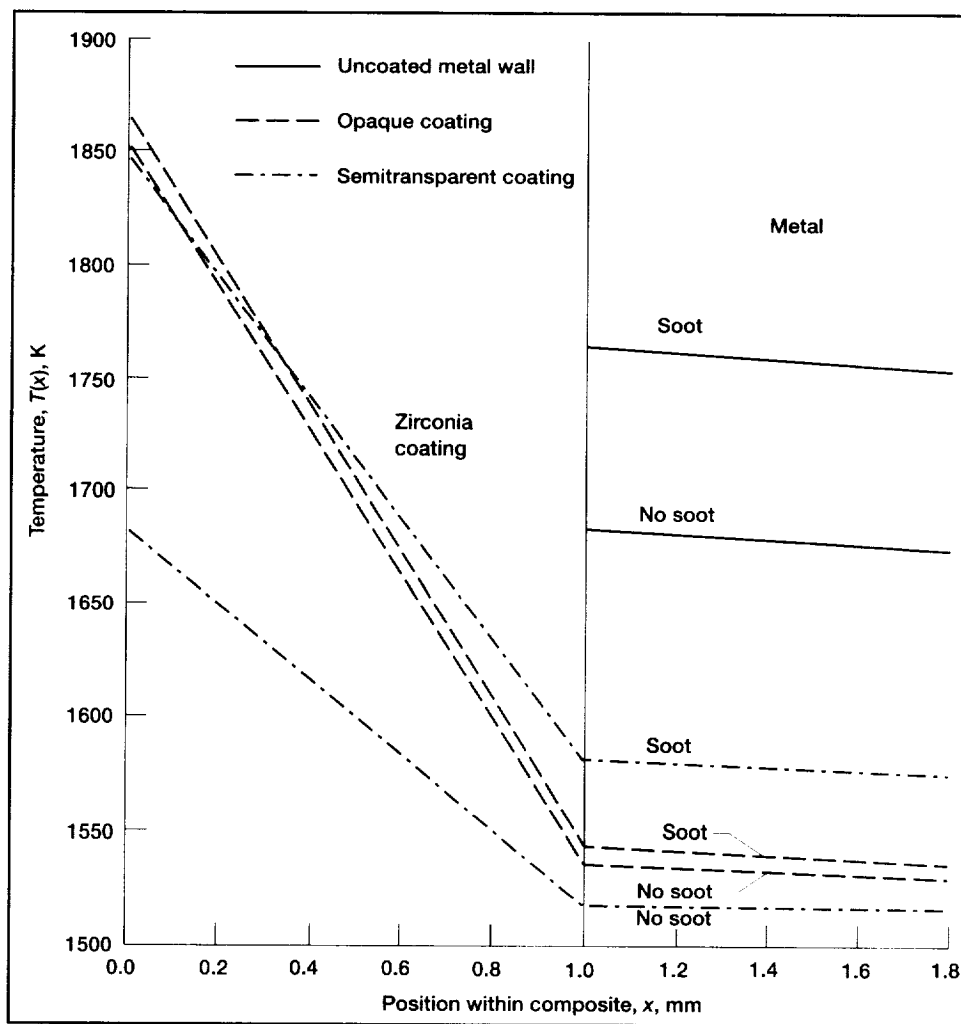
Since the radiative transfer equations are rather complex, especially when internal scattering is included, approximate methods are being investigated that might be convenient for computer design programs. An approximate two-flux method was used and verified by comparisons with solutions that used exact radiative transfer relations. The two-flux equations include scattering without increasing solution difficulty.

Illustrative transient temperatures are shown in the figure to the left for a translucent two-layer composite. This demonstrates that scattering in the first layer shields the second layer from incident radiation that is suddenly applied to the boundary at  $x = 0$ . Simultaneously, both boundaries are strongly cooled by convection. Scattering decreases radiation penetration to the second layer, and the transient temperatures in the second layer remain low. The maximum temperature is in the first layer.



Transient temperatures in a translucent, two-layer composite following the sudden application of radiation to the boundary at  $x = 0$ . Scattering in the first layer shields the second layer from incident radiation, resulting in low temperatures in the second layer. (Optical thickness of layer,  $\kappa$ ; refractive index,  $n$ ; scattering albedo,  $\Omega$ ; thickness of composite,  $D$ ; and initial temperature,  $T_i$ .)

Related behavior is examined in the figure below for a 1-mm-thick zirconia coating on a high-alloy steel combustion liner; zirconia has high scattering. The results are for typical steady-state engine conditions. The solid lines represent an uncoated metal wall, with the lower solid line for metal oxidized on both sides. The upper solid line is for metal covered with soot on the combustion side. The temperatures are above the metal melting point, so a thermal barrier coating would have to be used to protect the metal. For comparison, metal with a zirconia coating assumed opaque so it has no internal radiation (dashed lines) is shown. With the coating, the metal temperature is substantially reduced, and soot on the coating increases metal temperatures only slightly. If the coating can be kept clean, there is an additional benefit when the coating is translucent (dot-dash lines). The high scattering of the clean zirconia coating reflects away much of the incident radiation, and temperatures in the zirconia are decreased (lower dot-dash line), with the temperature of the hot side of the metal reduced about 20 K. If the zirconia is covered with soot, however, the metal temperatures increase. Incident radiation is absorbed by the soot, and the translucence of the zirconia acts like increased thermal conductivity that reduces the insulating ability of the coating (upper dot-dash line).



Combustor liner temperature distributions for oxidized metal without a coating, with an opaque thermal barrier coating, and with a semitransparent thermal barrier coating. All cases shown both with and without soot on the exposed surface.

## Bibliography

Siegel, R.: Green's Function and Two-Flux Analysis for Transient Radiative Transfer in a Composite Layer. ASME HTD-Vol. 325, National Heat Transfer Conference, Houston, Vol. 3, 1996, pp. 35-43.

Siegel, R.: Two-Flux Green's Function Analysis for Transient Spectral Radiation in a Composite, AIAA J. Thermophysics Heat Trans., vol. 10, no. 4, 1996, pp. 681-688.

Siegel, R.: Internal Radiation Effects in Zirconia Thermal Barrier Coatings, AIAA J. Thermophysics Heat Trans., vol. 10, no. 4, 1996, pp. 707-709.

## Lewis contact:

Dr. Robert Siegel, (216) 433-5831, robert.siegel@lerc.nasa.gov

Author: Dr. Robert Siegel

Headquarters program office: OA

# Technology Transfer

## Lewis Business and Industry Summit

On September 19, 1996, the NASA Lewis Research Center hosted its first Lewis Business and Industry Summit, which showcased the Center's technology and capabilities. The Summit was designed to create and strengthen new and continuing relationships between Lewis and the private sector, and to build recognition of Lewis as a key technology resource in the region.

The Summit featured tours, over 140 exhibits, breakout sessions, and demonstrations of key Lewis products, capabilities, and facilities in six core competencies: combustion and fluids, materials and structures, instrumentation and controls, communications and computing, power generation and management, and turbomachinery. Breakout sessions and exhibits on partnering, technology transfer, and commercialization enabled attendees to learn more about working with Lewis.

More than 500 individuals representing over 300 businesses and organizations (from as far away as California) attended the Summit, and NASA is following up nearly 400 inquiries regarding technology transfer opportunities. Twenty-eight different corporate, civic, and technology transfer organizations partnered with NASA Lewis to create and sponsor the Business and Industry Summit. NASA's Administrator, Daniel S. Goldin, attended the Summit and commented "What a great day for Cleveland!"

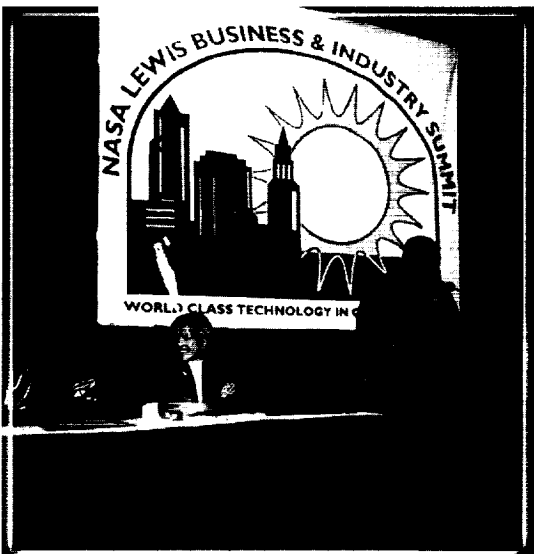
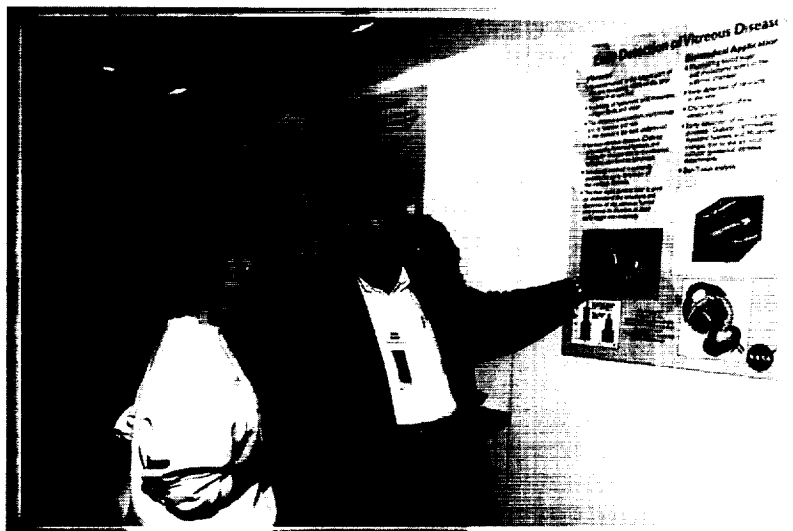
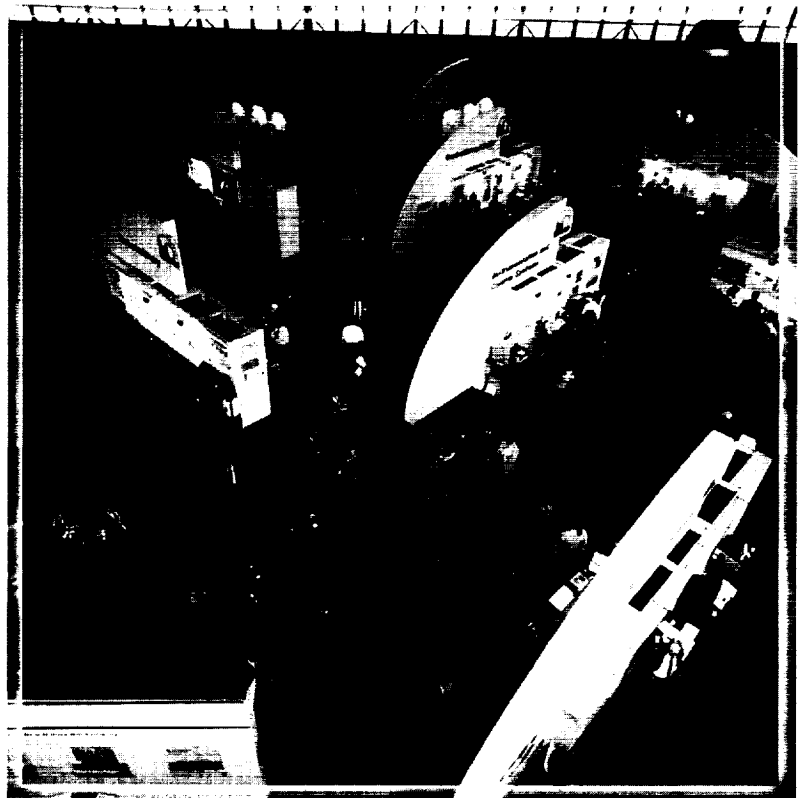
**Find out more about the Summit on the World Wide Web:**

<http://www.lerc.nasa.gov/LBIS/>

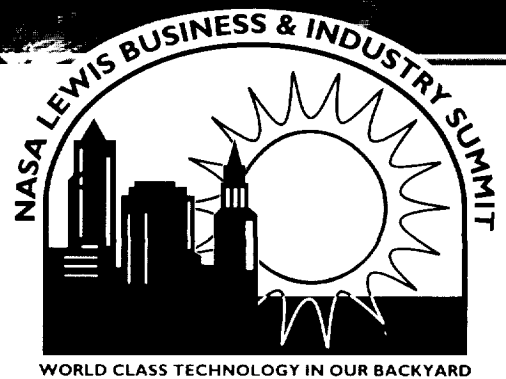
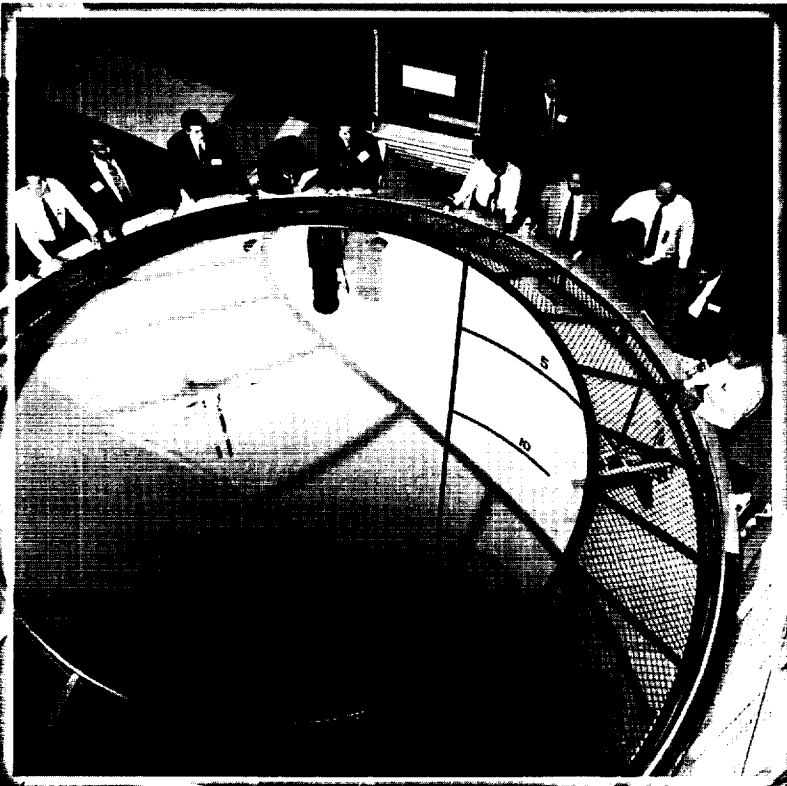
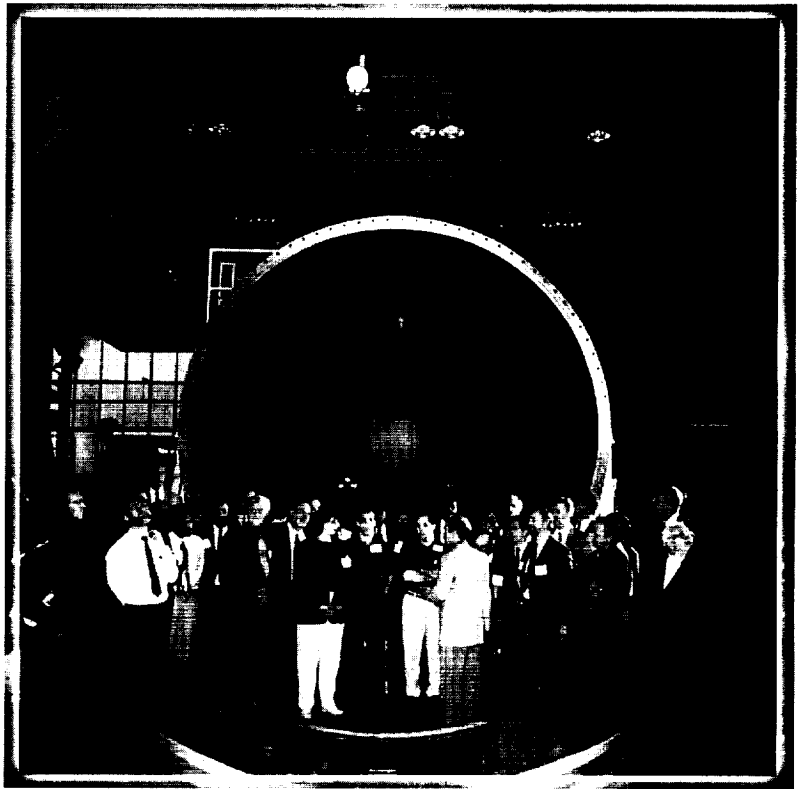
**Lewis contact:** Ann O. Heyward, (216) 433-3484, [Ann.O.Heyward@lerc.nasa.gov](mailto:Ann.O.Heyward@lerc.nasa.gov)

**Author:** Ann O. Heyward

**Headquarters program office:** OA







# Innovative Ultrasonic Imaging Method Wins R&D 100 Award

The NASA Lewis Research Center, Cleveland State University, and Sonix, Inc., teamed on a technology transfer project resulting in a single transducer ultrasonic imaging subsystem that is thickness independent. Sonix, an established manufacturer of ultrasonic imaging systems used worldwide for microelectronics, materials research, and commercial nondestructive evaluation, has incorporated this new system into several of their commercial ultrasonic imaging systems.

Because high-tech components are often made of composite materials where internal flaws and nonuniform internal microstructures can lead to catastrophic failure of the part, nondestructive evaluation of products is an increasingly important part of the manufacturing and quality assurance process. Nondestructive evaluation, which involves an internal inspection of virtually every part manufactured, rather than a random sampling of production parts, is an absolute necessity for high-tech components.

Using ultrasonic imaging systems is one approach to nondestructive evaluation of just-made, high-tech parts. Currently, in cases where extremely rigid quality control is required, parts that will be ultrasonically scanned must be precision machined to eliminate any superimposing effect of thickness variations present in the ultrasonic image. The single transducer subsystem developed by the Lewis/Cleveland State/Sonix team eliminates the effect of thickness variations in the image, thus eliminating the need to precisely machine the part. In addition, the number of samples needed to characterize a material is reduced by up to 50 percent in comparison to conventional ultrasonic imaging systems. Up to 20 percent of the cost of conventional systems is saved because less machining, less image interpretation time, less image processing, and fewer samples are needed.

The Single Transducer Thickness-Independent Ultrasonic Imaging Method subsystem was developed by NASA Lewis team leader Dr. Don J. Roth, Sonix team leader Mike Whalen, and Cleveland State University team leader Prof. John H. Hemann. Other team members included James R. Bodis of Cleveland State and J. Lynne Hendricks of Sonix. The Single Transducer Thickness-Independent Ultrasonic Imaging subsystem won a 1996 R&D 100 Award.

**Lewis contact:** Stephen M. Riddlebaugh, (216) 433-5565,  
Stephen.M.Riddlebaugh@lerc.nasa.gov

**Author:** Stephen M. Riddlebaugh

**Headquarters program office:** OA

## Lewis-Developed Ion Exchange Material Licensed to Several Companies

The NASA Lewis Research Center licensed its patented Ion Exchange Material (IEM) to several businesses this year. Three limited field-of-use licenses were issued to two firms, and a manufacturing license was issued to a third firm.

The Lewis IEM is a polymer-based material that adsorbs (collects on its surface) heavy metal ions from aqueous (water-based) solutions. A broad range of potential applications has been identified for this material from food processing to wastewater cleanup.

Licenses have been issued to Lee and Associates of Bolton, Vermont, to manufacture test kits to identify the presence and concentrations of heavy metals in aqueous solutions and to extract precious or heavy metals from raw or partially refined ore. The Invention Factory of Barre, Vermont, was issued a license to develop and manufacture food processing equipment that will remove lead from aqueous foodstuffs. Howard Industries of Columbus, Ohio, received a license to manufacture the Lewis IEM. Additional limited field-of-use licenses are presently being negotiated with several other companies.

### **Lewis contact:**

Stephen M. Riddlebaugh,  
(216) 433-5565,  
Stephen.M.Riddlebaugh@lerc.nasa.gov

**Author:** Stephen M. Riddlebaugh

**Headquarters program office:** OA

## Lewis Incubator for Technology

In 1996, the Lewis Incubator for Technology (LIFT) opened for business. LIFT is enabling entrepreneurs, startup companies, and emerging small companies to create new products, enterprises, and jobs by working with the NASA Lewis Research Center to acquire technology and technical expertise with high commercial potential. Enterprise Development, Inc., manages this program under a cooperative agreement with NASA Lewis. The State of Ohio's Department of Development also provides funding for this program. LIFT is located at BP America's world-class research facility in Warrensville Heights, Ohio, where LIFT tenants have access to outstanding laboratory and office space, small-scale production facilities, library research services, and other critical capabilities as they build their businesses.

A number of services geared toward the needs of entrepreneurial enterprises—such as education and hands-on assistance with strategic planning, business plan development, marketing, and accessing venture capital and other financial support—are available to LIFT tenants. LIFT's objective is to give access to NASA technology to create new products, services, companies, high-quality jobs, economic growth, and increased economic impact in the State of Ohio.

### **Lewis contacts:**

Kim A. Veris, (216) 433-6355,  
Kim.A.Veris@lerc.nasa.gov; and  
Ann O. Heyward, (216) 433-3484,  
ann.o.heyward@lerc.nasa.gov

### **Lift contact:**

Wayne Zeman, wzeman@ebtc.org

**Author:** Kim A. Veris

**Headquarters program office:** OA

# NASA Headquarters Program Offices

**OA**—Office of Aeronautics

**HPCCO**—High Performance Computing & Communications Office

**STD**—Subsonic Transportation Division

**OLMSA**—Office of Life & Microgravity Sciences & Applications

**MSAD**—Microgravity Science & Applications Division

**OSAT**—Office of Space Access and Technology

**OSF**—Office of Space Flight

**OSMA**—Office of Safety and Mission Assurance

**OSS**—Office of Space Science

# Index of Authors and Contacts

Both authors and contacts are listed in this index. Articles start on the page numbers following the names. When two articles start on the same page, the first article is indicated by the letter "a" after the number and the second article by a "b."

## A

Adamczyk, Dr. John J. 169

## B

Baaklini, Dr. George Y. 98  
Babrauckas, Theresa L. 36  
Bakhle, Milind A. 89  
Banks, Bruce A. 122  
Barankiewicz, Wendy S. 16  
Bartolotta, Dr. Paul A. 67, 84  
Beach, Raymond F. 121  
Benson, Thomas J. 15a  
Bhasin, Dr. Kul B. 127  
Bonacuse, Peter J. 85  
Bozzolo, Dr. Guillermo H. 49  
Brady, Dr. Michael P. 66, 67  
Bright, Michelle M. 9  
Brindley, Dr. William J. 66, 67  
Buffum, Dr. Daniel H. 24

## C

Canacci, Victor A. 33  
Carney, Kelly S. 166  
Chamis, Dr. Christos C. 72, 74, 75  
Chiamonte, Dr. Fran 140  
Chima, Dr. Rodrick V. 25

## D

Davidian, Kenneth O. 104  
Davis, Dr. David O. 17  
De Chant, Lawrence J. 1  
De Groh, Kim K. 122  
DeBonis, James R. 21  
DeLombard, Richard 151  
Dickman, John Ellis 123  
Dietrich, Daniel L. 150  
Dimofte, Dr. Florin 114

## E

Eckel, Andrew J. 54, 105

## F

Farmer, Dr. Serene C. 58  
Fellenstein, James A. 60  
Fernandez-Pello, Prof. A. Carlos 147  
Ferrante, Dr. John 49, 170  
Fincannon, James 155  
Fleming, Dr. David P. 90

Follen, Gregory J. 38, 39, 40  
Fox, Dennis 69  
Fralick, Gustave C. 3, 4  
Frate, David T. 150  
Freed, Dr. Alan D. 48  
Fusaro, Robert L. 92

## G

Gabb, Timothy P. 51  
Gaier, Dr. James R. 124  
Gard, Melissa Y. 139  
Garg, Dr. Anita 53  
Gayda, Dr. John 51  
Georgiadis, Nicholas J. 21  
Gholdston, E.W. 158  
Ghosn, Dr. Louis 99  
Ginty, Carol A. 47  
Gray, Dr. Hugh R. 47  
Griffin, Dr. DeVon W. 139

## H

Hall, Nancy Rabel 143  
Heidmann, James D. 26  
Heinen, Dr. Vernon O. 131  
Hemminger, Joseph A. 104  
Hendricks, Robert C. 114  
Herbell, Dr. Thomas P. 54  
Heyward, Ann O. 173, 177b  
Hoffman, Dave J. 153, 157  
Hojnicki, Jeffrey S. 155  
Hollansworth, James E. 128  
Horowitz, Dr. Jay G. 40, 161  
Hughes, Christopher E. 31

## I

Irvine, Thomas B. 33

## J

Jacobson, Dr. Nathan 69  
Jacobson, Thomas P. 143  
Janetzke, David C. 96  
Jankovsky, Amy L. 106  
Jaskowiak, Martha H. 56  
Jones, Dr. William R., Jr. 61  
Jones, Jeffrey A. 161

## K

Karimi, K. 158

Kascak, Albert F. 94  
Kashiwagi, T. 137  
Kaufman, Bradford A. 121  
Kerslake, Thomas W. 157  
Kim, Heechul 135  
Kiser, J. Douglas 59  
Klann, Gary A. 34  
Kory, Carol L. 131  
Koudelka, John M. 147  
Kurkov, Dr. Anatole P. 95

## L

Lam, David W. 23  
Lawrence, Dr. Charles 42  
Le, Dr. Dzu K. 163  
Lee, F.C. 158  
Lerch, Bradley A. 86  
Lewandowski, Beth 43  
Linne, Diane L. 108  
Liu, Dr. Nan-Suey 14  
Loyselle, Dr. Patricia L. 118  
Ludwiczak, Damian R. 168  
Lyons, Dr. Valerie J. 20

## M

Malarik, Diane C. 145  
Maloney, Dr. Thomas M. 118  
Manners, Bruce A. 158  
McKissock, Barbara I. 120  
McMillen, Joseph P. 162  
Mehmed, Oral 96  
Melcher, Kevin J. 11  
Meyer, William V. 142  
Miller, Dr. David P. 27  
Miranda, Dr. Félix A. 132, 133  
Morscher, Gregory N. 57  
Murthy, Dr. Pappu L.N. 76, 77  
Musgrave, Jeffrey L. 12

## N

Nadell, Shari-Beth 1  
Nemeth, Noel N. 100  
Neudeck, Dr. Philip G. 6  
Noebe, Dr. Ronald D. 49

## O

Oeftering, Richard C. 165  
Olson, Sandra L. 137

Opila, Dr. Elizabeth J. 69  
Otero, Angel M. 140  
Overton, Eric 125  
Owen, Dr. Albert K. 163

## **P**

Palaszewski, Bryan A. 109, 110  
Panov, Y. 158  
Patnaik, Dr. Surya N. 79  
Pereira, Dr. J. Michael 80, 81  
Piszczor, Michael F., Jr. 116  
Pline, Alexander D. 143  
Putt, Charles W. 42

## **R**

Radil, Kevin C. 62  
Rajagopalan, J. 158  
Richter, G. Paul 105  
Riddlebaugh, Stephen M. 176, 177a  
Roberts, Dr. Gary D. 81  
Roeder, James W., Jr. 34  
Rogers, Richard B. 142  
Romanofsky, Robert R. 132  
Roth, Dr. Don J. 102  
Rutledge, Sharon K. 126

## **S**

Sankovic, John M. 112  
Saravanos, Dimitris A. 82  
Sayir, Dr. Ali 54, 58, 105  
Scheiman, David A. 157  
Schneider, Dr. Steven J. 113  
Schoenenberger, Mark 17  
Schubert, Kathleen E. 148  
Seasholtz, Dr. Richard G. 8  
Sedlak, Deborah A. 143, 148, 151  
Shogrin, Brad 61  
Shyne, Rickey J. 29  
Siegel, Dr. Robert 171  
Singh, Dr. Mrityunjay 59  
Skor, Mike 153  
Smialek, Dr. James L. 66, 67, 70  
Sohn, Dr. Ki-Hyeon 29  
Spence, Rodney L. 130  
Steinetz, Dr. Bruce M. 97  
Stubbs, Dr. Robert M. 14  
Sutter, Dr. James K. 64

## **T**

Tweedt, Dr. Daniel L. 30

## **U**

Urban, Dr. David L. 139

## **V**

Van Drei, Donald E. 38  
Van Zante, Dale E. 15b  
Veres, Joseph P. 44  
Veris, Kim A. 177b  
Verrilli, Michael J. 87  
Viterna, Dr. Larry A. 159  
Vrotsos, Pete 151

## **W**

Warner, Joseph D. 127  
Whittenberger, Dr. J. Daniel 53  
Wilson, Richard M. 119  
Wilt, David M. 117  
Winsa, Edward A. 148  
Woodward, Richard P. 31

## **Z**

Zaman, Dr. Khairul B. 19  
Zeman, Wayne 177b  
Zurawski, Robert L. 143



# REPORT DOCUMENTATION PAGE

Form Approved  
OMB No. 0704-0188

Public reporting burden for this collection of information is estimated to average 1 hour per response, including the time for reviewing instructions, searching existing data sources, gathering and maintaining the data needed, and completing and reviewing the collection of information. Send comments regarding this burden estimate or any other aspect of this collection of information, including suggestions for reducing this burden, to Washington Headquarters Services, Directorate for Information Operations and Reports, 1215 Jefferson Davis Highway, Suite 1204, Arlington, VA 22202-4302, and to the Office of Management and Budget, Paperwork Reduction Project (0704-0188), Washington, DC 20503.

<b>1. AGENCY USE ONLY</b> (Leave blank)		<b>2. REPORT DATE</b> March 1997	<b>3. REPORT TYPE AND DATES COVERED</b> Technical Memorandum	
<b>4. TITLE AND SUBTITLE</b>  Research & Technology 1996			<b>5. FUNDING NUMBERS</b>  None	
<b>6. AUTHOR(S)</b>				
<b>7. PERFORMING ORGANIZATION NAME(S) AND ADDRESS(ES)</b>  National Aeronautics and Space Administration Lewis Research Center Cleveland, Ohio 44135-3191			<b>8. PERFORMING ORGANIZATION REPORT NUMBER</b>  E-10503	
<b>9. SPONSORING/MONITORING AGENCY NAME(S) AND ADDRESS(ES)</b>  National Aeronautics and Space Administration Washington, D.C. 20546-0001			<b>10. SPONSORING/MONITORING AGENCY REPORT NUMBER</b>  NASA TM-107350	
<b>11. SUPPLEMENTARY NOTES</b>  Responsible person, Walter S. Kim, organization code 9400, (216) 433-3742.				
<b>12a. DISTRIBUTION/AVAILABILITY STATEMENT</b>  Unclassified - Unlimited Subject Categories 01 and 31  This publication is available from the NASA Center for AeroSpace Information, (301) 621-0390.			<b>12b. DISTRIBUTION CODE</b>	
<b>13. ABSTRACT (Maximum 200 words)</b>  This report selectively summarizes the NASA Lewis Research Center's research and technology accomplishments for fiscal year 1996. It comprises 116 short articles submitted by the staff scientists and engineers. The report is organized into six major sections: Aeronautics, Aerospace Technology, Space Flight Systems, Engineering & Computational Support, Lewis Research Academy, and Technology Transfer. A table of contents, an author index, and a list of NASA Headquarters program offices have been included to assist the reader in finding articles of special interest. This report is not intended to be a comprehensive summary of all research and technology work done over the past fiscal year. Most of the work is reported in Lewis-published technical reports, journal articles, and presentations prepared by Lewis staff and contractors (for abstracts of these Lewis-authored reports, visit the Lewis Technical Report Server (LeTRS) on the World Wide Web— <a href="http://letrs.lerc.nasa.gov/LeTRS/">http://letrs.lerc.nasa.gov/LeTRS/</a> ). In addition, university grants have enabled faculty members and graduate students to engage in sponsored research that is reported at technical meetings or in journal articles. For each article in this report, a Lewis contact person has been identified, and where possible, reference documents are listed so that additional information can be easily obtained. The diversity of topics attests to the breadth of research and technology being pursued and to the skill mix of the staff that makes it possible. For more information about Lewis' research, visit us on the World Wide Web ( <a href="http://www.lerc.nasa.gov">http://www.lerc.nasa.gov</a> ). Also, this document is available on the World Wide Web ( <a href="http://www.lerc.nasa.gov/WWW/RT/">http://www.lerc.nasa.gov/WWW/RT/</a> ).				
<b>14. SUBJECT TERMS</b>  Aeronautics; Aerospace engineering; Space flight; Space power; Materials; Structures; Electronics; Space experiments; Technology transfer			<b>15. NUMBER OF PAGES</b> 195	
			<b>16. PRICE CODE</b> A09	
<b>17. SECURITY CLASSIFICATION OF REPORT</b> Unclassified	<b>18. SECURITY CLASSIFICATION OF THIS PAGE</b> Unclassified	<b>19. SECURITY CLASSIFICATION OF ABSTRACT</b> Unclassified	<b>20. LIMITATION OF ABSTRACT</b>	